

THE HIGH DENSITY LIPOPROTEIN AND ATHEROSCLEROSIS

**THE DEVELOPMENT OF ATHEROSCLEROSIS AND CORONARY
OCCLUSION IN THE MOUSE:
INVESTIGATING THE HIGH DENSITY LIPOPROTEIN SIGNALING
PATHWAY AND THE IMPACT OF THE SCAVENGER RECEPTOR CLASS B
TYPE 1**

By PEI YU, MBBS, MMED

**A Thesis Submitted to the School of Graduate Studies
in Partial Fulfillment of the Requirements for
the Degree Doctor of Philosophy.**

McMaster University © Copyright by Pei Yu, 2016

ABSTRACT

Coronary artery disease results from atherosclerotic plaque formation. High-density lipoprotein (HDL) has been shown to be inversely associated with the risk of coronary artery disease. It not only reduces lipid accumulation in atherosclerotic plaques by mediating reverse cholesterol transport, but also exerts direct protection on vascular cells via the scavenger receptor class B, type 1 (SR-B1).

Increased macrophage apoptosis is commonly observed in advanced or unstable atherosclerotic plaques. In this thesis, the anti-apoptotic effect and the signaling pathway of HDL in macrophages were investigated. We showed that HDL protected macrophages from endoplasmic reticulum (ER) stress induced apoptosis in a SR-B1 adaptor protein PDZK1 and Akt1 dependent manner. Also, atherogenic mice with PDZK1 deficiency in bone marrow-derived cells exhibited increased atherosclerotic plaque sizes with enlarged necrotic cores, which is a feature of rupture-prone plaques. We also found that HDL decreased the proapoptotic Bcl-2 related protein Bim in ER stressed macrophages, and Bim^{-/-} macrophages were resistant to tunicamycin-induced apoptosis. Our *in vitro* study suggests that Bim is likely to be the downstream factor in the HDL signaling pathway. Consistent with this, inactivation of Bim *in vivo* significantly reduced plaque area and necrotic core size in a mouse model with low circulating HDL.

We also characterized the SR-B1^{-/-}/apoE^{-/-}, a spontaneous coronary heart disease model, by treating them with the clinically used heart disease drug rosuvastatin, and found that rosuvastatin protected SR-B1^{-/-}/apoE^{-/-} mice against atherothrombosis and

attenuated myocardial fibrosis and cardiomegaly. This protection may be attributed to the ability of rosuvastatin to reduce oxidized LDL and inhibit macrophage foam cell formation. The work in this thesis contributes to a more detailed understanding of the impacts of HDL and SR-B1 on atherosclerosis.

ACKNOWLEDGEMENTS

Foremost, I would like to express my deepest gratitude to my advisor, Dr. Bernardo Trigatti, for his excellent guidance, continuous support and constructive suggestion throughout my Ph.D study. Dr. Trigatti gave me the freedom to explore the projects on my own, and patiently helped and directed me to overcome a lot of research difficulties. I have benefited greatly from Dr. Trigatti. I would never have been able to finish my dissertation without his help and suggestions. I would like to extend my thanks to my supervisory committee: Dr. Richard Austin and Dr. Jonathan Bramson, for their insightful comments and constructive feedback to my project over the years.

I feel very lucky to work in a great research team, including all of my former and current colleagues: Dr. Yi Zhang, Dr. Aishah Al-Jarallah, Dr. Mark Fuller, Dr. Omid Dadoo, David Wang, Leticia Gonzalez and Kristina Durham. I am very thankful for their various forms of support during my graduate study. We also have the best lab technician, Melissa MacDonald. Everyone was impressed by her excellent management on mouse colonies, reagent catalogues and research labware. She was always willing to help taking care of my mice, when I was on sick leave.

I would also like to thank my parents and my parents-in-law. Even though we are thousands of miles away, they were always supportive. I really appreciate all of the sacrifices that they made for us, and all of the valuable suggestions they gave to us when we were experiencing difficulties and challenges.

Last but not the least, I would like to thank my loving husband and best friend, Jason Jia Yang. I am grateful to my husband not only because he was always encouraging me whenever I felt frustrated, but also because he has given up so much to make my work a priority. Words can never say how grateful I am to my loving husband.

TABLE OF CONTENTS

ABSTRACT	III
ACKNOWLEDGEMENTS	V
LIST OF FIGURES AND TABLES	XII
CHAPTER I: GENERAL INTRODUCTION	1
PREFACE	1
1.1 Atherosclerosis	2
1.2. High-density lipoprotein (HDL)	8
1.3. The initiation of HDL signaling pathways	10
1.3.1 ApoA-I and ATP-binding cassette transporter A1 (ABCA1)	11
1.3.2 Mature HDL and ATP-binding cassette transporter G1 (ABCG1).....	12
1.3.3 HDL and SR-B1	13
1.3.4 Sphingosine 1-phosphate (S1P), apoM and S1P receptors (S1PR).....	14
1.4. Atheroprotective effects of HDL in vascular cells	15
1.4.1 Myeloid cells	15
1.4.2 Endothelial cells	22
1.4.3 Macrophages.....	38
1.4.4 Smooth muscle cells	45
1.5. Mouse models of atherosclerosis	49
1.5.1 ApoE ^{-/-} mouse model	50
1.5.2 LDLR ^{-/-} mouse model	51
1.5.3 ApoE ^{-/-} /LDLR ^{-/-} mice.....	53

1.5.4 SR-B1 ^{-/-} /apoE ^{-/-} mice	53
1.6. Objectives of the thesis	57
CHAPTER II	60
PREFACE.....	60
2.1 Abstract.....	61
2.2 Introduction.....	63
2.3 Materials and Methods.....	68
2.3.1 Materials	68
2.3.2 Mice.....	68
2.3.3 Preparation, culture and treatment of peritoneal macrophages	68
2.3.4 Apoptosis analysis	69
2.3.5 Measurement of UPR markers in cultured macrophages	71
2.3.6 Analysis of Akt phosphorylation.....	72
2.3.7 Macrophage polarization	73
2.3.8 Bone Marrow Transplantation.....	74
2.3.9 Analysis of atherosclerotic Lesions.....	74
2.3.10 Statistical analysis	76
2.4 Results	77
2.4.1 HDL, but not LDL, protected MPMs from apoptosis in a dose-dependent manner.	77
2.4.2 HDL did not reduce ER stress induced by tunicamycin.....	80
2.4.3 HDL mediated protection of macrophages from apoptosis requires PDZK1	80
2.4.4 HDL mediated cytoprotection of macrophages via PDZK1 involves Akt1	90
2.4.5 Bone marrow-specific deletion of PDZK1 increases diet induced atherosclerosis in LDLR ^{-/-} mice.....	94

2.4.6 Effects of PDZK1 inactivation on markers of macrophage polarization	99
2.5 Discussion.....	103
2.6 Supplementary Materials and Methods.....	111
2.6.1 Foam cell formation and oil red O staining:.....	111
2.6.2 Evaluation of Bone Marrow Reconstitution.....	111
2.6.3 Lipid profile.....	112
2.6.4 Enzyme-linked immunosorbent assay.....	112
2.6.5 Monocyte Recruitment	112
2.6.6 Immunofluorescence staining.....	113
2.7 Supplementary Figures	115
CHAPTER III.....	135
PREFACE.....	135
3.1 Abstract.....	136
3.2 Introduction.....	137
3.3 Materials and Methods.....	140
3.3.1 Materials	140
3.3.2 Mice.....	140
3.3.3 Macrophage culture and apoptosis induction	141
3.3.4 Detection of apoptotic cells	141
3.3.5 Real-time PCR.....	142
3.3.6 Western Blot.....	143
3.3.7 Bone Marrow Transplantation (BMT)	144
3.3.8 Atherosclerotic Lesions	144
3.3.9 Lipid analysis.....	145

3.3.10 Enzyme-linked immunosorbent assay	145
3.3.11 Flow cytometry	145
3.3.12 Statistical analysis	146
3.4 Results	147
3.4.1 HDL reduced Bim protein levels in macrophages.	147
3.4.2 ApoA-I gene inactivation results in increased necrotic core formation in high fat diet fed LDLR deficient mice.....	155
3.4.3 Knocking out Bim in BM reduced atherosclerosis and plaque necrosis in apoA-I ^{-/-} /LDLR ^{-/-} mice.	161
3.5 Discussion.....	171
CHAPTER IV	176
PREFACE.....	177
4.1 Abstract.....	178
4.2 Introduction.....	180
4.3 Materials and Methods.....	185
4.3.1 Materials	185
4.3.2 Mice.....	185
4.3.3 Atherosclerosis and myocardial fibrosis	186
4.3.4 Lipid analysis.....	186
4.3.5 SDS-PAGE and immunoblotting	187
4.3.6 Bone marrow cell preparation, culture and treatment	188
4.3.7 Real time PCR	188
4.3.8 Enzyme-linked immunosorbent assay	190
4.3.9 Immunofluorescence staining.....	190

4.3.10 Statistical analysis	191
4.4 Results	192
4.4.1 Rosuvastatin increased plasma cholesterol levels in SR-B1 ^{-/-} /apoE ^{-/-} mice.	192
4.4.2 Rosuvastatin attenuated atherosclerosis and cardiac pathology in SR-B1 ^{-/-} /apoE ^{-/-} mice.	196
4.4.3 Rosuvastatin reduced levels of oxLDL in plasma and atherosclerotic plaques	205
4.4.4 Rosuvastatin treatment of macrophages decreases CD36 expression and foam cell formation	208
4.5 Discussion.....	212
CHAPTER V: DISCUSSION	218
5.1 Summary of HDL anti-apoptotic signaling pathway.....	218
5.2 Akt1 as a therapeutic target for atherosclerosis	225
5.3 Study of atherosclerosis in macrophage-specific Bim knockout mice	227
5.4 Characterization of coronary atherosclerotic plaques in SR-B1^{-/-}/apoE^{-/-} mice	228
5.5 The effects of SR-B1 deficiency on the components and functions of HDL	231
5.6 Summary and Significance.....	233
REFERENCES.....	236

LIST OF FIGURES AND TABLES

Figure 1.1: Macrophages in atherosclerotic plaques.....	5
Figure 1.2: The effect of HDL on inhibiting hematopoietic cell proliferation.	18
Figure 1.3: ER stress and UPR activation.....	34
Figure 1.4: The signaling pathways of HDL in endothelial cells.	36
Figure 1.5: The signaling pathways of HDL in macrophages.	43
Figure 1.6: The signaling pathways of HDL in SMCs.	47
Figure 2.1: Serum lipoproteins, specifically HDL, protected macrophages from tunicamycin– and thapsigargin-induced apoptosis.	78
Figure 2.2: HDL did not reduce ER stress in macrophages.....	84
Figure 2.3: HDL reduced tunicamycin- and oxLDL-induced apoptosis in WT but not PDZK1 ^{-/-} macrophages.....	86
Figure 2.4: PDZK1 ^{-/-} macrophages were more sensitive to tunicamycin-induced apoptosis in vivo than WT macrophages.	88
Figure 2.5: HDL activated Akt1 signaling pathway in macrophages in a PDZK1 dependent manner.	92
Figure 2.6: LDLR ^{-/-} mice transplanted with PDZK1 ^{-/-} BM showed enlarged necrotic cores with increased cell apoptosis in atherosclerotic plaques.....	97
Figure 2.7: PDZK1 deficiency partially inhibited the polarization of M2 macrophages.	101
Supplementary Table 2.1: Primer sequences for RT-PCR	114
Supplementary Figure 2.1: HDL did not reduce ER stress in foam cells.	115

Supplementary Figure 2.2: HDL protected MPM-derived foam cells from tunicamycin-induced apoptosis in a PDZK1-dependent manner.....	117
Supplementary Figure 2.3: PDZK1 ^{-/-} BM derived macrophages are more sensitive than WT BM derived macrophages to tunicamycin-induced apoptosis in LDLR ^{-/-} mice.	119
Supplementary Figure 2.4: PDZK1 deficiency in BM-derived cells did not affect lipid profile or systemic inflammatory markers in LDLR ^{-/-} mice.	121
Supplementary Figure 2.5: Blood cell analysis of LDLR ^{-/-} mice with PDZK1 deficiency in BM-derived cells.....	123
Supplementary Figure 2.6: Quantification of plaque area and necrotic core area in a subgroup of LDLR ^{-/-} mice transplanted with WT and PDZK1 ^{-/-} BM.....	125
Supplementary Figure 2.7: LDLR ^{-/-} mice transplanted with WT and PDZK ^{-/-} BM showed similar levels of ER stress in plaque macrophages.	127
Supplementary Figure 2.8: LDLR ^{-/-} mice transplanted with PDZK1 ^{-/-} BM and WT BM showed similar levels of cell proliferation in aortic sinus atherosclerotic plaques..	129
Supplementary Figure 2.9: LDLR ^{-/-} mice transplanted with PDZK1 ^{-/-} and WT BM showed similar numbers of recruited monocytes into aortic sinus atherosclerotic plaques.	131
Supplementary Figure 2.10: PDZK1 deficiency did not affect M1 macrophage polarization.	133
Figure 3.1: HDL protected macrophages from tunicamycin-induced apoptosis.	149

Figure 3.2: Bim ^{-/-} macrophages showed reduced sensitivity to tunicamycin-induced apoptosis.	151
Figure 3.3: HDL reduced Bim protein, but not mRNA level in cultured macrophages. .	153
Figure 3.4: Effect of apoA-I deficiency on lipid and systemic inflammation in LDLR ^{-/-} mice.	157
Figure 3.5: ApoA-I ^{-/-} /LDLR ^{-/-} mice fed high-fat diet for 10 weeks developed more atherosclerosis with bigger necrotic cores than LDLR ^{-/-} mice.	159
Figure 3.6: Knocking out Bim in BM reduced atherosclerosis and plaque necrosis in apoA-I ^{-/-} /LDLR ^{-/-} mice.	163
Figure 3.7: Blood leukocyte population in apoA-I ^{-/-} /LDLR ^{-/-} mice transplanted with WT or Bim ^{-/-} BM.	165
Figure 3.8: Body and spleen weights of apoA-I ^{-/-} /LDLR ^{-/-} mice transplanted with WT or Bim ^{-/-} BM.	167
Figure 3.9: Reduced plasma lipids in the apoA-I ^{-/-} /LDLR ^{-/-} mice transplanted with Bim ^{-/-} BM.	169
Figure 4.1 Effects of rosuvastatin on plasma cholesterol in SR-B1 ^{-/-} /apoE ^{-/-} mice.	194
Figure 4.2: Treatment of SR-B1 ^{-/-} /apoE ^{-/-} mice mice with rosuvastatin reduced atherosclerosis development in the aortic sinus and coronary arteries.	199
Figure 4.3: Rosuvastatin treatment reduced CD41 immunostaining in coronary arteries of SR-B1 ^{-/-} /apoE ^{-/-} mice.	201
Figure 4.4: Rosuvastatin treatment attenuated myocardial fibrosis and cardiomegaly in SR-B1 ^{-/-} /apoE ^{-/-} mice.	203

Figure 4.5: Effects of rosuvastatin on SAA and oxLDL in SR-B1 ^{-/-} /apoE ^{-/-} mice.	206
Figure 4.6: Effects of rosuvastatin on scavenger receptor expression and foam cell formation in macrophages.....	210
Figure 5.1: The working model of SR-B1-mediated HDL anti-apoptotic signaling pathway in macrophages.....	220

LIST OF ABBREVIATIONS

ABCA1	ATP-binding Cassette Transporter A1
ABCG1	ATP-binding Cassette Transporter G1
ACAT	Acetyl-Coenzyme A Acetyltransferase
ADMA	Asymmetric Dimethylarginine
AIF	Apoptosis-inducing Factor
Apaf-1	Apoptotic Protease Activating Factor 1
Apo	Apolipoprotein
APOBEC-1	Apolipoprotein B mRNA Editing Catalytic Polypeptide-1
ATF	Activating Transcription Factor
BCR	Breakpoint Cluster Region Kinase
BH	Bcl-2 Homology
BM	Bone Marrow
BMT	Bone Marrow Transplantation
BOP	BH3 Domain-only Protein
CAD	Caspase Activated DNase
CD	Cluster of differentiation
CE	Cholesteryl Ester
CHD	Coronary Heart Disease
CHOP	CCAAT Enhancer Binding Protein Homologous Protein

COX-2	Cyclooxygenase Type 2
DAPI	4',6-Diamidino-2-Phenylindole Dihydrochloride
DDAH	Dimethylarginine Dimethylaminohydrolase
DFF40	DNA Fragmentation Factor 40
DIABLO	Direct Inhibitor of Apoptosis Protein Binding Protein with Low Isoelectric Point
ECL	Enhanced Chemiluminescence
ERK1/2	Extracellular signal-regulated kinases 1/2
eNOS	Endothelial Nitric Oxide Synthase
ER	Endoplasmic Reticulum
FADD	Fas-associated Death Domain
FasL	FAS Ligand
FBS	Fetal Bovine Serum
FC	Free Cholesterol
FPLC	Fast Protein Liquid Chromatography
GM-CSF	Granulocyte Macrophage Colony Stimulating Factor
GRP	Glucose Regulatory Protein
HDL	High Density Lipoprotein
HL	Hepatic Lipase
HRP	Horseradish Peroxidase
HUVEC	Human Umbilical Vein Endothelial Cell

i.p.	intraperitoneally
IAP	Inhibitor of Apoptosis Protein
ICAM-1	Intercellular Adhesion Molecule-1
IDL	Intermediate Low Density Lipoprotein
IL	Interleukin
iNOS	Inducible Nitric Oxide Synthase
IRE1	Inositol-requiring Enzyme 1
KO	Knockout
LCAT	Lecithin/Cholesterol Acyltransferase
LDL	Low Density Lipoprotein
LDLR	Low Density Lipoprotein Receptor
LPS	Lipopolysaccharide
LRP	Low Density Lipoprotein Receptor Related Protein
MCP-1	Monocyte Chemoattractant Protein-1
MCSF	Macrophage Colony Stimulating Factor
MCV	Mean Cell Volume
MPM	Mouse Peritoneal Macrophage
NADPH	Nicotinamide Adenine Dinucleotide Phosphate
NCLPDS	Newborn Calf Lipoprotein Deficient Serum
NCS	Newborn Calf Serum
NO	Nitric Oxide

NUC70	Endonuclease-70kD
OxLDL	Oxidized Low Density Lipoprotein
OxPL	Oxidized Phospholipid
PBA	4-Phenyl Butyric Acid
PBS	Phosphate Buffered Saline
PDGF	Platelet-derived Growth Factor
PDZK1	(Postsynaptic Density Protein/Drosophila Disc-large Protein/ Zonula Occludens Protein) PDZ-containing 1
PERK	Protein Kinase RNA-like Endoplasmic Reticulum Kinase
PGI2	Prostaglandin I2
PMA	Phorbol-12-Myristate-13-Acetate
PP2A	Protein Phosphatase 2A
RCT	Reverse Cholesterol Transport
RDW	Red Blood Cell Distribution Width
ROS	Reactive Oxygen Species
S1P	Sphingosine 1-phosphate
S1PR	Sphingosine 1-phosphate Receptor
SAA	Serum Amyloid A
SERCA	Sarco/Endoplasmic Reticulum Ca ²⁺ ATPase
Smac	Second Mitochondria-derived Activator of Caspase

SMC	Smooth Muscle Cell
SOCS	Suppressor of Cytokine Signalling
SPC	Sphingosylphosphorylcholine
SR-B1	Scavenger Receptor Class B type 1
SRA	Scavenger Receptor Class A
SREBP-2	Sterol Regulatory Element-binding Protein-2
STAT	Signal Transducer and Activator of Transcription
SUV	Small Unilamellar Vesicle
TGF	Transforming Growth Factor
tKO	Triple Knockout
TLR	Toll-like Receptor
TNF	Tumor Necrosis Factor
TRAIL-R	Tumor Necrosis Factor Related Apoptosis Inducing Ligand Receptor
TRAM	(TIR Domain Containing Adaptor Protein Inducing Interferon)
	TRIF
	Related Adaptor Molecule
TRIF	TIR Domain Containing Adaptor Protein Inducing Interferon
TUDCA	Tauroursodeoxycholic Acid
TUNEL	Terminal Deoxynucleotidyl Transferase dUTP Nick End Labeling

UC	Unesterified Cholesterol
UPR	Unfolded Protein Response
VCAM-1	Vascular Cell Adhesion Molecule-1
VLDL	Very Low Density Lipoprotein
WT	Wild Type

CHAPTER I: GENERAL INTRODUCTION

PREFACE

The major content of section 1.5 of this chapter is adapted from a review article entitled ‘Mouse Models of Coronary Artery Atherosclerosis’ by Leticia Gonzalez, Pei Yu and Bernardo Trigatti. At the time of writing of this thesis, this manuscript was in press in the *Journal of Cardiovascular Disorders*. The complete reference is: Gonzalez L, Yu P and Trigatti BL. Mouse Models of Coronary Artery Atherosclerosis. *J Cardiovasc Disord.* 2016; 3(1): 1021. © Austin Publishing Group.

1.1 Atherosclerosis

According to the recent report from the American Heart Association, the mortality of cardiovascular disease declined 30.8 % from 2001 to 2011 due to the increased use of evidence-based medical therapies (Mozaffarian et al., 2015). However, it still accounted for 31.3 % of all deaths in the U.S (Mozaffarian et al., 2015). Coronary heart disease, which culminates with fatal myocardial infarction, is the largest contributor (375,295 deaths; 47.7 %) of cardiovascular disease deaths (Mozaffarian et al., 2015).

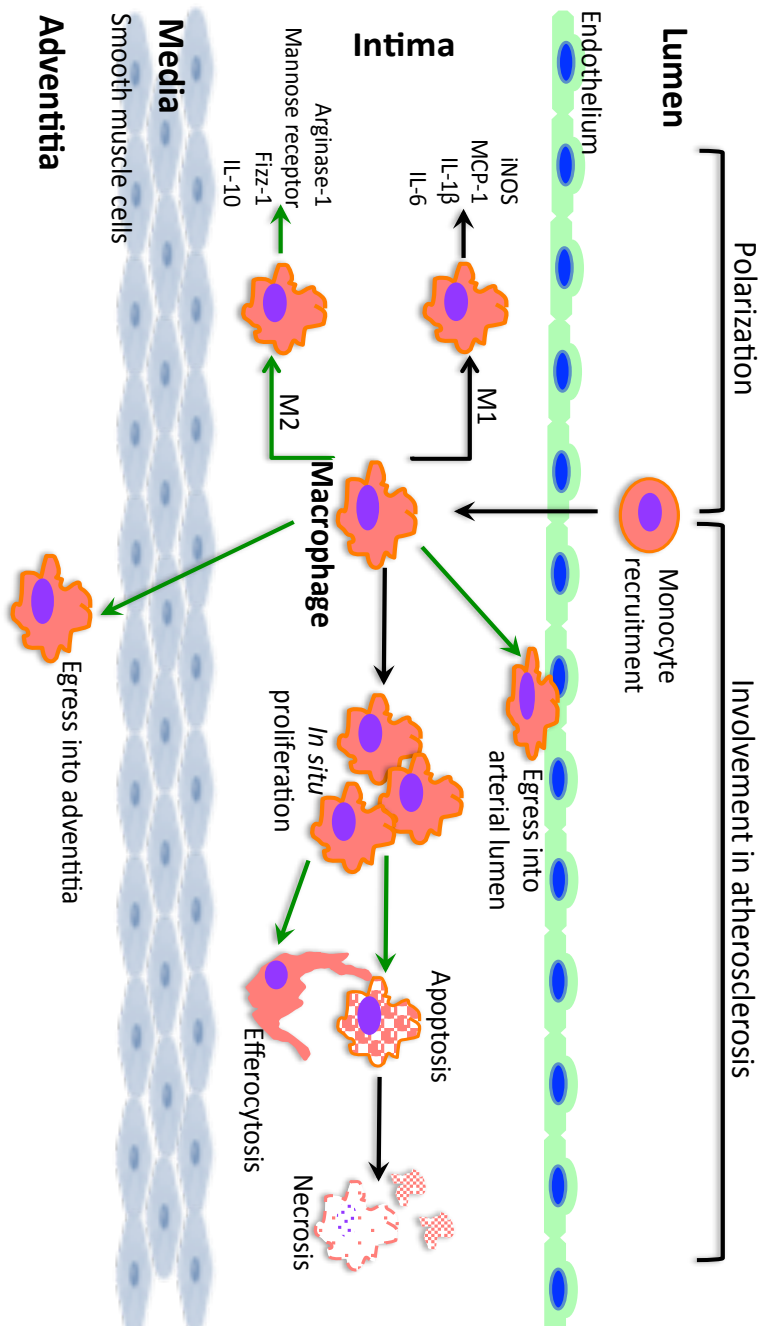
Atherosclerosis is the pathological process underlying coronary heart disease, occurring in the subendothelium in large- and medium- sized arteries. As the guardian of the vascular wall, endothelium is a nonadhesive and nonthrombogenic interface separating blood from the underlying vascular tissues. The endothelium produces various vaso-regulatory molecules, such as nitric oxide (NO), endothelin and angiotensin II, to maintain vascular homeostasis (Davignon and Ganz, 2004). However, the risk factors of atherosclerosis, such as hypercholesterolemia, smoking and certain inflammatory mediators (*e.g.* tumor necrosis factor (TNF)- α and interleukin (IL)-1 β), disrupt this homeostasis and lead to endothelial dysfunction and activation, which is the earliest sign of atherosclerosis (Davignon and Ganz, 2004). The consequences of endothelial dysfunction are: (1) the passive deposition of atherogenic lipoproteins, such as low-density lipoprotein (LDL), in the sub subendothelial spaces of the arterial wall and oxidative modification of LDL by various mechanisms (Daugherty et al., 1994; Yla-Herttuala et al., 1991); (2) overexpression of adhesion molecules on the endothelial

cells, such as selectins, vascular cell adhesion molecule 1 (VCAM-1/CD106) and intercellular adhesion molecule 1 (ICAM-1/CD54) (Springer, 1994). E-selectin (CD62E) is an endothelial-specific adhesion molecule important in the tethering and attachment of leukocytes to vascular endothelial cells. ICAM-1 and VCAM-1 are members of the immunoglobulin-like superfamily and involved in the firm adhesion of leukocytes to the endothelium (Moore et al., 2013; Springer, 1994).

Atherosclerosis is known as a chronic inflammatory disease, due to the involvement of inflammatory cells, such as neutrophils, monocytes and macrophages. Circulating monocytes first roll along the endothelial surface by interacting with endothelial selectins via glycoprotein ligands (Galkina and Ley, 2007; McNeill et al., 2010; Moore et al., 2013). Then, firm adhesion occurs through VCAM-1 and ICAM-1 interacting with monocyte integrin β_2 (CD11b/CD18) and integrin β_1 (CD49d/CD29) (Galkina and Ley, 2007; McNeill et al., 2010; Moore et al., 2013). As shown in Figure 1.1, monocytes migrate into the vessel wall in response to monocyte chemoattractant protein-1 (MCP-1) secreted by activated endothelium. In the subendothelium, monocytes differentiate into macrophages in response to macrophage colony stimulating factor (MCSF) and take up modified lipoproteins via scavenger receptors, such as scavenger receptor class A (SRA) and CD36 (Kzhyshkowska et al., 2012). This causes the accumulation of intracellular lipids, and gives macrophages a foamy appearance, at which stage the macrophages are also called foam cells. Recently, there has been increasing interest in the heterogeneity of macrophages in atherosclerotic plaques, particularly pro-inflammatory M1 and anti-inflammatory M2 macrophages, which are

differentiated under the stimulation of Th1- and Th2-derived cytokines, respectively (Chinetti-Gbaguidi et al., 2015). A great number of *in vitro* studies explored the gene expression patterns characterizing different subsets of macrophages (reviewed in (Chinetti-Gbaguidi et al., 2015)). Even though, the *in vivo* activation stimuli and definitive markers are not clearly demonstrated yet (Chinetti-Gbaguidi et al., 2015; Johnson and Newby, 2009), de Winther and colleagues showed that macrophages with M1 markers were predominant in the rupture-prone shoulder region of human atherosclerotic lesion (Stoger et al., 2012). On the contrary, M2 marker staining was pronounced in the adventitia (Stoger et al., 2012).

Figure 1.1: Macrophages in atherosclerotic plaques. This diagram shows the longitudinal section of arterial wall: lumen (top), intima, media and adventitia (bottom). Monocytes migrate through the endothelial monolayer into the intima and differentiate into macrophages. The polarization of macrophages (M1, M2 and cell markers) is shown on the left; the involvement of macrophages in atherosclerotic plaque development is on the right. The black arrows suggest pro-atherosclerotic effects (*e.g.* M1 polarization), whereas green arrows are anti-atherosclerotic (*e.g.* M2 polarization). Macrophages can migrate out of the plaque into either arterial lumen or adventitia to promote plaque regression, or accumulate or even proliferate to accelerate atherosclerosis. Under the influence of intracellular and extracellular stressors, macrophages undergo apoptosis, which is thought to be anti-atherosclerotic, because (1) apoptotic macrophages secrete anti-inflammatory cytokines; (2) they can attract other macrophages for efferocytosis, and thereby limit plaque size. However, the uncleared apoptotic macrophages developed to the final stage—necrosis, which is pro-inflammatory and pro-thrombotic.



Macrophages are the major cell type in atherosclerotic plaques (Figure 1.1). The number of macrophages in the plaque is determined by monocyte recruitment in the early stages of atherosclerosis, and by macrophage *in situ* proliferation in the advanced stages (Robbins et al., 2013). In contrast, under certain circumstances, the migration of macrophages out of the atherosclerotic lesions into the arterial lumen or through the media into the adventitial lymphatics may help reduce the plaque burden, contributing to plaque regression (Moore et al., 2013). However, the net egress of macrophages decreases with the development of atherosclerosis, leading to the retention of lipid-loaded macrophages in the plaques (Moore et al., 2013). The macrophages that accumulate in the lipid-rich, oxidative and pro-inflammatory plaques eventually undergo apoptosis induced by either the intrinsic pathway or the death-ligand-induced extrinsic pathway. It has been shown that macrophages represent the majority of apoptotic cells in human atherosclerotic lesions (Kolodgie et al., 2000). Apoptosis limits plaque expansion in the early stage of atherosclerosis, since apoptotic macrophages release cytokine or molecules serving as ‘find me’ or ‘eat me’ signals to attract phagocytes for clearance (Van Vre et al., 2012). The clearance of apoptotic cells by phagocytes is referred to as efferocytosis (Van Vre et al., 2012). It has been proposed that at the advanced stages of atherosclerosis development, impaired efferocytosis leads to the accumulation of apoptotic macrophages which become necrotic and contribute to necrotic core formation (Van Vre et al., 2012). The necrotic core size is prominent in determining plaque instability. It has been widely accepted that the stable plaques, which have small necrotic core and thick fibrous cap, are likely to be clinically silent for

decades (van der Wal and Becker, 1999). In contrast, the vulnerable plaque is characterized by big necrotic core and thin fibrous cap (van der Wal and Becker, 1999). These plaques are prone to undergo erosion and rupture and release thrombosis-initiator tissue factor, leading to occlusive thrombosis overlying the ruptured plaque in the coronary arteries, which is the pathologic base of myocardial infarction (van der Wal and Becker, 1999).

1.2. High-density lipoprotein (HDL)

A number of prospective clinical studies have established a strong inverse relationship between plasma HDL cholesterol level and the risk of coronary artery disease (Castelli et al., 1986; Emerging Risk Factors et al., 2009; Gordon and Rifkind, 1989; Gordon et al., 1977; Sharrett et al., 2001). Compared to other lipoproteins, HDL, with a mean size of 7.6-10.6 nm and density of 1.063-1.21 g/ml, is relatively small, dense, and rich in proteins (Blanche et al., 1981). HDLs are highly heterogeneous, consisting of several subpopulations varying in shape, density, size and composition. HDLs were separated into two subclasses by ultracentrifugation: the less dense HDL₂ (1.063-1.125 g/ml) and the more dense HDL₃ (1.125-1.21 g/ml) (De Lalla and Gofman, 1954). HDL₂ and HDL₃ can be further fractionated by non-denaturing polyacrylamide gradient gel electrophoresis into HDL_{3c}, 7.2-7.8 nm diameter; HDL_{3b}, 7.8-8.2 nm; HDL_{3a}, 8.2-8.8 nm; HDL_{2a}, 8.8-9.7 nm; and HDL_{2b}, 9.7-12.0 nm (Blanche et al., 1981). On the basis of surface charge and shape, agarose gel electrophoresis separates HDLs into α - and pre β -migrating particles, which represent the lipid-rich and lipid-poor HDLs,

respectively (Schaefer and Asztalos, 2007). Agarose gel and non-denaturing gradient gel electrophoresis can also be combined into a 2-dimensional electrophoresis that separates HDLs according to charge in the first run and size in the second run, followed by immunoblotting for apolipoprotein (apoA)-I, the major apolipoprotein of HDL. This method identifies up to 12 groups of apoA-I containing HDL particles: pre β (pre β 1 and pre β 2), α (α 1, α 2 and α 3) and pre α (pre α 1, pre α 2, pre α 3 and pre α 4) (Asztalos et al., 2000; Schaefer and Asztalos, 2007). Moreover, according to the apolipoprotein components, HDL can be separated into particles containing both apoA-I and apoA-II (LpAI:LpA-II) or particles containing only apoA-I (LpA-I) (Fruchart et al., 1993).

Even among the high-dose statin-treated coronary heart disease patients, whose LDL cholesterol had been reduced to < 70 mg/dL, the high-HDL subgroup had a lower risk of cardiovascular events than the low-HDL subgroup (Barter et al., 2007). Protective effects of HDL against atherosclerosis were also consistently seen in animal models by administering native HDL or by overexpressing apoA-I (Badimon et al., 1990; Badimon et al., 1989; Paszty et al., 1994; Plump et al., 1994; Rubin et al., 1991). The close correlation between plasma HDL and cardiovascular health is traditionally attributed to HDL-mediated reverse cholesterol transport (RCT), in which HDL particles shuttle cholesterol from peripheral tissue to liver (Al-Jarallah and Trigatti, 2010; Assmann and Nofer, 2003). Increasing number of studies, mainly *in vitro* or animal studies, have also postulated the pleiotropic atheroprotective effects of HDL in addition to RCT, such as anti-inflammatory, anti-oxidative and anti-thrombotic properties (Navab et al., 2011). However, the Mendelian randomization study on the causal relationship

between plasma HDL level and myocardial infarction showed that the genetic mechanism that raised plasma HDL did not reduce the risk of myocardial infarction (Voight et al., 2012). This suggests that the function or quality of HDL particles should be regarded as a parameter of importance. This chapter mainly highlights recent basic scientific studies on HDL-initiated intracellular signaling in the vascular cells related to the development of atherosclerosis, which are considered as the pleiotropic effects of HDL beyond its classical role in transporting and reducing cholesterol accumulation in peripheral tissue (*e.g.* arterial wall). The effective HDL components serving as the ligands and their corresponding receptors expressed on vascular cells will be briefly summarized. Then, the signaling pathways and consequent atheroprotective effects of HDL in each vascular cell type will be reviewed, followed by a diagram of the working model for HDL signaling at the end of each section. Also, some atherogenic mouse models lacking HDL's receptor protein scavenger receptor class B type 1 (SR-B1) will be discussed. At the end, the general research objectives for each chapter will be listed.

1.3. The initiation of HDL signaling pathways

Similar to other lipoproteins, each HDL particle consists of a hydrophobic core, containing triglycerides and cholesterol esters, surrounded by a hydrophilic shell of proteins, phospholipids and free cholesterol (FC). Proteomics and lipidomics showed that over 85 proteins and 200 lipids have been identified in HDL particle and that the list continues to grow (Kontush et al., 2013; Shah et al., 2013). However, the effects of the individual component on atherosclerosis have not been fully understood. This section

will introduce the proteins and lipids in HDL particles that initiate HDL signaling and the function of their corresponding receptors expressed on vascular cells.

1.3.1 ApoA-I and ATP-binding cassette transporter A1 (ABCA1)

ApoA-I is the major structural protein of human and mouse HDL, and accounts for approximately 70 % of total HDL protein. ApoA-I is synthesized by and secreted from the liver and small intestine, and circulates in blood with the secondary structure containing amphipathic α -helices, allowing the spontaneous interaction with lipids (Fitch, 1977; Frank and Marcel, 2000; Zannis et al., 2006). ABCA1, a ubiquitous protein that belongs to the ABC family of transporters, is expressed abundantly in various tissues and interacts with apoA-I, leading to the transfer of cellular phospholipids and cholesterol to lipid-poor apoA-I. In this way, the lipid-poor apoA-I is gradually lipidated and converted to discoidal particles enriched in FC (Rosenson et al., 2012). Plasma Lecithin/Cholesterol acyltransferase (LCAT), synthesized and released by the liver, is assembled into the discoidal HDL particle and activated by apoA-I (Rosenson et al., 2012). LCAT catalyzes the transfer of the 2-acyl group of lethin or phosphatidylethanolamine to FC, generating cholesteryl ester (CE), which forms a neutral lipid core, and converts the discoidal HDL to mature spherical HDL (Rosenson et al., 2012; Zannis et al., 2006). Cholesterol efflux can also be promoted by apoA-I mutations (e.g. apoA-I_{Milano} and apoA-I_{Paris}) or by apoA-I mimetic peptides, which resemble the amphipathic helices in apoA-I (Bielicki and Oda, 2002; Hovingh et al., 2010; Reddy et al., 2014; Stoekenbroek et al., 2015). The first apoA-I mimetic peptide

18A was synthesized in 1985 by Anantharamaiah *et al* (Anantharamaiah *et al.*, 1985). Subsequently, by increasing the number of phenylalanine (F) residues, more optimized apoA-I mimetic peptides with increased lipid binding affinity were generated, such as 2F, 3F, 4F, 5F, 6F, 7F (Hovingh *et al.*, 2010). The modified apoA-I mimetic peptides were also synthesized, such as FAMP (without phospholipids) and ETC-642 (complexed with sphingomyelin and phosphocholine) (Di Bartolo *et al.*, 2011a; Di Bartolo *et al.*, 2011b; Uehara *et al.*, 2013). It has been shown that these recombinant apoA-I or mimetic peptides exerted anti-atherosclerotic effects in human and animal models (Hovingh *et al.*, 2010; Reddy *et al.*, 2014; Stoekenbroek *et al.*, 2015; Uehara *et al.*, 2013; Zhang *et al.*, 2010b).

1.3.2 Mature HDL and ATP-binding cassette transporter G1 (ABCG1)

The lipidated apoA-I or small HDL particles can further accept cholesterol via another ABC transporter ABCG1. Unlike ABCA1, ABCG1 only promotes cholesterol efflux to HDL, but not to lipid-free apoA-I (Phillips, 2014). The cholesterol efflux via ABCG1, which is dependent on the aqueous diffusion pathway, does not require the binding of HDL to the receptor (Phillips, 2014). Additionally, ABCG1 promotes the efflux of 7-ketocholesterol from macrophages, which acquire this oxysterol from oxidized low-density lipoprotein (oxLDL) (Terasaka *et al.*, 2007). Also, ABCG1 not only delivers cholesterol to HDL particles, but also to other acceptors (*e.g.* cyclodextrin), which is likely to be the reason why some of HDL's effects on vascular

cells, such as inhibition of NF- κ B activation in endothelial cells, can be mimicked by incubating cells with cyclodextrin (Cheng et al., 2012).

The cholesterol transport from cells to apoA-I or small HDL particles via ABCA1/ABCG1 is not only the first step of RCT, but also the key mechanism of HDL biogenesis. Thus, the deficiency of either ABCA1 or ABCG1 causes low circulating HDL *in vivo* (McNeish et al., 2000; Oram, 2000; Wiersma et al., 2009). Most importantly, the alteration of lipid content in the cell membrane during cholesterol efflux has also been regarded as the trigger of many intracellular signaling pathways (Prosser et al., 2012).

1.3.3 HDL and SR-B1

SR-B1 is an integral membrane protein that belongs to the CD36 superfamily of scavenger receptor proteins and is encoded by the *Scarb1* gene,. It is a heavily glycosylated protein located in the plasma membrane with N- and C-terminal cytoplasmic domains, 2 transmembrane domains and a large central extracellular domain (Krieger, 2001). In 1996, Krieger and colleagues identified SR-B1 as an HDL receptor highly expressed in the liver and steroidogenic tissues. It mediates cholesterol uptake into cells by selectively transferring CE from an HDL particle into the cell without the degradation of the HDL particle itself (Acton et al., 1996). Consequently, the knockout of SR-B1 in wild type (WT) or apoE^{-/-} mice resulted in a remarkable disruption in HDL metabolism, including reduced lipid storage in steroidogenic tissues, elevated plasma HDL cholesterol and enlarged HDL particles (Rigotti et al., 1997; Trigatti et al., 1999).

On the other hand, SR-B1 expressed in COS cells also mediates the efflux of cellular FC to HDL (Phillips, 2014). However, the physiological role of SR-B1 in mediating cholesterol efflux from macrophages is still unclear (Yancey et al., 2007; Zhang et al., 2003). In spite of this, our and others' research has consistently shown that deletion of SR-B1 in bone marrow derived cells increased atherosclerosis in atherogenic mouse models (Covey et al., 2003; Tao et al., 2015; Zhang et al., 2003). This may indicate the atheroprotective effects of SR-B1 in macrophages are independent of cholesterol efflux.

1.3.4 Sphingosine 1-phosphate (S1P), apoM and S1P receptors (S1PR)

S1P is a bioactive sphingolipid metabolite, modulating multiple cell functions, such as cell proliferation, differentiation and migration (Hla, 2003; Olivera and Spiegel, 1993; Paik et al., 2001). Over 60 % S1P in the plasma is bound to HDL particles, with the remainder bound to albumin (Murata et al., 2000). Recent publications suggest apoM as an important carrier of S1P on HDL particles, and a determinant of plasma concentration of S1P (Christoffersen et al., 2011; Liu et al., 2014). S1P functions through G-protein-coupled receptors S1PR1-5 in the plasma membrane (Moolenaar and Hla, 2012). Though widely expressed, S1P receptors showed tissue-specific preferences, as S1PR1-3 are abundantly expressed in vascular tissues, whereas S1PR4 and 5 are mainly detected in immune cells and in the nervous system (Blaho and Hla, 2014). HDL/apoM-bound S1P, but not albumin-S1P (Galvani et al., 2015), has been found to be protective to vascular cells (Argraves and Argraves, 2007; Christoffersen et al., 2011; Kimura et al., 2003; Okajima et al., 2009), and low S1P levels have been

reported in patients with coronary artery disease and myocardial infarction (Argraves et al., 2011; Karuna et al., 2011; Sattler et al., 2010).

1.4. Atheroprotective effects of HDL in vascular cells

1.4.1 Myeloid cells

Inhibition of hematopoietic cell proliferation

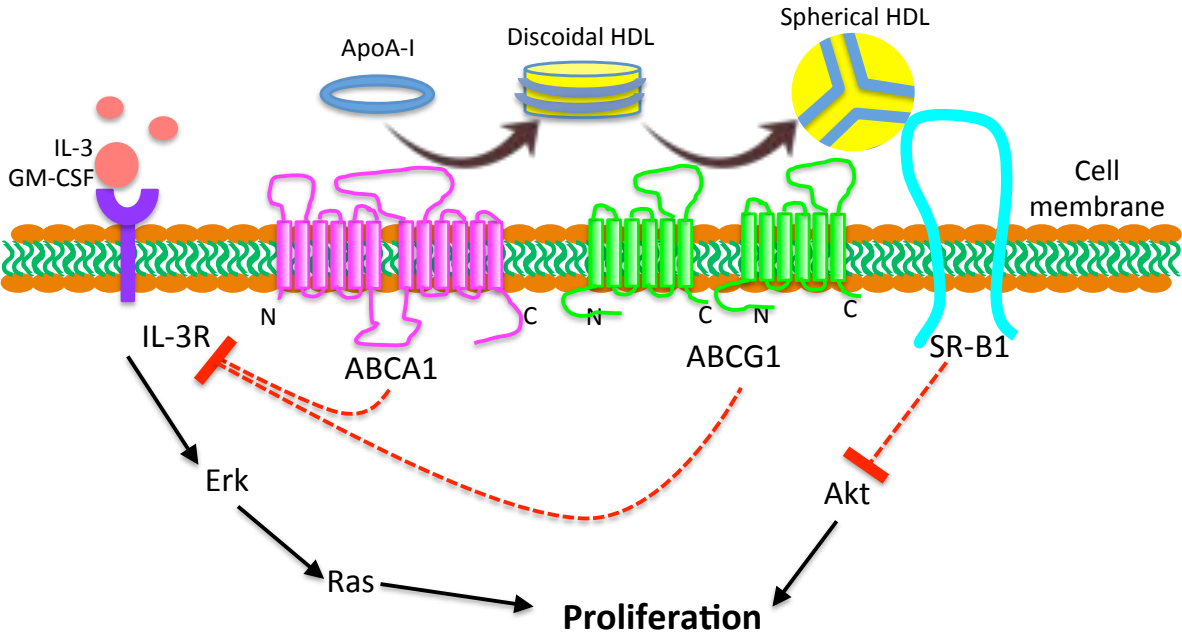
A number of clinical studies have established a direct relationship between white blood cell count and the morbidity and mortality of cardiovascular disease (Lee et al., 2001; Sweetnam et al., 1997). In particular, neutrophilia and monocytosis are closely correlated with atherosclerotic lesion development in mouse models. Disruption of CXC ligand-receptor interaction in apoE^{-/-} mice caused neutrophilia and increased neutrophil recruitment into plaques, associated with enlarged atherosclerotic lesion area (Zernecke et al., 2008). Similarly, LDLR^{-/-} or apoE^{-/-} mice with MCSF deficiency exhibited gene dose-dependent reduction in circulating monocytes, as well as significant decrease in plaque size (Qiao et al., 1997; Rajavashisth et al., 1998; Smith et al., 1995).

There is evidence suggesting that HDL may regulate myeloid cell proliferation, providing potential mechanisms for leukocytosis-associated atherosclerosis development. For example, in children with familial hypercholesterolemia, the level of HDL cholesterol was inversely related with monocyte count (Tolani et al., 2013). Also, in animal models, apoA-I^{+/-}LDLR^{-/-} mice, which have reduced HDL, showed increased monocyte and neutrophil counts, compared to LDLR^{-/-} mice (Tolani et al., 2013). Moreover, transplantation of ABCA1^{-/-}/ABCG1^{-/-} bone marrow increased myeloid cell

counts and accelerated atherosclerosis in LDLR^{-/-} (Yvan-Charvet et al., 2007) and LDLR^{+/-} (Yvan-Charvet et al., 2010a) mice. The underlying mechanism may involve the alteration of plasma membrane cholesterol content due to the deficiency of ABC transporters, followed by the upregulation of IL-3 receptor β unit, which activates ERK1/2 and Ras signaling, and increases cell sensitivity to proliferative molecules IL-3 and granulocyte macrophage colony stimulating factor (GM-CSF) (Figure 1.2) (Yvan-Charvet et al., 2010a). However, infusion of human apoA-I or reconstituted HDL into C57BL/6 mice effectively inhibited hematopoietic cell proliferation (Feng et al., 2012). Similarly, overexpression of apoA-I in the ABC transporter deficient BM-transplanted LDLR^{+/-} mice completely reversed the expansion of leukocytes and the enlargement of plaques in proximal aorta (Yvan-Charvet et al., 2010a). So, it is conceivable that the normal expression of ABC transporters guarantees the sufficiency of circulating HDL. However, myeloid stem cell proliferation suppressed by HDL may be independent of ABCA1 or ABCG1. Our lab found increased circulating monocytes and lymphocytes in SR-B1^{-/-}/LDLR^{-/-} mice when fed high fat high cholesterol diet, compared to LDLR^{-/-} mice (Fuller et al., 2014a). This was supported by the research done by Feng *et al.* showing that HDL receptor SR-B1, which was also highly expressed on hematopoietic stem and progenitor cells, was required by apoA-I/HDL-mediated modulation of leukocyte count (Feng et al., 2012; Gao et al., 2014). Their research also showed an inhibition of Akt phosphorylation by apoA-I in SR-B1 containing, but not in SR-B1^{-/-} hematopoietic cells (Figure 1.2). The expansion of SR-B1^{-/-} hematopoietic cells was significantly dampened by treating them with Akt phosphorylation inhibitor, suggesting

that Akt is the downstream factor of SR-B1 mediated signaling pathway in inhibiting the proliferation of hematopoietic stem and progenitor cells (Gao et al., 2014). However, it is still unclear why SR-B1 inhibits Akt activation in hematopoietic cells, whereas in other cells SR-B1 mediates HDL-dependent activation of Akt (Al-Jarallah et al., 2014; Mineo et al., 2003; Zhang et al., 2007).

Figure 1.2: The effect of HDL on inhibiting hematopoietic cell proliferation. ApoA-I is lipidated, and turns into discoidal HDL and spherical HDL via cholesterol efflux from ABCA1 and ABCG1. The diagrams of ABCA1 and ABCG1 are adapted from the topographic models proposed by Oram *et al.* (Oram and Vaughan, 2006). The apoA-I double-belt in discoidal HDL and trefoil in spherical HDL were derived from the apoA-I structural model raised by Silva *et al.* (Silva et al., 2008). The cholesterol content alteration in plasma membrane due to ABC transporter mediated cholesterol efflux inhibits the expression of IL-3 receptor, which in combination with IL-3 or GM-CSF activates ERK/Ras pathway, leading to cell proliferation. On the other hand, HDL also suppresses hematopoietic cell proliferation via SR-B1, which inhibits Akt phosphorylation.



Inhibition of leukocyte differentiation and activation

Besides hematopoietic cell proliferation, HDL also regulates the differentiation and activation of leukocytes. The proliferation of hematopoietic stem cells has been shown to occur in the splenic red pulp, which is the reservoir providing Ly-6C^{high} monocyte subset (Robbins et al., 2012). Compared to Ly-6C^{low} monocytes that patrol along the endothelium and produce anti-inflammatory cytokines against infection, Ly-6C^{high} monocytes are prone to adhere to and penetrate through the activated endothelium, and give rise to macrophages in atherosclerotic plaques (Moore et al., 2013; Swirski et al., 2007). HDL suppresses the differentiation of Ly-6C^{high} monocytes. Decreased percentage of myeloid progenitor cells from C57BL/6 mice differentiated to Ly-6C^{high} monocytes when incubated in the presence of HDL (Feng et al., 2012). In line with this is the *in vivo* study showing that chow-fed ABCA1^{-/-}ABCG1^{-/-} mice exhibited significantly more Ly-6C^{high} monocytes than C57BL/6 mice, and hypercholesterolemia induced by high-fat diet further stimulated the expansion of Ly-6C^{high} cells in these double knockout mice, but not in WT mice (Yvan-Charvet et al., 2010a). SR-B1 is also directly or indirectly involved in the differentiation of monocytes *in vivo*. Recent publication by our lab showed that knockout of SR-B1 significantly increased the proportion of circulating Ly-6C^{high} monocytes in the LDLR^{-/-} mice fed high-fat high-cholesterol cholate-containing diet (Fuller et al., 2014a). However, due to the alteration of HDL particles (*e.g.* increased HDL particle size and increased ratio of FC to CE) (Braun et al., 2003; Trigatti et al., 1999) in SR-B1 deficient mice, it is unclear if the

increase in inflammatory monocytes is a result of the disruption of HDL signaling due to the absence of SR-B1 or due to the altered HDL composition or function.

Neutrophils contribute to atherosclerotic lesion development by producing reactive oxygen species (Drechsler et al., 2010; Mazor et al., 2008). It has been shown that neutrophil activation was stimulated in hypercholesterolemia, and characterized by increased expression of CD11b (Drechsler et al., 2010; Mazor et al., 2008). Murphy *et al.* demonstrated the role of apoA-I/HDL on reducing CD11b expression in human neutrophils, and specified that the effects of lipid-free apoA-I and HDL were mediated by ABCA1 and SR-B1, respectively (Murphy et al., 2011). The physiological role of monocyte CD11b is to mediate monocyte adhesion. CD11b and CD49d are the receptors of ICAM-1 and VCAM-1, respectively (Galkina and Ley, 2007; McNeill et al., 2010; Moore et al., 2013). Murphy *et al.* reported that HDL inhibited PMA-induced CD11b expression in human monocytes in a dose-dependent manner (Murphy et al., 2008). This is mainly due to the apoA-I/ABCA1 mediated cholesterol efflux, leading to the reduction of lipid rafts in cell membrane (Murphy et al., 2008). Similarly, apoA-I or the apoA-I mimetic peptide 4F decreased both CD49d and CD11b expression in monocyte-derived macrophages (Smythies et al., 2010). Consequently, the adhesion of these macrophages to lipopolysaccharide (LPS)-activated human umbilical vein endothelial cells (HUVEC) was reduced by about 50 % (Smythies et al., 2010). Moreover, Pei *et al.* in our lab observed significantly increased abilities of monocytes from SR-B1 deficient mice to bind to ICAM-1 and VCAM-1 *in vitro*, compared to blood monocytes harvested from SR-B1 expressing mice (Pei et al., 2013). Consistent with

this, SR-B1^{-/-}/apoE^{hypomorphic} mice transplanted with SR-B1 containing bone marrow showed decreased monocyte recruitment into atherosclerotic plaques in the aortic sinus, compared to SR-B1^{-/-}/apoE^{hypomorphic} mice transplanted with autologous bone marrow (Pei et al., 2013). This suggests a potential mechanism of HDL-regulated adhesion molecule expression via SR-B1.

1.4.2 Endothelial cells

Inhibition of inflammation

HDL has been shown to inhibit TNF- α or IL-1 induced expression of VCAM-1, ICAM-1 and E-selectin in HUVECs, at the levels of both cell surface expression and steady state mRNA (Cockerill et al., 1995). The ability of HDL to reduce endothelial cell adhesion molecule expression has also been studied *in vivo*. Infusion of reconstituted HDL suppressed IL-1 induced E-selectin expression in the intradermal vessels from a porcine model of acute inflammation (Cockerill et al., 2001). In another study, apoE^{-/-} mice with carotid peri-arterial collars showed reduced VCAM-1 expression and monocyte infiltration after infused with reconstituted HDL containing apoA-I and phosphatidylcholine (Dimayuga et al., 1999). Moreover, infusion of the apoA-I mimetic peptide, ETC-642, also reduced the adhesion molecules expressed in rabbit thoracic aorta and carotid artery (Di Bartolo et al., 2011a; Di Bartolo et al., 2011b). As to a specific mechanism, many inflammatory cytokine-related genes are regulated by the transcription factors belonging to the NF- κ B family, which can be activated by TNF- α or IL-1 (Collins et al., 1995; de Martin et al., 1993; Read et al.,

1995; Read et al., 1994). However, the effect of HDL on NF- κ B translocation is controversial. Cockerill *et al.* found that HDL inhibited adhesion molecule expression without affecting the nuclear translocation or DNA binding of NF- κ B (Cockerill et al., 1999). On the contrary, reductions in TNF- α induced expression of MCP-1 and the NF- κ B p65 subunit were observed in reconstituted HDL and apoA-I mimetic peptide treated rabbits (Di Bartolo et al., 2011a). Schmidt *et al.* also observed a reduction of TNF- α induced NF- κ B translocation following PI3K-Akt pathway activation in the endothelial cells treated with HDL associated lysosphingolipids, sphingosylphosphorylcholine (SPC) or lysosulfatide (Schmidt et al., 2006). As shown in Figure 1.3, the upstream portions of the PI3K/Akt signaling pathway may involve, not only the binding of S1P to the S1P1 receptor (Kimura et al., 2006b), but also SR-B1 and its adapter PDZK1 (Kimura et al., 2006a), which have all been shown to play roles in inhibiting TNF- α induced adhesion molecule expression by HDL in cultured endothelial cells. In addition, the PI3K/Akt pathway mediated anti-inflammatory effects by HDL were partially dependent on another S1P receptor, S1PR3 (Nofer et al., 2003). Recently, our lab reported increased expression of ICAM-1 and VCAM-1 on the coronary arterial endothelium in SR-B1 deficient LDLR^{-/-} mice, compared to SR-B1 expressing LDL^{-/-} mice, suggesting the possible involvement of SR-B1 signaling pathway in regulating adhesion molecule expression *in vivo* (Fuller et al., 2014a). HDL particles also carry microRNAs, among which miR-223 is highly related to inflammation (Tabet et al., 2014). It has been demonstrated that the anti-inflammatory property of HDL can be

attributed in part to its ability to transfer miR-223 to endothelial cells to target and inhibit ICAM-1 mRNA (Tabet et al., 2014).

Activation of endothelial nitric oxide synthase (eNOS)

Another hallmark of endothelial dysfunction is the impaired endothelium-dependent vasodilation mediated by NO. NO not only regulates vascular tone, but also prevents platelet activation and smooth muscle cell proliferation (Mineo and Shaul, 2012b). NO is generated from the conversion of L-arginine to L-citrulline, which is catalyzed by eNOS in endothelial cells (Davignon and Ganz, 2004; Mineo and Shaul, 2012b). eNOS is anchored in caveolae on the endothelial cell membrane by N-terminal myristoylation and palmitoylation, and inactivated by binding with caveolin-1 and -3, the major proteins of caveolae (Davignon and Ganz, 2004; Garcia-Cardena et al., 1997; Ju et al., 1997; Mineo and Shaul, 2012b). Caveolin inhibits eNOS via interacting with calmodulin; the physiological activation of eNOS involves the binding of Ca^{2+} to calmodulin, leading to the dissociation of calmodulin from caveolin (Davignon and Ganz, 2004; Michel et al., 1997; Mineo and Shaul, 2012b). The localization of eNOS to caveolae is necessary for the production of NO. It has been shown that oxLDL altered the cholesterol environment in caveolae via the scavenger receptor CD36, leading to the displacement of eNOS from cell membrane, and thereby inhibiting eNOS activation (Blair et al., 1999; Uittenbogaard et al., 2000). However, co-incubation of cells with HDL maintained the cholesterol homeostasis in caveolae and prevented the redistribution of eNOS induced by oxLDL (Uittenbogaard et al., 2000). Also, anti-SR-

B1 IgG, which blocked the binding of HDL to SR-B1, completely prevented HDL from reversing the effect of oxLDL, suggesting that SR-B1 mediates the effects of HDL on cholesterol environment and eNOS localization in caveolae (Uittenbogaard et al., 2000). More notably, HDL also directly activates eNOS via SR-B1, and this process requires the binding of apoA-I, but not apoA-II, to SR-B1 (Assanasen et al., 2005; Yuhanna et al., 2001). Interestingly, small unilamellar vesicles (SUV) also has been shown to activate eNOS via wild type SR-B1. However, a mutant form of SR-B1, which could not transport cholesterol to SUV, only mediated eNOS activation by HDL, but not by SUV (Assanasen et al., 2005). This suggests that SR-B1 mediated eNOS activation via transporting cholesterol to HDL. In terms of specific domains of SR-B1 involved, this study using a series of chimeric mutants of SR-B1 showed that the C-terminal transmembrane domain is indispensable for HDL signaling (Assanasen et al., 2005). Moreover, it was also shown by using photoactive cholesterol that membrane cholesterol binds directly to the C-terminal transmembrane domain of SR-B1 (Assanasen et al., 2005). These findings may indicate the C-terminal transmembrane of SR-B1 acts as a cholesterol sensor in the caveolae. This study also compared the functions of SR-B1 and the SR-B1 mutant form SR-B1 Δ 509, which lacks the last amino acid in the C-terminal cytoplasmic domain of SR-B1, and found that, unlike SR-B1, SR-B1 Δ 509 could not mediate the HDL-initiated signal transduction (Assanasen et al., 2005). It has been demonstrated that the intact C-terminus of SR-B1 is required to interact with the PDZ domain-containing protein PDZK1 (Ikemoto et al., 2000; Silver, 2002). PDZK1, which is expressed in endothelium, is required for HDL-initiated activation of eNOS in

cultured endothelial cells (Zhu et al., 2008). Interestingly, PDZK1 does not regulate SR-B1 expression/localization, or HDL-SR-B1 binding, or SR-B1-mediated cholesterol efflux (Zhu et al., 2008). However, PDZK1 is required for HDL and SR-B1 to induce Src activation, which leads to the parallel activation of PI3K/Akt and MAPK and the subsequent phosphorylation of eNOS at Ser-1177 (Fulton et al., 1999; Mineo et al., 2003; Zhu et al., 2008).

In addition, it was also shown that S1P activated eNOS via the G_i-protein-coupled receptors S1PR1 (Wilkerson et al., 2012) and S1PR3 (Nofer et al., 2004), followed by the activation of PI3K/Akt pathway in human endothelial cells, as shown in Figure 1.4.

A novel mechanism of HDL-dependent NO production was reported in 2011, involving the dimethylarginine dimethylaminohydrolase (DDAH)/asymmetric dimethylarginine (ADMA) pathway (Peng et al., 2011). DDAH hydrolyzes ADMA, an endogenous competitive eNOS inhibitor, to L-citrulline and dimethylamine, thereby increasing NO production (Peng et al., 2011). Incubation of HUVECs with oxLDL significantly decreased DDAH activity, but increased ADMA levels, which were, however, reversed by pretreatment with HDL (Peng et al., 2011). Thus, the effect of HDL on the DDAH/ADMA pathway may also contribute to the activation of eNOS.

Stimulation of endothelial cell migration

A number of endothelial functions promoting endothelial monolayer integrity, such as migration, proliferation and survival, are critically associated with NO

production (DeMeester et al., 1998; Murohara et al., 1999; Napoli et al., 2013). Interestingly, HDL has been shown to stimulate endothelial cell migration independently of NO activation (Seetharam et al., 2006). The potential mechanisms were shown in Figure 1.4. Similar to the eNOS activation, HDL-induced endothelial migration also requires the expression of SR-B1 and PDZK1 and the activation of PI3K and MAPK pathways (Seetharam et al., 2006; Wu et al., 2015; Zhu et al., 2008). Additionally, HDL causes SR-B1-dependent Rac activation and lamellipodia formation, which is required for cell migration (Seetharam et al., 2006). Moreover, HDL-induced cell migration was mimicked by incubating cells with S1P, which bond to S1PR1 and S1PR3 and activated PI3K and Rho kinase (Kimura et al., 2003). In concert with the *in vitro* findings, apoA-I^{-/-}, SR-B1^{-/-} and PDZK1^{-/-} mice exhibited impaired re-endothelialization in the carotid arteries after perivascular electric injury (Seetharam et al., 2006; Zhu et al., 2008).

Apoptotic pathways

Morphologically, Apoptosis is characterized cytoplasmic and nuclear shrinkage, chromatin condensation, followed by plasma membrane blebbing and nuclear fragmentation (Saraste and Pulkki, 2000). Eventually, the plasma membrane starts extending and budding. The detached apoptotic bodies containing intact organelles and portions of the nucleus, are rapidly recognized and engulfed by neighboring cells (Saraste and Pulkki, 2000). Since apoptosis typically does not induce inflammation or tissue damage, it plays a role in cell turnover during embryogenesis and in normal tissue homeostasis (Renehan et al., 2001). The clearance of apoptotic cells prevents apoptosis

progress to post-apoptosis, or necrosis. During necrosis, cytoplasm and organelles are irreversibly swollen, and the plasma membrane loses integrity, leading to the release of cellular pro-inflammatory constituents and inflammatory response in surrounding tissue (Zong and Thompson, 2006).

Apoptosis can be induced via extrinsic or intrinsic pathways. The extrinsic, also called the death receptor-mediated, pathway is triggered by the ligation of death receptors and their corresponding ligand. The best-characterized death receptors include Fas, TNF related apoptosis inducing ligand receptor 1 (TRAIL-R1) and TRAIL-R2 (Guicciardi and Gores, 2009). The association of death receptors with their corresponding ligands, such as Fas ligand (FasL) and TRAIL, results in receptor trimerization, clustering of the receptors' death domains and recruitment of adaptor molecules Fas-associated death domain (FADD) (Guicciardi and Gores, 2009). FADD then recruits and activates initiator caspase-8, which propagates the apoptotic signal by direct cleavage of downstream effector caspases, such as caspase-3 (Guicciardi and Gores, 2009).

A variety of stimuli have been shown to activate the intrinsic pathway, including viral infections (Galluzzi et al., 2008), free radicals (von Harsdorf et al., 1999), radiation (Eliseev et al., 2005), toxins (Bantel et al., 2001; Tesh, 2010), hypoxia (Sawant et al., 2014; Weinmann et al., 2004) and hyperthermia (Shellman et al., 2008). These stimuli converge on mitochondria to induce outer mitochondrial membrane permeabilization (Decaudin et al., 1998; Green and Kroemer, 2004). Endoplasmic reticulum (ER) stress and unfolded protein response (UPR) has been regarded as the mechanism underlying

the activation of the mitochondrial pathway. The ER is the primary site of folding and modification of secreted and membrane-bound proteins, and the efficient functioning of ER is vital for cell survival. Several factors, such as ATP, Ca^{2+} and redox state, are critical for correct protein folding in the ER (Gaut and Hendershot, 1993). The disturbance of these factors results in the accumulation of unfolded and misfolded proteins, which is known as ER stress. To respond to the ER stress, cells activate UPR through three ER transmembrane receptors: Protein kinase RNA-like endoplasmic reticulum kinase (PERK), activating transcription factor (ATF)6 and inositol-requiring enzyme 1 (IRE1) (Basseri and Austin, 2012). In resting cells, all these receptors are maintained in the ER membrane by binding with ER chaperone proteins, such as glucose regulatory protein (GRP)78 and GRP94 (Basseri and Austin, 2012). However, the unfolded proteins accumulated in the ER lumen compete with the three receptors to bind with ER chaperone proteins, leading to the dissociation of ER chaperone proteins from the three receptors and the activation of UPR (Basseri and Austin, 2012). The UPR reduces protein synthesis, promotes protein folding and stimulates unfolded protein degradation, thereby reducing the accumulation of unfolded proteins and restoring normal ER function (Basseri and Austin, 2012; Schroder and Kaufman, 2005). However, if ER stress is persistent and severe, UPR signaling switches from pro-survival to pro-apoptotic by activating CHOP (CCAAT enhancer binding protein homologous protein) (Basseri and Austin, 2012). CHOP deficient embryonic fibroblasts and peritoneal macrophages have been shown to be more resistant to ER stress induced apoptosis than CHOP^{+/+} controls (Thorp et al., 2009; Zinszner et al., 1998). Even though, CHOP^{-/-}

mice were phenotypically normal, and had normal fertility and reproductive behavior (Zinszner et al., 1998), they exhibited significantly reduced cellular apoptosis in the proximal tubule epithelium (Zinszner et al., 1998). Notably, CHOP^{-/-} mice with apoE^{-/-} background showed decreased macrophage apoptosis and smaller necrotic cores in the aortic sinus atherosclerotic lesions, compared to CHOP^{+/+}/apoE^{-/-} mice (Thorp et al., 2009).

Bcl-2 family proteins have been suggested to be critically involved in the intrinsic apoptosis signaling pathway (Brunelle and Letai, 2009). These proteins contain at least one of the four BH domains, and the structural differences contribute to the opposite roles in the regulation of intrinsic apoptosis pathway. The pro-apoptotic multi-domain proteins (Bax and Bak) contain the BH1, BH2 and BH3 domains (Brunelle and Letai, 2009). Bax and Bak are the downstream effectors of the Bcl-2 family regulated apoptosis, which are able to oligomerize and pierce the mitochondrial outer membrane, leading to the release of cytochrome *c* from mitochondrial intermembrane space (Brunelle and Letai, 2009). However, in healthy cells, Bax and Bak are monomers and restrained by the interaction with anti-apoptotic Bcl-2 proteins (Bcl-2, Bcl-X_L, Mcl-1), which typically contain all four BH domains (BH1-BH4) (Brunelle and Letai, 2009). This balance can be disrupted by the third class of Bcl-2 family (Bim, Noxa, Puma, Bid and Bad), a group of pro-apoptotic BH3 domain-only proteins (BOPs). It has been suggesting that BOPs activate Bax and Bak by binding to anti-apoptotic Bcl-2 proteins to replace Bax and Bak or by directly binding to and activating Bax and Bak to form pores on the mitochondrial outer membrane (Brunelle and Letai, 2009). The roles of

BOPs in regulating apoptosis may have implications for the development of therapeutics to interfere with the Bcl-2 protein balance. It has been shown that CHOP suppressed pro-survival Bcl-2 transcription (McCullough et al., 2001), whereas CHOP activation by ER stress upregulated pro-apoptotic Bim expression. Also, overexpression of CHOP led to the translocation of Bax protein from the cytosol to the mitochondria (Oyadomari and Mori, 2004). Furthermore, CHOP activation induced by ER stress was shown to increase the transcription of Bim (Puthalakath et al., 2007).

The impaired integrity of the mitochondrial outer membrane causes the release of the pro-apoptotic factors, such as cytochrome c, apoptosis-inducing factor (AIF), Smac (second mitochondria-derived activator of caspase)/DIABLO (direct inhibitor of apoptosis protein (IAP)-binding protein with low isoelectric point), Omi/HtrA2 or endonuclease G from the mitochondrial inter-membrane space (Cande et al., 2002; Saelens et al., 2004). Cytochrome c released into the cytosol binds to the c-terminal region of apoptotic protease activating factor 1 (Apaf-1) and initiates caspase-9 activation (Jiang and Wang, 2004). Cytochrome c/APAF-1/caspase-9 form a complex, called apoptosome, and triggers executioner caspase-3 activation, whereas Smac/DIABLO and Omi/HtrA2 promote caspase activation by antagonizing the IAPs (Jiang and Wang, 2004). Caspase-3 then cleaves substrates, such as DNA fragmentation factor 40 (DFF40), caspase activated DNase (CAD) and endonuclease-70kD (NUC70), in the cytosol to mediate the double-stranded DNA fragmentation, the hallmarks of apoptosis (Enari et al., 1998; Sakahira et al., 1998; Urbano et al., 1998). Interplays between the extrinsic and the intrinsic pathways also play a role. The activation of

caspase-8 in the death receptor pathway may result in the cleavage of Bid, a BH3 domain only Bcl-2 family protein, which translocates to mitochondria upon activation to release cytochrome c, thereby initiating the mitochondria-dependent apoptotic pathway (Cory and Adams, 2002).

HDL-dependent protection against endothelial apoptosis

HDL has been demonstrated to protect endothelial cells from apoptosis (Mineo and Shaul, 2007; Nofer et al., 2001; Seetharam et al., 2006; Suc et al., 1997; Sugano et al., 2000), and it is to some degree dependent on NO production (Kwon et al., 2001). Many risk factors promoting atherosclerosis were shown to induce endothelial cell apoptosis *in vitro*, including oxLDL, angiotensin II, reactive oxygen species (ROS), TNF- α and high glucose (Baumgartner-Parzer et al., 1995; Dimmeler et al., 2002; Dimmeler et al., 1997; Suc et al., 1997; Sugano et al., 2000). However, HDL or apoA-I was consistently shown to protect endothelial cells from apoptosis induced by oxLDL (Suc et al., 1997), TNF- α (Sugano et al., 2000) or growth factor deprivation (Nofer et al., 2001). It was also reported that HDL induced PI3K/Akt activation and time-dependent phosphorylation of pro-apoptotic Bcl-2 protein Bad, leading to the dissociation of Bad from Bcl-X_L (Nofer et al., 2001) (Figure 1.4). The availability of Bcl-X_L allows it to neutralize Bax and Bak, which tend to oligomerize in and penetrate the outer membrane of mitochondria, leading to the mitochondria-dependent or intrinsic apoptotic pathway (Brunelle and Letai, 2009). Consistent with this, HDL inhibits a number of cell events characteristic of the activation of mitochondria-dependent

apoptosis, including increased cytoplasm Ca^{2+} concentration, mitochondrial transmembrane potential dissipation, cytochrome c release and caspase-3 and -9 activation (Nofer et al., 2001; Suc et al., 1997). In addition, S1P was also shown to mimic HDL's anti-apoptotic effect. However, unlike migration, which was stimulated by S1P via both S1PR1 and S1PR3, S1P protected HUVECs from serum-starvation induced apoptosis in a S1PR1, but not S1PR3, dependent manner (Kimura et al., 2003).

Figure 1.3: ER stress and UPR activation. The ER mediates the folding and post-translational modification (such as glycosylation) of secreted and transmembrane proteins. It is also a storage site for calcium ions, which are transported by the SERCA (sarco/endoplasmic reticulum Ca^{2+} -ATPase) in the ER membrane. Chemicals, such as tunicamycin and thapsigargin, which inhibit protein glycosylation or SERCA activation, cause the accumulation of unfolded or misfolded proteins in the ER cavity, called ER stress. GRP78, an ER chaperone protein that binds the ER transmembrane proteins PERK, IRE1 and ATF6 keeping them inactive, dissociates upon the accumulation of unfolded proteins, to help in protein folding. This dissociation leads to the homodimerization and autophosphorylation of PERK and IRE1, and the Golgi-translocation and proteolytic processing of ATF6, releasing a nuclear form that acts as a transcription factor (ATF6N). The activation of these pathways is known as the UPR, which aims to relieve ER stress by suppressing protein synthesis, upregulating ER chaperone protein expression and increasing ER-associated protein degradation (ERAD). However, under certain circumstances, ER stress can also induce apoptosis, which is dependent on PERK phosphorylation and mediated by the activation of CHOP.

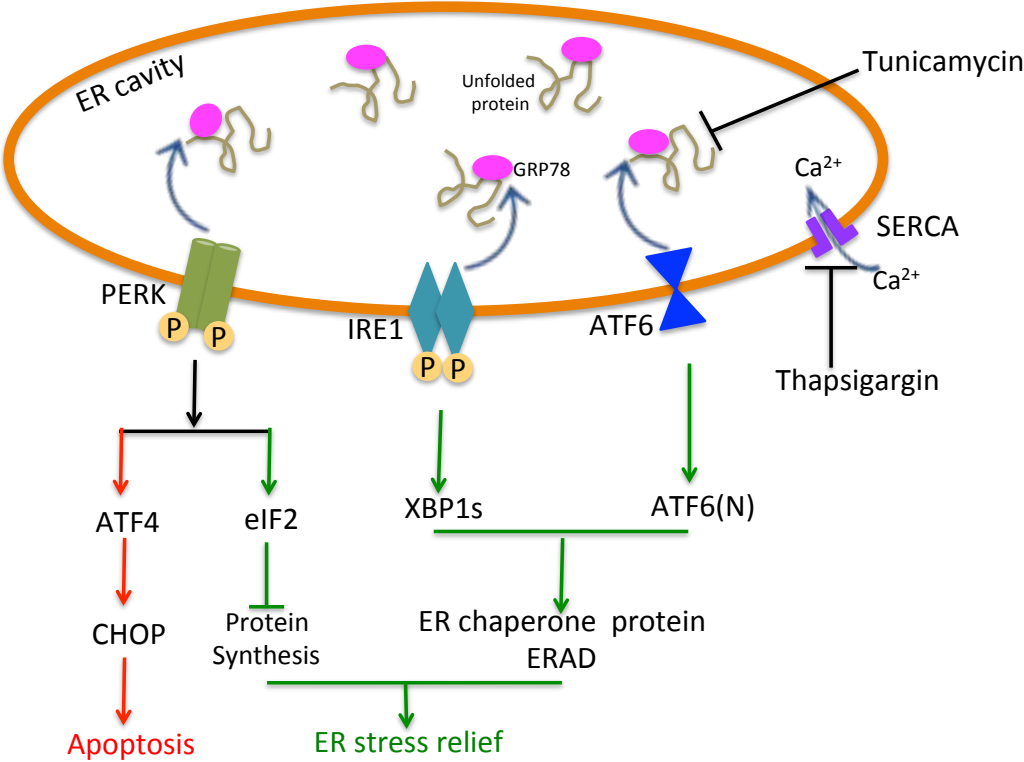
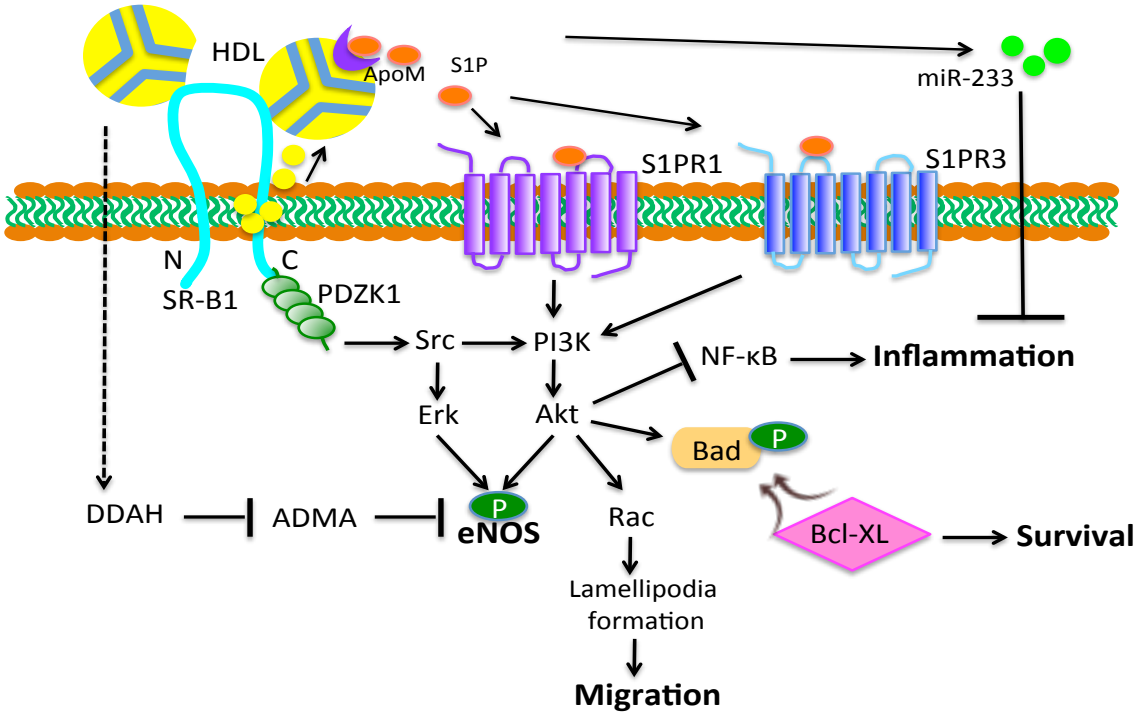


Figure 1.4: The signaling pathways of HDL in endothelial cells. There is a great overlap in HDL-initiated eNOS activation, cell migration, cell survival and anti-inflammatory signaling pathways. The C-terminal transmembrane domain of SR-B1 serves as a cholesterol sensor, and the C-terminal cytoplasmic domain binds to the adapter protein PDZK1. Both domains are required for the SR-B1-mediated HDL signaling. HDL also functions by carrying S1P to S1PR1 and S1PR3. The activation of eNOS depends on Src activation, followed by the parallel activation of both PI3K/Akt and MAPK pathways. HDL also activates eNOS via the DDAH/ADMA pathway, though the receptor-mediated this pathway is unclear. PI3K/Akt activation is commonly shared by all the pathways. It not only inhibits NF- κ B regulated inflammatory molecule expression, but also stimulates Rac-mediated endothelial cell migration. PI3K/Akt also phosphorylate Bcl-2 related protein Bad, leading to its dissociation from Bcl-X_L, which promotes cell survival. HDL also delivers miR-233 into endothelial cells to antagonize the mRNA of inflammatory molecules.



1.4.3 Macrophages

Induction of M2 polarization

HDL enhanced the polarization of M2 macrophages both *in vitro* and in atherosclerotic plaques. As summarized in Figure 1.5, Sanson *et al.* showed the ability of HDL to suppress iNOS, IL-6 and TNF- α (M1 markers) in IFN- γ untreated and treated bone marrow-derived macrophages, and to increase the transcripts of Arginase-1 and Fizz-1 (M2 markers) at both baseline and IL-4 stimulated levels by activating the signal transducer and activator of transcription (STAT)6 signaling pathway (Sanson *et al.*, 2013). They reported that HDL induced STAT6 phosphorylation via JAK1 and JAK2, unlike IL-4, which induces STAT6 phosphorylation via JAK1 and JAK3 (Sanson *et al.*, 2013). On the other hand, LPS induces M1 related genes through TLR4 signaling, involving activation of TRIF (TIR domain containing adaptor protein inducing interferon) and TRAM (TRIF related adaptor molecule) signaling. HDL inhibits LPS induced activation of TRIF and TRAM dependent signaling, independently of altering intracellular cholesterol content in macrophages (Suzuki *et al.*, 2010). On the contrary, the expression of M2 markers (mannose receptor, CD163, IL-10, IL1-RA, PPAR γ) in macrophages derived from human peripheral blood monocytes are not significantly increased by co-incubating with HDL (Colin *et al.*, 2014). This discrepancy may be due to the differences in species or cell culture conditions. However, the overall effects of HDL in mice appear to facilitate M2 polarization. For example, atherosclerotic aortic arches from apoE^{-/-} mice were transplanted to apoA-I expressing or apoA-I deficient mice. Compared to the apoA-I expressing mice, which had high levels of plasma HDL,

apoA-I^{-/-} mice with low HDL exhibited impaired plaque regression with reduced percentage of M2 macrophages within plaques (Feig et al., 2011). In another study, injection of native apoA-I into apoE^{-/-} mice resulted in a significant reduction in M1, but an increase in M2 macrophages in advanced atherosclerotic plaques (Hewing et al., 2014). Also, the plaques exhibited decreased lipid content and macrophage accumulation, but increased collagen content (Hewing et al., 2014). These findings suggest the role of macrophage polarization on plaque size and structure. The effects of HDL on macrophage polarization can be partially explained by the activity of S1P. Park *et al.* found that incubation of mouse peritoneal macrophages with S1P significantly inhibited LPS-induced M1 polarization, but restored LPS-inhibited M2 marker expression (Park et al., 2014). Consistent with the effect of HDL, they also found a concentration-dependent increase of STAT6 phosphorylation by incubating macrophages with S1P, which was followed by the upregulation of the suppressor of cytokine signaling (SOCS)1 and the suppression of SOCS3 (Park et al., 2014). However, S1P's effects, including SOCS1 activation, SOCS3 inhibition and Arginase-1 production, were completely blocked by adding an anti-IL-4 blocking antibody into the cell culture media (Park et al., 2014), suggesting the involvement of the IL-4 signaling pathway in the S1P induced M2 polarization. The effects of S1P were also confirmed *in vivo*, using a synthetic S1P analogue FTY720. LDLR^{-/-} mice administrated with FTY720 showed reduced LPS-elicited Nitrite/Nitrate and IL-6 (M1 markers), but increased IL-4-induced IL-1 receptor antagonist (M2 marker) in peritoneal macrophages (Nofer et al., 2007). Similar to the effects of HDL on plaque size, FTY720 reduced both

necrotic core size and atherosclerotic lesion size in the aortic root and brachiocephalic artery of LDLR^{-/-} mice (Nofer et al., 2007).

Stimulation of macrophage migration

The retention of lipid-loaded macrophages (foam cells) in atherosclerotic plaques is likely attributed to the impaired ability of emigration (Llodra et al., 2004), due to cholesterol accumulation in the cell membrane (Nagao et al., 2007; Qin et al., 2006). It has been shown that elevating membrane cholesterol led to the misregulation of Rho GTPase, including the activation of Rac1 and the inhibition of RhoA, and consequently affected cytoskeletal organization and macrophage migration (Nagao et al., 2007; Qin et al., 2006). However, infusion of recombinant apoA-I_{Milano} resulted in a significant decrease of atherosclerotic plaque volume in the patients with acute coronary syndromes (Nissen et al., 2003). Paralleling the human studies, apoE^{-/-} mice on high-cholesterol diet exhibited reduced plaque size and macrophage accumulation in the plaques 48 hours after single infusion of recombinant apoA-I_{Milano} (Shah et al., 2001). The role of HDL in atherosclerotic plaque regression is also supported by transplantation of the atherosclerotic thoracic aortic segments from apoE^{-/-} mice to the apoE^{-/-} mice with apoA-I transgene, which resulted in reduced macrophage content (>80%) in the transplanted plaques, compared to the autologous aorta transplantation (Rong et al., 2001). These findings suggest the impact of macrophage egress on plaque size and the effect of HDL on stimulating macrophage migration. A recent publication by Al-Jarallah *et al.* from our lab explored the mechanism by which HDL-induced macrophage migration, and

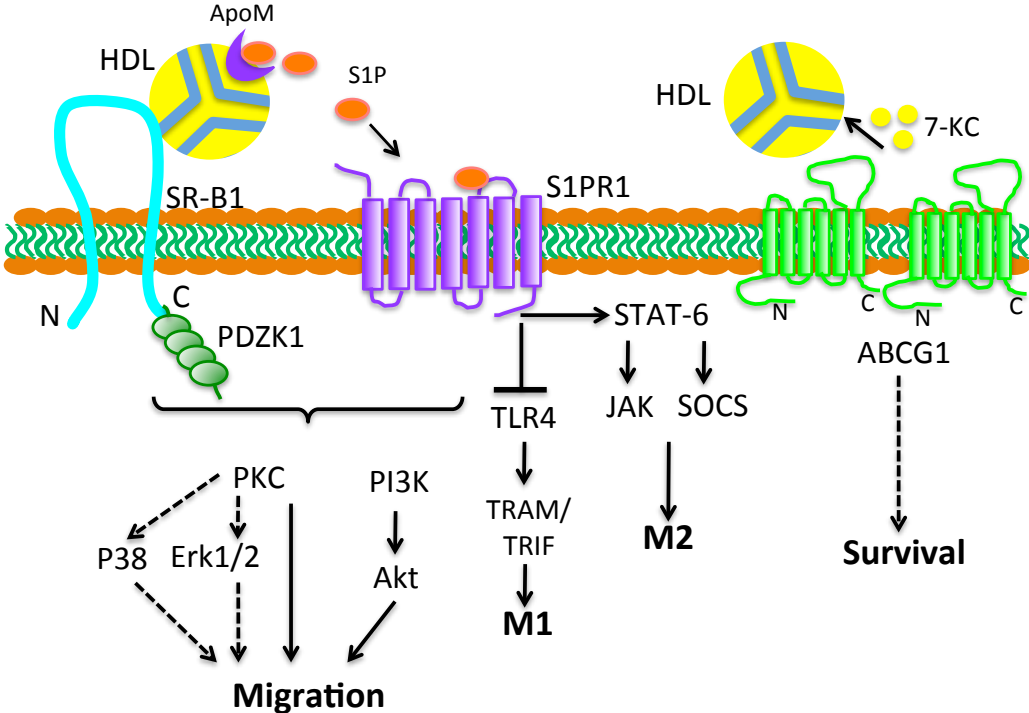
demonstrated that the SR-B1/PDZK1 pathway and the S1P/S1PR1 pathway were both required (Al-Jarallah et al., 2014) (Figure 1.5). The activation of the S1P/S1PR1 pathway can be inhibited by interrupting HDL binding to SR-B1 or blocking SR-B1-mediated cholesterol transport (Al-Jarallah et al., 2014). They also showed that the downstream signaling involved PI3K/Akt1, Rho kinase, PKC, p38 MAPK and ERK1/2 pathways (Al-Jarallah et al., 2014).

Inhibition of macrophage apoptosis

In advanced atherosclerotic plaques, foam cells accumulating in plaques eventually are thought to undergo apoptosis as a result of a variety of factors including oxidative and ER stress (Seimon and Tabas, 2009). Macrophage apoptosis can be induced by treating cells with oxLDL (Heinloth et al., 2002; Muller et al., 2001) or loading them with FC (Devries-Seimon et al., 2005; Yao and Tabas, 2001), and can be inhibited by co-incubating with HDL (Baldan et al., 2006; Terasaka et al., 2007; Yvan-Charvet et al., 2010b; Yvan-Charvet et al., 2007). *In vitro*, ABCG1^{-/-} or ABCA1^{-/-} ABCG1^{-/-} macrophages had increased sensitivity to oxLDL- or oxidized phospholipid (oxPL)-induced apoptosis (Baldan et al., 2006; Terasaka et al., 2007; Yvan-Charvet et al., 2010b; Yvan-Charvet et al., 2007). The protection against oxLDL-induced apoptosis was as reported to be dependent on ABCG1-mediated 7-ketocholesterol efflux from macrophages to HDL (Terasaka et al., 2007) (Figure 1.5). Consistent with the *in vitro* findings, transplantation of ABCG1^{-/-} bone marrow into LDLR^{-/-} mice led to increased apoptosis in atherosclerotic plaques, compared to the transplantation of WT bone

marrow (Baldan et al., 2006). Ongoing research from our lab showed that HDL also protected macrophages from apoptosis induced by cholesterol loading, OxLDL and ER stress via a pathway involving SR-B1 (Zhang and Al-Jarallah, manuscript in revision). The mechanisms by which HDL mediates protection against macrophage apoptosis induced by ER stress will be further discussed in Chapters 2 and 3. Macrophage apoptosis plays different roles in the development of atherosclerosis: In the early stages of atherosclerosis, macrophage apoptosis reduces plaque burden by decreasing the cellular content within the plaques; in the late stages of atherosclerosis, however, macrophage apoptosis accelerates plaque expansion, due to increased apoptotic cell accumulation and inflammation-induced monocyte recruitment (Gautier et al., 2009).

Figure 1.5: The signaling pathways of HDL in macrophages. HDL stimulates macrophage migration in a SR-B1/PDZK1 and S1p/S1PR1 dependent manner. The downstream signaling pathways are derived from the working model of HDL signaling pathway proposed by Al-Jarallah et al. (Al-Jarallah et al., 2014). HDL-induced macrophage polarization involves the signaling of S1P through S1PR1, which inhibits TLR4-regulated M1 polarization, but enhanced STAT6-mediated M2 polarization. The anti-apoptotic effect of HDL is mediated by ABCG1, which delivers 7-ketocholesterol to HDL.

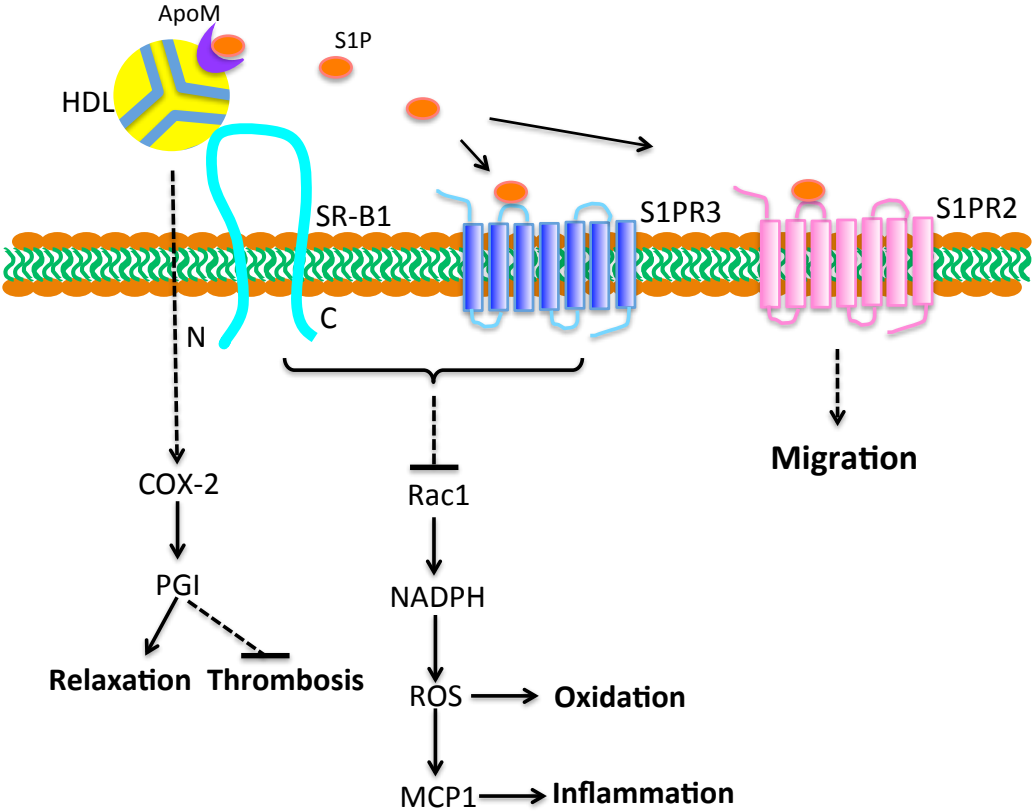


1.4.4 Smooth muscle cells

Vascular smooth muscle cells (SMCs) are involved in all stages of atherosclerosis, even though their functions are still under debate (Dzau et al., 2002). For example, in the early stages of atherosclerosis development, vascular SMCs secrete inflammatory molecules, such as MCP-1 and VCAM to promote atherosclerosis (Dzau et al., 2002). Also, inflammation-induced SMC proliferation and migration are thought to cause neointimal hyperplasia and lumen narrowing (Dzau et al., 2002). However, in the advanced plaques, SMCs not only comprise the fibrous cap, but also secrete collagen fibers to stabilize the plaque (Dzau et al., 2002). As shown in Figure 1.6, HDL regulates the functions of vascular SMCs via multiple pathways. For example, HDL stimulates SMCs to release prostaglandin I₂ (PGI₂) by upregulating cyclooxygenase type 2 (COX-2) expression (Vinals et al., 1997). This is considered to play roles in the regulation of SMC tone and the prevention of thrombosis formation (Vinals et al., 1997). The anti-inflammatory and anti-oxidative effects of HDL were evidenced by the study showing that HDL inhibited the Rac1-dependent activation of NADPH (nicotinamide adenine dinucleotide phosphate) oxidase, the source of ROS in SMCs, and subsequently reduced MCP-1, which was controlled by intracellular oxidative molecules (Tolle et al., 2008). This effect required the participation of S1P and SPC, but not apoA-I, in HDL particles (Tolle et al., 2008). Also, HDL, S1P or SPC failed to inhibit ROS or MCP-1 in the absence of SR-B1 or S1PR3 (Tolle et al., 2008). HDL also inhibited platelet-derived growth factor (PDGF)-induced SMC migration via S1P and S1PR2 interaction (Damirin et al., 2007; Tamama et al., 2005). Interestingly, PDZK1, which facilitates endothelial

cell migration, was shown to negatively regulate vascular SMC proliferation and migration in response to PDGF (Lee et al., 2015). This effect of PDZK1 is independent of SR-B1, but relies on an inhibitory interaction with the breakpoint cluster region kinase (BCR), which binds to the first PDZ domain of PDZK1 with its C-terminal STEV sequence and enhances SMC proliferation in the absence of PDZK1 (Lee et al., 2015). This study showed that PDZK1 regulated vascular cell function independently of SR-B1. Thus, it may indicate an effect of PDZK1 unattached to HDL signaling pathway, or that HDL signals to PDZK1 via other PDZK1-conjugated receptors.

Figure 1.6: The signaling pathways of HDL in SMCs. HDL stimulates PGI secretion in SMCs to regulate SMC tone and inhibit thrombosis formation. In a SR-B1 and S1PR3 dependent manner, HDL inhibits Rac1-stimulated ROS and MCP-1 production. The HDL-induced SMC migration is mediated by S1PR2.



1.5. Mouse models of atherosclerosis

Despite the attractive characteristics of the mouse as a model of atherosclerosis, no inbred strain is known to develop atherosclerotic plaques in the absence of inactivating mutations in one or more genes involved in lipoprotein homeostasis. Mice carry most of their plasma cholesterol in HDL, while in humans the main cholesterol carrier is the LDL class (de Silva et al., 1994). This difference between species might contribute to the protection seen in the mouse against atherosclerosis, since HDL is considered to be protective against coronary heart disease, while high LDL cholesterol is considered as a risk factor (Gordon et al., 1977). In 1985, Paigen and colleagues reported the results of feeding different inbred strains of mice a high fat, high cholesterol diet, containing cholate, in an effort to identify atherosclerosis susceptibility differences between strains (Paigen et al., 1985). The results of the study established that C57BL/6 mice were the most sensitive, whereas C3H mice were the most resistant to diet-induced atherosclerosis development. A gender difference has also been detected under similar conditions, with female mice being more susceptible to plaque development (Paigen et al., 1987). Yet, the atherosclerotic lesions in C57BL/6 mice on the “Paigen diet” arose only in the aortic root and the most proximal aorta and displayed features of early stages of plaque development (Mehrabian et al., 1991; Tangirala et al., 1995). Studies by Liao et al. suggested that the genetic differences in atherosclerosis susceptibility seen in the inbred strains of mice might be a consequence of differences in their inflammatory responses, suggesting the importance of inflammation in atherosclerosis development (Liao et al., 1993). The advent of gene targeting approaches in mice led to the

generation of two widely used mouse models for the study of atherosclerosis: the apoE^{-/-} and LDLR^{-/-} mouse models.

1.5.1 ApoE^{-/-} mouse model

ApoE, encoded by the *ApoE* gene, is a protein present on the surface of very low-density lipoproteins (VLDL), HDL and chylomicrons. A major role of apoE is to mediate binding of apoE-containing lipoproteins to the LDLR and other receptors, serving as a ligand for clearance of these lipoproteins by the liver (Imaizumi, 2011). In 1992, two groups independently reported the generation of and the characteristics of atherosclerosis development in apoE^{-/-} mice (Piedrahita et al., 1992; Plump et al., 1992; Zhang et al., 1992). Since then, several studies have contributed to evidence of its pleiotropic role on atherosclerosis development.

The absence of apoE in mice results in a phenotype resembling human type III hyperlipoproteinemia, with severe hypercholesterolemia due to accumulation of lipoprotein remnants, even on a normal chow diet (Ghiselli et al., 1981). Reports have shown that on a normal chow diet, apoE^{-/-} mice spontaneously develop lesions in the aortic sinus and aortic branches with foam cells appearing as early as 8 weeks of age (Nakashima et al., 1994). High-fat diet feeding accelerated lesion development and led to more advanced lesions similar in complexity to plaques found in humans (Reddick et al., 1994; Zhang et al., 1994). Consistent with the role of apoE in lipoprotein clearance, transgenic mice expressing human apoE2 – an isoform of apoE defective in receptor binding – are characterized by the presence of β -VLDL (chylomicron and VLDL

remnants) and spontaneous atherosclerotic lesions rich in foam cells and displaying small fibrous caps (Sullivan et al., 1998).

Besides the obvious role of apoE on cholesterol distribution among lipoproteins, there are several other effects of apoE that might contribute to its anti-atherogenic properties. It has been demonstrated that apoE expression in macrophages is crucial for atherosclerosis protection. Bone marrow transplantation experiments demonstrated that mice receiving macrophages lacking apoE developed significantly more atherosclerosis without affecting total plasma cholesterol (Fazio et al., 1997; Van Eck et al., 1997). ApoE has also been demonstrated to prevent expression of adhesion molecules in human endothelial cells (Stannard et al., 2001) and to inhibit platelet aggregation through the L-arginine-nitric oxide pathway (Riddell et al., 1997). Effects on modulation of vascular smooth muscle cell migration and proliferation have been reported as well (Swertfeger and Hui, 2001). Finally, apoE has also been shown to exert a wide variety of immunoregulatory effects: regulation of T cell proliferation and activation (Kelly et al., 1994; Zhang et al., 2010a), innate immunity (Roselaar and Daugherty, 1998), sepsis (Kattan et al., 2008) and more recently macrophage polarization (Baitsch et al., 2011).

1.5.2 LDLR^{-/-} mouse model

LDLR is a cell surface receptor that recognizes both apoB on LDL and apoE on different lipoproteins. Once lipoproteins bind the LDLR, the complex is internalized removing cholesterol from circulation (Goldstein and Brown, 1987). Deficiency of LDLR function in humans is the basis of familial hypercholesterolemia (Goldstein and

Brown, 1979). Individuals lacking both copies of the LDLR gene present high levels of LDL cholesterol in circulation and suffer myocardial infarction as early as the first decade of life. In 1993, Ishibashi and colleagues reported the generation of LDLR deficient mice (Ishibashi et al., 1993). Contrary to the phenotype observed in apoE^{-/-} mice, LDLR^{-/-} mice do not develop significant atherosclerosis while fed a normal chow diet. This might be explained by the ability of the LDL receptor related protein (LRP) pathway to clear apoB 48 containing lipoproteins from circulation, such that deletion of LDLR leads only to mild hypercholesterolemia in mice (Ishibashi et al., 1993; Wouters et al., 2005). Nevertheless LDLR^{-/-} mice are very sensitive to diet modifications. When fed high-fat and/or high-cholesterol diets, LDLR^{-/-} mice develop severe hypercholesterolemia and atherosclerotic lesions along much of the aortic tree (Lichtman et al., 1999; Tangirala et al., 1995). As mentioned previously, humans mostly carry cholesterol on apoB100-containing LDL. To generate animal models with plasma lipoproteins more closely resembling those in humans, Davidson and colleagues generated LDLR^{-/-} mice also lacking the apolipoprotein B mRNA editing catalytic polypeptide-1 (APOBEC-1) gene, rendering them able to synthesize only apoB100 (Powell-Braxton et al., 1998), while Hobbs and colleagues generated LDLR^{-/-} mice overexpressing a human apoB100 transgene (Sanan et al., 1998). Each of these mice secretes predominantly apoB100, exhibit elevated levels of circulating cholesterol and develop spontaneous atherosclerosis when fed a normal chow diet (Powell-Braxton et al., 1998; Sanan et al., 1998).

1.5.3 ApoE^{-/-}/LDLR^{-/-} mice

Mice lacking both apoE and the LDLR develop significant hypercholesterolemia and atherosclerosis in both the aorta and in coronary arteries in response to long term high fat diet feeding (Caligiuri et al., 1999). These mice also developed myocardial infarction in response to hypoxia or mental stress, reportedly mediated by the release of endothelin and consequent vasospasm of partially occluded coronary arteries, since it was reduced by treatment with an endothelin receptor A blocker (Caligiuri et al., 1999). In a separate study, Li and colleagues showed that high-fat diet fed ApoE^{-/-}/LDLR^{-/-} mice preconditioned by exposure to either ischemia/reperfusion or hyperoxia presented improved post-ischemic ventricular function and reduced myocardial infarct size (Li et al., 2001).

1.5.4 SR-B1^{-/-}/apoE^{-/-} mice

SR-B1^{-/-} mice were reported to have increased levels of oxidative stress due to a reduction in the circulating levels of HDL-associated antioxidant enzyme paraoxonase-1 (Van Eck et al., 2007). Furthermore, SR-B1 deficiency alters erythrocyte maturation and platelet structure and clearance resulting in the development of anemia and thrombocytopenia (Dole et al., 2008; Holm et al., 2002).

The impact of SR-B1 on atherosclerosis development has also been studied in both knockout and transgenic models. Hepatic overexpression of SR-B1 in heterozygous LDLR^{-/-} mice fed a high fat/cholesterol diet, containing the bile salt sodium cholate, decreased lesion area in the aortic root and cholesterol content in VLDL, LDL and HDL

(Arai et al., 1999). However, protection was not seen in transgenic homozygous LDLR^{-/-} fed a high fat/cholesterol diet (Arai et al., 1999). On the other hand, transient hepatic overexpression of SR-B1 in LDLR^{-/-} mice with early and advanced lesions reduced atherosclerosis (Kozarsky et al., 2000). Reduction in lesion size was correlated with HDL cholesterol levels (Kozarsky et al., 2000). Overexpression of SR-B1 in a human apoB transgenic mouse was shown to be protective against diet-induced fatty streak formation in the aorta as well (Ueda et al., 2000). Krieger and colleagues first reported the effects of complete inactivation of SR-B1 on atherosclerosis (Trigatti et al., 1999). SR-B1^{-/-} mice were crossed with apoE^{-/-} mice to generate SR-B1^{-/-}/apoE^{-/-} mice, which were reported to exhibit substantially increased cholesterol associated with VLDL sized particles and abnormally large HDL like particles (Trigatti et al., 1999). When fed normal chow diets, these mice developed accelerated aortic sinus atherosclerosis at 5 weeks of age, at which age no atherosclerosis was detected in littermate apoE^{-/-} control mice. In a subsequent publication Krieger and colleagues reported that SR-B1^{-/-}/apoE^{-/-} mice fed a normal chow diet developed substantial, occlusive atherosclerosis in coronary arteries as well, and that this was associated with extensive myocardial fibrosis, cardiomegaly, cardiac conductance abnormalities, reduced cardiac function, and mortality of the SR-B1^{-/-}/apoE^{-/-} mice between 5 and 8 weeks of age (50% mortality by 6 weeks of age) (Braun et al., 2002).

The nature of the phenotype observed in SR-B1^{-/-}/apoE^{-/-} mice has been further explored. Lymphocyte-dependent inflammation is known to influence atherosclerosis development, thus Karackattu et al. explored a role for T and B cells on CAD

development (Karackattu et al., 2005). To do so, RAG-2/SR-B1/apoE triple KO (tKO) mice were generated, where the absence of RAG-2 gene expression prevents lymphocyte maturation (Shinkai et al., 1992). No differences in coronary atherosclerosis, myocardial infarction or cardiac dysfunction were found between triple and control SR-B1^{-/-}/apoE^{-/-} mice, indicating that the absence of circulating B and T lymphocytes does not affect the development of coronary atherosclerosis or myocardial infarction, or improve cardiac function in these mice (Karackattu et al., 2005). Hepatic lipase (HL) hydrolyzes triglycerides and phospholipids and it has been suggested that it can influence atherosclerosis, although the mechanism is not clear (Jansen et al., 2002). Deletion of HL in SR-B1^{-/-}/apoE^{-/-} mice significantly delayed the development of atherosclerosis in both the aortic root and coronary arteries despite the increase in total cholesterol (Karackattu et al., 2006). This study also confirmed that in these mice the extent of atherosclerosis in coronary arteries rather than in the aortic root is more closely correlated with cardiac dysfunction and lifespan (Karackattu et al., 2006). Bone marrow transplantation of either wild type or SR-B1^{-/-}/apoE^{-/-} bone marrow into SR-B1^{-/-}/apoE^{-/-} mice significantly reduced serum cholesterol. Transplantation of wild type bone marrow also reduced aortic atherosclerosis and prolonged survival on SR-B1^{-/-}/apoE^{-/-} mice indicating that restoration of macrophage SR-B1 and/or apoE can reduce atherosclerosis in these mice (Yu et al., 2006). In a separate study, microarray mRNA profiling of hearts from SR-B1^{-/-}/apoE^{-/-} mice at different stages of cardiac disease progression revealed a significant increase (80-fold) of apoD in hearts with extensive myocardial infarction (Tsukamoto et al., 2013). Using a model of ischemia/reperfusion-induced

myocardial infarction, Krieger and colleagues showed that apoD could reduce myocardial infarction potentially through its antioxidant activity (Tsukamoto et al., 2013). This, therefore, led to the identification of apoD as a cardioprotective factor that is induced in hearts upon myocardial infarction.

Pharmacological studies have also been performed in the SR-B1^{-/-}/apoE^{-/-} mice to test the effect of drugs of interest on coronary heart disease. Probucol is a potent antioxidant and anti-inflammatory drug reported to prevent atherosclerosis development (Yamashita and Matsuzawa, 2009). Treatment with probucol significantly extended the lifespan of SR-B1^{-/-}/apoE^{-/-} mice (from a mean of 6 to a mean of 36 weeks) and almost completely reversed the cardiac pathology (Braun et al., 2003). From this study it was also possible to conclude that most of the pathological features leading towards premature death arise between 3-5 weeks of age, providing a window where the drug could be administered to alter disease progression (Braun et al., 2003). In a similar study, SR-B1^{-/-}/apoE^{-/-} mice were treated with either ezetimibe (inhibition of intestinal cholesterol absorption) or SC-435 (inhibition of intestinal bile acid absorption) for three weeks (Braun et al., 2008b). Both drugs were capable of significantly reducing cholesterol in the IDL/LDL fraction and extending survival of these mice. Treatment with ezetimibe significantly delayed onset or progression of atherosclerosis in the aortic root and coronary arteries; myocardial fibrosis and cardiomegaly were reduced as well (Braun et al., 2008b). Finally, the effect of pomegranate extract, rich in polyphenolic antioxidants, on coronary artery disease development was tested (Al-Jarallah et al., 2013). Treatment of SR-B1^{-/-}/apoE^{-/-} mice with pomegranate extract reduced levels of

oxidative stress and inflammation in the plaque. Coronary atherosclerosis and myocardial fibrosis were also reduced, even though treatment increased cholesterol in the VLDL fraction (Al-Jarallah et al., 2013). Despite the reduction in atherosclerosis in the aortic root and coronary arteries, survival was not extended in SR-B1^{-/-}/apoE^{-/-} mice receiving pomegranate extract.

1.6. Objectives of the thesis

We have substantial understanding of the mechanisms by which HDL exerts anti-atherosclerotic effects in endothelial cells. However, its roles and signaling pathways in macrophages are not fully investigated. Macrophage accumulation dominantly contributes of the plaque volume (summarized in Figure 1.1). More importantly, macrophage apoptosis is a critical contributor of plaque instability. Consistent with others' findings showing that HDL protected macrophages from oxLDL-induced apoptosis (Baldan et al., 2006; Terasaka et al., 2007; Yvan-Charvet et al., 2010b; Yvan-Charvet et al., 2007), research done Zhang *et al.* in our lab (Zhang and Al-Jarallah, manuscript in revision), as well as my unpublished data (Figure 2.1), showed that HDL also inhibited mouse peritoneal macrophages (MPMs) from endoplasmic reticulum (ER) stress-induced apoptosis in a dose-dependent manner. Paralleling the *in vitro* findings, decreasing circulating HDL by knocking out apoA-I resulted in increased necrotic core sizes in atherosclerotic plaques (Figure 3.5). Despite the ABCG1-mediated anti-apoptotic pathway in macrophages (Figure 1.5), Zhang *et al.* also demonstrated the indispensable role of SR-B1 in HDL-dependent protection of macrophages from

apoptosis (Zhang and Al-Jarallah, manuscript in revision). The second chapter of the thesis is focusing on the downstream signaling factors following SR-B1, especially the role of SR-B1's adapter protein PDZK1. The specific aims of this chapter are: (1) to clarify the effects of plasma lipoproteins (LDL and HDL) on protecting MPMs from apoptosis; (2) to test the effect of HDL on tunicamycin-induced ER stress in macrophages; (3) to further explore this signaling pathway by detecting the activation of Akt; (4) to investigate the role of PDZK1 in protection from macrophage apoptosis, and in the necrotic core formation in atherosclerotic plaques; (5) to test the effect of PDZK1 on M1 and M2 macrophage polarization.

The third chapter is completing the HDL signaling pathway in macrophages by testing the involvement of the pro-apoptotic Bcl-2 family protein, Bim, in ER stress induced apoptosis in macrophages and atherosclerosis development *in vivo*. This chapter mainly investigated on the BH-3 domain only protein Bim, because (1) Bim is highly-expressed in hematopoietic cells; (2) The data from Zhang et al. in our lab showed a time-dependent decrease of Bim protein in macrophages treated with HDL for the first 2 hours (Zhang and Al-Jarallah, manuscript in revision). In this chapter, the role of Bim in HDL signaling pathway was demonstrated by testing the following aims: (1) to analyze the effects of HDL on macrophage Bim at both mRNA and protein levels; (2) to test if Bim^{-/-} macrophages are resistant to apoptosis, even without the protection by HDL; (3) to test the effect of reducing HDL on atherosclerosis and plaque necrosis by characterizing apoA-I^{-/-}/LDLR^{-/-} mice; (4) to utilize apoA-I^{-/-}/LDLR^{-/-} mice as recipients and test the function of Bim in bone marrow derived cells on atherosclerosis.

In the fourth chapter, I utilized the SR-B1^{-/-}apoE^{-/-} mouse model of spontaneous coronary artery atherosclerosis and myocardial infarction to explore mechanisms by which rosuvastatin protects against coronary heart disease. The aims for this project include: (1) to analyze cholesterol levels and metabolism in control and rosuvastatin-treated SR-B1^{-/-}/apoE^{-/-} mice; (2) to test the effect of rosuvastatin on coronary atherosclerosis, platelet activation and cardiac pathology; (3) to investigate on the mechanism by which rosuvastatin affect atherosclerosis in the SR-B1^{-/-}/apoE^{-/-} mice, such as levels of oxidized phospholipid and foam cell formation.

CHAPTER II

Contribution of PDZK1 to protection against macrophage apoptosis and necrotic core formation in atherosclerotic plaques.

Author list: Pei Yu, Kelvyn Fernandes and Bernardo L. Trigatti

PREFACE

This project was designed by Pei Yu and Professor Bernardo Trigatti. Pei Yu conducted all the experiments, except the analysis of lipid staining and ER stress markers in foam cells (Supplementary Figure 2.1 and 2.2), which was designed by Pei Yu and carried out by Kelvyn Fernandes under the supervision of Pei Yu. All data were interpreted by Pei Yu with guidance from Professor Trigatti. The manuscript was written by Pei Yu with guidance and editing from Professor Trigatti. This manuscript has been submitted to the journal *Atherosclerosis, Thrombosis and Vascular Biology*.

2.1 Abstract

Macrophage apoptosis contributes to the formation of necrotic cores in atherosclerotic plaques, increasing the risk of plaque rupture, leading to clinical events. High-density lipoprotein (HDL) is well-known to protect against atherosclerosis, and this process may involve the HDL receptor SR-B1 (scavenger receptor class B, type 1). In this study, we tested the role of the adaptor protein, PDZK1, known to bind to the carboxy terminal cytoplasmic domain of SR-B1, in HDL dependent protection against macrophage apoptosis and its contribution to protection against atherosclerosis. We induced apoptosis of mouse peritoneal macrophages *in vitro* with endoplasmic reticulum (ER) stress inducing agents including tunicamycin. Cell death was assessed by terminal deoxynucleotidyl transferase dUTP nick end labeling (TUNEL) and cleaved caspase-3 staining. Only low levels of tunicamycin-induced apoptosis were observed when macrophages were cultured with lipoproteins. However, tunicamycin-stimulated apoptosis was substantially increased when lipoproteins were removed from the culture medium. The addition of purified HDL, but not LDL suppressed tunicamycin-induced apoptosis without alleviating ER stress. However, HDL did not inhibit macrophage apoptosis *in vitro* when PDZK1 was deleted, which was consistent with the observation that peritoneal injection of tunicamycin induced significantly more apoptosis *in vivo*, in thioglycollate-elicited macrophages lacking PDZK1. PDZK1 deficient macrophages also exhibited partially impaired M2 polarization. HDL increased phosphorylation of Akt1 in wild-type, but not in PDZK1^{-/-} macrophages. Consistent with a role for HDL induced Akt1 in protection against macrophage apoptosis, HDL treatment of

macrophages from Akt1^{-/-} mice failed to protect them from tunicamycin-induced apoptosis. In order to test the role of PDZK1 on atherosclerosis, LDLR^{-/-} mice were transplanted with either PDZK1^{-/-} or wild-type bone marrow and challenged with a high-fat, western type diet to induce atherosclerosis. Both lesion size and necrotic core area were significantly larger in mice with bone marrow specific deletion of PDZK1. Consistent with a role for PDZK1 in protection against apoptosis, significantly increased TUNEL and cleaved caspase 3 staining and reduced immunostaining for mannose receptor, a marker of M2 polarization, was observed in atherosclerotic plaques in mice with bone marrow specific deletion of PDZK1. These data demonstrate that PDZK1 is required for the HDL-dependent protection against macrophage apoptosis and that PDZK1 in bone marrow derived cells, plays a role in protecting macrophages from apoptosis and suppressing the development of necrotic cores in atherosclerotic plaques.

2.2 Introduction

Atherosclerotic cardiovascular disease is a leading cause of mortality and morbidity in both the US and Europe (Perk et al., 2012; Roger et al., 2012). Myocardial infarction, a life-threatening manifestation of atherosclerosis, is a result of local vascular occlusion with an acute thrombus overlying a preexisting atherosclerotic plaque (Falk et al., 1995). Plaque erosion or rupture has been shown to be responsible for the transition from an asymptomatic atheroma to acute thrombosis formation (Falk et al., 1995).

These culprit lesions are commonly characterized by large necrotic cores, which are derived from dead lipid-loaded macrophages (foam cells) (Moore and Tabas, 2011; Sakakura et al., 2013). The large necrotic core is thought to contribute to plaque vulnerability through increased expression/release of proteases including matrix metalloproteinase leading to degradation of the fibrous cap and smooth muscle cell apoptosis, causing thinning of the fibrous cap (Moore and Tabas, 2011). Macrophage apoptosis contributes to plaque instability by increasing the volume of necrotic cores. Macrophages in atherosclerotic lesions have been shown to be exposed to a number of pro-apoptotic stimuli, including oxidative stress, oxysterol loading, activation of Fas death pathway and ER stress, triggering the intrinsic or extrinsic apoptotic pathways (Seimon and Tabas, 2009). Among these, ER stress (the accumulation of unfolded proteins in the ER) is relatively better known to induce macrophage apoptosis in atherosclerotic lesions from studies of both clinical samples and mouse models (Seimon and Tabas, 2009). *In vivo*, ER stress can be induced by insulin resistance, glucosamine, serum starvation, oxidized phospholipids, free cholesterol (FC) accumulation and

peroxynitrite (Seimon and Tabas, 2009). Tunicamycin (an inhibitor of protein N-glycosylation) and thapsigargin (an inhibitor of the Serca ER calcium pump) are also commonly used tools to induced ER stress in cultured cells or model systems (Timmins et al., 2009). Under physiological conditions, ER stress leads to the activation of the unfolded protein response (UPR), characterized by the upregulation of ER chaperones to assist in protein folding, and the attenuation of protein biosynthesis, in an attempt to relieve ER stress (Scull and Tabas, 2011). However, with prolonged ER stress and sustained UPR activation, there is a switch from activation of pro-survival to pro-apoptotic pathways (Scull and Tabas, 2011). This process involves the activation of CEBP (CCAAT-enhancer-binding proteins)-homologous protein (CHOP), which has been shown to regulate the expression and activation of pro-apoptotic Bcl-2 family proteins and mediate mitochondria-dependent apoptosis (Puthalakath et al., 2007; Scull and Tabas, 2011).

High-density lipoprotein (HDL) has been well-known to protect against atherosclerosis by mediating reverse cholesterol transport (Al-Jarallah and Trigatti, 2010). Growing evidence also demonstrates the direct functions of HDL (*e.g.* anti-inflammation, anti-apoptosis, anti-thrombosis and pro-migration) on a number of cell types, such as monocytes, endothelial cells, macrophages and smooth muscle cells, that contribute to atherosclerosis (Al-Jarallah et al., 2014; Al-Jarallah and Trigatti, 2010; Feng et al., 2012; Mineo and Shaul, 2012a; Terasaka et al., 2007). The scavenger receptor class B type 1 (SR-B1), a high-affinity HDL receptor expressed on these vascular cells, is critically involved in the signaling pathways initiated by HDL (Al-

Jarallah et al., 2014; Feng et al., 2012; Kimura et al., 2006a; Seetharam et al., 2006; Yuhanna et al., 2001). Globally knocking out of SR-B1 in normal chow-fed apoE^{-/-} (Braun et al., 2002), or high cholesterol diet-fed apoE^{hypomorphic} (Zhang et al., 2005) or LDLR^{-/-} (Fuller et al., 2014a) mice leads to increased aortic sinus atherosclerosis and occlusive coronary atherosclerosis, which can be reversed by restoring SR-B1 expression in bone marrow (BM) derived cells (Pei et al., 2013; Yu et al., 2006), indicating the importance of bone marrow derived-cell expressed SR-B1 in plaque development *in vivo*.

Krieger and colleagues have characterized PDZK1 as an adaptor protein that binds to the C-terminal cytoplasmic three amino acids of SR-B1 with both PDZ1 and PDZ3 domains (Ikemoto et al., 2000; Kocher et al., 2010; Kocher et al., 2011; Silver, 2002). PDZK1^{-/-} mice do not display any gross phenotypic abnormalities, but do show increased plasma cholesterol and abnormally large HDL particles, which are similar to what has been observed in SR-B1^{-/-} mice (Kocher et al., 2003a; Yesilaltay et al., 2006). PDZK1 deficient mice exhibit very low levels of SR-B1 protein in liver (~5 % of normal) and ~ 50 % of SR-B1 protein in intestine, but normal levels of SR-B1 protein in the adrenal gland, endothelial cells, macrophages and other cell types, suggesting that PDZK1 is required in a tissue selective manner, for stabilization of SR-B1 protein (Al-Jarallah et al., 2014; Kocher et al., 2003b; Kocher et al., 2008; Zhu et al., 2008). The similarly increased HDL total cholesterol and HDL size seen in PDZK1 and SR-B1 deficient mice are due to the drastic reduction in hepatic SR-B1 protein levels in PDZK1 deficient mice (Kocher et al., 2003b).

Global deletion of PDZK1 in apoE deficient mice has been shown to increase high fat diet induced atherosclerosis in the aortic sinus (Kocher et al., 2008) and to trigger high fat, high cholesterol cholate-containing diet-induced coronary artery atherosclerosis (Yesilaltay et al., 2009). This resembled the occlusive coronary artery atherosclerosis that develops (albeit spontaneously) in SR-B1^{-/-}/apoE^{-/-} mice (Braun et al., 2002).

PDZK1 has also been reported to play an important role in HDL signaling mediated by SR-B1 in endothelial cells and macrophages. In these cells, the absence of PDZK1 does not appear to affect SR-B1 protein levels or cell surface distribution (Al-Jarallah et al., 2014; Kocher et al., 2008). However, deletion of the C-terminal, PDZK1 interacting motif from SR-B1 abolished HDL-dependent endothelial nitric oxide synthase (eNOS) activation (Assanasen et al., 2005). Similarly, knockdown of PDZK1 impairs HDL dependent activation of Akt phosphorylation and endothelial cell migration *in vitro* (Wu et al., 2015; Zhu et al., 2008). Consistent with *in vitro* findings, PDZK1^{-/-} mice with reconstitution of PDZK1 expression in liver exhibit impaired re-endothelialization following perivascular electric injury (Zhu et al., 2008). In macrophages, knockout of either SR-B1 or PDZK1 prevents HDL induced migration (Al-Jarallah et al., 2014). The involvement of PDZK1 in macrophages in HDL dependent protection against apoptosis and its contribution to protection against atherosclerosis, however, has not been described.

In this study, we report that the adaptor protein PDZK1 is required by HDL to protect macrophages against apoptosis induced by ER stress. HDL signaling does not

appear to affect the induction of the UPR, but rather leads to transient Akt1 activation in a PDZK1 dependent manner. *In vivo*, mice deficient in PDZK1 either globally or in bone marrow derived cells, exhibit increased tunicamycin induced apoptosis in peritoneal macrophages recruited by thioglycollate. LDLR^{-/-} mice lacking PDZK1 in exclusively bone marrow derived cells exhibited increased high fat diet induced atherosclerosis in their aortic sinuses and atherosclerotic plaques were characterized by increased apoptosis and increased necrotic core sizes compared to LDLR^{-/-} mice expressing PDZK1 in bone marrow derived cells. These results suggest that PDZK1 plays a key role in protecting macrophages against apoptosis both *in vitro* and *in vivo*, and this contributes to protection against atherosclerosis development and plaque stabilization.

2.3 Materials and Methods

2.3.1 Materials

All materials were purchased from Sigma Aldrich (St. Louis, Missouri, USA) unless otherwise stated.

2.3.2 Mice

All procedures involving mice were approved by the McMaster University Animal Research Ethics Board and were in accordance with the guidelines of the Canadian Council on Animal Care. Sources of mice: C57BL6/J (control for Akt1^{-/-}); B6129SF2/J (control for PDZK1^{-/-}); PDZK1^{-/-} and LDLR^{-/-}: The Jackson Laboratory (Bar Harbor, ME, USA); Akt1^{-/-}: Professor Morris Birnbaum, University of Pennsylvania. All mice were bred and housed in the Thrombosis and Atherosclerosis Research Institute (TaARI) Animal Facility in ventilated cages with automatic watering and had free access to food and water. Mice were maintained on normal chow (Teklad#2018, 18% protein diet, Harlan Laboratories, Mississauga, ON, Canada), or, for induction of atherosclerosis, on a Western type diet (containing 21 % butter fat and 0.15 % cholesterol, #112286, Dyets Inc., Bethlehem, PA, USA).

2.3.3 Preparation, culture and treatment of peritoneal macrophages

Primary mouse peritoneal macrophages (MPMs) were prepared by injecting mice intraperitoneally (i.p.) with 1 ml of 10 % thioglycollate. Mice were euthanized 4 d later

and cells were recovered by peritoneal lavage as described previously (Al-Jarallah et al., 2014). Cells were plated (1.5×10^5 cells/well) in 8-well NuncTM Lab-TekTM II ChamberslidesTM (Thermo Scientific, Waltham, MA, USA) and cultured in DMEM containing 2mM L-glutamine and 50 U/ml penicillin/50 µg/ml streptomycin (Medium 1) with 10% fetal bovine serum (FBS) over night. Before each experiment, cell culture medium was changed to Medium 1 with 3 % newborn calf lipoprotein deficient serum (NCLPDS) (Zhang et al., 2007) and cells were cultured for 24 hrs. At the start of each experiment, the medium was changed to fresh Medium 1 containing 3 % newborn calf serum (NCS, Life Technologies Inc., Burlington, ON, Canada), or 3 % NCLPDS without or with supplementation of different concentrations of human HDL or LDL (Biomedical Technologies Inc, Boston, MA, USA), without or with addition of various agents to induce ER or oxidative stress as indicated. ER or oxidative stress inducing agents and concentrations used were: tunicamycin (10 µg/ml tunicamycin); thapsigargin (5 µM); oxidized LDL (100 µg protein/ml; Biomedical Technologies Inc, Boston, MA, USA). In all cases, controls contained an equivalent amount of vehicle (0.1 % DMSO) for tunicamycin or thapsigargin.

2.3.4 Apoptosis analysis

For cleaved caspase-3 or TUNEL staining, cells were treated for 24 hrs before fixation with 2 % paraformaldehyde. Cleaved caspase-3 (Asp175) antibody was purchased from Cell Signaling Technology (Danvers, MA, USA) and diluted 1:200 for immunofluorescence staining, followed by incubation with Alexa Fluor 488 F(ab')₂

fragment of goat anti-rabbit IgG (H+L) antibody (Life Technologies Inc., Burlington, ON, Canada), diluted 1:500 in phosphate buffered saline (PBS). TUNEL staining was performed using S7110 ApopTag® fluorescein *in situ* apoptosis detection kit (Millipore Canada Ltd., Etobicoke, ON, Canada), following the manufacturer's instructions. Nuclei were counterstained with 300 nM 4',6-diamidino-2-phenylindole dihydrochloride (DAPI). Fluorescent images were captured using a Zeiss Axiovert 200M inverted fluorescence microscope (Carl Zeiss Canada Ltd. Toronto, ON, Canada).

For apoptosis induction *in vivo*, mice were injected i.p. with 10 % thioglycollate on day 0. Tunicamycin (1 mg/kg of body weight) was dissolved in 150 mM dextrose and injected i.p. on day 3 (Timmins et al., 2009; Yamamoto et al., 2010). Macrophages were harvested 24 hrs later and stained with 1 µg/ml propidium iodide, followed by fixation with 4 % paraformaldehyde at 37 °C for 10 min. Cells were permeabilized with ice-cold methanol and incubated with anti-cleaved caspase-3 (Asp175) antibody (1:800 diluted in FACS Buffer: PBS containing 0.1 % BSA and 0.1% sodium azide) at room temperature for 1 hr, followed by incubation with Alexa Fluor 488 labeled F(ab')₂ fragment of goat anti-rabbit IgG (H+L) antibody (1:1000 diluted in FACS Buffer, Life Technologies Inc., Burlington, ON, Canada) for 30 min. Monocytes were identified by APC-conjugated rat anti-mouse CD11b antibody (Life Technologies Inc., Burlington, ON, Canada). Samples were analyzed by a BD FACScalibur™ flow cytometer (BD Biosciences, San Jose, CA, USA). 30,000 events were analyzed and data was processed by FlowJo data analysis software (FlowJo, LLC., Oregon, OR, USA).

2.3.5 Measurement of UPR markers in cultured macrophages

2×10^6 MPMs were plated in 3 cm dishes and treated with or without 10 $\mu\text{g/ml}$ tunicamycin, in the presence or absence of 50 $\mu\text{g/ml}$ HDL, as described above. GRP78 and GRP94 were detected by western blot as the 78 kD and 94 kD protein bands using an anti-KDEL antibody (Watson et al., 2003). Briefly, cells were lysed on ice with RIPA buffer (containing 50 mM Tris-HCl PH7.4; 150mM NaCl; 1 % Triton X-100; 1 % sodium deoxycholate; 0.1 % SDS; 1 mM EDTA) in the presence of protease inhibitors (1 $\mu\text{g/ml}$ pepstatin A; 1 $\mu\text{g/ml}$ leupeptin; 10 $\mu\text{g/ml}$ aprotinin; 50 μM APMSF) and centrifuged at 1200 rpm at 4°C for 5 min using an Allegra™ X-220 centrifuge (Beckman Coulter, Mississauga, ON, Canada) to collect supernatant. Protein concentrations were determined using the BCA protein assay kit (Pierce Biotechnology, Rockford, Illinois, USA). 20-50 μg proteins were subjected to SDS-PAGE, as described previously (Trigatti et al., 1991), using a 15 % acrylamide gel for separation of GRP78 and GRP94 and loading control GAPDH (38 kD). Electrophoretic transfer of proteins to PVDF membranes and immunoblotting was as previously described (Trigatti et al., 1991). Briefly, membranes were blocked in Blocking Solution (5 % skim milk in TBS supplemented with 0.1 % Tween-20) for 1 hr at room temperature before incubation with mouse anti-mouse KDEL antibody (Enzo Life Sciences, Inc., Farmingdale, NY, USA, diluted 1: 1000 in Blocking Solution) at 4°C overnight. Membranes were then washed and incubated with horseradish peroxidase (HRP)-conjugated donkey anti-mouse antibody (Jackson Immunoresearch laboratory, West Grove, Pennsylvania, USA, diluted 1:10000 in Blocking Solution) at room temperature for 1 hr. HRP was detected

using the Amersham Enhanced Chemiluminescence (ECL) kit (GE Healthcare Life Sciences, Baie d'Urfe, QC, Canada). Then, the membrane was re-probed for GAPDH by incubating with HRP-conjugated anti GAPDH antibody (Abcam Inc. Toronto, ON, Canada, 1:5000 in the Blocking Solution) for 1 hr at room temperature. The bands of HRP were imaged as described above. The intensities of the protein bands were measured using a Gel Doc instrument (Bio-Rad Laboratories, Hercules, CA, USA).

CHOP was detected by RT-PCR. Total RNA from cultured macrophages was extracted and purified using the RNeasy Mini Kit (Qiagen Inc., Toronto, ON, Canada) and quantified using a SpectraMax Plus384 spectrophotometer (Molecular Devices, Sunnyvale, CAA, USA). cDNA synthesis was performed from 1 µg of total RNA using QuantiTect Reverse Transcription Kit (Qiagen Inc., Toronto, ON, Canada). Real-time quantitative PCR for CHOP or GAPDH was performed using Platinum Sybr Green dye (Invitrogen Life Technologies Inc., Burlington, ON, Canada) in an Applied Biosystems 7300 Real Time PCR system (Applied Biosystems, Foster City, CA, USA) with default settings. All primers were synthesized by Invitrogen Life Technologies (Burlington, ON, Canada). Primer sequences used are listed in Supplementary Table 2.1.

2.3.6 Analysis of Akt phosphorylation

Thioglycollate-elicited MPMs were plated (2×10^6 cells/well) and cultured in Medium 1 with 10 % FBS, as described above. The next day, cells were incubated in Medium 1 containing 3 % NCLPDS instead of 10 % FBS for 24 hrs. Before HDL treatment, cells were serum-starved in DMEM for 2 hrs. Then, they were incubated with

50 µg/ml HDL for up to 3 hrs. Cells were lysed with lysis buffer containing protease inhibitors and PhosSTOP phosphatase inhibitors (Roche, Mannheim, Germany). Immunoblotting was performed as described above. The protein levels of phospho-Akt (Ser473) was determined by incubating with rabbit monoclonal antibodies purchased from Cell Signaling (1:1000 in 3 % BSA, Danvers, MA, USA), followed by HRP-conjugated donkey anti-rabbit secondary antibody (1:10000 in Blocking Solution, Jackson ImmunoResearch laboratory, West Grove, PA, USA). Imaging was performed as described above. Then, membranes were incubated in stripping buffer for 15 min and reblocked in Blocking Solution for 1 hr at room temperature. Total Akt was blotted by incubating the membrane with rabbit anti-Akt antibody (1:1000 in 3 % BSA, Cell Signaling, Danvers, MA, USA). HRP-conjugated secondary antibody incubation and imaging was performed as above. Finally, the protein loading control β -actin was detected using HRP-conjugated anti- β -actin antibody (1:5000 in 3 % BSA, Cell Signaling, Danvers, MA, USA).

2.3.7 Macrophage polarization

Thioglycollate-elicited MPMs were incubated in Medium 1 + 10 % FBS, as described above. MPMs were exposed to either lipopolysaccharide (LPS) or interleukin (IL)-4 (each at 10 ng/ml) for 6 hrs. RNA extraction and RT-PCR were performed as described above. Primer sequences for markers of M1 (IL-6, IL-1 β , monocyte chemoattractant protein (MCP)-1) or M2 polarization (Arginase-1, Fizz-1, mannose receptor) are listed in Supplementary Table 2.1.

2.3.8 Bone Marrow Transplantation

Bone marrow cells were collected from the femurs and tibias of donor mice by flushing with sterile medium as described previously (Covey et al., 2003). Male LDLR^{-/-} mice (10-12 weeks old) were lethally irradiated using a Gammacell 3000 small animal irradiator (Best® Theratronics Ltd. Ottawa, ON, Canada) at a split dose of 1400 rad and immediately thereafter, injected i.v. with 3×10^6 bone marrow cells. After bone marrow transplantation, mice were treated for 2 weeks with antibiotics in their drinking water as described previously (Covey et al., 2003).

2.3.9 Analysis of atherosclerotic Lesions

Beginning at 4 weeks after bone marrow transplantation, LDLR^{-/-} mice were fed Western type diet for 10 weeks to induce atherosclerosis. After the Western diet feeding period, mice were fasted for 4 hrs prior to isoflurane anesthesia and euthanasia by thoracotomy. Blood was collected by cardiac puncture and tissue was perfused with 0.9 % sodium chloride containing 10 U of heparin/ml, followed by 10 % formalin. Hearts were harvested and immersion-fixed in 10 % formalin overnight. Tissues were either embedded in paraffin or frozen in Shandon Cryomatrix (Thermo Fisher Scientific, Ottawa, ON, Canada). Transverse sections (5 μ m for paraffin sections or 10 μ m for cryosections) of aortic sinus, where the three valve leaflets are intact, were stained with oil red O and hematoxylin (frozen sections) or Mayer's hematoxylin and eosin (H&E)

(paraffin sections). Images were captured using a Zeiss Axiovert 200M inverted microscope (Carl Zeiss Canada Ltd., Toronto, ON, Canada). The necrotic core was defined as acellular area (negative for hematoxylin/eosin staining). The total plaque areas and necrotic core areas were determined by quantitative morphometry using Axiovision 3.1.2.1 software (Carl Zeiss Canada Ltd., Toronto, ON, Canada).

Apoptosis in atherosclerotic lesions was detected by staining aortic sinus cryosections, using the TUNEL kit as described above, or by staining paraffin sections with cleaved caspase 3 antibody. For cleaved caspase-3 immunostaining, paraffin sections were first deparaffinized (xylene: 5min×3; 100% ethanol: 10min×2; and 70% ethanol: 10min×3) and then subjected to antigen retrieval using the Vector Antigen Unmasking Solution (Vector Laboratories, Inc., Burlingame, CA, USA). Sections were then incubated in Blocking Solution (PBS containing 3 % goat serum) for 1 hr at room temperature, followed by incubation with rabbit anti-cleaved caspase-3 (Asp175) antibody (Cell Signaling Technology, Danvers, MA, USA; 1:200 in Blocking Solution) at 4°C overnight and with Alexa Fluor 488 F(ab')₂ fragment of goat anti-rabbit IgG (H+L) antibody (Life Technologies Inc., Burlington, Ontario, Canada; 1:500 diluted in PBS) for 1 hr at room temperature.

For immunostaining for mannose receptor and Mac-3, cryosections were fixed in 4 % paraformaldehyde for 20 min and incubated with Blocking Solution as described above. Sections were then incubated with rabbit anti-mannose receptor antibody (Abcam Inc. Toronto, ON, Canada; 1:500 in Blocking Solution) and rat anti-mouse CD107b (Mac3) antibody (BD Biosciences, San Jose, CA, USA; 1:50 in Blocking

Solution) at 4°C overnight. Primary antibodies were detected by goat anti-rabbit Alexa Fluor 488 (1:500 in PBS, Life Technologies Inc., Burlington, ON, Canada) and goat anti-rat Alexa Fluor 568 (1:200 in PBS, Life Technologies Inc., Burlington, ON, Canada). Fluorescent images were captured using a Zeiss Axiovert 200M inverted fluorescence microscope (Carl Zeiss Canada Ltd. Toronto, ON, Canada), as described above.

2.3.10 Statistical analysis

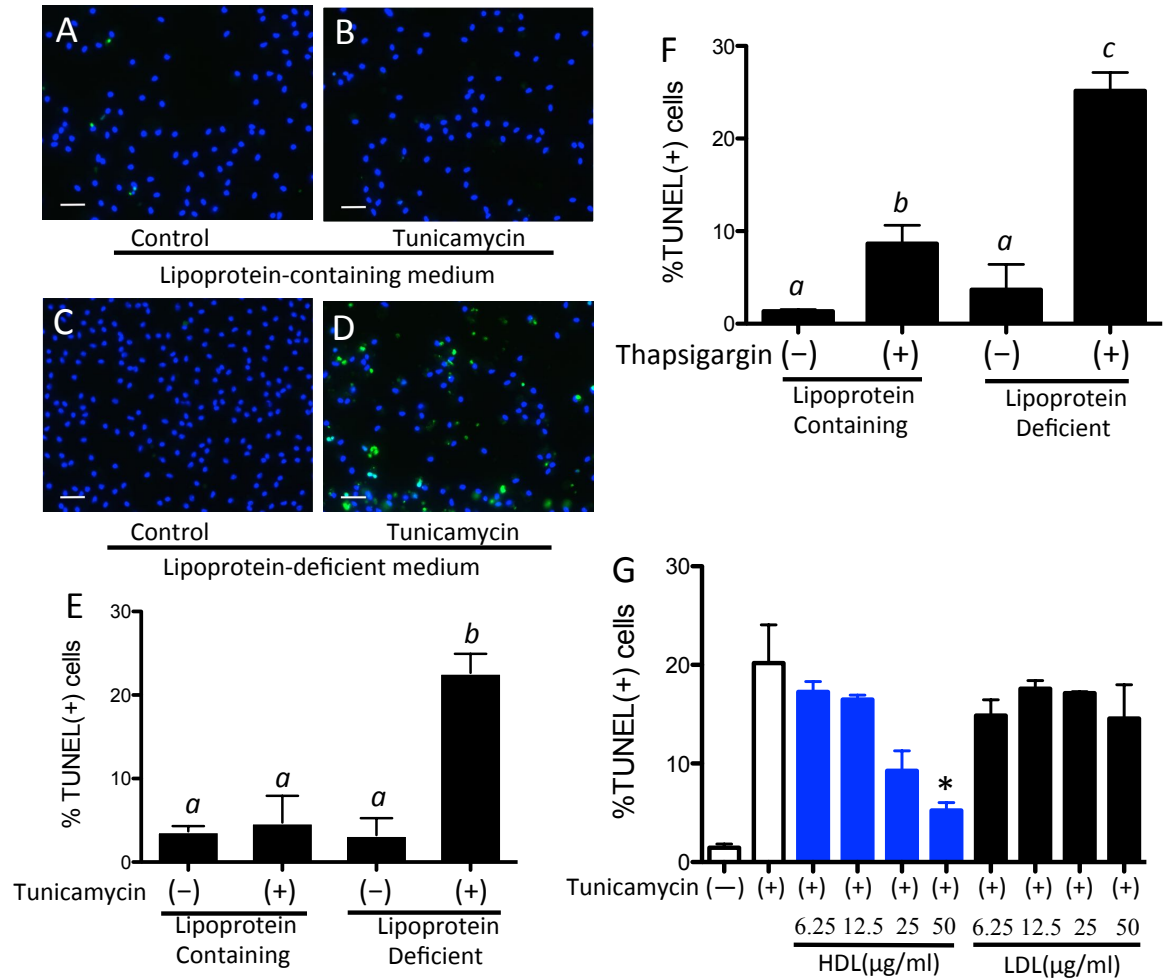
Sigma Plot statistical analysis software was used. For two groups, data was subjected to the Shapiro-Wilk test for normality and F test for equality of variances. Those that passed were analyzed by the Student's t-test (2-tailed, unpaired). Those that failed either test were analyzed by the Mann-Whitney Rank Sum test. Data from multiple groups were analyzed with one-way or two-way ANOVA with post hoc tests for pairwise comparisons: If the data passed the Shapiro-Wilk normality test and the variance test, they were analyzed by the Holm-Sidak method; If not, they were subjected to the Tukey test; Dunnett's test was used to compare multiple groups to a single control group; Dunn's test was used when the group sizes were unequal. Data are presented as mean±standard error of the mean. P values <0.05 were considered statistically significant.

2.4 Results

2.4.1 HDL, but not LDL, protected MPMs from apoptosis in a dose-dependent manner.

In order to test the overall effect of plasma lipoproteins on cell survival from ER stressors, we incubated thioglycollate-elicited MPMs in lipoprotein-containing medium or in lipoprotein-deficient serum, and induced apoptosis with tunicamycin for 24 hrs. As shown in Figure 2.1A-E, MPMs harvested from wild type (WT) mice showed similar baseline levels of apoptosis when they were incubated in the media containing (Bar 1) and lacking (Bar 3) plasma lipoproteins. The addition of tunicamycin did not significantly alter the percentage of apoptotic macrophages in the presence of lipoproteins (Bar 3). However, the depletion of lipoproteins significantly increased tunicamycin-stimulated apoptosis (Bar 4). Similar results were also observed in the macrophages incubated with another ER stress inducer thapsigargin (Figure 2.1F). In order to test the effects of individual lipoproteins, macrophages were cultured in the medium supplemented with newborn calf lipoprotein-deficient serum (NCLPDS) and treated with tunicamycin as described above. Varying concentrations (6.25-50 $\mu\text{g/ml}$) of purified HDL or LDL were added (Figure 2.1G). As described above, macrophages were sensitive to tunicamycin-induced apoptosis when the culture medium lacked lipoproteins (open bars). However, increasing concentrations of HDL reduced the level of tunicamycin-induced apoptosis in a dose-dependent manner (blue bars) and the reduction was significant at the concentration of 50 $\mu\text{g/ml}$. On the other hand, LDL did not show any anti-apoptotic effects, when added to the culture medium (black bars).

Figure 2.1: Serum lipoproteins, specifically HDL, protected macrophages from tunicamycin- and thapsigargin-induced apoptosis. Thioglycollate-elicited MPMs were incubated in lipoprotein-containing (A, B) and lipoprotein-deficient (C, D) medium with (B, D) or without (A, C) tunicamycin for 24 hrs. Apoptotic cells were detected by TUNEL staining (green). Cell nuclei were counterstained with DAPI (blue). Scale bar=20µm. Data was expressed as the percentage of TUNEL⁺ cells in total number of cells (E) and analyzed by two-way ANOVA followed by Holm-Sidak pairwise comparison (n=3, p<0.01 *a* vs. *b*). Similar experiment was performed by using thapsigargin, instead of tunicamycin, to induce MPM apoptosis (F). The percentage of TUNEL⁺ cells was analyzed by two-way ANOVA followed by Holm-Sidak pairwise comparison (n=3, p<0.05 *a* vs. *b*, p<0.001 *a* vs. *c*, p<0.001 *b* vs. *c*). MPMs were incubated in lipoprotein-deficient serum and apoptosis was induced with tunicamycin (G). Increasing concentrations of HDL and LDL, as labeled, were added. Cell apoptosis was quantified, as described above, and analyzed by one-way ANOVA followed by Dunnett's method. (n=3, *p<0.05vs. tunicamycin-treated control).



2.4.2 HDL did not reduce ER stress induced by tunicamycin.

Prolonged ER stress and activation of the UPR induces apoptosis through upregulation of CHOP (Puthalakath et al., 2007). We therefore tested if the protective effect of HDL was a result of attenuation of the UPR. MPMs harvested from WT mice were treated with or without tunicamycin and HDL, as described above. SDS-PAGE and immunoblotting were carried out using anti-KDEL antibody, to detect the ER chaperone, GRP78 and GRP94, which are induced in response to ER stress, and frequently used as markers of the UPR (Lee, 2005). As shown in Figure 2.2A-C, tunicamycin substantially increased GRP78 and GRP94, whereas HDL did not affect their levels in either control or tunicamycin treated cells. Tunicamycin treatment also substantially induced expression of CHOP, while HDL treatment had no effect (Figure 2.2D). Similarly results were obtained when macrophages were first converted to foam cells by incubation with acetylated-LDL (100 µg/ml for 24 hrs) prior to treatment with/without tunicamycin and HDL (Supplementary Figure 2.1).

2.4.3 HDL mediated protection of macrophages from apoptosis requires PDZK1

To test if PDZK1 is required for the ability of HDL to protect macrophages against apoptosis, MPMs from PDZK1^{-/-} mice and control WT mice were cultured and treated with or without tunicamycin in the presence or absence of 50 µg/ml HDL. Apoptosis was analyzed by immunofluorescence staining for cleaved caspase-3, which is the activated form of caspase-3 (Cullen and Martin, 2009). As shown in Figure 2.3A-I, both WT and PDZK1^{-/-} MPMs were sensitive to tunicamycin-induced apoptosis when

cultured in the absence of serum lipoproteins (C vs. A; G vs. E). Consistent with what we observed above, HDL treatment attenuated tunicamycin induced apoptosis in WT MPMs (D vs. C). However, HDL was not able to reduce the level of tunicamycin induced apoptosis in PDZK1^{-/-} macrophages (H vs. G). Similar results was also seen when WT and PDZK1^{-/-} macrophages were first converted to foam cells by incubation with acLDL for 24 hrs prior to treatment with or without tunicamycin in the presence or absence of HDL (Supplementary Figure 2.2). Oxidized low-density lipoprotein (oxLDL) has been shown to be a potent macrophage apoptosis inducer (Heinloth et al., 2002; Muller et al., 2001; Seimon and Tabas, 2009). In order to test if HDL is also able to protect macrophages from apoptosis triggered by a physiologically relevant inducer, we treated WT and PDZK1^{-/-} MPMs with 100 µg/ml oxLDL in the presence or absence of HDL. Consistent with observations reported by others (Heinloth et al., 2002), increased cell apoptosis was seen in WT macrophages treated with oxLDL, and HDL treatment attenuated oxLDL induced apoptosis (Figure 2.3J). Similar to our findings above, oxLDL also induced significant apoptosis in PDZK1^{-/-} macrophages, however HDL was unable to protect PDZK1^{-/-} macrophages from oxLDL induced apoptosis (Figure 2.3J).

We next tested the sensitivity of PDZK1^{-/-} macrophages to apoptosis *in vivo* (Figure 2.4). WT and PDZK1^{-/-} mice were injected intraperitoneally with thioglycollate to recruit peritoneal macrophages. Three days later, mice were injected intraperitoneally with either tunicamycin (1 mg/kg) or vehicle, and 24 hrs afterwards, mice were euthanized and peritoneal cells were collected by peritoneal lavage and analyzed by flow cytometry for CD11b (to detect myeloid cells), cleaved caspase 3 (to detect cells

undergoing apoptosis) and propidium iodide (to detect necrotic cells). Greater than 90 % of the collected cells were positive for CD11b (Figure 2.4B) (Ding et al., 1987). There appeared to be a trend towards a proportion of peritoneal cells that were undergoing apoptosis (positive for cleaved caspase 3) at baseline (without tunicamycin) in PDZK1^{-/-} compared to WT mice, although the differences did not reach statistical significance (Figure 2.4H Bar 1 vs.3). Intraperitoneal injection of tunicamycin into WT mice did not increase apoptosis of elicited peritoneal macrophages at the concentration of tunicamycin used (Figure 2.4H Bar 2 vs.1). In contrast, i.p. injection of the same concentration of tunicamycin into PDZK1^{-/-} mice substantially increased the proportion of elicited peritoneal macrophages undergoing apoptosis (Figure 2.4H Bar 4 vs.3). No propidium iodide staining was detected (Figure 2.4D-G), indicating the absence of necrosis. PDZK1^{-/-} mice have been reported to have increased plasma total cholesterol associated with enlarged HDL particles, as described in SR-B1^{-/-} mice (Kocher et al., 2003a; Yesilaltay et al., 2006). To verify that the increased sensitivity of elicited peritoneal macrophages from PDZK1^{-/-} mice to tunicamycin induced apoptosis compared to those from WT mice is the result of a lack of PDZK1 in the macrophages themselves, we carried out a similar experiment using wild type mice that had been lethally irradiated and transplanted with bone marrow from either PDZK1^{-/-} or control WT mice. Eight weeks post-BMT, blood cell genotyping showed that WT PDZK1 was completely replaced by the mutant PDZK1 allele in the WT mice transplanted with PDZK1^{-/-} BM (Supplementary Figure 2.3A). As above, mice were injected i.p. with thioglycollate to elicit peritoneal macrophages. Three days later, tunicamycin was

injected i.p. and peritoneal cells were harvested by lavage 24 hrs later and analyzed by flow cytometry for CD11b, propidium iodide and cleaved caspase 3. As observed for global PDZK1^{-/-} mice, BM-specific deficiency of PDZK1 resulted in increased basal and tunicamycin induced apoptosis of elicited peritoneal macrophages, compared to control mice expressing PDZK1 in BM derived cells. This suggests that macrophages deficient in PDZK1 are more sensitive to apoptosis *in vivo* (Supplementary Figure 2.3B).

Figure 2.2: HDL did not reduce ER stress in macrophages. MPMs were incubated for 24 hrs with or without tunicamycin (10 $\mu\text{g/ml}$) in the presence or absence of HDL (50 $\mu\text{g/ml}$). Then, cells were lysed and the lysates were subjected to SDS-PAGE for immunoblotting (A-C); or RNA was extracted for real time PCR analysis (D). (A): Immunoblots of GRP78, GRP94 and GAPDH in the MPMs treated with or without tunicamycin or HDL. Data was expressed as fold change of GRP78 (B) and GRP94 (C) relative to GAPDH protein and analyzed by two-way ANOVA followed by Holm-Sidak pairwise comparison ($n=3$, $p<0.05$ *a* vs. *b*). (C): The levels of CHOP mRNA was quantified by RT-PCR, and normalized to the levels of GAPDH mRNA. The relative levels of CHOP were analyzed by two-way ANOVA followed by Holm-Sidak pairwise comparison. ($n=3$, $p<0.001$ *a* vs. *b*)

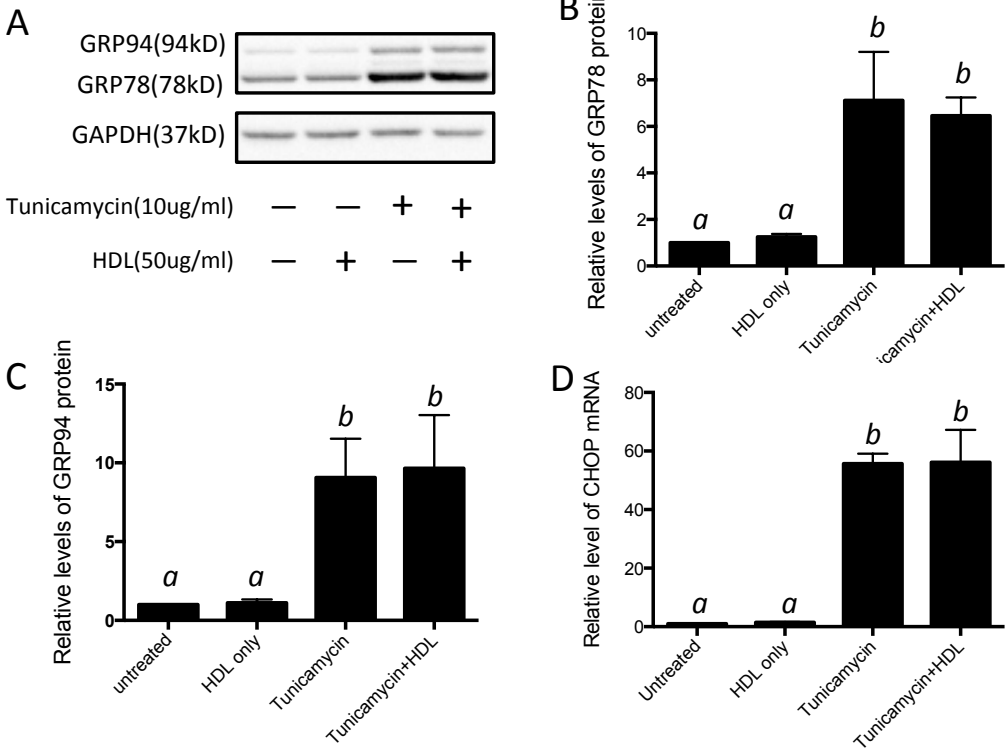


Figure 2.3: HDL reduced tunicamycin- and oxLDL-induced apoptosis in WT but not PDZK1^{-/-} macrophages. Thioglycollate-elicited MPMs from WT and PDZK1^{-/-} mice were treated with 10 µg/ml of tunicamycin in the presence or absence of 50 µg/ml HDL for 24 hrs. Then, cells were fixed and cleaved caspase-3 immunofluorescent staining was done to detect apoptotic cells (A-H: Green). Nuclei were stained with DAPI (A-H: Blue). Scale bar=20µm. Data was expressed as the percentage of cleaved caspase-3 positive cells vs. DAPI positive nuclei (I). Data was analyzed by two-way ANOVA with Holm-Sidak method, n=3, ***p<0.001, vs. untreated control; ### p<0.001, vs. tunicamycin-treated cells. J: WT and PDZK1^{-/-} MPMs were treated with 100 µg/ml of oxLDL in the presence or absence of 50 µg/ml HDL for 24 hrs. Then, cells were fixed, and stained with TUNEL to detect apoptotic cells. Data was expressed as the percentage of TUNEL⁺ nuclei. Two-way ANOVA with Holm-Sidak method was carried out for statistical analysis, n=4, **p<0.01, ***p<0.001 vs. untreated control; ## p<0.01, vs. tunicamycin-treated cells.

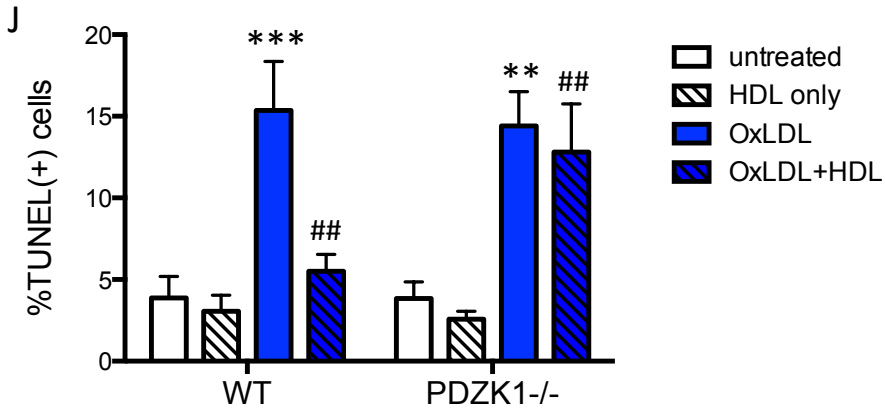
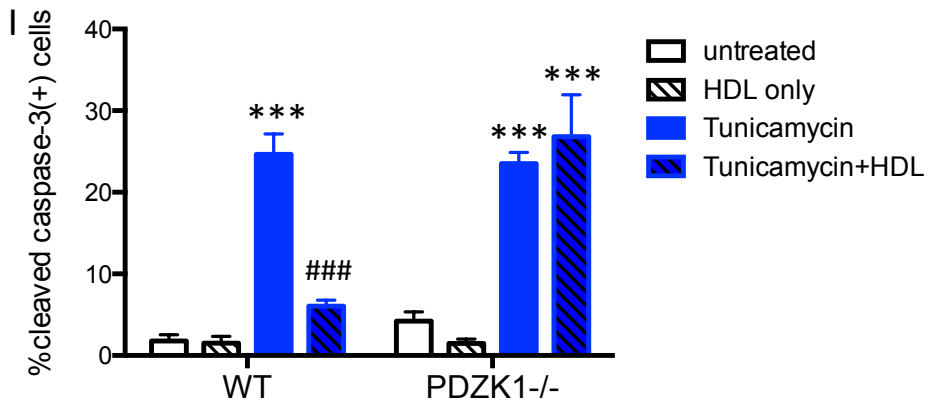
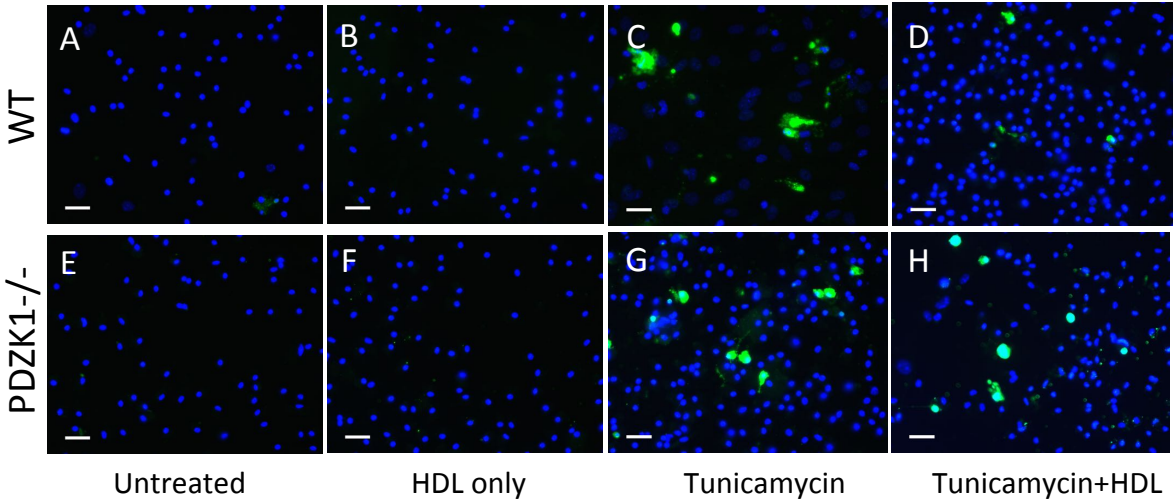
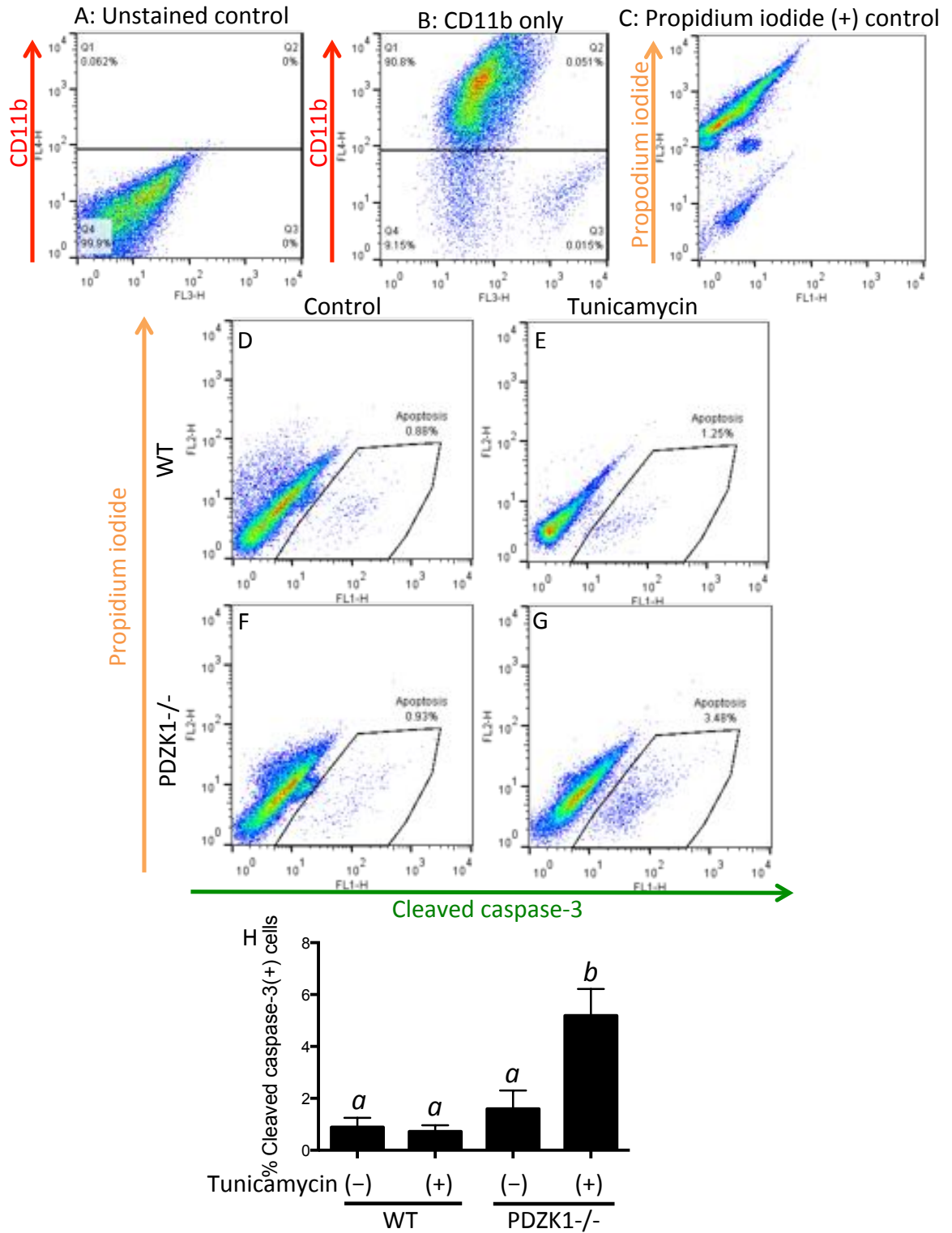


Figure 2.4: PDZK1^{-/-} macrophages were more sensitive to tunicamycin-induced apoptosis *in vivo* than WT macrophages. Tunicamycin (1 mg/kg of body weight) was injected i.p. after macrophages were recruited into peritoneal cavity. Peritoneal macrophages were harvested 24 hrs after tunicamycin injection. Macrophages were defined as CD11b⁺ cells (A: unstained and B: CD11b stained). Propidium iodide (+) cells are considered as necrotic cells (C). Apoptosis (X axis: cleaved caspase-3 stained cells) and necrosis (Y axis: PI positive cells) in control and tunicamycin-treated WT and PDZK1^{-/-} macrophages are shown in D-G. The percentage of apoptotic macrophages was analyzed by two-way ANOVA, followed by Holm-Sidak comparison (H: n=3, p<0.05 *a vs. b*).

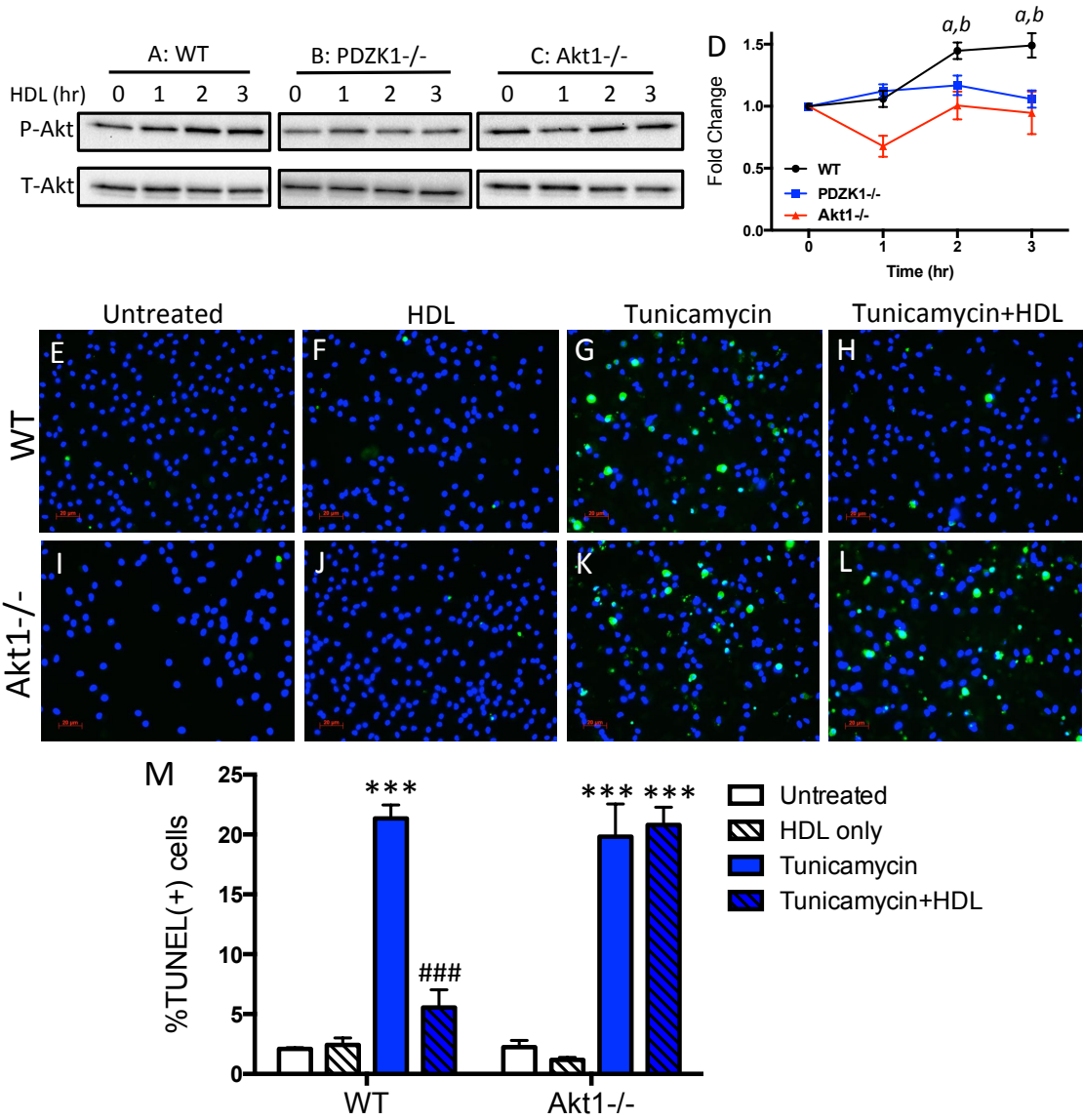


2.4.4 HDL mediated cytoprotection of macrophages via PDZK1 involves Akt1

Akt represents one of the most frequently activated pathways mediating cell survival (Song et al., 2005; Yu et al., 2015). Previous studies have shown that HDL can mediate the activation of Akt in a variety of cell types, including endothelial cells (Mineo et al., 2003), Chinese hamster ovary derived cells (Zhang et al., 2007) cultured murine RAW264.7 macrophage-like cells (Al-Jarallah et al., 2014) and hematopoietic stem progenitor cells (Gao et al., 2014) in a manner involving SR-B1. To test if HDL treatment of elicited peritoneal macrophages induced Akt activation, MPMs collected from WT, PDZK1^{-/-} or Akt1^{-/-} mice were cultured in the absence of lipoproteins, followed by incubation with HDL for up to 3 hrs. Phospho-Akt was detected by immunoblotting using an antibody that detects the activated, phosphorylated forms of all three Akt isoforms (Akt1, 2 and 3) at Ser residues equivalent to Ser473 of Akt1. As shown in Figure 2.5A-D, after 2 and 3 hours of incubation with HDL, Akt phosphorylation was significantly increased in macrophages from WT mice, but not macrophages from PDZK1^{-/-} or Akt1^{-/-} mice. The absence of HDL induced Akt phosphorylation in macrophages from Akt1^{-/-} mice demonstrates that HDL treatment leads to activation of Akt1 but not other isoforms of Akt. The absence of HDL induced Akt phosphorylation in macrophages from PDZK1^{-/-} mice demonstrates that PDZK1 is required for HDL induced activation of Akt1 in macrophages. To verify that Akt1 is required for HDL induced survival signaling in macrophages, MPMs from either Akt1^{-/-} or WT control mice were elicited, cultured in the absence of lipoproteins and treated with or without tunicamycin for 24 hr in the absence or presence of HDL. Apoptosis

was detected by TUNEL staining. As observed for macrophages deficient in PDZK1, macrophages lacking Akt1 were not protected by HDL from tunicamycin-induced apoptosis (Figure 2.5E-M). Thus, HDL induced activation of Akt1 in macrophages in a PDZK1 dependent manner, and Akt1, together with PDZK1 is required for HDL dependent protection against apoptosis induced by ER stressors.

Figure 2.5: HDL activated Akt1 signaling pathway in macrophages in a PDZK1 dependent manner. (A-D): MPMs from WT (A), PDZK1^{-/-} (B) and Akt1^{-/-} (C) mice were treated with HDL (50 µg/ml) for 0, 1, 2 and 3 hrs. Phospho-Akt (P-Akt) and total-Akt (T-Akt) in macrophage lysates were immunoblotted. Graph D shows the fold change of P-Akt/T-Akt ratios. Data was analyzed by two-way ANOVA followed by Holm-Sidak pairwise comparison. n=4; *a*, p<0.05 WT vs. PDZK1^{-/-}; *b*, p<0.05 WT vs. Akt1^{-/-}. (E-L): WT and Akt1^{-/-} MPMs were treated with or without tunicamycin in the presence or absence of HDL for 24 hrs. (M): Cell apoptosis was determined by TUNEL staining. Data was analyzed by two-way ANOVA with Holm-Sidak method, n=4, ***p<0.001, vs. untreated control; ### p<0.001, vs. tunicamycin-treated cells.



2.4.5 Bone marrow-specific deletion of PDZK1 increases diet induced atherosclerosis in LDLR^{-/-} mice

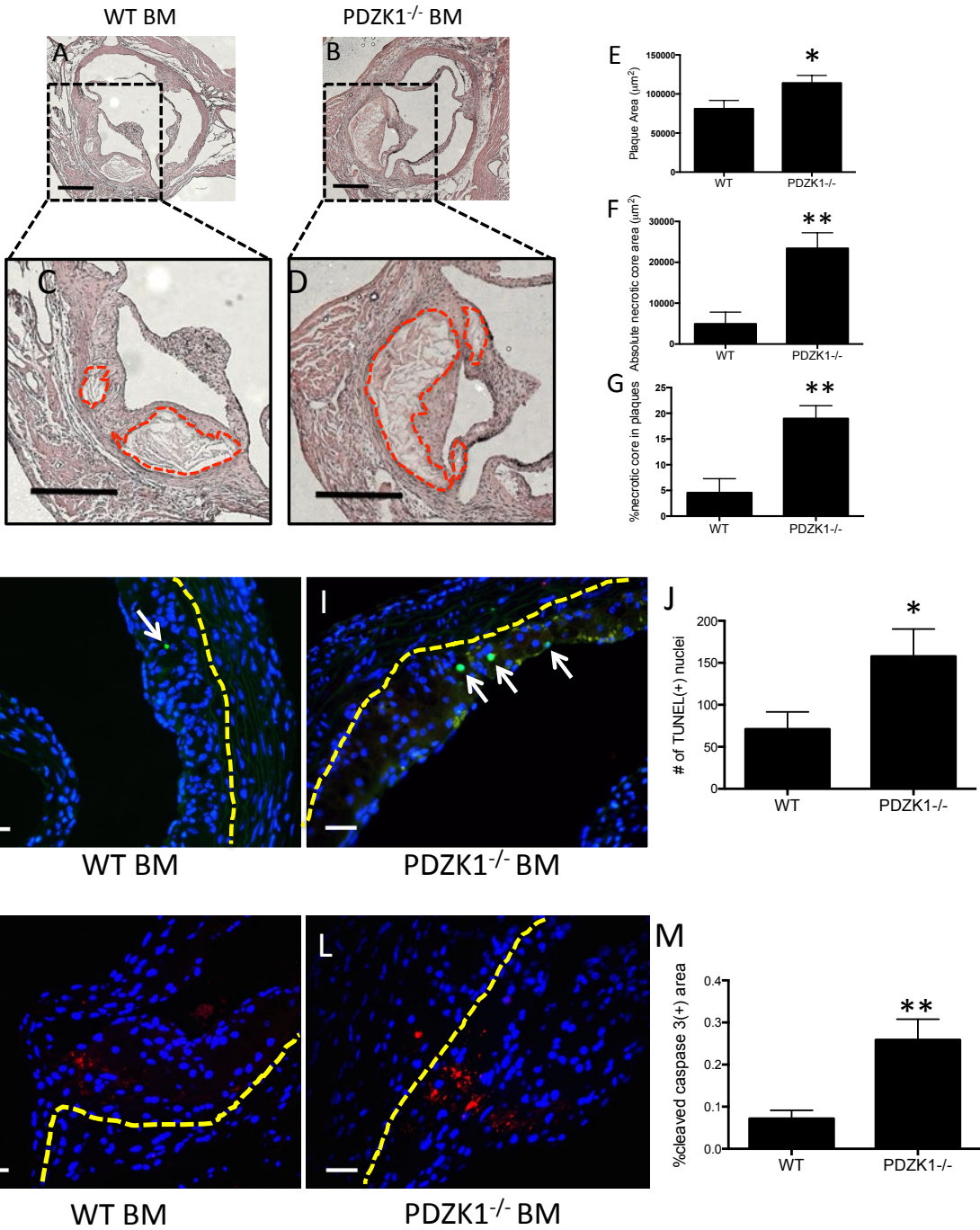
Given the importance of macrophage apoptosis in atherosclerosis development, we hypothesized that deletion of PDZK1 in macrophages might impact the development of atherosclerotic plaques and necrotic cores within those plaques. To test this, we used BM transplantation using male LDLR knockout (KO) mice as recipients and PDZK1KO or control WT mice as BM donors to generate chimeric LDLR KO mice that either lacked PDZK1 expression in bone marrow derived cells including macrophages (LDLR KO^{BM-PDZK1KO} mice) or control LDLR^{-/-} mice with intact PDZK1 in all tissues/cell types (LDLR KO^{BM-WT} mice). After recovery from BM transplantation, mice were placed on a western-type high-fat diet for 10 weeks. BM specific deletion of PDZK1 did not significantly affect plasma total cholesterol or lipoprotein cholesterol profiles, or the levels of circulating inflammatory cytokines, IL-6 or TNF- α (Supplementary Figure 2.4). LDLR KO^{BM-PDZK1 KO} mice did, however, exhibit statistically significant alterations in parameters associated with red blood cells; specifically, reduced hematocrit and mean cell volume (MCV) (Supplementary Figure 2.5A), suggesting small sized red blood cells. The slightly increased red blood cell distribution width (RDW) suggests increased variance in the size of red blood cells. Furthermore, flow cytometry analysis revealed a slight increase in the proportion of leukocytes positive for the B cell marker, B220, with no statistically significant alterations in the proportions of CD3⁺ (T lymphocytes) or CD11b⁺ cells (myeloid cells) (Supplementary Figure 2.5B-H).

LDLR KO mice with BM specific inactivation of PDZK1 exhibited a 40% increase in the average size of atherosclerotic plaques in the aortic sinus compared to LDLR KO mice transplanted with WT bone marrow (Figure 2.6A,B, E). LDLR KO^{BM-PDZK1 KO} mice exhibited more pronounced increases in the sizes of cell free necrotic cores compared to control LDLR KO^{BM-WT} mice, either when the absolute area of necrotic cores (Figure 2.6F) or the area of necrotic core relative to the atherosclerotic plaque cross-sectional area (Figure 2.6G) was measured. To eliminate the potential confounding effect of larger atherosclerotic plaques driving increased necrotic core development, we compare the necrotic core sizes in a subgroup of mice with statistically identical plaque sizes (Supplementary Figure 2.6A,B). Again, LDLR KO^{BM-PDZK1KO} mice exhibited an approximately three-fold greater absolute necrotic core size than did LDLR KO^{BM-WT} mice (Supplementary Figure 2.6C).

Apoptosis in atherosclerotic plaques from the LDLR KO^{BM-PDZK1 KO} and control LDLR KO^{BM-WT} mice was detected by TUNEL staining (Figure 2.6J-L) or immunostaining for activated (cleaved) caspase 3 (Figure 2.6M-O). We detected an approximately 2-fold increase in the number of TUNEL⁺ nuclei in atherosclerotic lesions from the mice transplanted with PDZK1^{-/-} compared to those transplanted with WT BM. Similarly, we detected approximately 3-fold increased activated caspase 3 immunostaining in plaques from mice with BM specific deficiency of PDZK1. No differences were seen in the levels of immunostaining for ER chaperones (anti-KDEL) as a measure of ER stress/UPR activation in plaques (Supplementary Figure 2.7A, B, H), the abundance of macrophages (Mac-3 immunostaining) (Supplementary Figure 2.7C, D,

G) or the numbers of nuclei positive for Ki67, a marker of cellular proliferation (Amano et al., 2014; Robbins et al., 2013; Scholzen and Gerdes, 2000) (Supplementary Figure 2.8). We also did not detect significant differences in recruitment of phagocytic cells into atherosclerotic plaques (Supplementary Figure 2.9), using a well characterized fluorescent bead based assay to label and track circulating phagocytic monocytes and their recruitment into atherosclerotic plaques (Pei et al., 2013; Tacke et al., 2007). Together these results suggest that PDZK1 in macrophages or other BM derived cells does not affect the degree of induction of ER stress in macrophages, or the overall abundance of macrophages, cell proliferation or recruitment of monocytes into atherosclerotic plaques in high fat diet fed LDLR^{-/-} mice.

Figure 2.6: LDLR^{-/-} mice transplanted with PDZK1^{-/-} BM showed enlarged necrotic cores with increased cell apoptosis in atherosclerotic plaques. Hearts from LDLR^{-/-} mice transplanted with WT BM (A) and PDZK1^{-/-} BM (B) were cross-sectioned and stained to visualize plaques and necrotic cores in aortic sinus. A and B are H&E stained aortic sinus from LDLR^{-/-} mice transplanted with WT and PDZK1^{-/-} BM, respectively. C and D are magnified images of necrotic cores (outlined by red dash lines) in atherosclerotic plaques from A and B. Scale bar=200µm. Plaque size (E) and necrotic core size (F) were quantified. The size of necrotic cores was normalized to total plaque area (G). Student t-test or Rank Sum test was performed. n=12, *p<0.05, **p<0.01 PDZK1^{-/-} vs. WT. TUNEL staining of atherosclerotic plaques in aortic sinuses from LDLR^{-/-} mice transplanted with WT BM (H) and PDZK1^{-/-} BM (I). White arrows point to the TUNEL⁺ nuclei in the plaques (green). Sections were counter-stained by DAPI to visualize nuclei (blue). Yellow dash lines outline the arterial walls. Scale bar=20µm. The numbers of TUNEL⁺ nuclei were counted and normalized to the area of nuclei-containing area (J: n=12). Data was analyzed by Rank Sum test. *P<0.05. Cleaved caspase-3 staining (red) of atherosclerotic plaques in aortic sinuses from LDLR^{-/-} mice transplanted with WT BM (K, n=6) and PDZK1^{-/-} BM (L, n=4). DAPI staining shows all the nuclei (blue). Arterial wall is outlined by yellow dash line. Scale bar=20µm. The intensity of cleaved caspase-3 was normalized to the total plaque area (M). Student t-test was performed. **P<0.01.

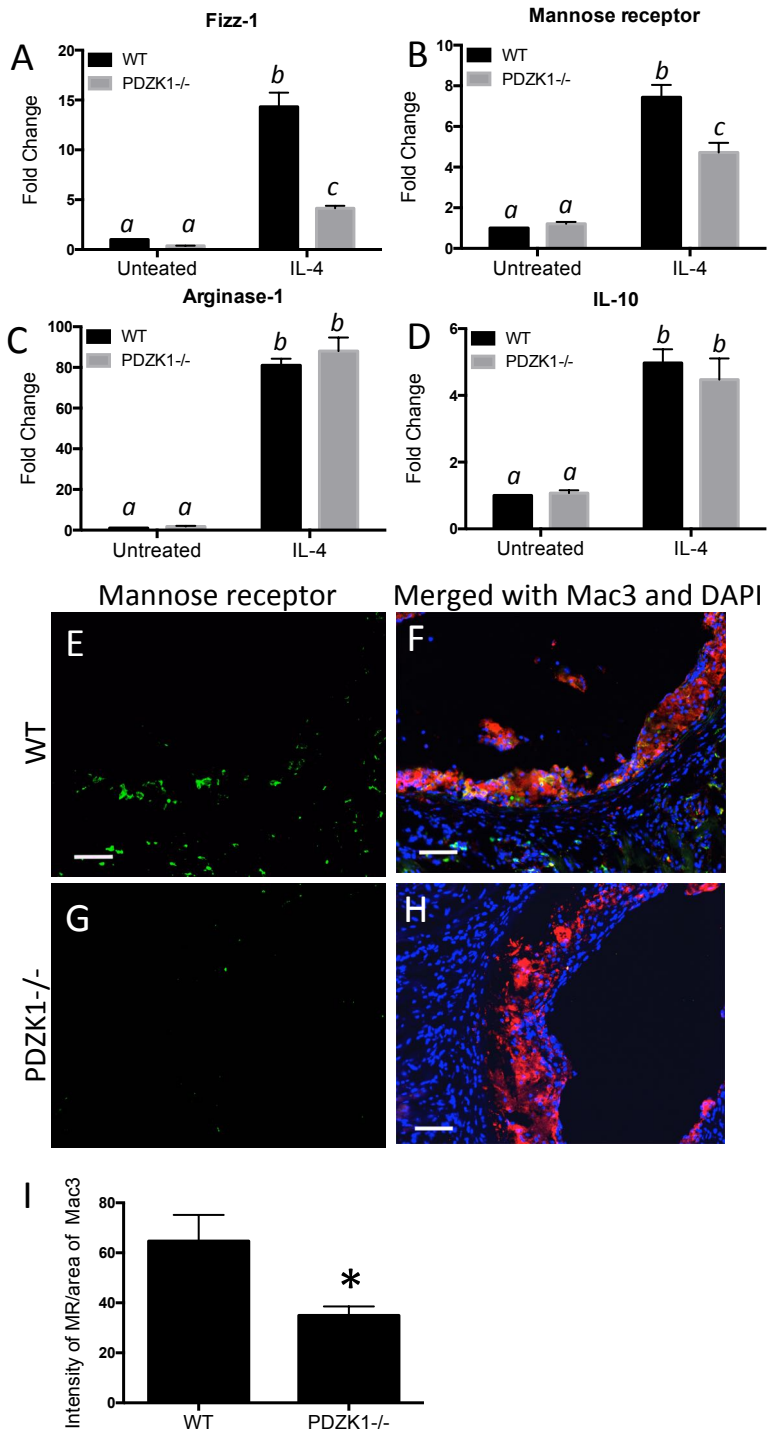


2.4.6 Effects of PDZK1 inactivation on markers of macrophage polarization.

Macrophages are heterogeneous and have been broadly divided into M1, or classically activated macrophages, which promote inflammatory responses, and M2, or alternatively activated macrophages, which attenuate inflammatory responses and promote tissue repair (Murray and Wynn, 2011). Both M1 and M2 macrophages are present in atherosclerotic plaques and appear to influence plaque inflammation, formation and stability, with macrophages in rupture prone areas of unstable plaques exhibiting M1 characteristics while macrophages localized to more stable, lipid rich regions of plaques away from necrotic cores exhibiting M2 characteristics (Leitinger and Schulman, 2013). To examine if PDZK1 deletion affected the capacity of macrophages to be M1 or M2 polarized, we cultured MPMs with either 10 ng/ml of LPS (M1 polarizing) or 10 ng/ml IL-4 (M2 polarizing) for 6 hrs and detected the mRNA levels IL-1 β , IL-6 and MCP-1 (M1 markers), or Fizz-1, mannose receptor, IL-10 or arginase-1 (M2 markers). The transcripts of IL-1 β , IL-6 and MCP-1 were remarkably upregulated by LPS in both WT and PDZK1^{-/-} macrophages (Supplementary Figure 2.10). However, no significant differences were observed between WT and PDZK1^{-/-} macrophages, suggesting that deficiency of PDZK1 may not affect macrophage M1 polarization under the conditions employed. WT and PDZK1^{-/-} macrophages did not differ significantly in the baseline levels of the M2 polarization markers, Fizz-1, mannose receptor, IL-10 or arginase-1. Upon treatment with IL-4, PDZK1^{-/-} macrophages showed attenuated induction of Fizz-1 and mannose receptor compared to WT macrophages. No differences in the levels of induction of arginase-1 and IL-10 were observed, however

(Figure 2.7A-D). Consistent with above results, we detected less mannose receptor immunoreactivity in atherosclerotic plaques from high fat diet fed LDLR KO^{BM-PDZK1} mice than from LDLR KO^{BM-WT} mice (Figure 2.7E-I). These findings suggest that inactivation of PDZK1 partially attenuates macrophage M2 polarization *in vitro* and in atherosclerotic plaques *in vivo*.

Figure 2.7: PDZK1 deficiency partially inhibited the polarization of M2 macrophages. MPMs were treated with 10 ng/ml IL-4 for 6 hrs. RT-PCR was performed to determine the mRNA levels of M2 macrophage markers: (A) Fizz-1, (B) Mannose receptor, (C) Arginase-1, (D) IL-10. Data was analyzed by two-way ANOVA followed by Holm-Sidak method. $N=4$, $p<0.001$ *a* vs. *b* and *b* vs. *c*. Cross-sections of aortic sinus from LDLR^{-/-} mice transplanted with WT (E, F) and PDZK1^{-/-} (G, H) BM were stained for mannose receptor (Green) and Mac-3 (Red) and counterstained with DAPI (Blue). Scale bar=20 μ m. The intensity of mannose receptor staining was normalized to the size of Mac-3 positive area (I: n=6). Data was analyzed by Rank Sum test. * $p<0.05$.



2.5 Discussion

ER stress has been shown to be present at all stages in atherosclerotic plaques (Zhou et al., 2005) and contributes to apoptosis of macrophages in culture (Puthalakath et al., 2007; Scull and Tabas, 2011). Under standard culture conditions, in which serum replete with lipoproteins is used, macrophages appear to be resistant to apoptosis induced by ER stress inducing agents (Figure 2.1). This is consistent with research reported by Tabas and co-workers, who demonstrated that a “second hit” involving engagement of pattern recognition receptors (SR-AI/II, TLR-4, CD36) by their ligands, together with ER stress inducing agents, was required to induce apoptosis in cultured macrophages [reviewed in (Seimon and Tabas, 2009; Tabas, 2009)]. Here, we demonstrate that removal of lipoproteins from the culture medium (by using serum depleted of lipoproteins by KBr gradient centrifugation) was sufficient to sensitize macrophages to apoptosis induced by ER stress inducing agents. We also demonstrated that supplementation of medium prepared with lipoprotein deficient serum with HDL, but not with LDL, was sufficient to confer protection against apoptosis induced by ER stress inducing agents. Similarly, we found that HDL was able to protect macrophages from apoptosis induced by incubation with oxLDL when macrophages were cultured in medium containing serum otherwise depleted of lipoproteins. This is consistent with previous reports that HDL protects endothelial cells against apoptosis induced by multiple factors (Nofer et al., 2001; Suc et al., 1997; Sugano et al., 2000). This HDL specific effect was lost when macrophages were prepared from mice lacking expression of either PDZK1 or Akt1, suggesting that it was due to HDL elicited responses in the

macrophages themselves, rather than direct effects of HDL on the concentration of ER stressors (tunicamycin or thapsigargin) or the activity of oxidized LDL. We saw similar effects in macrophages that were first incubated with acLDL for 24 hrs to induce foam cell formation. Others have previously reported that HDL protection of macrophages against apoptosis mediated by oxLDL or oxysterols involves ABCG1 dependent oxysterole efflux (Baldan et al., 2006; Terasaka et al., 2007). Further research is required to determine if ABCG1 mediated sterol efflux contributes to the PDZK1-dependent HDL mediated protection against apoptosis that we have seen.

Exposure of macrophages or lipid loaded foam cells to HDL did not appear to reduce the extent of ER stress/UPR activation by tunicamycin since HDL treatment had no effect on the degree of induction of either GRP78 protein or CHOP mRNA. Our findings suggest that HDL treatment did not suppress the extent of ER stress when cells were incubated with both HDL and tunicamycin. In contrast, others have reported that when lipid loaded THP-1 macrophages were first treated with tunicamycin for 24 hrs, and then allowed to recover from tunicamycin treatment in the absence or presence of HDL for an additional 24 hrs, cells treated with HDL exhibited lower levels of ER stress markers during the recovery phase (Niculescu et al., 2013). These findings may suggest that while HDL may be able to accelerate recovery from ER stress induced by tunicamycin or other agents, it does not appear to be able to prevent the induction of ER stress from occurring in the first place.

Instead, HDL treatment resulted in increased phosphorylation of Akt in wild type macrophages, but not in macrophages lacking Akt1, suggesting that the increased Akt

phosphorylation was due to activation of Akt1, but not other Akt isoforms (Akt2 or 3). Akt1 is known to play a central role in cell survival signaling [reviewed in (Datta et al., 1999; Hers et al., 2011)]. Consistent with this, Akt1 was required for HDL mediated protection against apoptosis, since HDL was able to protect macrophages prepared from Akt1 expressing mice but not macrophages from Akt1^{-/-} mice from apoptosis induced by tunicamycin (Figure 2.5E-M). We have previously reported that HDL stimulated the directional migration of macrophages via a pathway that involved the HDL receptor, SR-B1, the adaptor protein PDZK1, and Akt1 (Al-Jarallah et al., 2014). Similarly, others have reported that HDL signaling in endothelial cells, leading to Akt activation, involves SR-B1 and PDZK1 activity (Assanasen et al., 2005; Seetharam et al., 2006; Yuhanna et al., 2001; Zhu et al., 2008). In research to be reported elsewhere (Zhang, Al-Jarallah, manuscript in revision), we found that expression of SR-B1 is also required for HDL mediated protection induction of macrophages against apoptosis induced by ER stress inducing agents. Consistent with this, we demonstrate herein that HDL dependent signaling, leading to Akt1 phosphorylation, as well as HDL dependent protection of macrophages against tunicamycin induced apoptosis, both required PDZK1 expression. Consistent with the finding that inactivation of PDZK1 resulted in increased sensitivity to tunicamycin induced apoptosis in the presence of HDL in cultured macrophages, elicited peritoneal macrophages were more sensitive to tunicamycin induced apoptosis *in vitro* both in PDZK1^{-/-} compared to WT mice as well as in WT mice with BM specific deficiency of PDZK1 (Supplementary figure 2.3), suggesting that PDZK1 expression also protects macrophages from tunicamycin induced apoptosis *in vivo*.

Consistent with the increased sensitivity of PDZK1^{-/-} macrophages to apoptosis induced *in vitro* and *in vivo* upon peritoneal injection of tunicamycin, we also observed significantly more apoptosis (TUNEL⁺ nuclei or cleaved caspase 3 positive immunostaining) and bigger necrotic cores in atherosclerotic plaques from LDLR^{-/-} mice transplanted with PDZK1^{-/-} BM (Figure 2.6). These findings suggest that PDZK1 may play a role in protection of macrophages or other BM derived cells in atherosclerotic plaques from apoptosis. We cannot, however, rule out the possibility that the increased evidence of apoptotic cells in atherosclerotic plaques from LDLR^{-/-} mice lacking PDZK1 in bone marrow derived cells may reflect impaired efferocytosis. SR-B1 is known to mediate efferocytosis and it has recently been reported that this involves SR-B1 dependent signaling in macrophages in response to apoptotic cells, that involves a PI3K/Rac1 signaling pathway (Tao et al., 2015). The extent to which PDZK1 is involved in this signaling pathway has, to our knowledge, not been described and remains to be evaluated.

We have also found that inactivation of PDZK1 appears to partially attenuate the extent of M2 macrophage polarization in response to IL-4 treatment, since levels of induction of Fizz-1 and mannose receptor were reduced in IL-4 treated PDZK1^{-/-} compared to WT macrophages. No differences were detected in the levels of IL-4 mediated induction of two other M2 polarization markers: arginase 1 and IL-10, however. Consistent with this, we detected reduced mannose receptor immunofluorescence in atherosclerotic plaques in LDLR^{-/-} mice with bone marrow specific deficiency in PDZK1 compared to those in LDLR^{-/-} mice with intact PDZK1.

We attempted to stain for Fizz-1 as well but found that Fizz-1 immunoreactivity was localized to perivascular tissues and was absent from atherosclerotic plaques themselves (data not shown). Together, this suggests that PDZK1 deficiency partially attenuates macrophage M2 polarization *in vitro* and in atherosclerotic plaques. M2 macrophages have been reported to secrete anti-inflammatory cytokines including IL-10, transforming growth factor (TGF)- β , and IL-1 receptor antagonist (Gordon, 2007; Mantovani et al., 2001). It has also been shown that M2 macrophages play a dominant role in efferocytosis of apoptotic macrophages (Zizzo et al., 2012). The reduced population of M2 macrophages in atherosclerotic plaques may also indicate a defective clearance of dead cells.

The increased levels of apoptotic cells in atherosclerotic plaques of LDLR^{-/-} mice with PDZK1 deficiency in BM derived cells, was accompanied by a substantial ~4-fold increase in average necrotic core sizes and an ~ 50 % increase in atherosclerotic plaque cross sectional area. The increased necrotic core sizes are consistent with increased evidence of apoptosis observed in plaques from mice lacking PDZK1 in BM derived cells and are in agreement with other reports that in advanced atherosclerotic plaques, increased macrophage apoptosis (and/or defective efferocytosis) contributed to increased necrotic core development, while plaque size was less affected (Feng et al., 2003b; Han et al., 2006; Lim et al., 2008). Nevertheless, our findings of increased atherosclerotic plaque sizes, plaque apoptosis and necrotic core sizes in mice lacking PDZK in BM derived cells are consistent with similar effects of BM specific inactivation of SR-B1 in LDLR^{-/-} and apoE^{-/-} mice (Covey et al., 2003; Tao et al., 2015; Zhang et al., 2003).

Despite the increased evidence of apoptosis in atherosclerotic plaques, we did not observe differences in the total macrophage content based on Mac3 staining. Monocyte recruitment and macrophage proliferation have both been reported to contribute to macrophage content in atherosclerotic plaques (Robbins et al., 2013). Consistent with our finding of similar macrophage content in atherosclerotic plaques from LDLR^{-/-} mice with or without BM specific PDZK1 deficiency, we detected no apparent differences in the recruitment of monocytes (using a well characterized fluorescent bead assay for recruitment of circulating monocytes into plaques) or cell proliferation within plaques (numbers of Ki67⁺ nuclei). It is perhaps surprising that we have detected no differences in macrophage content and even slight increases in plaque sizes in mice with BM specific PDZK1 deficiency in the face of increased apoptosis and apparently unaltered renewal of macrophages (proliferation + monocyte recruitment). Perhaps the increased loss of macrophages through apoptosis is balanced by reductions in other pathways of macrophage loss so as to account for the unaltered macrophage content in the presence or absence of PDZK1. Others have reported that macrophage egress from atherosclerotic plaques may be another factor that contributes to macrophage turnover (Moore et al., 2013). We have recently reported that HDL can induce the migration of cultured macrophages in a manner that is dependent on SR-B1 and PDZK1 and involves Akt1 (Al-Jarallah et al., 2014). Specifically, we found that inactivation of PDZK1 gene expression impaired macrophage migration in response to HDL or the sphingosine 1 phosphate receptor agonist FTY720. This raises the possibility that impaired migration in PDZK1 deficient macrophages may contribute to reduced egress from atherosclerotic

plaques and maintenance of total macrophage content within atherosclerotic plaques of LDLR KO mice with BM specific PDZK1 deficiency. Further research is required to determine if this is the case.

In conclusion, we have demonstrated that PDZK1 is required for HDL mediated protection of macrophages from apoptosis *in vitro*, and that inactivation of PDZK1 renders macrophages more susceptible to apoptosis *in vivo* in a peritonitis model. We have also shown that expression of PDZK1 in bone marrow derived cells, which include macrophages, normally contributes to protection against atherosclerotic plaque growth, apoptosis in atherosclerotic plaques, and necrotic core development, and contributes to macrophage M2 polarization. This suggests that macrophage PDZK1 may contribute to atherosclerotic plaque stabilization. *In vitro*, PDZK1 dependent protection against apoptosis involves signaling by HDL, a process which also requires the HDL receptor SR-B1 (Yi Zhang, A. Al-Jarallah, manuscript in revision) and Akt1 signaling. Inactivation of SR-B1 (Tao et al., 2015) or Akt1 (Fernandez-Hernando et al., 2007) are also accompanied by increased macrophage apoptosis in atherosclerotic plaques and increased necrotic core sizes, although in the case of SR-B1, this has been attributed to reduced efferocytosis. Whether HDL signaling contributes to these effects *in vivo* in atherosclerotic plaques remains to be determined. If so then HDL signaling via SR-B1/PDZK1/Akt1 in macrophages may represent an important pathway contributing to suppression of necrotic core formation and plaque stabilization. Consistent with this, we have recently reported that a subset of atherosclerotic plaques in coronary arteries from high fat, high cholesterol diet fed SR-B1^{-/-}/LDLR^{-/-} mice exhibit immunodetectable

staining for CD41, a marker of activated platelets, raising the possibility that these may represent platelet rich thrombi which have developed in these atherosclerotic coronary arteries, possibly reflecting thrombosis after plaque rupture. The extent to which this occurs in PDZK1^{-/-}/apoE^{-/-} mice, which also develop coronary artery atherosclerosis and myocardial fibrosis (Yesilaltay et al., 2009), is not clear and remains to be determined.

2.6 Supplementary Materials and Methods

2.6.1 Foam cell formation and oil red O staining:

Thioglycollate-elicited MPMs were plated and incubated in chamber slides as described above. 24 hrs before experiment, cells were incubated in Medium 1 with 3 % NCLPDS, and acetylated LDL (acLDL: 100 µg protein/ml, Biomedical Technologies Inc, Boston, MA, USA) was added to induce foam cell formation. Then, cells were treated with or without HDL (50 µg protein/ml, Biomedical Technologies Inc, Boston, MA, USA) in the presence or absence of 10 µg/ml tunicamycin for another 24 hrs before fixation with 2% paraformaldehyde. Slides were incubated for 2 hrs with Oil red O staining solution (0.42 g oil red O in 120 ml isopropanol and 90 ml PBS). The macrophage marker F4/80 was detected by rat anti-mouse F4/80 antibody (Abcam, Boston, MA, USA), followed by incubation with goat anti-rat alexa-488 secondary antibody (Invitrogen Life Technologies Inc., Burlington, ON, Canada).

2.6.2 Evaluation of Bone Marrow Reconstitution

10-week old male WT mice were transplanted with WT or PDZK1^{-/-} BM. 8 weeks after bone marrow transplantation, about 200 µl of blood was collected from facial vein of recipient mice. Genomic DNA was extracted using blood genomic DNA isolation kit (Norgen Biotek Corp., Thorold, ON, Canada). PDZK1 wild type and mutant alleles were detected by PCR amplification using primers oIMR5953 (5'-CATTCTACCAAGTTTGAGAGTCAG-3') in the combination with either oIMR5955

(5'- CAGGTGACCATCAGTGTCTTCTC-3') or oIMR5954 (5'- TGCGAGGCCAGAGGCCACTTGTGTAGC-3').

2.6.3 Lipid profile

Plasma was fractioned by gel filtration fast-protein liquid chromatography (FPLC) using an AKTA system with a Tricorn Superose 6 HR10/300 column (GE Healthcare Life Sciences, Baie d'Urfe, QC, Canada). Enzymatic assay kits were used to measure total cholesterol (Thermo Fisher Scientific, Ottawa, ON, Canada) in whole or fractionated plasma (Al-Jarallah et al., 2013; Fuller et al., 2014b).

2.6.4 Enzyme-linked immunosorbent assay

Plasma IL-6 and tumor necrosis factor-alpha (TNF- α) levels were measured by ELISA, using kits from Biolegend (San Diego, CA, USA), following manufacturer's instructions.

2.6.5 Monocyte Recruitment

Monocyte recruitment into atherosclerotic plaques was analyzed by labeling circulating monocytes with fluorescent beads, as previously described (Pei et al., 2013; Tacke et al., 2007). Mice were injected i.v. with 250 μ l PBS containing 1.5×10^{11} Fluoresbrite[®] YG microspheres (0.5 μ m, Polysciences, Inc., Warrington, PA, USA). 24 hrs after injection, mice were euthanized, and hearts were harvested and frozen in

Shandon Cryomatrix (Thermo Fisher Scientific, Ottawa, ON, Canada). 10 μ m transverse cryosections of aortic sinus were stained with oil red O. The number of green beads were counted and quantified as previously described (Pei et al., 2013).

2.6.6 Immunofluorescence staining

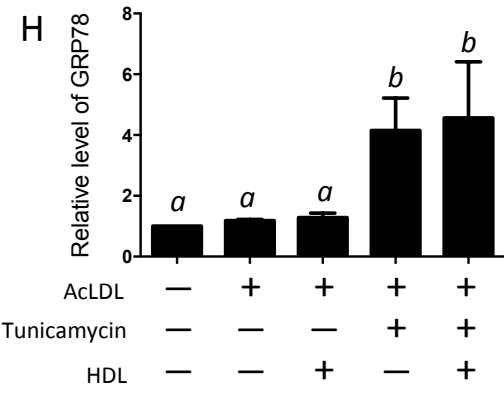
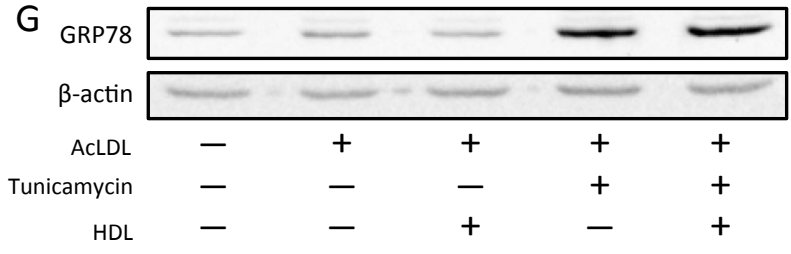
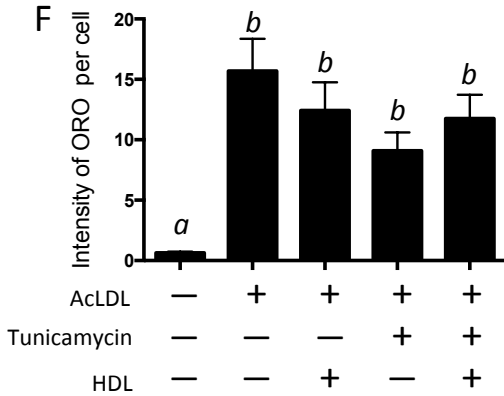
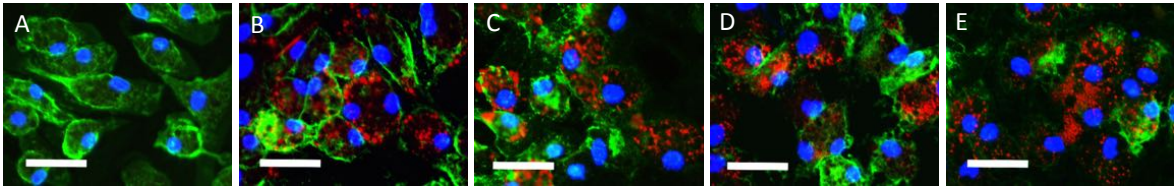
To determine ER stress in macrophages in atherosclerotic plaques, ER chaperone proteins was detected using Vector®M.O.M.[™] immunodetection kit (Vector Laboratories, Inc., Burlingame, CA, USA) with anti-KDEL antibody (Enzo Life Sciences, Inc. Farmingdale, NY, USA). Macrophages were stained with rat anti-mouse CD107b (Mac3) antibody followed by goat anti-rabbit alexa fluoro-488 secondary antibody (Invitrogen Life Technologies Inc., Burlington, ON, Canada). Cell proliferation was determined by staining atherosclerotic plaques with Rabbit monoclonal (SP6) ki67 antibody (Abcam Inc, Toronto, ON, Canada), followed by goat anti-rabbit alexa fluoro-488 secondary antibody (Invitrogen Life Technologies Inc., Burlington, ON, Canada). Sections were also co-stained with DAPI to visualize nuclei. Fluorescent images were captured using a Zeiss Axiovert 200M inverted fluorescence microscope (Carl Zeiss Canada Ltd. Toronto, ON, Canada).

Supplementary Table 2.1: Primer sequences for RT-PCR

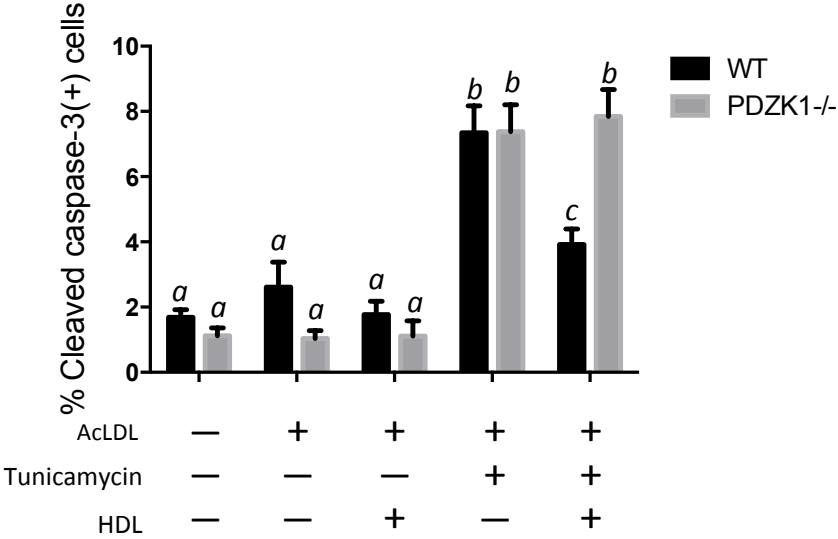
Genes	Primer sequences	References
Arginase-1	Forward: 5'-GCTCAGGTGAATCGGCCTTTT-3'	(Sanson et al., 2013)
	Reverse: 5'-TGGCTTGCGAGACGTAGAC-3'	
Fizz-1	Forward: 5'-CACCTCTTCACTCGAGGGACAGTTG-3'	(Sanson et al., 2013)
	Reverse: 5'-GGTCCCAGTGCATATGGATGAGACC-3'	
IL-10	Forward: 5'-GGTTGCCAAGCCTTATCGGA-3'	(Overbergh et al., 1999)
	Reverse: 5'-ACCTGCTCCACTGCCTTGCT-3'	
Mannose receptor	Forward: 5'-AAACACAGACTGACCCTTCCC-3'	(Stein et al., 1992)
	Reverse: 5'-GTTAGTGTACCGCACCTCC-3'	
CHOP	Forward: 5'-CCTAGCTTGGCTGACAGAGG-3'	(Averous et al., 2004)
	Reverse: 5'-CTGCTCCTTCTCCTTCATGC-3'	
GAPDH	Forward: 5'-ACCACAGTCCATGCCATCAC-3'	(Zhong et al., 2008)
	Reverse: 5'-TCCACCACCCTGTTGCTGTA-3'	
IL-6	Forward: 5'-TAGTCCTTCCTACCCCAATTTC-3'	(Sanson et al., 2013)
	Reverse: 5'-TTGGTCCTTAGCCACTCCTCC-3'	
MCP-1	Forward: 5'-TTCCTCCACCACCATGCAG-3'	(Trojan et al., 2002)
	Reverse: 5'-CCAGCCGGCAACTGTGA-3'	
IL-1 β	Forward: 5'-AGGCAGGCAGTATCACTCATTGT-3'	(Li et al., 2004)
	Reverse: 5'-GGAAGGTCCACGGGAAAGA-3'	

2.7 Supplementary Figures

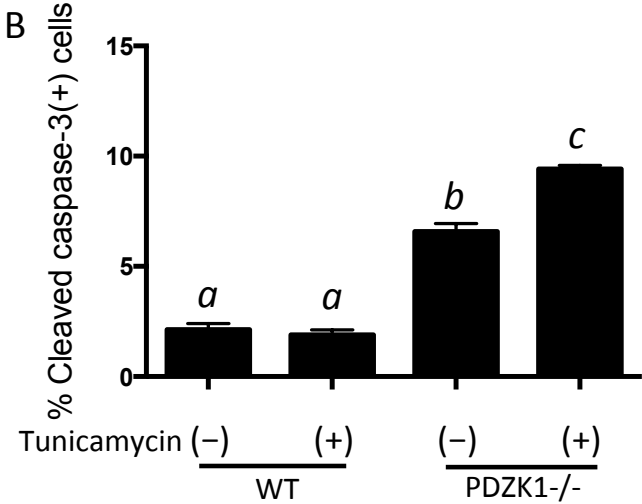
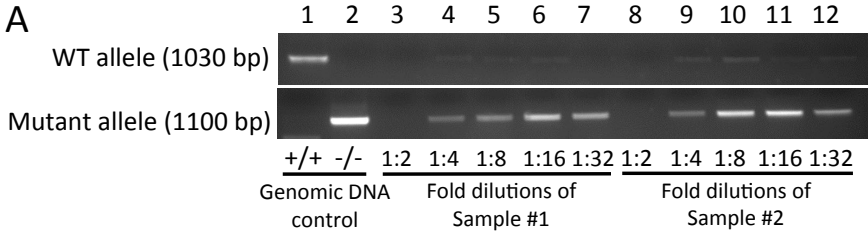
Supplementary Figure 2.1: HDL did not reduce ER stress in foam cells. MPMs were pre-incubated with acLDL (100 $\mu\text{g/ml}$) for 24 hrs and then treated with or without tunicamycin (10 $\mu\text{g/ml}$) in the presence or absence of HDL (50 $\mu\text{g/ml}$) for another 24 hrs. Cells were co-stained with oil red O (red), anti-F4/80 antibody (green) and DAPI (blue). Scale bar=20 μm . The intensity of oil red O per cell was shown in (F: $n\geq 9$). Data was analyzed by one-way ANOVA, and pairwise comparison was done by Dunn's method. $p < 0.05$ *a* vs. *b*. Levels of ER chaperone protein GRP78 were determined by immunoblotting (G, H). Data was analyzed by one-way ANOVA, followed by Tukey test. $n=4$, $p < 0.05$ *a* vs. *b*.



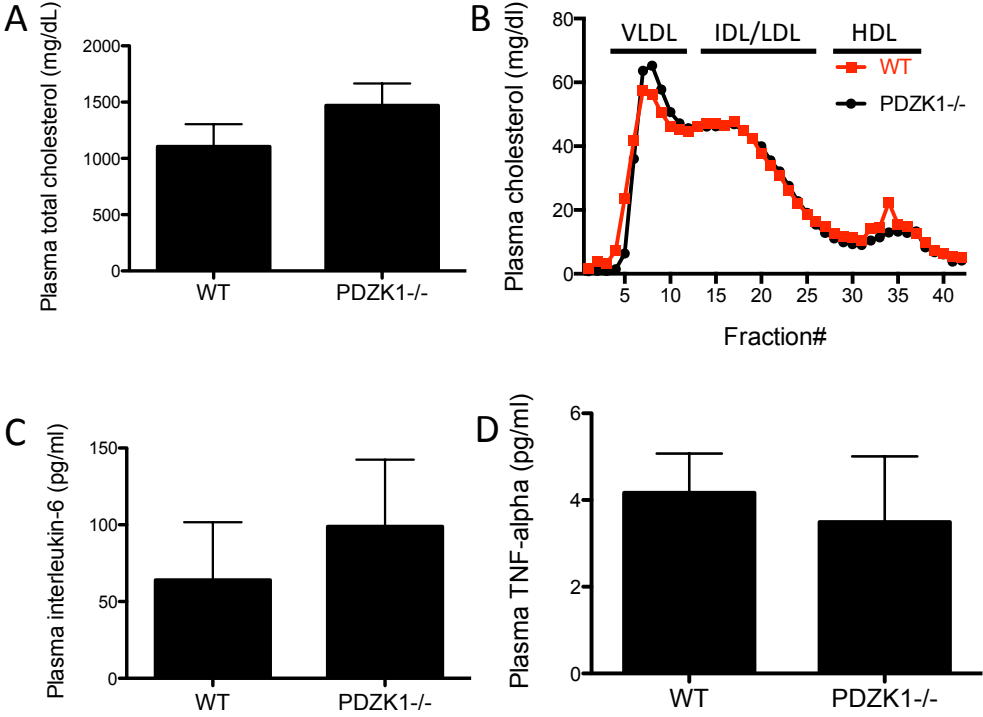
Supplementary Figure 2.2: HDL protected MPM-derived foam cells from tunicamycin-induced apoptosis in a PDZK1-dependent manner. MPMs were pre-incubated with acLDL (100 µg/ml) for 24 hrs and then treated with or without tunicamycin (10 µg/ml) in the presence or absence of HDL (50 µg/ml) for another 24 hrs. Then, cells were fixed and stained with anti-cleaved caspase-3 antibody and DAPI. The percentage of cleaved caspase-3 (+) cells was quantified and analyzed by two-way ANOVA, followed by Holm-Sidak method. $n \geq 3$, $p < 0.001$ a vs. b; $p < 0.001$ b vs. c; $p < 0.05$ a vs. c.



Supplementary Figure 2.3: PDZK1^{-/-} BM derived macrophages are more sensitive than WT BM derived macrophages to tunicamycin-induced apoptosis in LDLR^{-/-} mice. (A): 8 weeks post BM transplantation, blood cell DNA was genotyped for WT (upper panel) and mutant (lower panel) PDZK1. Lane 1 and 2 show the genotyping of DNA from WT and PDZK1^{-/-} mice respectively. The samples shown in lanes 3-7 and lanes 8-12 are collected from 2 LDLR^{-/-} mice transplanted with PDZK1^{-/-} BM. DNA templates were fold-diluted to optimize the loading amount. (B): 8 weeks after BM transplantation, recipient mice were intraperitoneally injected with 10 % thioglycollate to recruit macrophages. Macrophage apoptosis was induced *in vivo* by tunicamycin. 24 hrs later, macrophages were collected and subjected to CD11b, cleaved caspase-3 and propidium iodide staining. Cell apoptosis was quantified by flow cytometry. $n \geq 3$, $p < 0.001$ *a* vs. *b*; $p < 0.001$ *b* vs. *c*.



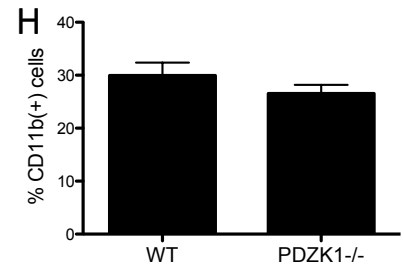
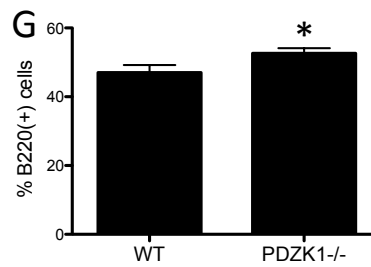
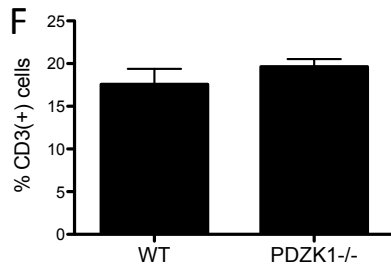
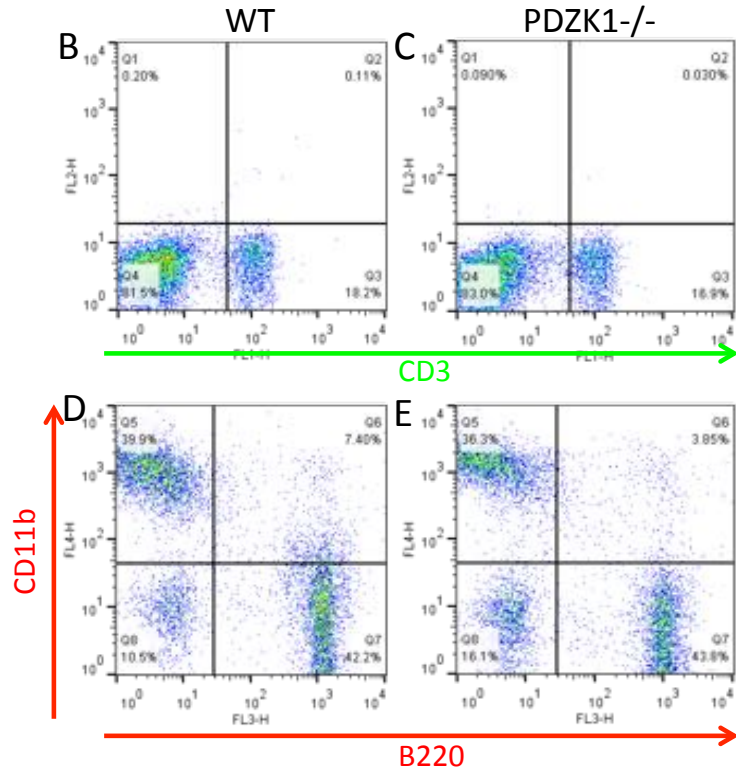
Supplementary Figure 2.4: PDZK1 deficiency in BM-derived cells did not affect lipid profile or systemic inflammatory markers in LDLR^{-/-} mice. (A): Plasma total cholesterol levels from LDLR^{-/-} mice transplanted with WT and PDZK1^{-/-} BM was determined by using enzymatic kit. (n=6, 4; p>0.05 by student *t* test). (B): Plasma lipoproteins were fractionated by FPLC, and total cholesterol in each fraction was determined. Representative profiles from WT and PDZK1^{-/-} BM transplanted mice are shown. The ranges of VLDL, IDL/LDL and HDL lipoproteins were determined by human lipoprotein controls. (C, D): Plasma levels of IL-6 (n=6, 4; p>0.05 by Rank Sum test) and TNF- α (n=6, 4; p>0.05 by student *t* test) were determined by ELISA kits.



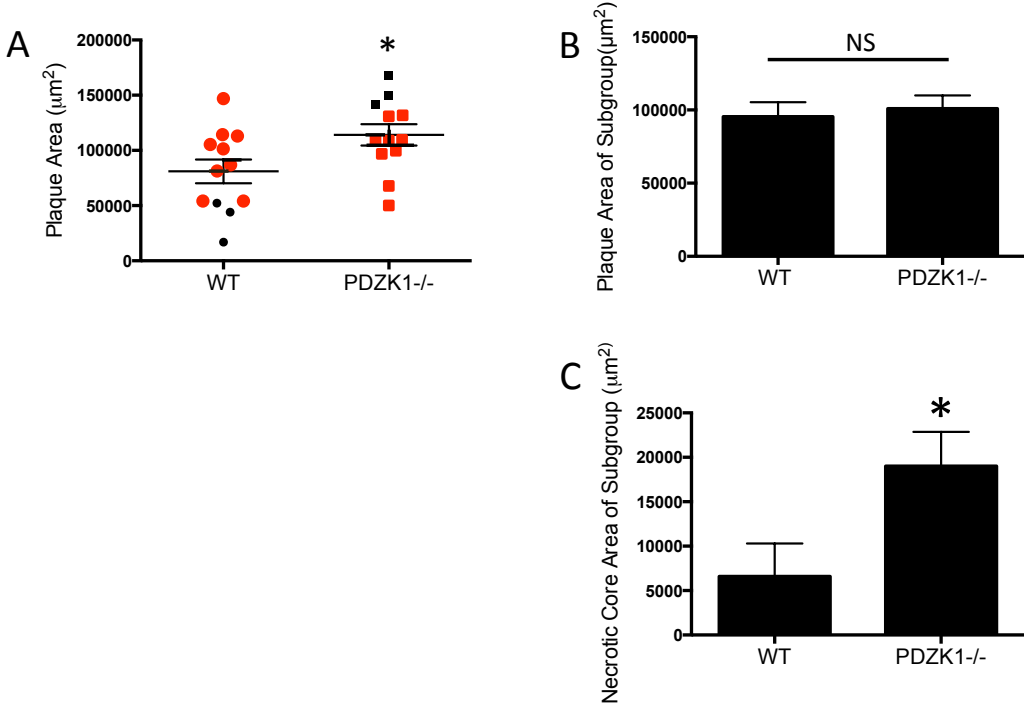
Supplementary Figure 2.5: Blood cell analysis of LDLR^{-/-} mice with PDZK1 deficiency in BM-derived cells. (A): Characteristics of Red blood cells were analyzed by Hemavet Multi-species Hematology System. Statistical analysis was done by Student *t* test (n=3, 4). (E-H): White blood cell populations were determined by flow cytometry. The percentages of CD3⁺ cells (B, C, F), B220⁺ cells (D, E, G) and CD11b⁺ cells (D, E, H) in the mice transplanted with WT and PDZK1^{-/-} BM were analyzed by Student *t* test. n=9, 11, *p<0.05.

A

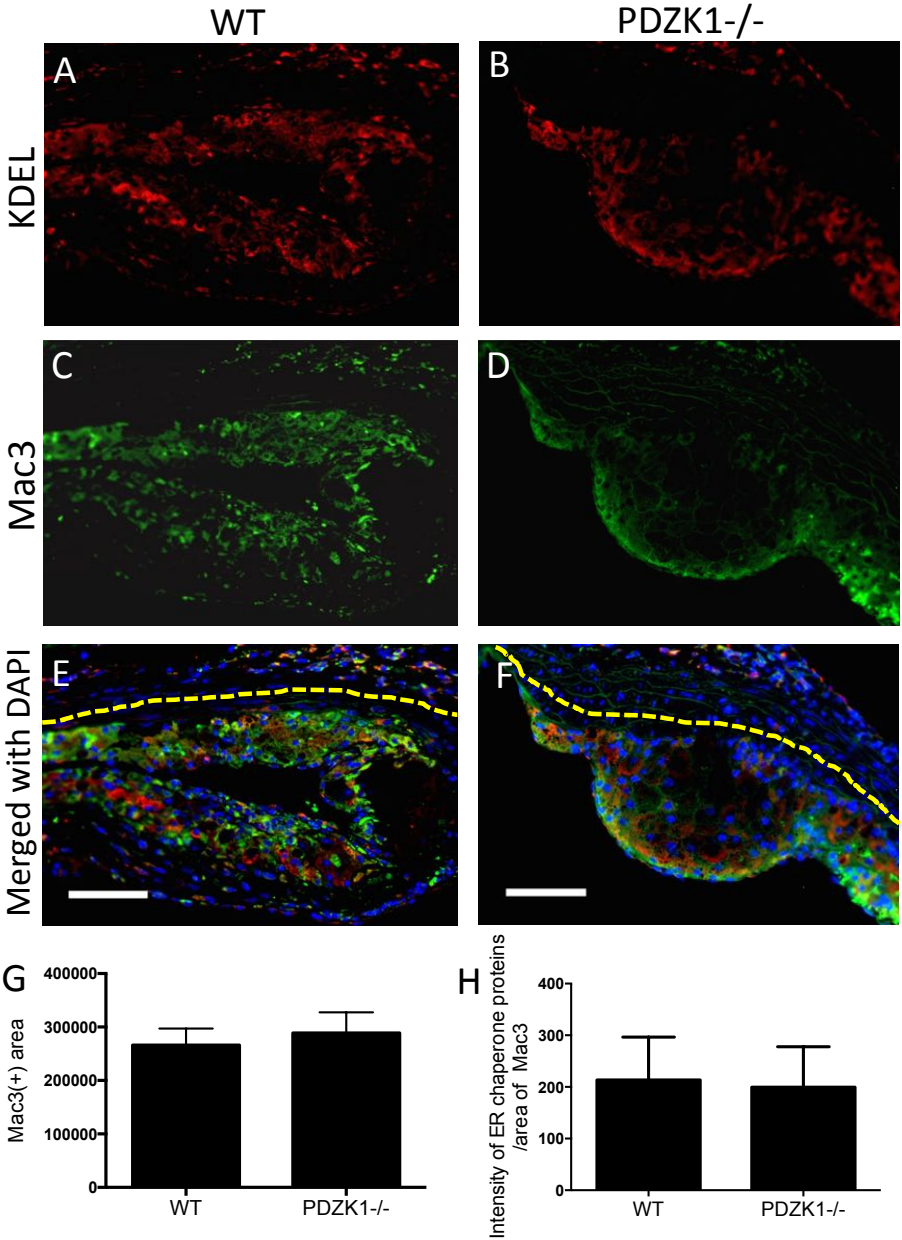
	WT	PDZK1 ^{-/-}	P
Hematocrit(%)	46.03±3.76	36.83±1.82	<0.001
MCV (fL)	50.13±0.4	44.2±0.68	<0.001
RDW (%)	17.5±0.17	19.03±0.49	<0.01



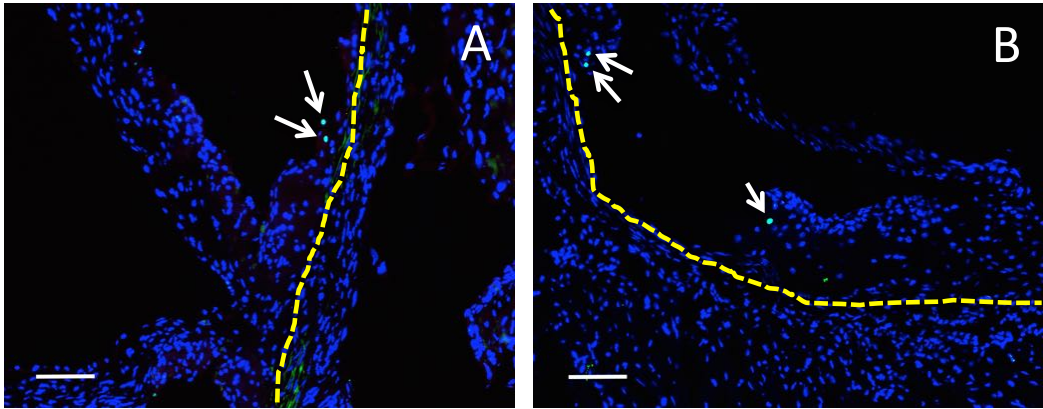
Supplementary Figure 2.6: Quantification of plaque area and necrotic core area in a subgroup of LDLR^{-/-} mice transplanted with WT and PDZK1^{-/-} BM. A: plaque sizes in the LDLR^{-/-} mice transplanted with WT and PDZK1^{-/-} BM in Figure 2.6E were shown as scatter plots. In order to get a subgroup with similar plaque sizes, 3 values in each group (black dots in WT group and black squares in PDZK1^{-/-} group) were removed. The rest samples (n=9: red dots in WT group and red squares in PDZK1^{-/-} group) were graphed in B. There is no significant difference in the total plaque area in these subgroups (p>0.05 by Student *t*-test). Quantification of necrotic core area in the subgroups was shown in C. *p<0.05 by Rank Sum test.



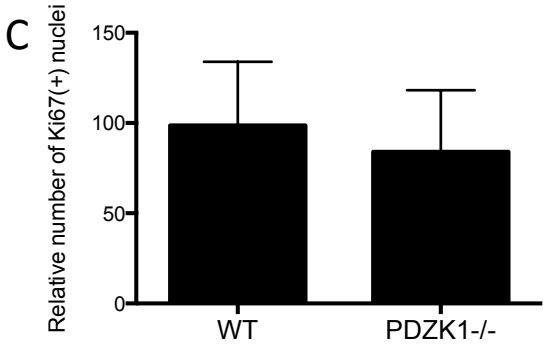
Supplementary Figure 2.7: LDLR^{-/-} mice transplanted with WT and PDZK^{-/-} BM showed similar levels of ER stress in plaque macrophages. Cross-sections of aortic sinus atherosclerotic plaques from LDLR^{-/-} mice transplanted with WT (A, C, E, n=6) and PDZK^{-/-} (B, D, F, n=4) BM were co-stained with anti-KDEL antibody (Red), anti-Mac3 antibody (Green) and DAPI. The Mac-3⁺ area was quantified. The intensity of ER chaperone proteins was normalized to the size of Mac-3⁺ area (E). Data was analyzed by Student *t* test. $p > 0.05$.



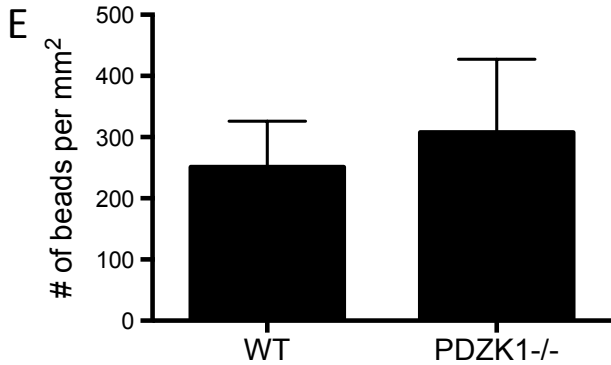
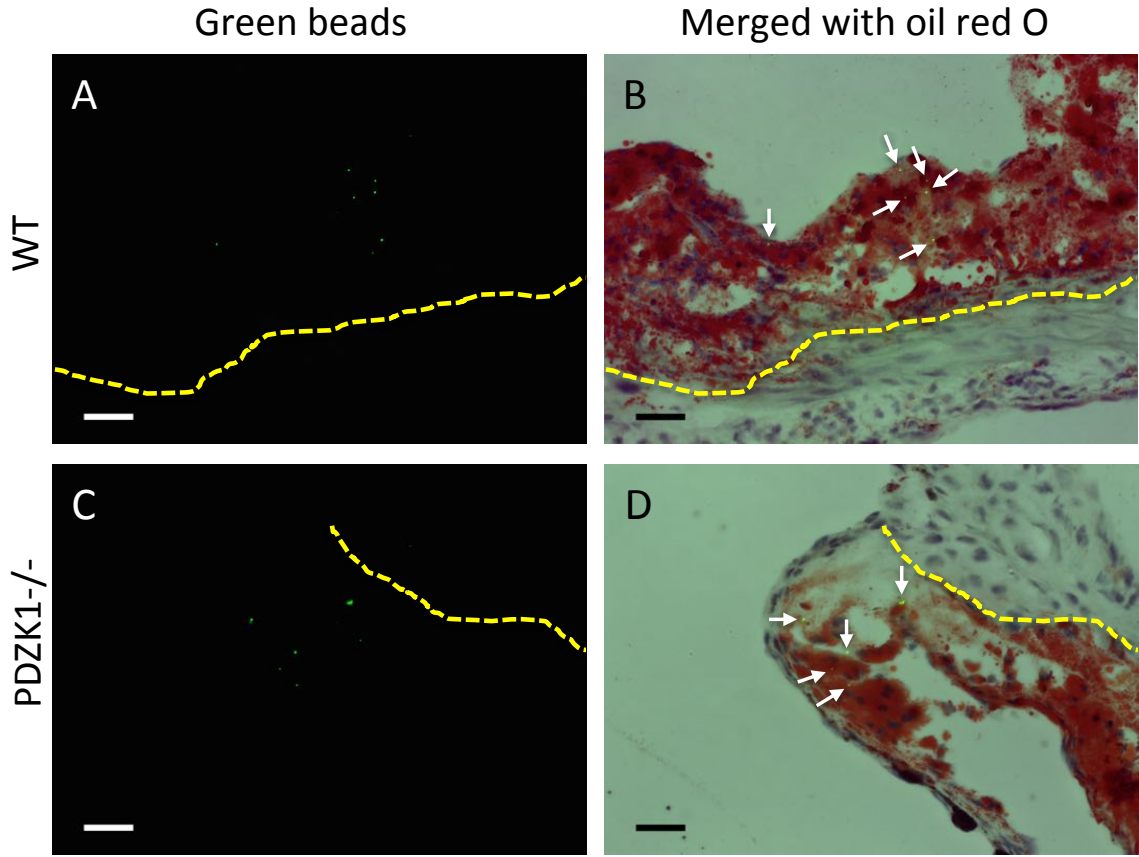
Supplementary Figure 2.8: LDLR^{-/-} mice transplanted with PDZK1^{-/-} BM and WT BM showed similar levels of cell proliferation in aortic sinus atherosclerotic plaques. The aortic sinus cross-sections were stained for Ki67⁺ nuclei (green, white arrows point to) and counter-stained with DAPI (blue). Arterial wall is outlined by yellow dash line. A: Sections from mice transplanted with WT BM (n=8). B: Sections from mice transplanted with PDZK1^{-/-} BM (n=10). Scale bar=50µm. C: The number of Ki67⁺ nuclei in atherosclerotic plaques was normalized to total plaque area. Data was analyzed by Rank Sum test. p>0.05.



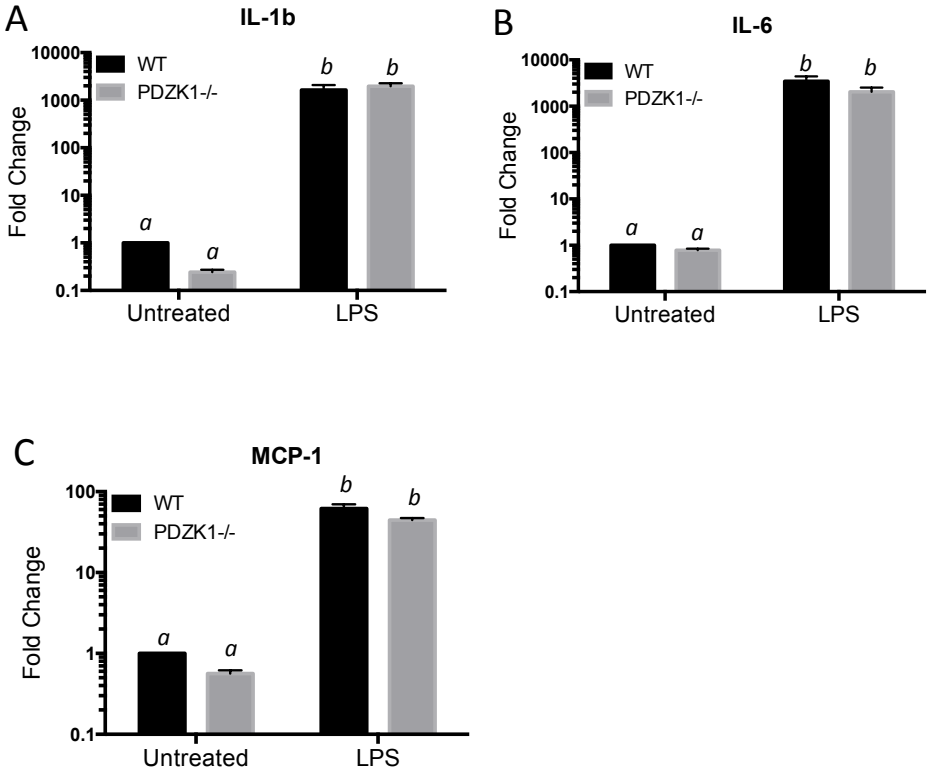
WT PDZK1^{-/-}



Supplementary Figure 2.9: LDLR^{-/-} mice transplanted with PDZK1^{-/-} and WT BM showed similar numbers of recruited monocytes into aortic sinus atherosclerotic plaques. BM transplanted LDLR^{-/-} mice were injected with FITC-Conjugated plain microspheres 24hrs before harvesting. The aortic sinuses were cross-sectioned and stained with oil red O. The green beads in atherosclerotic plaques from mice transplanted with WT BM and PDZK1^{-/-} BM were shown in A (n=9) and C (n=10), respectively, and merged with oil red O staining (B and D). The numbers of green beads were normalized to the total area of plaques (E). Data was analyzed by Rank Sum test. p>0.05.



Supplementary Figure 2.10: PDZK1 deficiency did not affect M1 macrophage polarization. MPMs were treated with 10 ng/ml LPS for 6 hrs. RT-PCR was performed to determine the mRNA levels of M1 macrophage markers: (A) IL-1 β , (B) IL-6, (C) MCP-1. Data was analyzed by two-way ANOVA followed by Holm-Sidak method. N=4, $p < 0.001$ *a* vs. *b*.



CHAPTER III

Inactivation of Bcl-2 homology (BH)-3 only protein Bim protects macrophages from apoptosis and inhibited atherosclerosis and plaque necrosis *in vivo*

Author list: Pei Yu, Leticia Gonzalez Jara and Bernardo L. Trigatti

PREFACE

This manuscript is in the process of being submitted. This project was designed by Pei Yu and Professor Bernardo Trigatti in 2013. All animals were set up by Pei Yu. Specimens were collaboratively collected by Pei Yu and Leticia Gonzalez. The majority data was collected and analyze by Pei Yu. Leticia Gonzalez assisted with bone marrow transplantation, and collected plasma cholesterol and inflammatory cytokine data (Figure 3.5 and 3.9). All data was interpreted by Pei Yu with guidance from Professor Trigatti. This manuscript was written by Pei Yu with guidance from Professor Trigatti.

3.1 Abstract

Macrophage apoptosis contributes to necrotic core formation in atherosclerotic plaques, which is one of the main characteristics of vulnerable plaques. Endoplasmic reticulum (ER) stress triggers macrophage apoptosis by increasing the Bcl-2 homology (BH)3-only protein Bim. In contrast, we showed in this study that high-density lipoprotein (HDL) reduced Bim protein levels in ER-stressed mouse peritoneal macrophages without altering Bim transcription, suggesting that HDL regulated Bim expression at post-transcriptional level. Consistent with this, ER stress induced apoptosis was attenuated in $Bim^{-/-}$ macrophages, and HDL treatment did not provide further protection, implicating Bim as a downstream factor in the HDL signaling pathway. A deficiency of apoA-I, the major apolipoprotein of HDL, reduced HDL levels and increased diet induced atherosclerotic plaque formation and the formation of necrotic cores within plaques in $LDLR^{-/-}$ mice. The deficiency of Bim in bone marrow derived cells, on the other hand, reduced atherosclerotic plaque sizes and inhibited necrotic core formation in high fat diet fed $apoA-I^{-/-}/LDLR^{-/-}$ mice. Decreased plasma cholesterol and reduced proportions of circulating $CD11b^{+}$ cells were also observed in the mice transplanted with $Bim^{-/-}$ bone marrow, which may contribute to the reduction in atherosclerotic plaque size. This study demonstrates for the first time that reduction of Bim levels can reduce atherosclerosis plaque size and protect against the development of large necrotic cores within atherosclerotic plaques.

3.2 Introduction

It has been shown both in humans and in animal models that atherosclerosis initiates with the subendothelial accumulation of apolipoprotein (apo)B-containing lipoproteins, leading to their accumulation within atherosclerotic plaques and modification by a variety of pathways, including oxidation (Moore and Tabas, 2011). Macrophages, which derive from circulating monocytes, play important roles in the clearance of modified, apoB-containing lipoproteins in the artery wall (Moore and Tabas, 2011). However, with the progress of the atherosclerosis, increasing numbers of lipid-loaded macrophages (foam cells) are retained in the subendothelium and exposed to a number of death inducers, including oxidized low-density lipoprotein (LDL), tumor necrosis factor- α (TNF- α), Fas ligand, hypoxia and intracellular accumulation of free cholesterol (FC) (Seimon and Tabas, 2009). Increased macrophage apoptosis and impaired efferocytosis in advanced plaques have been proposed to lead to secondary macrophage necrosis and contribute to the development of a large lipid rich, cell free necrotic core (Seimon and Tabas, 2009; Tabas, 2005). Large necrotic cores in atherosclerotic plaques increase the risk of plaque rupture and acute thrombosis and necrotic core size is closely related to the incidence of myocardial infarction (Falk et al., 1995; Moore and Tabas, 2011; Sakakura et al., 2013).

Sustained endoplasmic reticulum (ER) stress followed by unfolded protein response (UPR) activation is a relatively well-established mechanism causing apoptosis of macrophages in culture (Puthalakath et al., 2007; Scull and Tabas, 2011; Seimon and Tabas, 2009). Increased ER stress has also been detected in vulnerable atherosclerotic

plaques from human coronary arteries and mouse aortic sinus (Myoishi et al., 2007; Zhou et al., 2005). In contrast, pharmacological reduction of ER stress using small molecules, such as 4-phenyl butyric acid (PBA) and tauroursodeoxycholic acid (TUDCA) has been shown to decrease plaque sizes in atherogenic mouse models (Dong et al., 2010; Erbay et al., 2009). Similarly, disruption of UPR pathway by inactivation of CEBP homologous protein (CHOP) significantly reduced plaque size and necrotic core formation in advanced plaques (Thorp et al., 2009; Tsukano et al., 2010).

BH-3 only proteins (BOPs), including Bid, Noxa, Puma, bad and Bim, constitute a subgroup of the Bcl-2 protein family, and are essential in promoting apoptosis in various cell types (Bouillet et al., 1999; Jeffers et al., 2003; Kiryu-Seo et al., 2005; Ranger et al., 2003; Yin et al., 1999). Among them, Bim, which is encoded by the *Bcl2l1* gene, is a critical initiator of apoptosis in hematopoietic cells (Bouillet et al., 1999). ER stress in a variety of cell types including macrophages was shown by Puthalakath *et al.* to increase Bim protein levels by two pathways: upregulation of CHOP-mediated Bim gene transcription; and protein phosphatase 2A (PP2A) mediated dephosphorylation of Bim, preventing its ubiquitination and proteasomal degradation (Puthalakath et al., 2007). Consistent with this, they found that peritoneal macrophages, thymocytes and MCF-7 cells became refractory to ER stressor (tunicamycin or thapsigargin) induced apoptosis, when Bim was knocked out or silenced by using siRNA (Puthalakath et al., 2007).

We have previously reported that HDL protects cultured macrophages from apoptosis induced by ER stress in a manner dependent on the HDL receptor scavenger

receptor class B, type 1 (SR-B1), SR-B1's adapter protein PDZK1 and Akt1. However, HDL-treatment did not prevent ER stress or upregulation of CHOP (Zhang and Al-Jarallah, manuscript in revision; Chapter 2: Yu and Fernandes, manuscript in preparation), suggesting that the HDL-initiated signaling may interfere with the apoptotic pathway downstream of ER stress. We now demonstrate that HDL treatment of macrophages triggers a decrease in levels of Bim protein, and that this underlies HDL mediated protection of macrophages from apoptosis. We also demonstrate that a reduction of HDL levels in LDLR^{-/-} mice by inactivation of apoA-I, HDL's major apolipoprotein is accompanied by increased diet induced development of necrotic cores within atherosclerotic plaques and that bone marrow selective inactivation of Bim in apoA-I^{-/-}LDLR^{-/-} mice reduces both diet induced atherosclerosis and necrotic core formation, consistent with the notion that targeting Bim in macrophages in atherosclerotic plaques may contribute to plaque stabilization by reducing macrophage apoptosis.

3.3 Materials and Methods

3.3.1 Materials

All the materials were purchased from Sigma Aldrich (St. Louis, MO, USA) unless otherwise stated.

3.3.2 Mice

All procedures involving mice were approved by the McMaster University Animal Research Ethics Board and were in accordance with the guidelines of the Canadian Council on Animal Care. All mice were on a C57BL/6J background. C57BL6/J, $Bim^{-/-}$, $apoA-I^{-/-}$ and $LDLR^{-/-}$ mice were purchased from the Jackson Laboratory (Bar Harbor, ME, USA). $apoA-I^{-/-}/LDLR^{-/-}$ and control $apoA-I^{+/+}/LDLR^{-/-}$ mice were generated by breeding $apoA-I^{-/-}$ mice with $LDLR^{-/-}$ mice to generate double heterozygous offspring. These were mated to $LDLR^{-/-}$ mice to generate $apoA-I^{+/-}/LDLR^{-/-}$ offspring. Male and female $apoA-I^{+/-}/LDLR^{-/-}$ mice were mated together to generate founder $apoA-I^{-/-}/LDLR^{-/-}$ and $apoA-I^{+/+}/LDLR^{-/-}$ mice, which were used to establish the lines of $apoA-I^{-/-}/LDLR^{-/-}$ and $apoA-I^{+/+}/LDLR^{-/-}$ mice used in this study. All mice were bred and housed in the Thrombosis and Atherosclerosis Research Institute animal facility in ventilated cages with automatic watering and had free access to normal chow (#2018 Teklad 18% protein diet, Harlan Laboratories, Mississauga, ON, Canada). Atherosclerosis was induced by feeding mice a western type, high-fat diet (containing 21 % butter fat and 0.15 % cholesterol, #112286, Dyets Inc., Bethlehem, PA, USA) for 10 weeks.

3.3.3 Macrophage culture and apoptosis induction

Peritoneal macrophages were elicited by i.p. injection of 1 ml of sterile 10 % thioglycollate. Four days later, mice were euthanized by CO₂ asphyxiation, and peritoneal cells were collected by lavage of the peritoneal cavity with 10 ml of PBS containing 1 mM EDTA. Cells were washed, counted and cultured in DMEM containing 2mM L-glutamine and 50 U/ml penicillin/50 µg/ml streptomycin (Medium 1) with 10% FBS. Before each experiment, cells were pre-incubated in Medium 1 with 3 % newborn calf lipoprotein deficient serum (NCLPDS), instead of 10 % FBS, for 24 hrs. Then, mouse peritoneal macrophages (MPMs) were treated with 10 µg/ml tunicamycin or 5mM thapsigargin in the presence or absence of 50 µg/ml HDL for another 24 hrs.

3.3.4 Detection of apoptotic cells

Cultured cells were fixed in 2 % paraformaldehyde for 20 min and washed 3 times for 5 min each with PBS, before TUNEL or cleaved caspase-3 staining was performed. TUNEL staining was carried out using S7110 ApopTag® fluorescein *in situ* apoptosis detection kit (Millipore Canada Ltd., Etobicoke, ON, Canada), following the manufacture's instructions. For cleaved caspase-3 staining, fixed cells were incubated in 3 % goat serum at room temperature for 1 hr, and then incubated with anti-cleaved caspase-3 (Asp175) antibody (1:200 in Blocking Solution, Cell Signaling, Danvers, MA, USA) at 4°C overnight. After washing as described above, the cells were

incubated with Alexa Fluor 488 goat anti-rabbit IgG (H+L) antibody (1:500 in PBS, Life Technologies Inc., Burlington, ON, Canada). Cells were then counter-stained with 300 nM 4',6-diamidino-2-phenylindole (DAPI) to visualize nuclei. Fluorescent images were captured using a Zeiss Axiovert 200M inverted fluorescence microscope (Carl Zeiss Canada Ltd. Toronto, ON, Canada).

3.3.5 Real-time PCR

Total RNA from cultured macrophages was extracted and purified using the RNeasy Mini Kit (Qiagen Inc., Toronto, ON, Canada) and quantified using a SpectraMax Plus384 spectrophotometer (Molecular Devices, Sunnyvale, CA, USA). cDNA synthesis was performed from 1 µg of total RNA using QuantiTect reverse Transcription Kit (Qiagen Inc., Toronto, ON, Canada). Real-time quantitative PCR was performed using Platinum Sybr Green dye (Invitrogen Life Technologies Inc., Burlington, ON, Canada) in an Applied Biosystems 7300 Real Time PCR system (Applied Biosystems, Foster City, CA, USA) with default settings. Bim primers, which amplify a common fragment in all three Bim isoforms (Bim_{EL}, Bim_L and Bim_S) were synthesized by Invitrogen Life Technologies (Burlington, ON, Canada) and the sequences are: Forward: 5'-CGA CAG TCT CAG GAG GAA CC-3'; Reverse: 5'-CCT TCT CCA TAC CAG ACG GA-3' (Lin et al., 2013). The primer sequences for control GAPDH are: Forward: 5'-ACC ACA GTC CAT GCC ATC AC-3'; Reverse: 5'-TCC ACC ACC CTG TTG CTG TA-3'

3.3.6 Western Blot

MPMs were lysed in the presence of protease inhibitors. Cell lysates were centrifuged to isolate the supernatant. Protein concentrations were determined using the BCA protein assay kit (Pierce Biotechnology, Rockford, IL, USA). Approximately 30 μg proteins were subjected to SDS-PAGE, using 15 % acrylamide for the separation of Bim (EL: 23kD; L: 15kD; S: 12kD), Mcl-1 (35kD) and β -actin (38kD). Proteins were transferred to PVDF membranes, and then blocked in 5 % skim milk in TBS containing 0.1 % Tween-20 (TBS-T: Blocking Solution) for 1 hr at room temperature. Immunoblotting was performed by incubating the PVDF membrane with rabbit anti-Bim antibody (1: 1000 in 3 % BSA, Cell Signaling, Danvers, MA, USA) at 4°C overnight, followed by washing 3 times for 10 min each with TBS-T. Then, membranes were incubated with the peroxidase affipure donkey anti-rabbit IgG (H+L) (1:10000 in Blocking Solution, Jackson ImmunoResearch, West Grove, PA, USA) at room temperature for 1 hr. After washing as described above, the peroxidase on the membranes was detected using the Amersham Enhanced Chemiluminescence (ECL) kit (GE Healthcare Life Sciences, Baie d'Urfe, QC, Canada). The bands were imaged and analyzed using a Gel Doc instrument (Bio-Rad Laboratories, Hercules, CA, USA). For sequential immunoblotting, membranes were incubated in stripping buffer for 15 min and then re-blocked in Blocking Solution for 1 hr at room temperature, followed by membrane washing as described above. Then, membranes were incubated with rabbit anti-Mcl-1 antibody (1: 1000 in 3 % BSA, Cell Signaling, Danvers, MA, USA) at 4°C overnight. The incubation with secondary antibody and the detection of protein bands

were as described above. Finally, HRP- conjugated anti- β -actin antibody (1:5000 in 3 % BSA, Cell Signaling, Danvers, MA, USA) was incubated with membranes at room temperature for 1hr. Then, the membranes were washed, and the protein bands were imaged as described above.

3.3.7 Bone Marrow Transplantation (BMT)

BM cells were collected from the femurs and tibias of male donor mice as described previously (Covey et al., 2003). Male apoA-I^{-/-}/LDLR^{-/-} mice at 10 weeks of age were lethally irradiated using a Gammacell 3000 small animal irradiator (Best® Theratronics Ltd. Ottawa, ON, Canada) at a split dose of 1400 rad and immediately injected i.v. with 3×10^6 BM cells. After BMT, mice received normal chow diet and water supplemented with antibiotics as described previously (Covey et al., 2003). Four weeks post-BMT, recipients were fed western type diet for 10 weeks to induce atherosclerosis.

3.3.8 Atherosclerotic Lesions

Mice were euthanized under isoflurane anesthesia by thoracotomy. Blood was collected by cardiac puncture. Tissues were harvested and weighed. Hearts were fixed in 10 % formalin overnight before embedding in Shandon Cryomatrix (Thermo Fisher Scientific, Ottawa, ON, Canada). Transverse, 10 μ m thick sections of the aortic sinus were collected using a Shandon CryotomeTM (Thermo Fisher Scientific, Ottawa, ON,

Canada). Sections where the three valve leaflets were intact were stained for lipid with oil red O and nuclei were counterstained with hematoxylin. Bright field images were captured using a Zeiss Axiovert 200M inverted microscope (Carl Zeiss Canada Ltd., Toronto, ON, Canada). The necrotic core was defined as acellular area (negative for hematoxylin staining). The total plaque and necrotic core areas were quantified morphometry using Axiovision 3.1.2.1 software (Carl Zeiss Canada Ltd., Toronto, ON, Canada).

3.3.9 Lipid analysis

Plasma total cholesterol (Thermo Fisher Scientific, Ottawa, ON, Canada), FC, HDL cholesterol (HDL-C) and triglycerides (Wako Diagnosis, Richmond, VA, USA) were analyzed with enzymatic assay kits, following manufacturers' instructions.

3.3.10 Enzyme-linked immunosorbent assay

Plasma interleukin-6 (IL-6) was measured by ELISA, using a kit from Biolegend (San Diego, CA, USA), following manufacturer's instructions.

3.3.11 Flow cytometry

100 μ l of blood was collected by facial puncture 1 day before mice were harvested. Red blood cells were lysed using mouse lyse buffer (R&D Systems, Minneapolis, MN, USA), and white blood cells were pelleted by centrifugation at

1200rpm for 5 min using an Allegra™ X-220 centrifuge (Beckman Coulter, Mississauga, ON, Canada) with the SX4250 rotor. CD3, B220 and CD11b expressed on leukocytes were stained with FITC rat anti-mouse CD3 (BD Biosciences, Franklin Lakes, NJ, USA), PerCP-Cy5.5 anti-human/mouse CD45R (B220) (eBioscience Inc., San Diego, CA, USA) and APC anti-mouse CD11b (Life technologies, Eugene, OR, USA) for 1 hr in the dark on ice. Samples were analyzed by a BD FACScalibur™ flow cytometer (BD Biosciences, San Jose, CA, USA), and data was processed by FlowJo data analysis software (FlowJo, LLC., Oregon, OR, USA).

3.3.12 Statistical analysis

Sigma Plot statistical analysis software was used. Data was subjected to the Shapiro-Wilk test for normality and F test for equality of variances. Those that passed were analyzed by the Student's t-test (2-tailed, unpaired). Those that failed either test were analyzed by the Mann-Whitney Rank Sum test. Data from multiple groups were analyzed by ANOVA with post hoc tests for pairwise comparisons. Data are presented as mean \pm standard error of the mean. P values <0.05 were considered statistically significant.

3.4 Results

3.4.1 HDL reduced Bim protein levels in macrophages.

Macrophage apoptosis can be induced by treating them with oxidized LDL (oxLDL) or loading them with FC (Heinloth et al., 2002; Muller et al., 2001; Yao and Tabas, 2001), and this can be prevented by co-incubating the cells with HDL (Terasaka et al., 2007; Yvan-Charvet et al., 2010b; Yvan-Charvet et al., 2007). Similarly, treatment of macrophages in culture with the ER stress inducing agent tunicamycin significantly increased apoptosis detected by TUNEL staining for DNA degradation (Figure 3.1), consistent with previous reports (Puthalakath et al., 2007). In contrast, incubation of macrophages with HDL (50 µg protein/ml) prevented tunicamycin induced apoptosis (Figure 3.1). In a separate experiment, we compared the ability of tunicamycin to induce apoptosis, measured as immunofluorescence for activated caspase 3, in macrophages prepared from either wild type or *Bim*^{-/-} mice. Consistent with previous reports (Puthalakath et al., 2007), the degree of tunicamycin induced apoptosis was reduced in macrophages that lacked Bim expression, compared to those from wild type mice (Figure 3.2I: Bar6 vs. Bar5). As detected with TUNEL staining (Figure 3.1), treatment of wild type macrophages with HDL, together with tunicamycin, substantially dampened the induction of caspase 3 activation, compared to WT macrophages exposed to tunicamycin alone (Figure 3.2I: Bar7 vs. Bar5). In contrast, HDL treatment did not further reduce the already low level of apoptosis in tunicamycin treated *Bim*^{-/-} macrophages (Figure 3.2I: Bar8 vs. Bar6). This suggests that HDL was unable to further

protect macrophages lacking Bim from apoptosis, raising the possibility that Bim may be a downstream target of HDL's signaling pathway in macrophages.

To test this, we exposed WT MPMs to either tunicamycin or thapsigargin in the presence or absence of HDL. After 24 hrs, levels of Bim RNA and protein were tested by RT-PCR and immunoblotting, respectively. Bim_S, Bim_L and Bim_{EL} are the most abundant forms of Bim detected in most cells (Adachi et al., 2005; Mouhamad et al., 2004). Immunoblotting revealed that Bim_{EL} (23 kDa) was the major isoform detected in MPMs; the Bim_L (15 kDa) isoform was also detected though it appeared to be less abundant, whereas the Bim_S isoform (12 kDa) was not detected (Figure 3.3A). Levels of both the Bim_{EL} and Bim_L isoforms were reduced in HDL-treated cells (Figure 3.3A). On the other hand, the levels of total Bim transcript were not statistically significantly different (Figure 3.3B). A variety of studies suggest that the BOPs bind to the anti-apoptotic Bcl-2 proteins (e.g. Mcl-1) and neutralize them, therefore allowing the oligomerization of Bax and Bak (Ewings et al., 2007a; Hinds et al., 2007), suggesting that in addition to the absolute amounts of BOPs the ratio of BOPs to anti-apoptotic Bcl-2 family members is a key parameter in determining in the activation of apoptosis. Immunoblotting for Mcl-1 did not reveal any HDL dependent changes in its levels (Figure 3.3A). Therefore treatment with HDL resulted in reductions in both the absolute amount of Bim_{EL} and Bim_L and the relative amounts of these Bim isoforms to Mcl-1 (Figure 3.3A).

Figure 3.1: HDL protected macrophages from tunicamycin-induced apoptosis.

Thioglycollate-elicited MPMs were cultured in lipoprotein-deficient medium. Cells were treated with or without 10 µg/ml tunicamycin in the presence or absence of 50 µg/ml of HDL for 24 hrs. Then, Cells were stained by TUNEL (Green) and counterstained with DAPI (Blue) (A-C). The percentage of TUNEL(+) cells was quantified and analyzed by one-way ANOVA followed by Holm-Sidak method (D). (n=3, *p<0.05 vs. untreated; #p<0.05 vs. tunicamycin-treated)

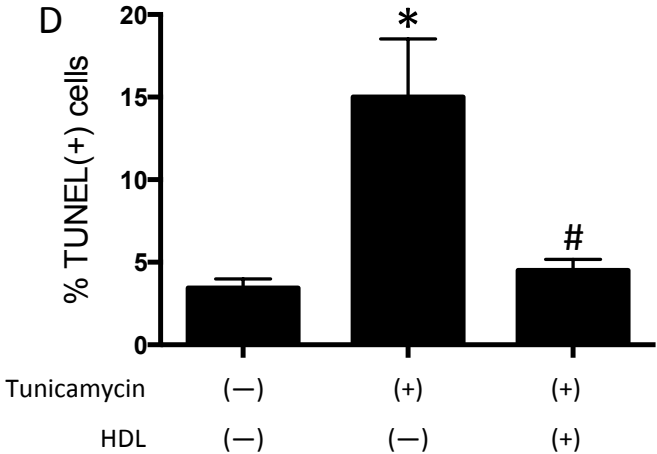
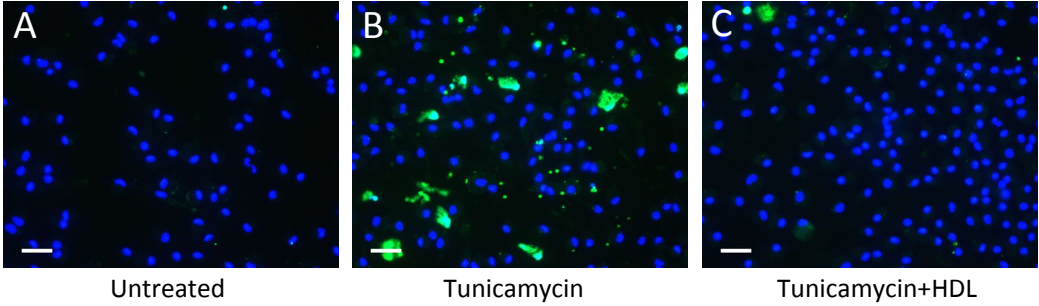


Figure 3.2: $Bim^{-/-}$ macrophages showed reduced sensitivity to tunicamycin-induced apoptosis. A-H): Thioglycollate-elicited MPMs from WT and $Bim^{-/-}$ mice were treated with 10 $\mu\text{g/ml}$ of tunicamycin in the presence or absence of 50 $\mu\text{g/ml}$ HDL for 24 hrs. Then, cells were fixed and cleaved caspase-3 immunofluorescent staining was done to detect apoptotic cells (green). Nuclei were stained with DAPI (blue). Data were expressed as the percentage of cleaved caspase-3 positive cells vs. DAPI positive nuclei. I): Data were analyzed by three-way ANOVA, *** $P < 0.001$, tunicamycin vs. untreated in WT. Bar graph is representative of three independent experiments.

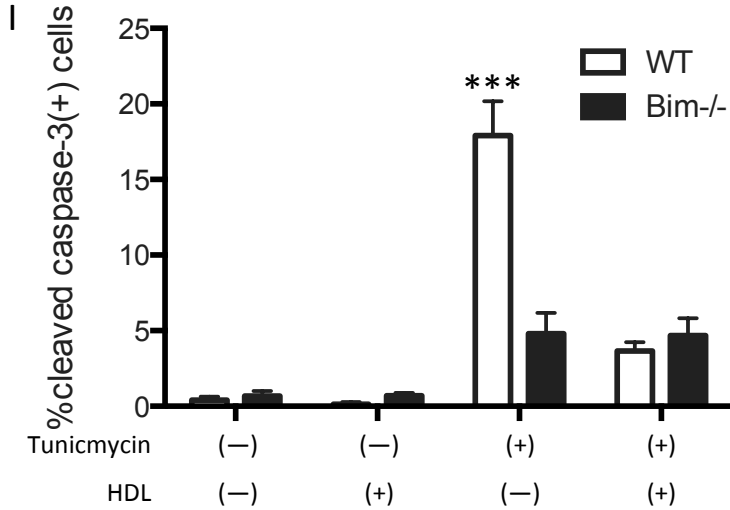
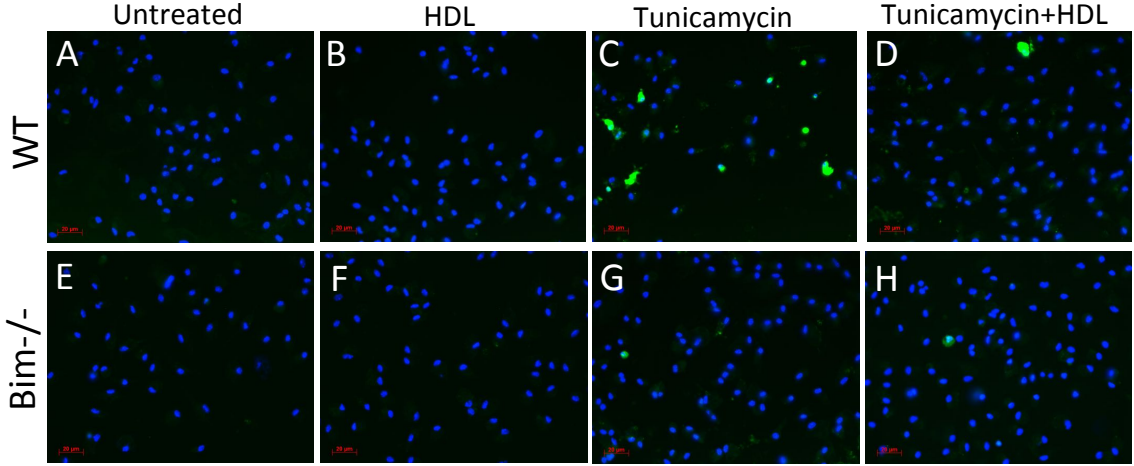
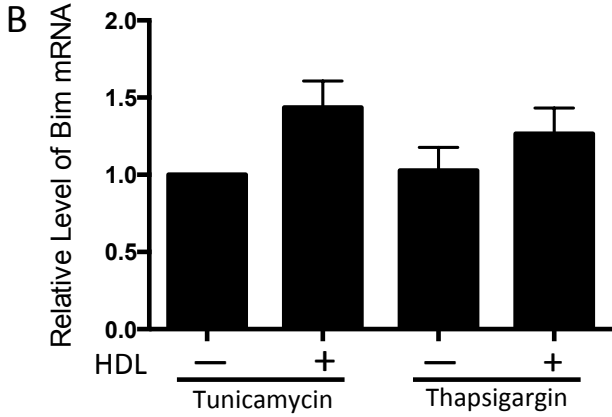
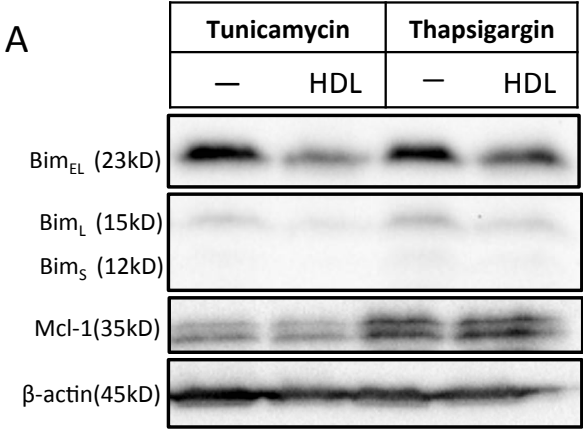


Figure 3.3: HDL reduced Bim protein, but not mRNA level in cultured macrophages. A): Thioglycollate-elicited MPMs were incubated with ER stressor (10 μ g/ml tunicamycin or 5 mM thapsigargin) in the presence or absence of 50 μ g/ml HDL for 24 hrs (n=3). Cell lysates were subjected to SDS-PAGE and immunoblotting for Bim (EL, L and S), Mcl-1 and β -actin. B): MPMs were treated as described in A). RNA was extracted and RT-PCR for Bim and GAPDH was performed. Bim mRNA levels were normalized to the levels of GAPDH and expressed as fold change relative to tunicamycin treated cells. Data were analyzed by one-way ANOVA followed by Holm-Sidak method. n=3, P>0.05.



3.4.2 ApoA-I gene inactivation results in increased necrotic core formation in high fat diet fed LDLR deficient mice.

Our *in vitro* findings suggest that HDL protected MPMs from apoptosis by reducing the levels of the pro-apoptotic BH3-only protein Bim. Because macrophage apoptosis is believed to contribute to necrotic core formation in atherosclerotic plaques, we reasoned that reduction in HDL levels might affect the sizes of necrotic cores in atherosclerotic plaques. To test this, we generated apoA-I^{-/-}/LDLR^{-/-} mice and examined atherosclerotic plaque formation in male mice after high fat diet feeding for 10 weeks. ApoA-I^{+/+}/LDLR^{-/-} male mice fed the same diet for the same duration were used as controls. We first measured plasma HDL and non-HDL total cholesterol levels and plasma triglyceride in both groups of mice. Plasma total cholesterol levels were slightly but statistically significantly lower in male, high fat diet fed apoA-I^{-/-}/LDLR^{-/-} mice compared to apoA-I^{+/+}/LDLR^{-/-} controls, as were non-HDL total cholesterol levels, which accounted for the majority of plasma total cholesterol (Figure 3.4A,C). HDL cholesterol accounted for only a small fraction of plasma total cholesterol, consistent with previous reports for high fat diet fed LDLR^{-/-} mice (Fuller et al., 2014a; Nakaya et al., 2009; Zabalawi et al., 2003). HDL cholesterol levels were ~50 % lower in apoA-I^{-/-}/LDLR^{-/-} mice compared to apoA-I^{+/+}/LDLR^{-/-} controls (Figure 3.4B), consistent with previous reports that genetic inactivation of apoA-I results in substantially reduced HDL levels in mice (Plump et al., 1997; Williamson et al., 1992; Zabalawi et al., 2003). We detected no significant differences in plasma triglyceride (Figure 3.4D) or IL-6 levels (Figure 3.4E).

Consistent with previous reports in chow or atherogenic diet fed apoA-I^{-/-} mice on LDLR^{-/-}, apoE^{-/-} or human apoB-Transgenic backgrounds (Boisvert et al., 1999; Hughes et al., 1997; Moore et al., 2003; Voyiaziakis et al., 1998; Zabalawi et al., 2003), we observed a statistically significant, 50 % increased average size of atherosclerotic plaques in 10-week high fat diet fed male apoA-I^{-/-}/LDLR^{-/-} mice compared with age and gender matched apoA-I^{+/+}/LDLR^{-/-} mice fed the same diet for the same duration (Figure 3.5A,B,E). Furthermore, atherosclerotic plaques in apoA-I^{-/-}/LDLR^{-/-} mice exhibited substantially larger necrotic cores than those from control apoA-I^{+/+}/LDLR^{-/-} mice (Figure 3.5C,D,F). This data demonstrates that inactivation of apoA-I gene expression, which led to reduced circulating HDL, was also accompanied by increased atherosclerotic plaque necrotic core development and is consistent with our *in vitro* data that HDL treatment protects macrophages from apoptosis.

Figure 3.4: Effect of apoA-I deficiency on lipid and systemic inflammation in LDLR^{-/-} mice. Plasma samples from 10-week western diet fed apoA-I^{-/-}/LDLR^{-/-} and LDLR^{-/-} control mice were analyzed for A): Plasma total cholesterol, B): Plasma HDL cholesterol, C): Plasma non-HDL cholesterol, D): Triglyceride and E): Interleukin-6. (n=24, 18), *P<0.05; ***P<0.001.

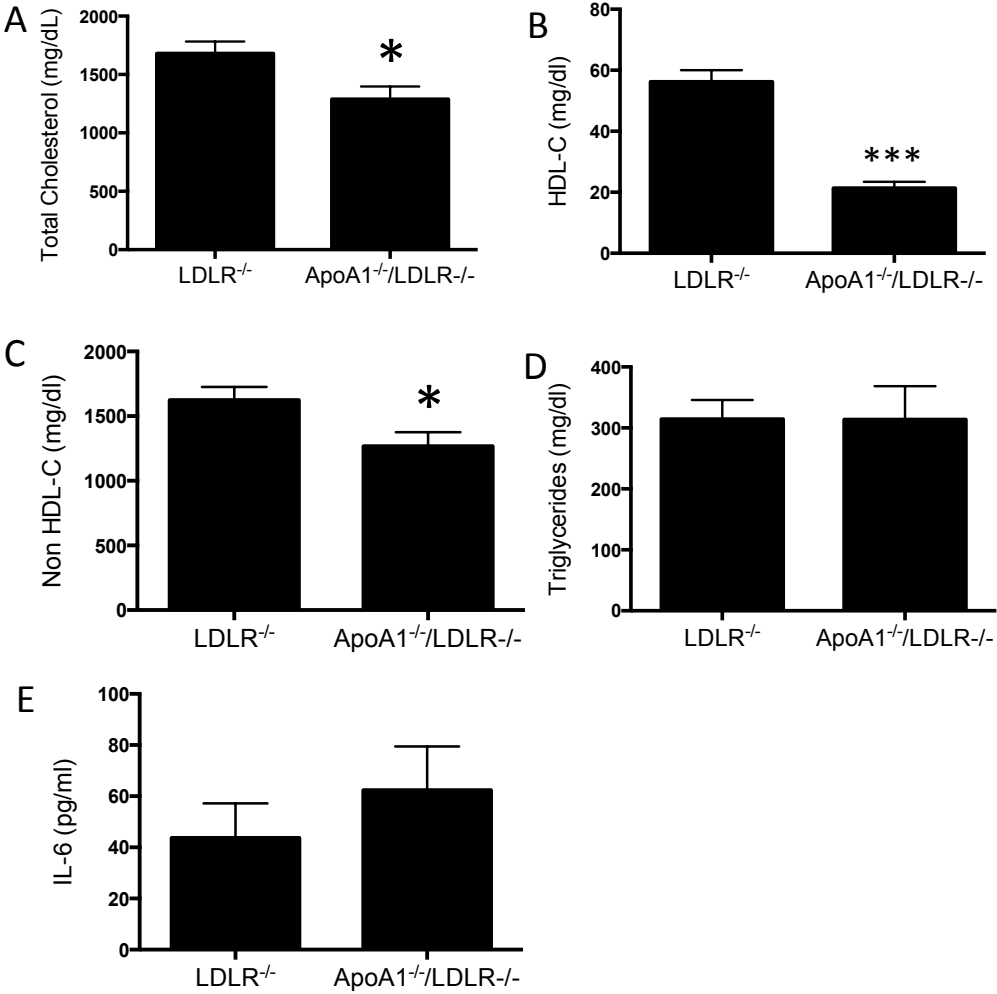
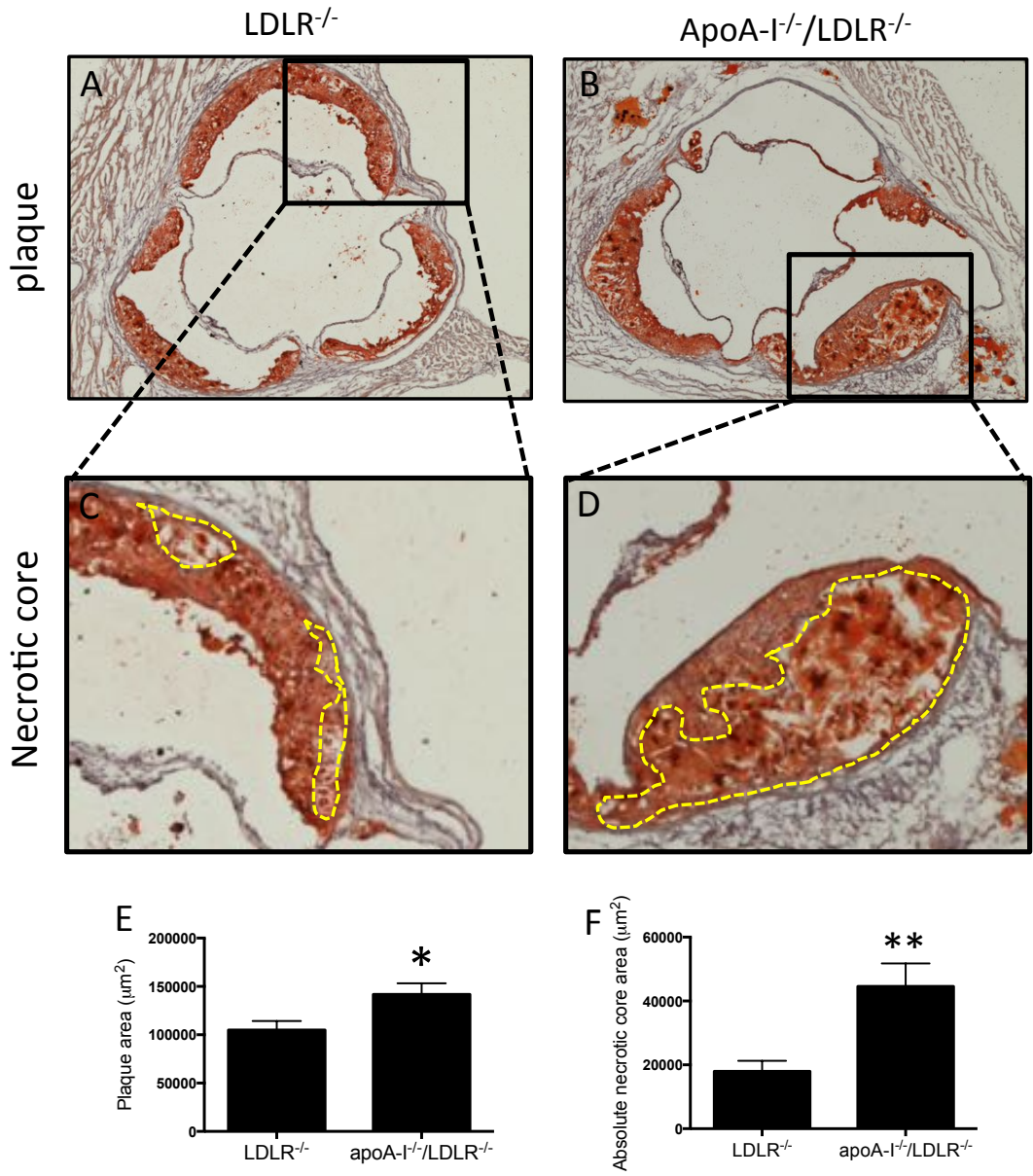


Figure 3.5: ApoA-I^{-/-}/LDLR^{-/-} mice fed high-fat diet for 10 weeks developed more atherosclerosis with bigger necrotic cores than LDLR^{-/-} mice. 10-week old LDLR^{-/-} and apoA-I^{-/-}/LDLR^{-/-} mice were challenged with high-fat western diet for 10 weeks. Representative images of oil red O/hematoxylin-stained cross sections of aortic sinus from A) LDLR^{-/-} mice and B) apoA-I^{-/-}/LDLR^{-/-} mice. Images were taken with 5X objective lens. C) and D) are magnified images of necrotic cores (outlined by yellow dash lines) in the atherosclerotic plaques from A) and B). E) Quantification of aortic sinus atherosclerotic plaque size. F) Quantification of necrotic core size. (n=22, 20) *P<0.05, **P<0.01.



3.4.3 Knocking out Bim in BM reduced atherosclerosis and plaque necrosis in apoA-I^{-/-}/LDLR^{-/-} mice.

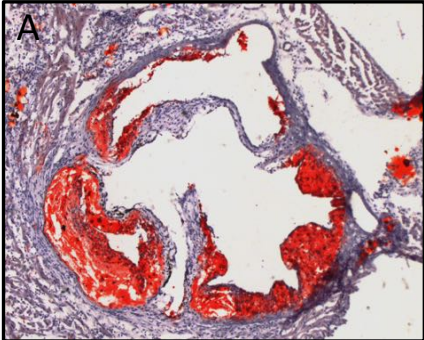
Since HDL treatment reduced Bim protein levels in ER-stressed macrophages and Bim^{-/-} macrophages were resistant to ER stress induced apoptosis, we hypothesized that inactivation of Bim expression in macrophages would reduce macrophage apoptosis in plaques, thereby limiting necrotic core size, even in the context of apoA-I deficiency. To test this, we transplanted BM from Bim^{-/-} or control WT mice into lethally irradiated apoA-I^{-/-}/LDLR^{-/-} recipient mice. After recovery from BM transplantation for 4 weeks, chimeras were fed a high fat diet for 10 weeks prior to analysis of atherosclerosis in the aortic sinus. ApoA-I^{-/-}/LDLR^{-/-} mice with BM specific Bim deficiency exhibited substantial reductions in both total plaque size (50 %) (Figure 3.6 A-C) and necrotic core size (70 %) (Figure 3.6D) compared to control apoA-I^{-/-}/LDLR^{-/-} mice reconstituted with Bim^{+/+} BM.

Mice deficient in Bim show many abnormalities that resemble human lymphocytic leukemia, including increased white blood cell counts and splenomegaly (Bouillet et al., 1999). Consistent with this, flow cytometry analysis of blood cells revealed significantly increased proportions of cells that were positive for B220, a marker of B lymphocytes (Figure 3.7A), a trend (not statistically significant) towards increased percentage of CD3 positive T cells (Figure 3.7B), and a reduction in the percentage of cells that were positive for CD11b staining (Figure 3.7C) in the mice transplanted with Bim^{-/-} BM. Bim^{-/-} mice have also been reported to exhibit splenomegaly (Bouillet et al., 1999). Consistent with this, increased spleen weight

(Figure 3.8A,C) was also observed in the apoAI^{-/-}/LDLR^{-/-} mice transplanted with Bim^{-/-} BM compared to those transplanted with BM from WT mice, after high fat diet feeding. We also noticed a slight but significantly lower body weight in the mice transplanted with Bim^{-/-} BM, compared to those transplanted with BM from WT mice, after high fat diet feeding (Figure 3.8B).

To our surprise, there was a 50 % reduction of plasma total, unesterified and esterified cholesterol (Figure 3.9A-C) in the apoAI^{-/-}/LDLR^{-/-} mice with BM specific Bim deficiency, compared to those with Bim^{+/+} BM. HDL-C levels were similar between the dKO mice transplanted with WT and Bim^{-/-} BM (Figure 3.9D), whereas non-HDL-C was significantly reduced in BM Bim^{-/-} group (Figure 3.9E). We also found that triglyceride levels were reduced by almost half (Figure 3.9F). The mechanism of reduced lipids in these mice is not clear. However, hypocholesterolemia has previously been observed in patients with hematological malignancies and the extent of hypocholesterolemia was related to tumor burden in patients (Gilbert and Ginsberg, 1983; Pandolfino et al., 1997; Reverter et al., 1988). This suggests that the reduced plasma cholesterol levels may be driven by increased circulating lymphocytes. The extents to which the reduced plasma non-HDL cholesterol and plasma TG levels contribute to the reduced atherosclerotic plaque and/or necrotic core sizes are not currently clear.

Figure 3.6: Knocking out Bim in BM reduced atherosclerosis and plaque necrosis in apoA-I^{-/-}/LDLR^{-/-} mice. Hearts from apoA-I^{-/-}/LDLR^{-/-} mice transplanted with A) WT BM and B) Bim^{-/-} BM were cross-sectioned and stained with oil red O for lipid deposition and hematoxylin for nuclei in the aortic sinus atherosclerotic plaques. (C): The total area of atherosclerotic plaques. (D): Absolute necrotic core size. (n=19, 11) *P<0.05, **P<0.01.



Bone marrow WT



Bim-/-

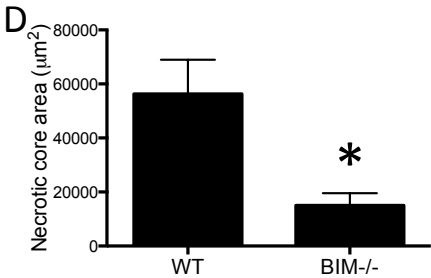
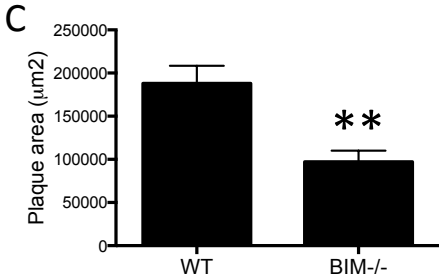


Figure 3.7: Blood leukocyte population in apoA-I^{-/-}/LDLR^{-/-} mice transplanted with WT or Bim^{-/-} BM. 200µl of blood was collected from each mouse. Red blood cells were lysed and leukocytes were stained with anti-CD11b(APC), anti-CD3(FITC) and anti-B220(PE) antibodies for monocytes, T lymphocytes and B lymphocytes, respectively. Then, samples from mice transplanted with WT BM (n=6) and Bim^{-/-} BM (n=3) were analyzed by flow cytometry and data was expressed as the percentage of A): B220(+), B): CD3(+) and C): CD11b(+) cells in all the blood leukocytes. *P<0.05, ***P<0.001.

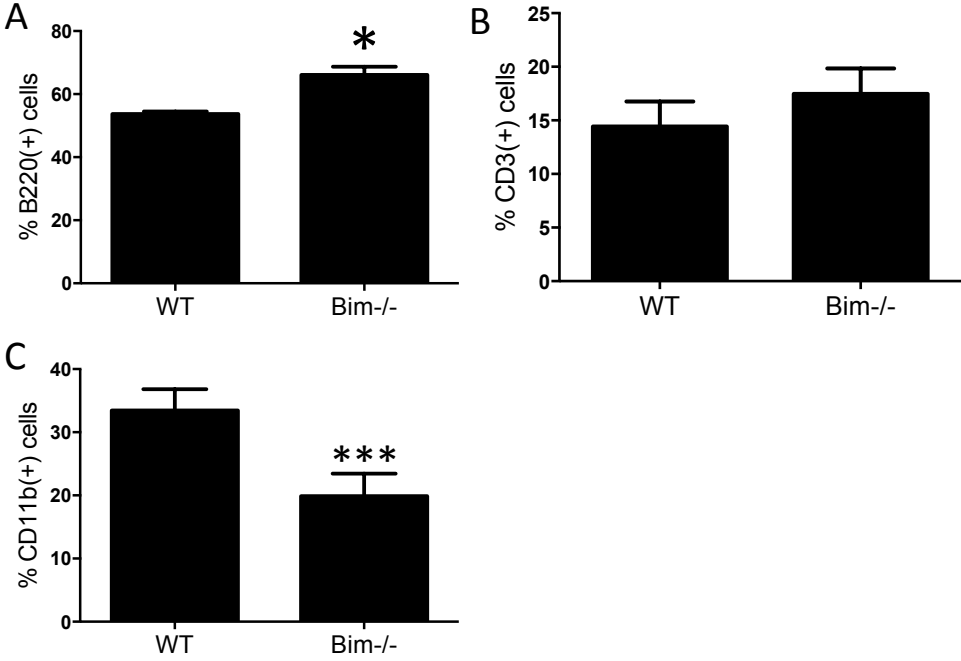


Figure 3.8: Body and spleen weights of apoA-I^{-/-}/LDLR^{-/-} mice transplanted with WT or Bim^{-/-} BM. A) spleen weights and B) body weights were measured after mice were harvested. C): spleen weights are normalized to body weights. (n=20, 12)
*P<0.05, ***P<0.001.

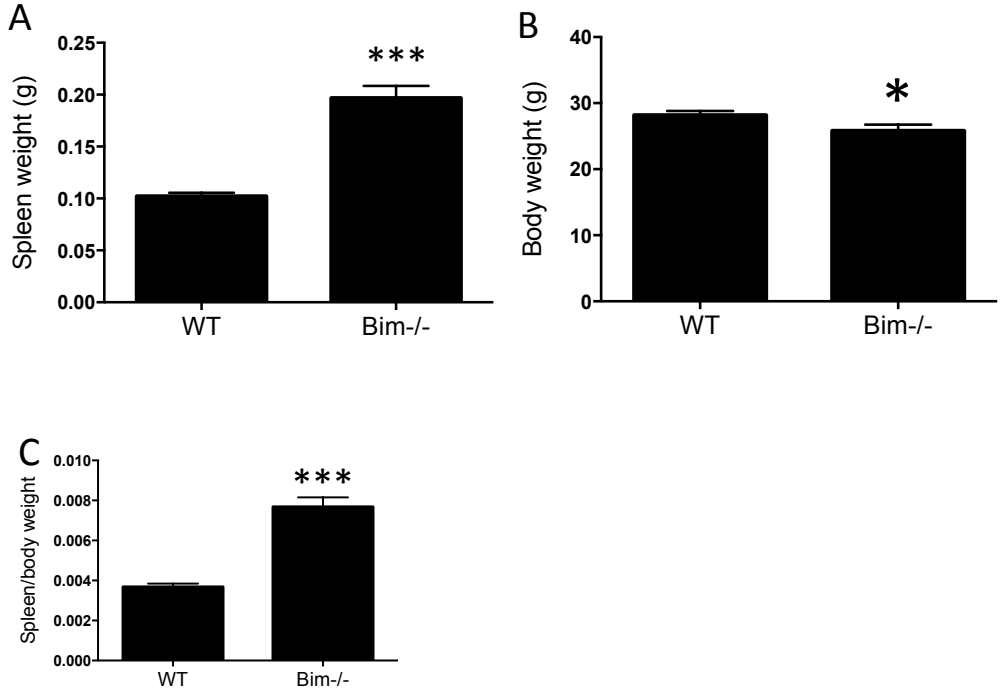
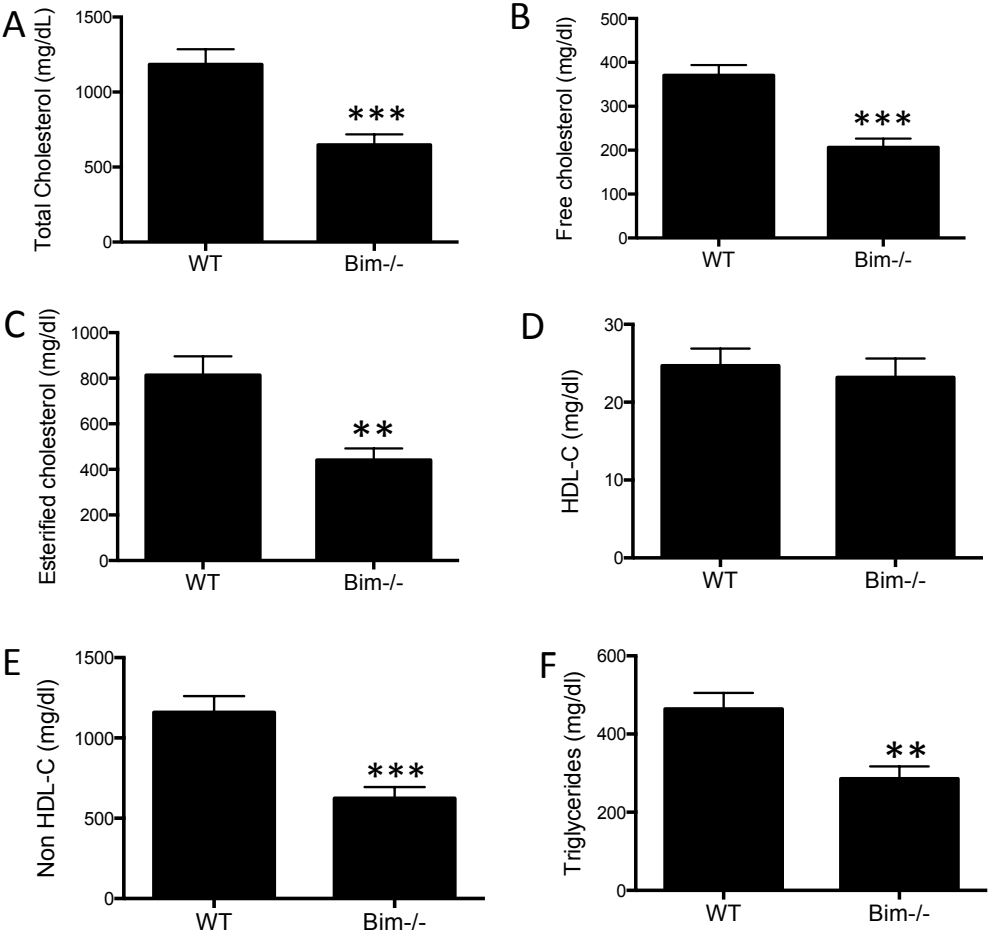


Figure 3.9: Reduced plasma lipids in the apoA-I^{-/-}/LDLR^{-/-} mice transplanted with Bim^{-/-} BM. Plasma samples from 10-week western diet fed apoA-I^{-/-}/LDLR^{-/-} mice transplanted with WT and Bim^{-/-} BM were analyzed for A): Plasma total cholesterol, B): Free cholesterol, C): Esterified cholesterol, D): Plasma HDL cholesterol and E): Non-HDL cholesterol and F): Triglycerides (n=13, 12), **P<0.01; ***P<0.001.



3.5 Discussion

Macrophage apoptosis can be induced *in vitro* by incubation with oxLDL (Heinloth et al., 2002; Muller et al., 2001) or loading with FC (Devries-Seimon et al., 2005; Yao and Tabas, 2001), which are abundant in atherosclerotic plaques. One of the well-established mechanisms underlying macrophage apoptosis is the sustained ER stress induced by FC (Devries-Seimon et al., 2005; Yao and Tabas, 2001). ER stress regulates Bim expression in multiple cell types at both transcriptional and post-translational levels (Puthalakath et al., 2007). ER stress upregulates the expression of CHOP, a transcription factor that induces Bim gene expression (Puthalakath et al., 2007). Bim protein is phosphorylated by different pathways, leading to its ubiquitinylation and proteasomal degradation; ER stress has been reportedly leads to PP2A mediated dephosphorylation of Bim, preventing its degradation (Puthalakath et al., 2007). Thus ER stressors lead to accumulation of Bim protein, promoting apoptosis, presumably through enhanced inhibition of anti-apoptotic Bcl-2 family members such as Mcl1 (Brunelle and Letai, 2009). Bim appears to play a central role in ER stress induced apoptosis, because inactivation of Bim gene expression in different cell types attenuates apoptosis induced by ER stress inducers, such as tunicamycin or thapsigargin (Puthalakath et al., 2007), which is consistent with our observations in Bim^{-/-} MPMs (Figure 3.2).

HDL is able to protect macrophages from apoptosis induced by a variety of stressors, including tunicamycin, thapsigargin (Chapter 2, Yu and Fernandes, manuscript in preparation), FC (Zhang and Al-Jarallah, manuscript in revision) or oxLDL (Heinloth

et al., 2002; Muller et al., 2001). We demonstrated that HDL did not relieve ER stress in tunicamycin or FC treated macrophages (Chapter 2, Yu and Fernandes, manuscript in preparation; Zhang and Al-Jarallah, manuscript in revision). Instead, HDL treatment of macrophages activated phosphorylation of Akt1 ((Al-Jarallah et al., 2014); Chapter 2, Yu and Fernandes, manuscript in preparation) and JNK1 (Zhang, Al-Jarallah and Yu, manuscript in revision) and led to reductions in the amount of Bim_{EL} (Zhang, Al-Jarallah and Yu, manuscript in revision; Figure 3.2). HDL dependent reductions in Bim_{EL} were dependent on JNK1 expression since they did not occur in JNK1 deficient macrophages, and both HDL dependent phosphorylation of JNK1 and reduction of Bim required SR-B1, since they were not seen in SR-B1 deficient macrophages. Likewise, HDL was not able to protect JNK1 deficient macrophages from apoptosis induced by ER stress inducing agents (Zhang et al, manuscript in revision). Similarly, HDL dependent activation of Akt1 phosphorylation required the SR-B1 adaptor protein, PDZK1, and was necessary for HDL dependent protection against apoptosis, since HDL was unable to protect Akt1 deficient macrophages from ER stress induced apoptosis (Chapter 2, Yu and Fernandes, manuscript in preparation). PI3K/Akt signalling has been shown to regulate Bim both at the transcriptional and post-translational levels in diverse cell types (Dijkers et al., 2000; Lv et al., 2013; Qi et al., 2006; Senokuchi et al., 2008; Stahl et al., 2002). Akt1 activation down-regulates Bim gene expression through the phosphorylation of Foxo3a, preventing its nuclear localization (Dijkers et al., 2000; Lv et al., 2013; Stahl et al., 2002). However, we did not observe reduced Bim gene expression in HDL treated macrophages. The activation of the PI3K/Akt signaling

pathway has also been reported to stimulate the phosphorylation of ERK1/2 (Harfouche et al., 2003). Activated ERK1/2 has been reported to phosphorylate Ser65 in exon 3, present in Bim_{EL} (but not other isoforms of Bim) (Clybouw et al., 2012), which both facilitates Bim dissociation from pro-survival Bcl-2 proteins and tags Bim for ubiquitination and proteasomal degradation in lymphocytes and cultured cell lines (Ewings et al., 2007a; Ewings et al., 2007b; Ley et al., 2003; Ley et al., 2005). Moreover, Akt can also dampen the pro-apoptotic activity of Bim by phosphorylating Bim at Ser87, leading to the association and sequestration of Bim by 14-3-3 protein, so that it cannot interact with pro-survival Bcl-2 family proteins (Qi et al., 2006).

The characterization of apoA-I^{-/-}/LDLR^{-/-} mice showed a decrease of total cholesterol, associated both HDL, and non-HDL fractions. The reason why the deficiency of apoA-I could lead to a reduction of non-HDL cholesterol is not clear. However, this phenotype in atherogenic diet fed LDLR^{-/-} mice lacking apoA-I was also reported by others (Boisvert et al., 1999; Zabalawi et al., 2003). Despite the reduction in non-HDL-C (Figure 3.4), atherosclerotic plaque sizes in the aortic sinus, and the sizes of necrotic cores within plaques were significantly increased in apoA-I^{-/-}/LDLR^{-/-} mice compared to apoA-I^{+/+}/LDLR^{-/-} controls when they were fed the high-fat diet (Figure 3.5). The increased atherosclerotic plaque size in mice deficient in apoA-I is consistent with previous reports (Hughes et al., 1997; Moore et al., 2003; Voyiaziakis et al., 1998) and likely reflects impaired reverse cholesterol transport and the absence of other protective effects of HDL on vascular cells. The substantially larger necrotic core sizes in apoA-I^{-/-}/LDLR^{-/-} mice compared to apoA-I^{+/+} LDLR^{-/-} controls when each were fed

the high-fat diet is consistent with our in vitro observations that HDL can protect macrophages from apoptosis induced by a variety of factors including ER stress inducing agents (Figure 3.1), FC loading (Zhang and Al-Jarallah, manuscript under revision) and oxLDL (Chapter 2, Yu et al, manuscript in preparation).

To test the role of Bim in atherosclerosis and necrotic core development within atherosclerotic plaques, we used BM transplantation to generate apoA-I^{-/-}LDLR^{-/-} mice that either expressed normal levels or lacked Bim in all BM derived cells, including monocyte derived macrophages. Knockout of Bim in BM-derived cells lead to a significant reduction in plaque size and an even larger reduction in necrotic size (Figure 3.6). This is the first time that the effects of Bim on atherosclerosis and necrosis in the plaques have been reported, and the underlying mechanism is undoubtedly complex. The reduced necrotic core sizes in mice with BM specific deficiency of Bim is consistent with our findings in cultured macrophages, and those of others, that Bim plays a key role in ER-stress induced apoptosis in macrophages (Figure 3.2;(Puthalakath et al., 2007)), and that HDL treatment of macrophages reduces levels of Bim protein (Figure 3.2; also, Zhang and Al-Jarallah et al manuscript in revision). Surprisingly, apoA-I^{-/-}LDLR^{-/-} mice with BM specific deletion of Bim exhibited a marked reduction in plasma total, esterified and unesterified cholesterol and triglyceride, likely reflecting reduced cholesterol associated with non-HDL lipoproteins (Figure 3.9). This may be associated with the increased levels of circulating lymphocytes, consistent with reports of increased lymphocytes in global Bim^{-/-} mice (Bouillet et al., 1999). Bouillet *et al.* (Bouillet et al., 1999), however also reported increased numbers of circulating monocytes and

granulocytes in global $Bim^{-/-}$ mice, whereas we observed apparent reductions in the proportion of circulating $CD11b^{+}$ cells in mice with BM specific inactivation of Bim (Figure 3.7). This discrepancy is likely because we analyzed the relative proportions of T and B lymphocytes and myeloid ($CD11b^{+}$) cells rather than their absolute numbers, and likely reflects a greater increase in the absolute numbers of T and B lymphocytes than myeloid cells in the mice with BM specific deficiency of Bim compared to controls with intact Bim expression.

In conclusion, this study demonstrates that HDL protects macrophages against ER stress induced apoptosis by triggering a reduction in the levels of the pro-apoptotic Bim_{EL} protein. We also demonstrate that reduction of HDL *in vivo* in mice results in development of atherosclerotic plaques with larger necrotic cores and that inactivation of Bim in BM derived cells, including monocyte derived macrophages, can limit necrotic core development and indeed atherosclerotic plaque development. These findings shed light on important pathways by which HDL protects against atherosclerosis development, namely development of necrotic cores, and implicates Bim_{EL} as a potential target for therapeutic intervention to limit the development of large necrotic cores, a key feature of unstable plaques.

CHAPTER IV

Rosuvastatin reduces aortic sinus and coronary artery atherosclerosis in SR-B1/apoE double knockout mice independently of plasma cholesterol lowering

Author list: Pei Yu, Christine B. Tenedero, Melissa E. MacDonald, Bernardo L. Trigatti

PREFACE

This manuscript has been submitted to *Arteriosclerosis, Thrombosis and Vascular Biology*. The reviewers' comments are being addressed and the manuscript will be resubmitted.

The research described herein was initiated by Pei Yu and Christine Tenedero in 2009 under the supervision of Professor Bernardo Trigatti. The majority of the data were collected by Pei Yu. All data were analyzed and interpreted by Pei Yu under the guidance of Professor Trigatti. The manuscript was written by Pei Yu with guidance from Professor Trigatti. Christine Tenedero assisted with mouse injection and harvesting, and contributed to some of the plaque staining and quantification. Mouse colonies were maintained and genotyped by Melissa MacDonald. Plasma apoA-I levels were analyzed by Melissa MacDonald (Figure 4.1G,H). We also thank Fatima Igdoura for technical assistance on Trichrome staining.

This research was supported by grants from AstraZeneca Inc. (DC-990-0324) and the Canadian Institutes for Health Research (MOP74765) to BLT.

4.1 Abstract

Objective: Rosuvastatin has been widely used in the primary and secondary prevention of coronary heart disease (CHD). However, its anti-atherosclerotic properties have not been tested in a mouse model that could mimic human CHD. The present study was designed to test the effects of rosuvastatin on coronary artery atherosclerosis and myocardial fibrosis in scavenger receptor class B type 1(SR-B1) and apolipoprotein E (apoE) double knockout mice.

Approach and Results: 3-week-old SR-B1^{-/-}/apoE^{-/-} mice were injected daily with 10 mg/kg of rosuvastatin for two weeks. Compared with saline-treated mice, rosuvastatin-treated mice showed increased levels of hepatic PCSK9 and LDLR message, but decreased levels of hepatic LDLR protein and increased plasma total cholesterol associated with apolipoprotein B (apoB)-containing lipoproteins. In spite of this, rosuvastatin treatment was associated with decreased atherosclerosis in both the aortic sinus and coronary arteries and reduced platelet accumulation in atherosclerotic coronary arteries. Cardiac fibrosis and cardiomegaly were also attenuated in rosuvastatin-treated SR-B1^{-/-}/apoE^{-/-} mice. Two-week treatment with rosuvastatin resulted in significant decreases in markers of oxidized LDL in both plasma and atherosclerotic plaques. *In vitro* analysis showed that incubation of bone marrow-derived macrophages with rosuvastatin substantially down-regulated CD36 and inhibited oxidized LDL-induced foam cell formation.

Conclusions: Rosuvastatin protected SR-B1^{-/-}/apoE^{-/-} mice against atherothrombosis and attenuated myocardial fibrosis and cardiomegaly, despite increased plasma total

cholesterol. The ability of rosuvastatin to reduce oxidized LDL and inhibit macrophage foam cell formation contributed to this protection.

4.2 Introduction

Atherosclerosis, a major underlying cause of coronary heart disease (CHD), is a consequence of both dysregulated lipid metabolism as well as dysregulated inflammatory processes that involve the recruitment of monocytes to susceptible areas of arteries, differentiation to macrophages and development into foam cells (Tuttolomondo et al., 2012). The accumulation of foam cells gives the appearance of fatty streaks in the intima of arterial walls at the early stages of atherosclerosis and finally forms atherosclerotic plaques as the disease develops (Tuttolomondo et al., 2012). The 3-hydroxy-3-methylglutaryl coenzyme A reductase inhibitors (statins) are potent inhibitors of cholesterol synthesis. A number of large-scale clinical trials have consistently demonstrated the effects of statins in plasma lipid lowering and in the primary and secondary prevention of CHD (Maron et al., 2000). Recent studies, however, suggest that the beneficial effects of statins may extend beyond their effects on serum cholesterol levels (Davignon, 2004; van der Meij et al., 2013). These studies suggest that statins likely protect the cardiovascular system against atherosclerosis via plasma lipid lowering-dependent and -independent mechanisms. Rosuvastatin (Crestor), a potent statin, has shown several beneficial characteristics, including a long half-life, a favorable safety profile, and low propensity for cytochrome P450 drug interactions (Cheng-Lai, 2003).

To study the pleiotropic effects of rosuvastatin, a number of mouse models have been used (Enomoto et al., 2009; Gronros et al., 2008; Li et al., 2005; Monetti et al., 2007; Schafer et al., 2005a; Schafer et al., 2005b; Schroeter et al., 2009; Verreth et al.,

2007). The most widely used mouse model of atherosclerosis is the apolipoprotein E (apoE)^{-/-} mouse (Enomoto et al., 2009; Gronros et al., 2008; Monetti et al., 2007; Schroeter et al., 2009). In apoE^{-/-} mice, total plasma cholesterol levels are approximately 5 times higher than in wild-type mice, due to increased very-low-, intermediate- and low-density lipoproteins (VLDL, IDL and LDL) (Plump et al., 1992; Zhang et al., 1992). ApoE^{-/-} mice fed a normal chow diet develop atherosclerosis by 3 months of age (Zhang et al., 1992), and the pathological process can be accelerated by feeding the mice high-fat and/or high-cholesterol diets (Plump et al., 1992). A number of studies demonstrated that rosuvastatin treatment (1-20 mg/kg of body weight) reduced inflammation, adhesion, thrombosis, and apoptosis in the aortic sinus and proximal aortas of apoE^{-/-} mice, even though the plasma cholesterol and triglyceride levels were not altered (Enomoto et al., 2009; Gronros et al., 2008; Monetti et al., 2007; Schroeter et al., 2009). While apoE^{-/-} mice exhibit severe atherosclerotic plaque formation in the aortic sinus, aortic arch and brachiocephalic arteries, their coronary arteries are comparatively resistant to atherosclerotic plaque formation (Braun et al., 2008a; Braun et al., 2002; Covey et al., 2003; Plump et al., 1992). Even though apoE^{-/-} mice fed normal chow diet for an extended time (8 months) have shown evidence of some atherosclerotic coronary arteries, subsequent myocardial infarction and heart dysfunction do not appear to develop (Plump et al., 1992).

In contrast, apoE^{-/-} mice that are also deficient in the scavenger receptor class B type 1 (SR-B1) exhibit spontaneous coronary artery atherosclerosis, which develops rapidly by 5 weeks of age (Al-Jarallah et al., 2013; Braun et al., 2002). SR-B1 is a cell

surface high-density lipoprotein (HDL) receptor, expressed in liver, intestine, steroidogenic tissues (e.g. adrenal gland, ovary and testis) and vascular cells (e.g. macrophages and endothelial cells) (Rigotti et al., 2003). SR-B1 in the liver and steroidogenic tissues mediates selective HDL lipid uptake, and hepatic SR-B1 drives reverse cholesterol transport to remove cholesterol from peripheral tissues for biliary excretion (Rigotti et al., 1997). SR-B1 has also been shown to enhance cholesterol efflux from cells and to mediate HDL-dependent activation of cellular signaling pathways in diverse cells including endothelial cells (Al-Jarallah and Trigatti, 2010) and macrophages (Al-Jarallah et al., 2014). Mice lacking both SR-B1 and apoE develop increased atherosclerosis in their aortic sinus and coronary arteries leading to both stenosis and complete occlusion of arteries between 3 and 5 weeks of age (Al-Jarallah et al., 2013; Braun et al., 2002). They also exhibit extensive myocardial fibrosis, cardiac functional and conductance abnormalities and reduced life span (6-8 weeks of age) compared with their apoE^{-/-} littermates (Braun et al., 2002). Krieger and co-workers have tested a number of pharmacological interventions on these phenotypes in SR-B1^{-/-}/apoE^{-/-} mice. Probucol, an anti-oxidant and lipid-lowering drug, corrected the lipoprotein abnormalities in SR-B1^{-/-}/apoE^{-/-} mice and delayed development of coronary artery atherosclerosis, and cardiac pathology, and extended their life span to 36 weeks (Braun et al., 2003). Ezetimibe, an inhibitor of intestinal cholesterol absorption, lowered LDL cholesterol and reduced aortic sinus and coronary arterial atherosclerosis and myocardial fibrosis and also increased the survival of SR-B1^{-/-}/apoE^{-/-} mice (Braun et al., 2008b). Similar results were obtained when SR-B1^{-/-}/apoE^{-/-} mice were treated with SC-

435, an apical sodium codependent bile acid transporter inhibitor, which prevents intestinal absorption of bile acid, resulting in decreased plasma LDL cholesterol (Braun et al., 2008b). Recent research from our lab demonstrated that oral supplementation of drinking water with pomegranate extract reduced oxidative stress and inflammation in coronary arteries of SR-B1^{-/-}/apoE^{-/-} mice and reduced atherosclerosis and myocardial fibrosis and delayed the development of ECG abnormalities, even though plasma cholesterol levels were increased (Al-Jarallah et al., 2013). These studies suggest that the SR-B1^{-/-}/apoE^{-/-} mouse may be a useful model system in which to analyze mechanisms of pharmacological protection against CHD.

To investigate the effects of rosuvastatin treatment on the development of coronary artery atherosclerosis and myocardial infarction in mice, we treated SR-B1^{-/-}/apoE^{-/-} mice with or without rosuvastatin. Treatment began at 3 weeks of age, preceding the start of atherosclerosis development in the aortic sinus or coronary arteries (Al-Jarallah et al., 2013). In this study, we show that daily treatment of SR-B1^{-/-}/apoE^{-/-} mice for 2 weeks with rosuvastatin (10 mg/kg of body weight) reduced aortic sinus and coronary artery atherosclerosis, cardiac enlargement and cardiac fibrosis. These changes were observed despite an increase in plasma lipoprotein cholesterol, due most likely to increased levels of hepatic PCSK9 gene expression and reduced levels of hepatic LDL receptor (LDLR) protein in rosuvastatin-treated mice. The reduction in atherosclerosis, however, was accompanied by reduced levels of oxidized LDL (oxLDL) in plasma and in the walls of the aortic sinus and coronary arteries. Furthermore, rosuvastatin treatment of cultured macrophages from SR-B1^{-/-}/apoE^{-/-} mice resulted in reduced levels

of CD36 and oxLDL-driven foam cell formation. Therefore, rosuvastatin protects against the development of coronary artery atherosclerosis and associated CHD in SR-B1^{-/-}/apoE^{-/-} mice by reducing the levels of oxLDL in circulation, their accumulation in the walls of arteries and uptake by macrophages.

4.3 Materials and Methods

4.3.1 Materials

Rosuvastatin calcium was provided by AstraZeneca, UK. All other materials were purchased from Sigma Aldrich (St. Louis, Missouri, USA) unless otherwise stated.

4.3.2 Mice

All procedures involving mice were approved by the McMaster University Animal Research Ethics Board and were in accordance with the guidelines of the Canadian Council on Animal Care. All mice were bred and housed in the Central and the TaARI animal facilities at McMaster University and had free access to normal chow (Teklad 18% protein diet, Harlan Laboratories, Mississauga, Ontario, Canada) and water. SR-BI^{-/-}/apoE^{-/-} and SR-BI^{+/+}/apoE^{-/-} mice were produced by breeding SR-BI^{+/-}/apoE^{-/-} mice (mixed C57BL/6J and 129/Sv background, from a colony originally established from founders obtained from Dr. Monty Krieger, MIT, Cambridge, USA). SR-BI^{-/-}/apoE^{-/-} mice and apoE^{-/-} littermates were weaned at age 3 weeks at which time daily injections of rosuvastatin (10mg/kg body weight) in 0.9% saline or vehicle solution (0.9% saline) were administered i.p. Rosuvastatin or saline administration continued until mice were 5 weeks of age, at which point they were fasted for 4 hours prior to anesthesia and euthanasia. Blood was collected by cardiac puncture and tissues were perfused with phosphate buffered saline containing 10 U of heparin/ml. Hearts were harvested and frozen in Shandon Cryomatrix (Thermo Fisher Scientific, Ottawa, Ontario, Canada) and stored at -80 °C for further analysis. Livers were rapidly frozen in liquid nitrogen for

protein analysis or stored at -80 °C in RNAlater (Invitrogen Life Technologies Inc., Burlington, Ontario, Canada). Plasma was prepared by centrifugation of blood at 8,000 rpm for 5 min in a microcentrifuge at 4°C and was stored at -80 °C prior to further analysis.

4.3.3 Atherosclerosis and myocardial fibrosis

Transverse cryosections (10µm) of the heart and aortic sinus were stained for lipids with oil red O as previously described and for fibrosis with Masson's Trichrome (Thermo Fisher Scientific, Ottawa, Ontario, Canada), which stains healthy myocardium red and collagen fibers blue (Al-Jarallah et al., 2013; Fuller et al., 2014b). Atherosclerotic plaque area and area of fibrosis were determined as previously described (Al-Jarallah et al., 2013; Fuller et al., 2014b).

4.3.4 Lipid analysis

Plasma was fractioned by gel filtration fast-protein liquid chromatography (FPLC) using an AKTA system with a Tricorn Superose 6 HR10/300 column (GE Healthcare Life Sciences, Baie d'Urfe Quebec, Canada). Enzymatic assay kits were used to measure total cholesterol (Thermo Fisher Scientific, Ottawa, Ontario, Canada) and unesterified cholesterol (Wako Diagnosis, Richmond, Virginia, USA), in whole or fractionated plasma (Al-Jarallah et al., 2013; Fuller et al., 2014b).

4.3.5 SDS-PAGE and immunoblotting

For hepatic membrane proteins, all procedures were carried out at 4 °C. Liver (1 g) was homogenized on ice using an Ultra-Turrax tissue homogenizer in buffer containing 20mM Tris-HCl (pH 7.5), 2 mM MgCl₂ and protease inhibitors (1 mM PMSF, 1 µg/ml pepstatin A, 1mg/ml leupeptin and 2 µg/ml aprotinin). Nuclei and cell debris were pelleted by centrifugation at 3,000xg. The supernatant was subjected to centrifugation at 100,000x g to pellet membranes. Membranes were suspended in 50 µl of 10mM sodium phosphate, pH 7, containing the protease inhibitors listed above and protein concentrations were determined using the BCA protein assay kit (Pierce Biotechnology, Rockford, Illinois, USA). Samples were either used immediately or stored at -80°C prior to further use. Plasma (0.5µl) or liver membranes (50 µg) were solubilized and subjected to SDS-PAGE using 6% acrylamide for separation of apoB or 15 % acrylamide for separation of apoA-1 from plasma, or 12 % acrylamide for separation of liver membrane proteins, as described previously (Trigatti et al., 1991). Electrophoretic transfer of proteins to PVDF membranes and immunoblotting was as previously described (Trigatti et al., 1999; Trigatti et al., 1991). Briefly, membranes were blocked in 5% skim milk powder for 1 hr at room temperature prior to incubation with goat anti-human apoA-I or goat anti-human/mouse apoB (both from Midland Bioproducts (Boone, Iowa, USA), goat anti-mouse LDLR (R&D, Minneapolis, Minnesota, USA) or mouse anti-mouse Na⁺/K⁺ ATPase α-1 (Upstate Technology, Lake Placid, New York, USA). Primary antibodies were diluted 1:1000 in blocking solution and incubated with membranes at 4°C over night. Membranes were then washed and

incubated with horseradish peroxidase (HRP) conjugated rabbit anti-goat or donkey anti-mouse IgG (Jackson ImmunoResearch laboratory, West Grove, Pennsylvania, USA). Secondary antibodies were diluted 1:10000 in blocking solution and incubated with membranes for 1 hr at room temperature. HRP was detected using the Amersham Enhanced Chemiluminescence (ECL) kit (GE Healthcare Life Sciences Baie d'Urfe Quebec, Canada). The intensities of the protein bands were measured using a Gel Doc instrument (Bio-Rad Laboratories, Hercules, California, USA).

4.3.6 Bone marrow cell preparation, culture and treatment

Bone marrow was flushed out of femurs and tibias from SR-B1^{-/-}/apoE^{-/-} mice into DMEM containing 10% FBS, 2mM L-glutamine 50 µg/ml penicillin and 50 U/ml streptomycin (Medium 1). Cells were dispersed and plated in 35 mm cell culture dishes for 12 hrs. After this, suspended cells were recovered, pelleted by centrifugation at 500 x g and re-suspended in Medium 1 supplemented with 20% L-cell conditioned medium. After 7 days in culture, the differentiated macrophages were treated with oxLDL (50µg protein/ml) with or without 10 µM rosuvastatin for 24 hrs at 37 °C and then fixed with paraformaldehyde and subjected to immunofluorescence or oil red O staining.

4.3.7 Real time PCR

Total RNA was extracted from 15-20 mg of liver tissue or cultured cells that were either fresh or stored in RNAlater. RNA was purified using the RNeasy Mini kit

(Qiagen Inc., Toronto, Ontario, Canada) and quantified using a SpectraMax Plus384 spectrophotometer (Molecular Devices, Sunnyvale, California, USA). cDNA synthesis was performed from 1 µg of total RNA using QuantiTect reverse Transcription Kit (Qiagen Inc., Toronto, Ontario, Canada). Real-time quantitative PCR was performed using Platinum Sybr Green dye (Invitrogen Life Technologies Inc., Burlington, Ontario, Canada) in an Applied Biosystems 7300 Real Time PCR system (Applied Biosystems, Foster City, California, USA) with default settings. All primers were synthesized by Invitrogen Life Technologies (Burlington, Ontario, Canada) and the sequences are: LDLR (forward): 5'-TCCAATCAATTCAGCTGTGG-3'; LDLR (reverse): 5'-GAGCCATCTAGGCAATCTCG-3'; PCSK-9 (forward): 5'-TTGCAGCAGCTGGGAACTT-3'(Ai et al., 2012); PCSK-9 (reverse): 5'-CCGACTGTGATGACCTCTGGA-3'(Ai et al., 2012); CD36 (forward): 5'-TTTCCTCTGACATTTGCAGGTCTA-3'; CD36 (reverse): 5'-AAAGGCATTGGCTGGAAGAA-3'; SR-A (forward): 5'-CTTTACCAGCAATGACAAAAGAGA-3'; SR-A (reverse): 5'-ATTCACGGATTCTGAACTGC-3'; GAPDH (forward): 5'-ACCACAGTCCATGCCATCAC-3'; GAPDH (reserve): 5'-TCCACCACCCTGTTGCTGTA-3'. Primer sequences were selected using Pubmed's primer-BLAST, unless otherwise stated.

4.3.8 Enzyme-linked immunosorbent assay

Plasma serum amyloid A (SAA) and oxidized LDL (oxLDL) levels were measured by ELISA using kits from Invitrogen Life Technologies (Burlington, Ontario, Canada) or Usen Life Science Inc. (Wuhan, Hubei, PRC), respectively.

4.3.9 Immunofluorescence staining

For bone marrow derived macrophages, intracellular lipid was stained by oil red O and CD36 was detected by rabbit anti-mouse CD36 (Santa Cruz Biotechnology, Dallas, Texas, USA) followed by goat anti-rabbit alexa-594 secondary antibody (Invitrogen Life Technologies Inc., Burlington, Ontario, Canada). F4/80 (macrophage marker) was detected by rat anti-mouse F4/80 antibody (Abcam, Boston, Massachusetts USA), followed by incubation with goat anti-rat alexa-488 secondary antibody (Invitrogen Life Technologies Inc., Burlington, Ontario, Canada). For tissues, oxLDL was detected by mouse anti-mouse E06 IgM (Avanti Polar Lipids Inc, Alabaster, Alabama, USA), followed by alexa-488 goat anti-mouse IgM (Invitrogen Life Technologies Inc., Burlington, Ontario, Canada). Rat anti-mouse CD41 antibody and goat anti-rat alexa-488 secondary antibody (both from Invitrogen Life Technologies Inc., Burlington, Ontario, Canada) were used to detect activated platelets. Nuclei in fixed cells or tissues were visualized by 4', 6'-diamidino-2-phenylindole (DAPI). Fluorescent images were captured using a Zeiss Axiovert 200M inverted fluorescence microscope (Carl Zeiss Canada Ltd. Toronto, Ontario, Canada).

4.3.10 Statistical analysis

Sigma Plot statistical analysis software was used. Data was subjected to the Shapiro-Wilk test for normality and F test for equality of variances. Those that passed were analyzed by the Student's *t*-test (2-tailed, unpaired). Those that failed either test were analyzed by the Mann-Whitney Rank Sum test. Data from multiple groups were analyzed with one-way ANOVA: Data that passed normality and F tests was analyzed by Holm-Sidak method; those that failed normality and equal variance tests were subjected to Kruskal-Wallis one-way ANOVA on Ranks and Tukey post hoc test. Data with 2 independent variables were analyzed by two-way ANOVA. Data are presented as mean \pm standard error of the mean. P values <0.05 were considered statistically significant.

4.4 Results

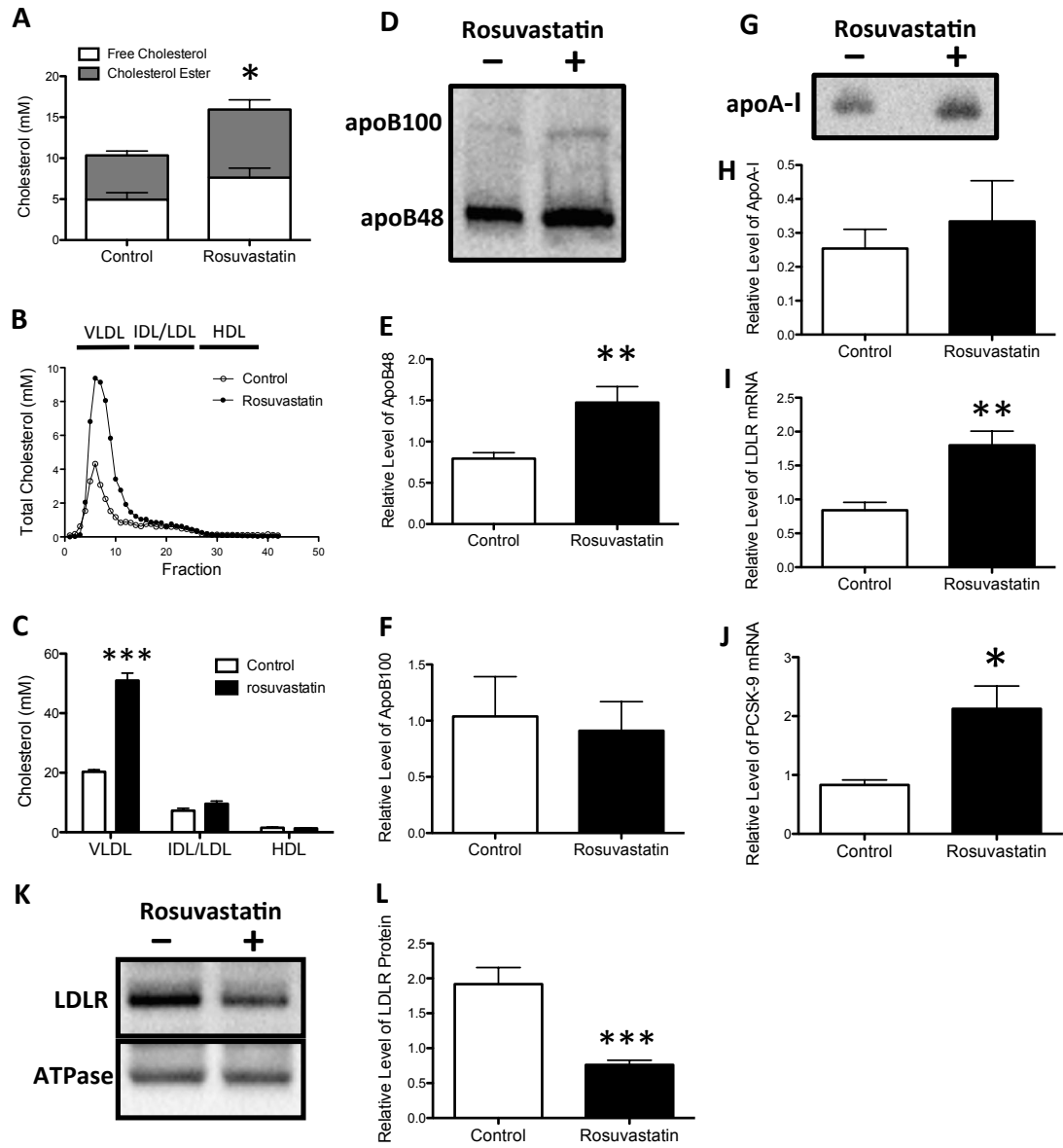
4.4.1 Rosuvastatin increased plasma cholesterol levels in SR-B1^{-/-}/apoE^{-/-} mice.

It has previously been shown that 4- to 7-week-old SR-B1^{-/-}/apoE^{-/-} mice develop severe hypercholesterolemia with a significant increase of VLDL-sized lipoproteins (size fractionated by fast protein liquid chromatography, FPLC) (Trigatti et al., 1999). It has also been reported that plasma lipoproteins from SR-B1^{-/-}/apoE^{-/-} mice contain abnormally high levels of free cholesterol, compared with apoE^{-/-} littermates, and that this may contribute to the coronary artery atherosclerosis and/or cardiac pathology observed (Braun et al., 2003). Similarly, our data showed that the average plasma cholesterol in 5-week-old SR-B1^{-/-}/apoE^{-/-} mice was about 10 mM and that the majority of cholesterol was associated with VLDL-sized fractions (Figure 4.1A-C). However, daily treatment of SR-B1^{-/-}/apoE^{-/-} mice, beginning at age of 3 weeks and lasting 2 weeks, increased plasma total cholesterol by 33 % (Figure 4.1A). Rosuvastatin treatment did not correct the abnormally high free cholesterol:total cholesterol ratio in rosuvastatin-treated SR-B1^{-/-}/apoE^{-/-} mice (Figure 4.1A). The lipoprotein cholesterol profiles of saline- or rosuvastatin-treated SR-B1^{-/-}/apoE^{-/-} mice revealed that rosuvastatin treatment increased cholesterol associated with VLDL-sized particles without substantially altering cholesterol associated with IDL/LDL- or HDL-sized lipoproteins (Figure 4.1B-C). Consistent with these findings, rosuvastatin treatment increased the plasma levels of apolipoprotein B (apoB) 48, but not apoB100 (which was present at much lower levels than apoB48) or apoA-I in SR-B1^{-/-}/apoE^{-/-} mice (Figure 4.1D-H). In humans, statin treatment leads to increased expression of LDLR in liver, promoting the

clearance of LDL from blood (Liao and Laufs, 2005). Likewise, rosuvastatin treatment of SR-B1^{-/-}/apoE^{-/-} mice resulted in an approximately 2-fold increase in the amount of LDLR transcript in liver as detected by RT-PCR (Figure 4.1I). Despite this, immunoblotting revealed an approximate 2-fold reduction in LDLR protein levels in liver membrane extracts from rosuvastatin-treated SR-B1^{-/-}/apoE^{-/-} mice (Figure 4.1K and L). This reduction in LDLR protein levels, despite the increased transcript levels, is likely explained by increased expression of PCSK9 in livers of rosuvastatin-treated SR-B1^{-/-}/apoE^{-/-} mice (Figure 4.1J), since PCSK9 gene expression, like that of LDLR, is upregulated by inhibition of cholesterol biosynthesis, but PCSK9 itself promotes the degradation of LDLR in hepatocytes (Horton et al., 2007; Urban et al., 2013). In turn, the reduced hepatic LDLR protein level likely explains the increased levels of apoB and cholesterol associated with plasma and VLDL-sized lipoproteins.

Figure 4.1 Effects of rosuvastatin on plasma cholesterol in SR-B1^{-/-}/apoE^{-/-} mice.

(A): Free cholesterol (white bars) and cholesterol ester (grey bars) in plasma samples from control saline- or rosuvastatin-treated SR-B1^{-/-}/apoE^{-/-} mice (n=10, 10). (B): Plasma lipoproteins were fractionated by FPLC, and total cholesterol in each fraction was determined. Representative profiles from control saline- or rosuvastatin-treated SR-B1^{-/-}/apoE^{-/-} mice are shown. (C) Total cholesterol in pooled fractions corresponding to VLDL-, IDL/LDL- and HDL-sized lipoproteins (n=5, 5). (D): Serum samples from control saline- or rosuvastatin-treated SR-B1^{-/-}/apoE^{-/-} mice were subjected to SDS-PAGE and immunoblotting for apoB. Positions of apoB48 (250kD) and apoB100 (500kD) are shown. Quantification of relative amounts of apoB48 (E) (n=9, 8), apoB100 (F; n=6, 8). (G) Representative immunoblot and (H) quantification of apoA-I (25kD) in serum from control saline- or rosuvastatin-treated SR-B1^{-/-}/apoE^{-/-} mice (n=5, 4). RT-PCR analysis of hepatic (I) LDLR and (J) PCSK9 transcript levels in control saline- or rosuvastatin-treated SR-B1^{-/-}/apoE^{-/-} mice (n=9, 10). Transcript levels are expressed as fold change relative to control saline-treated SR-B1^{-/-}/apoE^{-/-} mice and were normalized to GAPDH mRNA. (K) Representative immunoblot and (L) quantification of LDLR protein (normalized to Na⁺/K⁺ ATPase) in liver membranes from control saline- or rosuvastatin-treated SR-B1^{-/-}/apoE^{-/-} mice (n=9, 8). Mann-Whitney rank sum test was used for data in A, F, J and K. Student's *t*-test was used for all other comparisons except for panel C, which was analyzed by 2-way ANOVA. *P<0.05, **P<0.01 and ***P<0.001 vs. control.



4.4.2 Rosuvastatin attenuated atherosclerosis and cardiac pathology in SR-B1^{-/-}/apoE^{-/-} mice.

Consistent with previous reports, saline-treated SR-B1^{-/-}/apoE^{-/-} mice developed substantial aortic sinus atherosclerosis (Figure 4.2A) as well as atherosclerosis in coronary arteries by 5 weeks of age (Al-Jarallah et al., 2013; Braun et al., 2002) (Figure 4.2D-H). Despite the increase in lipoprotein cholesterol levels, atherosclerosis was substantially reduced in both the aortic sinus (Figure 4.2B,C) and in coronary arteries (Figure 4.2I) of rosuvastatin-treated compared with saline-treated SR-B1^{-/-}/apoE^{-/-} mice. Rosuvastatin treatment resulted in an approximate 44 % reduction in the cross-sectional areas of atherosclerotic plaques in the aortic sinus (Figure 4.2A-C). The majority of coronary arteries that developed atherosclerosis in SR-B1^{-/-}/apoE^{-/-} mice were in the upper portion of the heart, more proximal to the aorta (data not shown), which is consistent with the concept that atherosclerosis is a disease involving large- and medium-sized arteries (Galkina and Ley, 2009). Of coronary arteries observed in this region of hearts from saline-treated SR-B1^{-/-}/apoE^{-/-} mice at 5 weeks of age, 60 % exhibited no lipid accumulation (Figure 4.2D) or only fatty streaks (Figure 4.2E), while approximately 40 % exhibited raised atherosclerotic plaques (Figure 4.2F-H). However, SR-B1^{-/-}/apoE^{-/-} mice treated with rosuvastatin exhibited substantially fewer atherosclerotic coronary arteries (14 % of total coronary arteries observed; Figure 4.2I).

We have recently reported that SR-B1^{-/-}/LDLR^{-/-} mice fed a high-fat, high-cholesterol, cholate-containing diet rapidly developed coronary artery atherosclerosis leading to coronary artery stenosis or occlusion and that a substantial percentage of

atherosclerotic coronary arteries in these mice were characterized by abundant staining for CD41, a marker of platelet activation, suggesting that coronary artery disease development in these mice may involve thrombosis in addition to atherosclerosis (Fuller et al., 2014b). To determine if similar processes are involved in the development of coronary artery disease in the SR-B1^{-/-}/apoE^{-/-} mice and if they were modulated by rosuvastatin treatment, we performed immunostaining for CD41 in sections of atherosclerotic coronary arteries of saline- and rosuvastatin-treated SR-B1^{-/-}/apoE^{-/-} mice (Figure 4.3). This revealed that a substantial proportion (50 %) of atherosclerotic coronary arteries in 5-week-old SR-B1^{-/-}/apoE^{-/-} mice were positive for CD41 staining (Figure 4.3I). Both the proportion of atherosclerotic coronary arteries that were positive for CD41 staining (Figure 4.3I), and the average extent of CD41 staining in atherosclerotic coronary arteries (Figure 4.3J) were substantially reduced in 5-week-old SR-B1^{-/-}/apoE^{-/-} mice that had been treated for 2 weeks with rosuvastatin. This was seen both for coronary arteries that were virtually completely occluded by atherosclerotic plaques (Figure 4.3C and G) as well as coronary arteries that contained raised atherosclerotic plaques associated with coronary artery stenosis (<50 %) (Figure 4.3A and E). In contrast, we detected only two instances of atherosclerotic plaques in the aortic sinus that showed CD41-positive staining (not shown), out of approximately 27 aortic sinus sections analyzed. Together, these data suggest that in addition to reducing the degree of coronary artery atherosclerosis, rosuvastatin treatment reduced the accumulation of activated platelets in coronary artery atherosclerotic plaques in SR-B1^{-/-}/apoE^{-/-} mice.

Atherosclerosis in SR-B1^{-/-}/apoE^{-/-} mice is accompanied by myocardial fibrosis and cardiomegaly (Al-Jarallah et al., 2013; Braun et al., 2002). Fibrotic tissue in hearts was detected by Masson's trichrome staining, and cardiomegaly was assessed by measuring the heart:body weight ratios (Al-Jarallah et al., 2013; Braun et al., 2002; Fuller et al., 2014b). As reported previously (Al-Jarallah et al., 2013; Braun et al., 2002; Fuller et al., 2014b), we found that hearts from 5-week-old SR-B1^{-/-}/apoE^{-/-} mice exhibit extensive collagen deposition, as indicated by blue Masson's trichrome staining (healthy myocardium stains red) (Figure 4.4A). In contrast, collagen deposition was substantially reduced in hearts from rosuvastatin-treated SR-B1^{-/-}/apoE^{-/-} mice (Figure 4.4B-C), suggesting that rosuvastatin attenuated cardiac fibrosis in SR-B1^{-/-}/apoE^{-/-} mice. At 5 weeks of age, SR-B1^{-/-}/apoE^{-/-} mice exhibited significantly higher heart weights and lower body weights than saline-treated apoE^{-/-} littermates (Figure 4.4D-E), corresponding to significantly higher heart:body weight ratios (Figure 4.4F), which is consistent with previous studies (Al-Jarallah et al., 2013; Braun et al., 2002). Rosuvastatin did not affect the body weights of SR-B1^{-/-}/apoE^{-/-} mice (Figure 4.4E). However heart weights and heart:body weight ratios were significantly reduced in SR-B1^{-/-}/apoE^{-/-} mice treated for two weeks with rosuvastatin, compared with saline-treated mice (Figure 4.4D-F).

Figure 4.2: Treatment of SR-B1^{-/-}/apoE^{-/-} mice with rosuvastatin reduced atherosclerosis development in the aortic sinus and coronary arteries.

Representative images of oil red O/hematoxylin-stained cross sections of aortic sinus from (A) control saline-treated, and (B) rosuvastatin-treated SR-B1^{-/-}/apoE^{-/-} mice (scale bar = 200 μ m). (C) Quantification of aortic sinus atherosclerotic plaque size (n=10, 10). (D-H) Representative sections of oil red O/hematoxylin-stained coronary arteries with various extents of atherosclerosis (D: no plaque, E: fatty streaks, F: <50% stenosis, G: >50% stenosis and H: 100% occluded. Scale bar=50 μ m). (I) Quantification of the percentage of coronary arteries/section with raised atherosclerotic plaques in saline- or rosuvastatin-treated SR-B1^{-/-}/apoE^{-/-} mice (n=10, 10). Data were analyzed by Student's *t*-test. *P<0.05 and ***P<0.001.

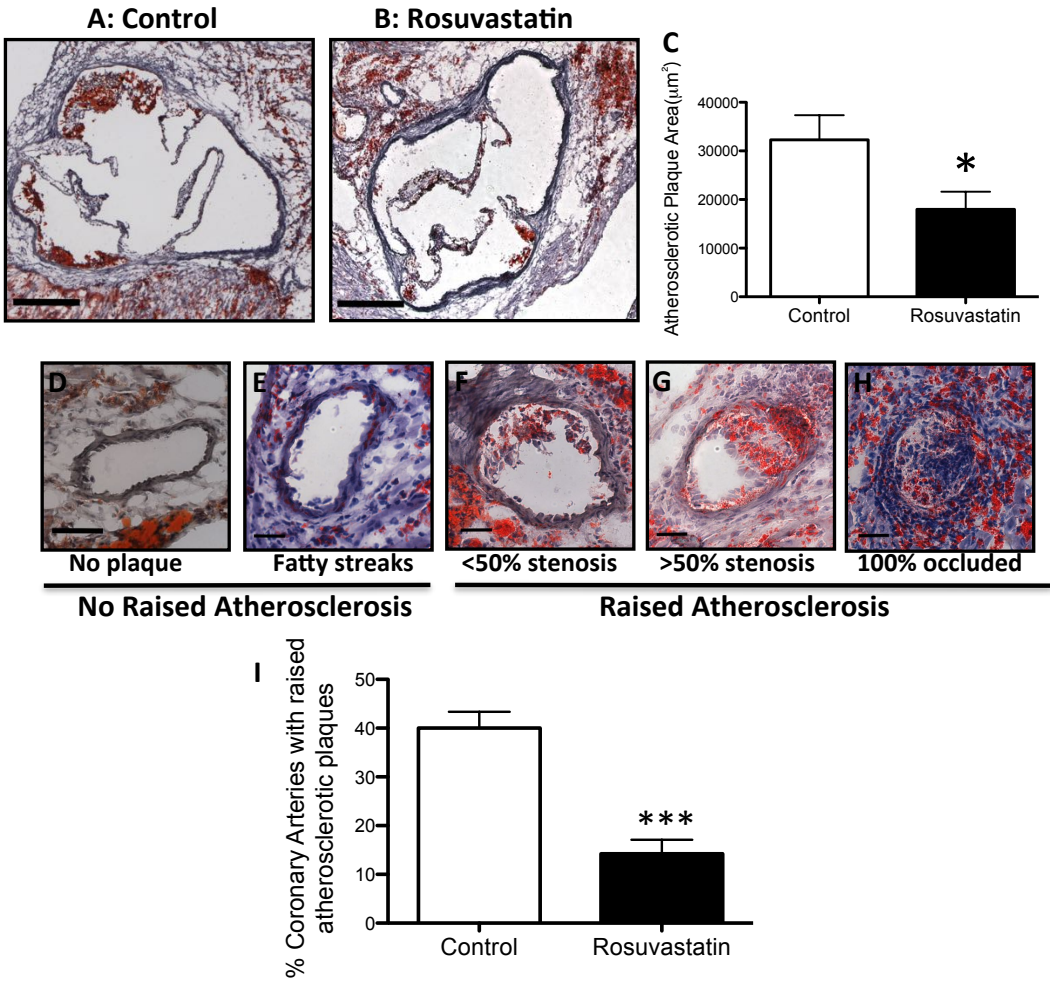


Figure 4.3: Rosuvastatin treatment reduced CD41 immunostaining in coronary arteries of SR-B1^{-/-}/apoE^{-/-} mice. Indirect immunofluorescence staining (green) for CD41, a marker of activated platelets, is shown in panels A, C, E, and G (nuclear DNA stained blue with DAPI). Oil red O/hematoxylin-stained adjacent sections are shown in panels B, D, F, and H. (A, B) Stenotic (C, D) completely occluded coronary arteries from control saline-treated SR-B1^{-/-}/apoE^{-/-} mice. (E, F) Stenotic and (G, H) completely occluded coronary arteries from rosuvastatin-treated SR-B1^{-/-}/apoE^{-/-} mice. Scale bar= 50 μ m. (I) The percentage of CD41-positive atherosclerotic coronary arteries and (J) the intensity of CD41 staining (normalized to plaque area) in positive coronary arteries from control saline- (n=13) and rosuvastatin-treated (n=14) SR-B1^{-/-}/apoE^{-/-} mice. Data in I were analyzed by Student's *t*-test and in J by the Mann-Whitney rank sum test. *P<0.05 and **P<0.01 vs. control saline-treated SR-B1^{-/-}/apoE^{-/-} mice.

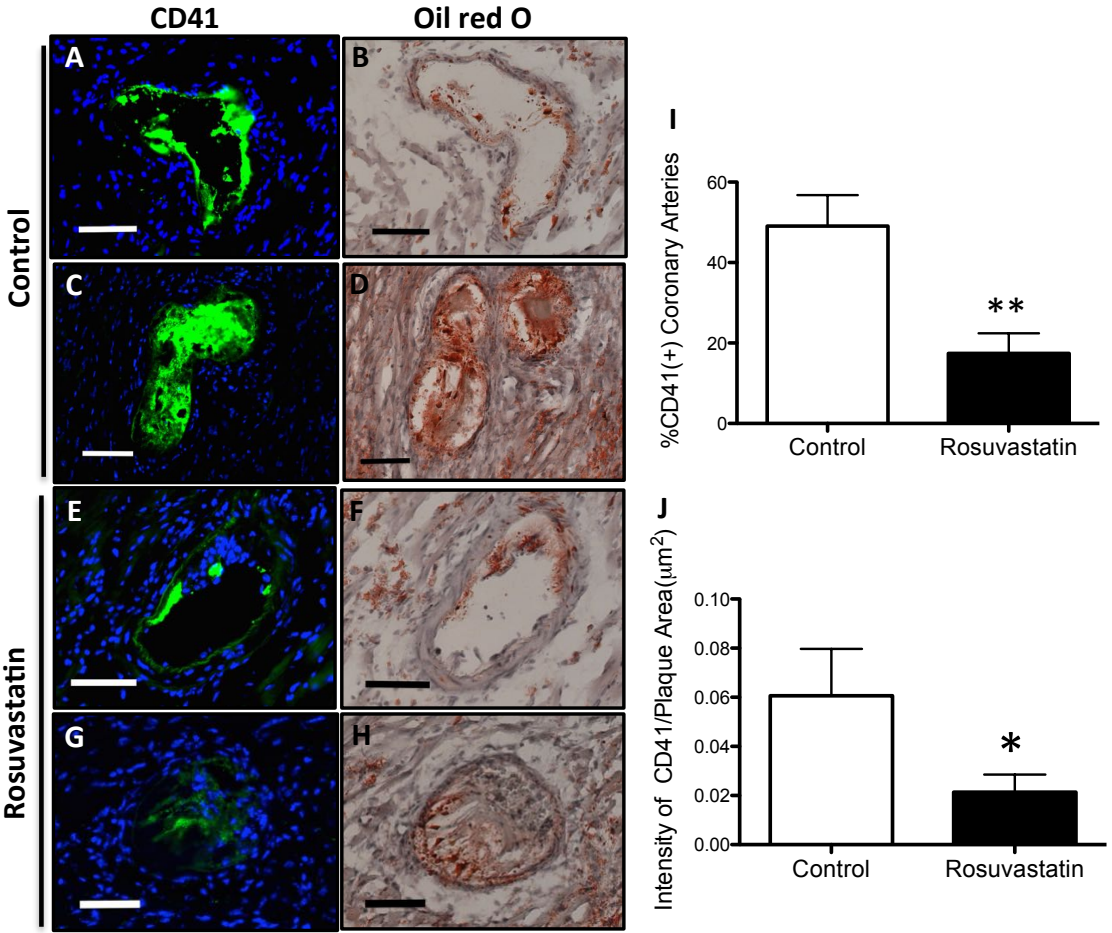
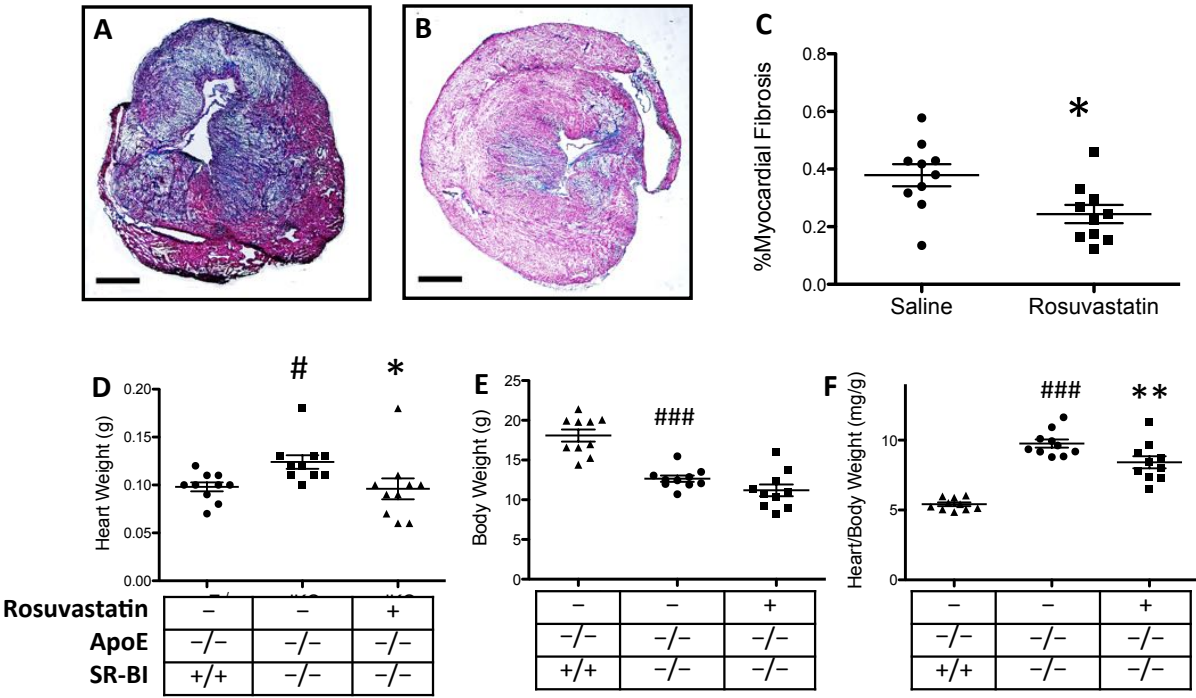


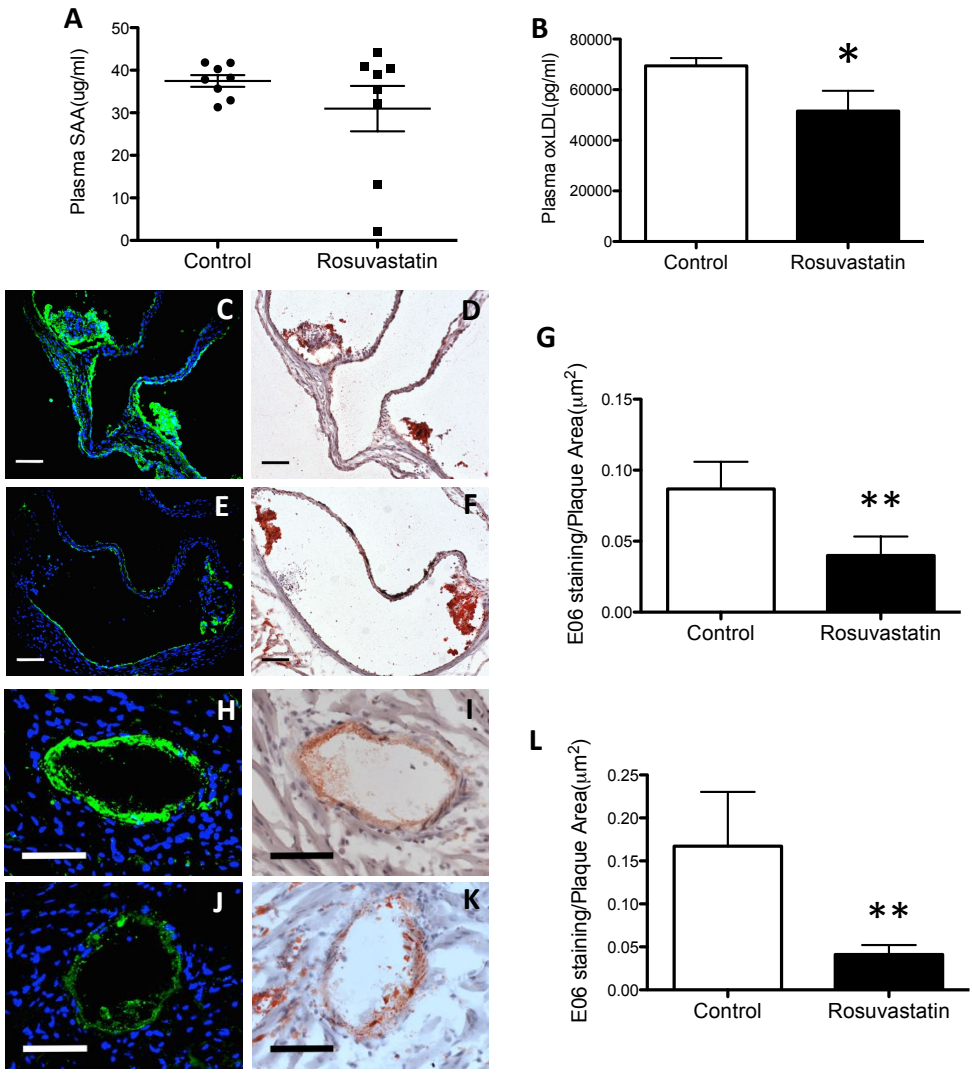
Figure 4.4: Rosuvastatin treatment attenuated myocardial fibrosis and cardiomegaly in SR-B1^{-/-}/apoE^{-/-} mice. (A, B) Representative images of Trichrome-stained transverse sections of upper portions of hearts from control saline- and rosuvastatin-treated SR-B1^{-/-}/apoE^{-/-} mice (scale bar=800 μ m). Collagen stains blue and healthy myocardium stains red. (C) The fibrotic area relative to the total cross-sectional area of the myocardium was quantified in each section for n=10 mice per group. (D) Heart weights, (E) body weights and (F) heart:body weight ratios, for control saline- or rosuvastatin-treated SR-B1^{-/-}/apoE^{-/-} mice (n=10, 10). Heart weights, body weights and heart:body weight ratios of saline-treated apoE^{-/-} mice (n=10) are shown for reference. Data in C were analyzed by Student's *t*-test. Data in D were analyzed by the Kruskal-Wallis one-way ANOVA on Ranks and Tukey post-hoc test. Data in E and F were analyzed by one-way ANOVA and Holm-Sidak post-hoc test. *P<0.05 and **P<0.01 vs. saline-treated SR-B1^{-/-}/apoE^{-/-} mice. #P<0.05 and ####P<0.001 vs. saline-treated apoE^{-/-} mice.



4.4.3 Rosuvastatin reduced levels of oxLDL in plasma and atherosclerotic plaques

Statins have been reported to attenuate systemic inflammation as well as lipoprotein oxidation (Davignon, 2004; Liao and Laufs, 2005). To investigate potential mechanisms involved in the anti-atherogenic effects of rosuvastatin in the face of increased lipoprotein cholesterol levels in SR-B1^{-/-}/apoE^{-/-} mice, we analyzed levels of the acute-phase inflammatory marker serum amyloid alpha (SAA) as well as levels of markers of oxidized lipoproteins (Douglas et al., 2012) in plasma and in the aortic sinus and coronary artery walls. Rosuvastatin did not significantly alter the levels of SAA in plasma of the SR-B1^{-/-}/apoE^{-/-} mice (Figure 4.5A). On the other hand, rosuvastatin treatment resulted in substantially reduced levels oxLDL, as detected by ELISA, in plasma of SR-B1^{-/-}/apoE^{-/-} mice (Figure 4.5B). In order to test for markers of oxLDL in histological sections of the aortic sinus and coronary arteries of saline- or rosuvastatin-treated SR-B1^{-/-}/apoE^{-/-} mice, we carried out indirect immunofluorescence staining using the E06 primary antibody, which detects oxidized phospholipids in oxLDL in atherosclerotic plaques (Napoli et al., 2004). We detected substantial E06 immunoreactivity in the aortic sinus in both atherosclerotic plaques and in regions of the artery wall that were devoid of atherosclerosis (Figure 4.5C). Substantial E06 immunoreactivity was also detected in fatty streaks in coronary arteries of SR-B1^{-/-}/apoE^{-/-} mice (Figure 4.5H). Reduced levels of E06 immunoreactivity were observed in both the aortic sinus (Figure 4.5E-G) and coronary arteries (Figure 4.5J-L) of rosuvastatin-treated SR-B1^{-/-}/apoE^{-/-} mice. This suggests reduced levels of oxidized lipids associated with oxLDL in the walls of arteries in rosuvastatin-treated mice.

Figure 4.5: Effects of rosuvastatin on SAA and oxLDL in SR-B1^{-/-}/apoE^{-/-} mice. (A) SAA levels in plasma from control saline- and rosuvastatin-treated SR-B1^{-/-}/apoE^{-/-} mice (n=8, 8). (B) OxLDL levels in plasma from control saline- and rosuvastatin-treated SR-B1^{-/-}/apoE^{-/-} mice (n=10, 10). OxLDL in atherosclerotic plaques in the aortic sinus (C-G) and coronary arteries (H-L) was analyzed by indirect immunofluorescence staining (oxLDL: green; nuclei: blue). Immunofluorescence (C, E, H, J) and oil red O (D, F, I, K) staining in adjacent sections are shown. Scale bars= 50 µm. The intensity of oxLDL in (G) the aortic sinus and (L) coronary arteries from control saline-treated (n=13) and rosuvastatin-treated (n=14) SR-B1^{-/-}/apoE^{-/-} mice was quantified and normalized to plaque area. Data in A, G and L were analyzed by the Mann-Whitney rank sum test. Data in B were analyzed by Student's *t*-test. *P<0.05 and **P<0.01 vs. saline-treated SR-B1^{-/-}/apoE^{-/-} mice.

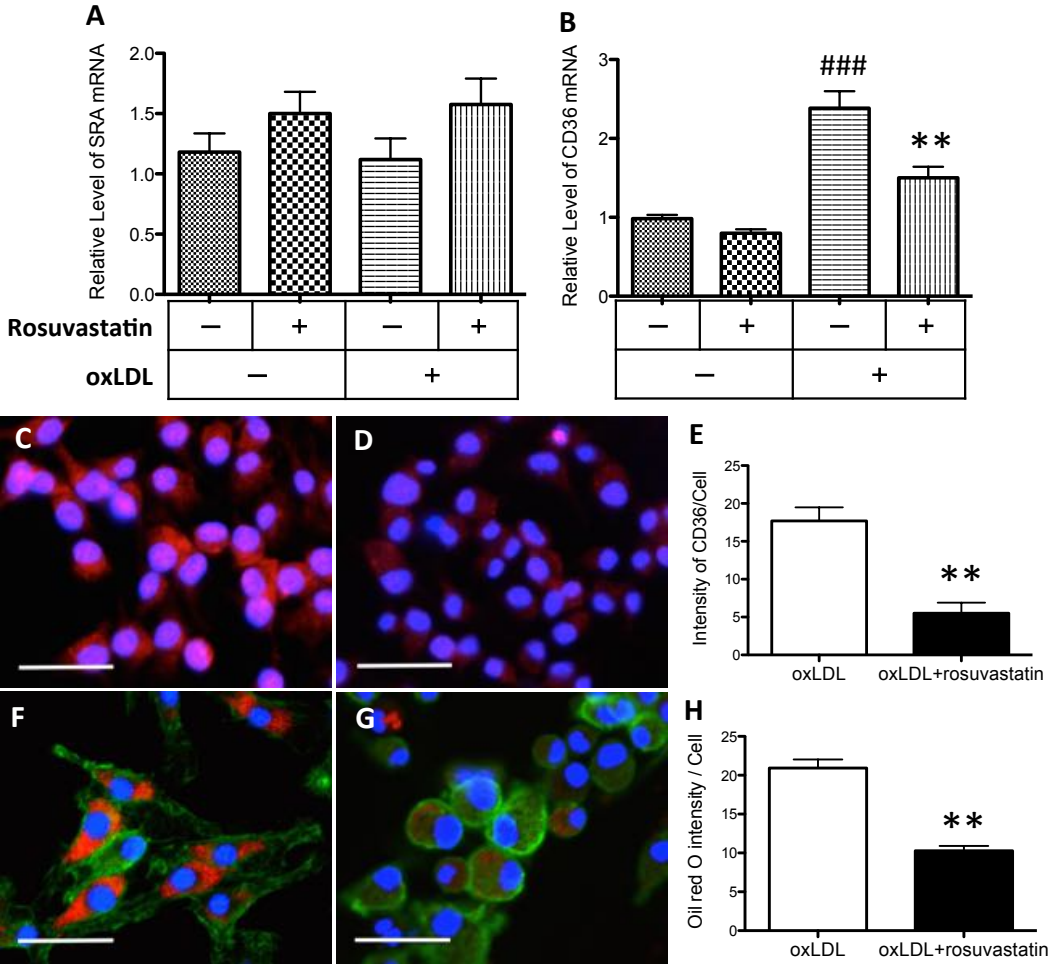


4.4.4 Rosuvastatin treatment of macrophages decreases CD36 expression and foam cell formation

To determine if rosuvastatin treatment also altered the ability of macrophages from SR-B1^{-/-}/apoE^{-/-} mice to accumulate lipids derived from oxLDL, we analyzed the expression of CD36 and scavenger receptor class A (SRA), the two major receptors mediating oxLDL-dependent conversion of macrophages to foam cells (Shashkin et al., 2005). Bone marrow prepared from SR-B1^{-/-}/apoE^{-/-} mice was differentiated into macrophages in culture and treated with or without rosuvastatin in the presence or absence of oxLDL (Figure 4.6). Neither rosuvastatin, oxLDL, nor the combination of rosuvastatin and oxLDL significantly affected the levels of SRA transcripts as detected by RT-PCR (Figure 4.6A). Consistent with previous reports that oxLDL upregulated CD36 expression (Jedidi et al., 2006), we observed a substantial increase of CD36 transcripts in oxLDL-treated cells (Figure 4.6B). Rosuvastatin substantially reduced CD36 gene expression in oxLDL-treated but not untreated cells (Figure 4.6B). Similarly, rosuvastatin treatment of bone marrow-derived macrophages exposed to oxLDL substantially reduced CD36 protein levels as detected by indirect immunofluorescence staining (Figure 4.6C-E). To examine the effects of rosuvastatin on foam cell formation, cultured macrophages treated with oxLDL with or without rosuvastatin were stained for neutral lipid droplets with oil red O. As expected, oxLDL treatment of cultured bone marrow-derived macrophages resulted in substantial formation of intracellular lipid droplets (Figure 4.6F). In contrast, co-incubation with rosuvastatin significantly suppressed lipid accumulation in macrophages (Figure 4.6G, H). Together, these results

demonstrate that rosuvastatin suppresses CD36 expression and oxLDL-driven foam cell formation.

Figure 4.6: Effects of rosuvastatin on scavenger receptor expression and foam cell formation in macrophages. (A, B) Levels of SR-A and CD36 mRNA in bone marrow-derived macrophages from SR-B1^{-/-}/apoE^{-/-} mice after treatment with or without oxLDL (100 µg protein/ml) and/or rosuvastatin (10 µM). Data are expressed as fold change relative to untreated cells and are normalized to levels of GAPDH mRNA. Cells from 3 mice were analyzed. (C, D) CD36 immunofluorescence staining of bone marrow-derived macrophages treated with oxLDL in the presence (C) or absence (D) of rosuvastatin (CD36: red; nuclei: blue). (E) The level of CD36 immunofluorescence staining per cell. (F, G) Oil red O staining of bone marrow-derived macrophages treated with oxLDL in the presence (F) or absence (G) of rosuvastatin (oil red O: red; F4/80: green; nuclei: blue). Scale bars in C, D, F, G =20 µm. (H) The level of oil red O staining per cell. Data in E and H represent 3 independent experiments and were confirmed with macrophages derived from bone marrow cells harvested from 2 additional mice. Data in A were analyzed by Kruskal-Wallis one-way ANOVA on Ranks. Data in B were analyzed by one-way ANOVA with the Holm-Sidak post hoc test. Data in E and H were analyzed by Student's *t*-test. ####P<0.001 vs. untreated control (no rosuvastatin/no oxLDL). **P<0.01 vs. treatment with oxLDL but no rosuvastatin.



4.5 Discussion

SR-B1^{-/-}/apoE^{-/-} mice do not begin to develop aortic sinus or coronary artery atherosclerosis until after 3 weeks of age (Al-Jarallah et al., 2013; Braun et al., 2003). However, they rapidly develop extensive coronary atherosclerosis, myocardial infarction and cardiac enlargement by 5 weeks of age when fed a normal chow diet (Al-Jarallah et al., 2013; Braun et al., 2002). SR-B1^{-/-}/apoE^{-/-} mice have been reported to exhibit substantially reduced survival, dying between 6 and 8 weeks of age (Braun et al., 2002; Braun et al., 2008b; Karackattu et al., 2006). In order to examine the effects of rosuvastatin treatment on the development of atherosclerosis in the aortic sinus and coronary arteries of these mice, we initiated treatment in mice at 3 weeks of age and euthanized mice at 5 weeks of age, after two weeks of daily treatment. By analyzing mice at 5 weeks of age, i.e. prior to onset of spontaneous death, we avoided potential confounding effects of the rapid decline in the health of mice.

Two-week treatment with rosuvastatin resulted in substantial reductions in the development of atherosclerosis in the aortic sinus and in coronary arteries of SR-B1^{-/-}/apoE^{-/-} mice (Figure 4.2). A significant proportion of atherosclerotic plaques in coronary arteries of SR-B1^{-/-}/apoE^{-/-} mice exhibited positive staining for CD41 (Figure 4.3), a marker of activated platelets, whereas CD41 staining was seen only very infrequently in atherosclerotic plaques in the aortic sinus (not shown). This suggests the development of platelet-rich thrombi in atherosclerotic plaques in the coronary arteries of SR-B1^{-/-}/apoE^{-/-} mice and is consistent with similar observations SR-B1^{-/-}/LDLR^{-/-} mice in which coronary artery atherosclerosis was induced to develop rapidly (within 3

weeks) by feeding the mice a highly atherogenic diet (Fuller et al., 2014b). Statins are known to prevent platelet activation and thrombosis, independent of their lipid-lowering effects (Liao and Laufs, 2005). Rosuvastatin has been reported to inhibit platelet activation in an animal model with endothelial dysfunction (Schafer et al., 2005a). Consistent with this, we observed that fewer atherosclerotic coronary arteries stained positive for CD41 and that in those that were positive, the extent of CD41 staining was reduced in mice treated for 2 weeks with rosuvastatin compared with saline-treated mice (Figure 4.3). These observations suggest that rosuvastatin treatment reduces the development of atherosclerosis and thrombosis in coronary arteries of SR-B1^{-/-}/apoE^{-/-} mice.

A consequence of coronary artery atherothrombosis in SR-B1^{-/-}/apoE^{-/-} mice is the development of myocardial infarction, as characterized by extensive cardiac fibrosis and cardiac enlargement. Treatment with rosuvastatin substantially reduced the extent of cardiac fibrosis in SR-B1^{-/-}/apoE^{-/-} mice (Figure 4.4A-C). Furthermore, rosuvastatin appeared to prevent the pathological increase in heart weights in SR-B1^{-/-}/apoE^{-/-} mice: Heart weights from saline-treated SR-B1^{-/-}/apoE^{-/-} mice were substantially larger, whereas those from rosuvastatin-treated SR-B1^{-/-}/apoE^{-/-} mice were no different than those of littermate saline-treated apoE^{-/-} mice (Figure 4.4D). These protective effects of rosuvastatin on cardiac morphology are most likely secondary to its effects on coronary artery atherothrombosis, although we cannot rule out the possibility that rosuvastatin treatment may have also protected cardiomyocytes directly against ischemia-induced

cell death and/or prevented the fibrotic response, as has been proposed by others (Ludman et al., 2009).

To understand the mechanisms by which rosuvastatin treatment reduced atherosclerosis development in SR-B1^{-/-}/apoE^{-/-} mice, we first examined the effects of rosuvastatin treatment on plasma and lipoprotein total and/or free cholesterol levels. Others have reported that treatment with different statins, including rosuvastatin, either slightly reduced or did not affect plasma lipoprotein total cholesterol levels in apoE^{-/-} mice in various studies (Enomoto et al., 2009; Gronros et al., 2008; Monetti et al., 2007; Schroeter et al., 2009; Zadelaar et al., 2007). However, we were surprised to see that rosuvastatin substantially increased plasma levels of apoB48 and cholesterol associated with VLDL-sized lipoprotein particles in plasma of SR-B1^{-/-}/apoE^{-/-} mice (Figure 4.1). An important mechanism of action of statins in plasma cholesterol lowering is the relief of the negative feedback inhibition of the cholesterol biosynthetic pathway on the transcription factor, sterol regulatory element-binding protein-2 (SREBP-2) in the liver (Horton et al., 2007). This results in increased processing of active SREBP-2 and increased expression of SREBP-2-regulated genes, including the gene encoding LDLR. The resulting increases in LDLR protein levels would lead to increased clearance of apoB- and apoE-containing lipoproteins from blood, reducing LDL (and VLDL) cholesterol levels (Horton et al., 2007). Indeed, we observed increased LDLR transcript levels in livers of rosuvastatin-treated SR-B1^{-/-}/apoE^{-/-} mice (Figure 4.1F). Conversely, we observed a greater than 50 % reduction in the amount of LDLR protein in liver membranes from the same rosuvastatin-treated SR-B1^{-/-}/apoE^{-/-} mice (Figure 4.1G,H).

This is likely explained by the increased expression of PCSK9 in the livers of SR-B1^{-/-}/apoE^{-/-} mice treated with rosuvastatin. PCSK9 gene expression is coordinately regulated with LDLR by SREBP-2 (Horton et al., 2007). PCSK9 that is either secreted by hepatocytes, or acting intracellularly, can bind to the LDLR and trigger its degradation, reducing LDLR protein levels and attenuating the effects of SREBP-2-mediated upregulation of LDLR gene expression (Horton et al., 2007). Consistent with this, the JUPITER (Justification for the Use of statins in Prevention: an Intervention Trial Evaluating Rosuvastatin) study showed that treatment with 20 mg of rosuvastatin resulted in a 28% increase in PCSK9 in men and 35% in women (Awan et al., 2012). Various studies suggest that mice are highly sensitive to the upregulation of PCSK9, which may explain why statin treatment is much less effective at lowering lipoprotein total cholesterol levels in mice than in humans (Horton et al., 2007).

We observed reduced aortic sinus atherosclerosis and reduced coronary artery atherothrombosis, accompanied by reduced cardiac fibrosis and attenuated cardiac enlargement in the SR-B1^{-/-}/apoE^{-/-} mice that had been treated with rosuvastatin, despite the substantially increased levels of apoB and of total cholesterol associated with VLDL-sized lipoproteins. This suggested that rosuvastatin protected against atherothrombosis via pathways distinct from LDLR-mediated plasma total cholesterol lowering. It has been reported that the concentrations of oxLDL in plasma were elevated in patients with CHD and that circulating oxLDL was found to be a strong predictor for acute CHD events (Holvoet et al., 1998; Meisinger et al., 2005). Indeed, despite the substantially increased levels of plasma total cholesterol in rosuvastatin-

treated SR-B1^{-/-}/apoE^{-/-} mice, we observed reduced levels of oxLDL in plasma as detected by ELISA (Figure 4.5B). We also observed abundant oxidized phospholipid immunoreactivity in atherosclerotic plaques as detected by immunostaining using the E06 monoclonal antibody, in all stages of atherosclerotic plaque development in both the aortic sinus and coronary arteries of SR-B1^{-/-}/apoE^{-/-} mice (Figure 4.5C, H). Treatment with rosuvastatin substantially reduced oxidized phospholipid immunoreactivity in atherosclerotic plaques in both aortic sinus and in coronary arteries (Figure 4.5C-L). This is consistent with reports of reduced oxLDL in the aortic arch of obese hyperlipidemic mice treated with rosuvastatin (Verreth et al., 2007).

CD36 appears to be a major receptor for oxLDL in macrophages, mediating its uptake and subsequent foam cell formation (Collot-Teixeira et al., 2007). CD36 expression is also upregulated by oxLDL in macrophages (Jedidi et al., 2006). Rosuvastatin attenuated the oxLDL-mediated upregulation of CD36 message and reduced CD36 protein levels, but did not alter SRA gene expression in oxLDL-treated bone marrow-derived macrophages prepared from SR-B1^{-/-}/apoE^{-/-} mice (Figure 4.6A-E). This is consistent with reports that pitavastatin downregulates CD36 expression by reducing PPAR- γ gene expression and increasing PPAR- γ protein phosphorylation (Han et al., 2004). It is unknown, however, if rosuvastatin acts through the same mechanism. OxLDL-driven foam cell formation is a consequence of CD36-mediated uptake of oxLDL by macrophages (Shashkin et al., 2005). Consistent with the ability of rosuvastatin to suppress oxLDL-stimulated CD36 gene expression and to reduce CD36

protein levels, rosuvastatin also suppressed oxLDL-mediated foam cell formation in cultured bone marrow-derived macrophages from SR-B1^{-/-}/apoE^{-/-} mice (Figure 4.6F-H). Together these studies demonstrate that rosuvastatin reduces the levels of oxLDL and oxLDL-derived lipids in plasma and in the artery wall as well as the ability of macrophages to take up oxLDL and become foam cells through suppression of oxLDL-induced CD36 expression. This reduction in oxLDL-driven foam cell formation, together with attenuated platelet activation, likely accounts for the reduced atherothrombosis and consequent reductions in cardiac fibrosis and cardiac enlargement, in the face of increased plasma total cholesterol in SR-B1^{-/-}/apoE^{-/-} mice treated with rosuvastatin.

CHAPTER V: DISCUSSION

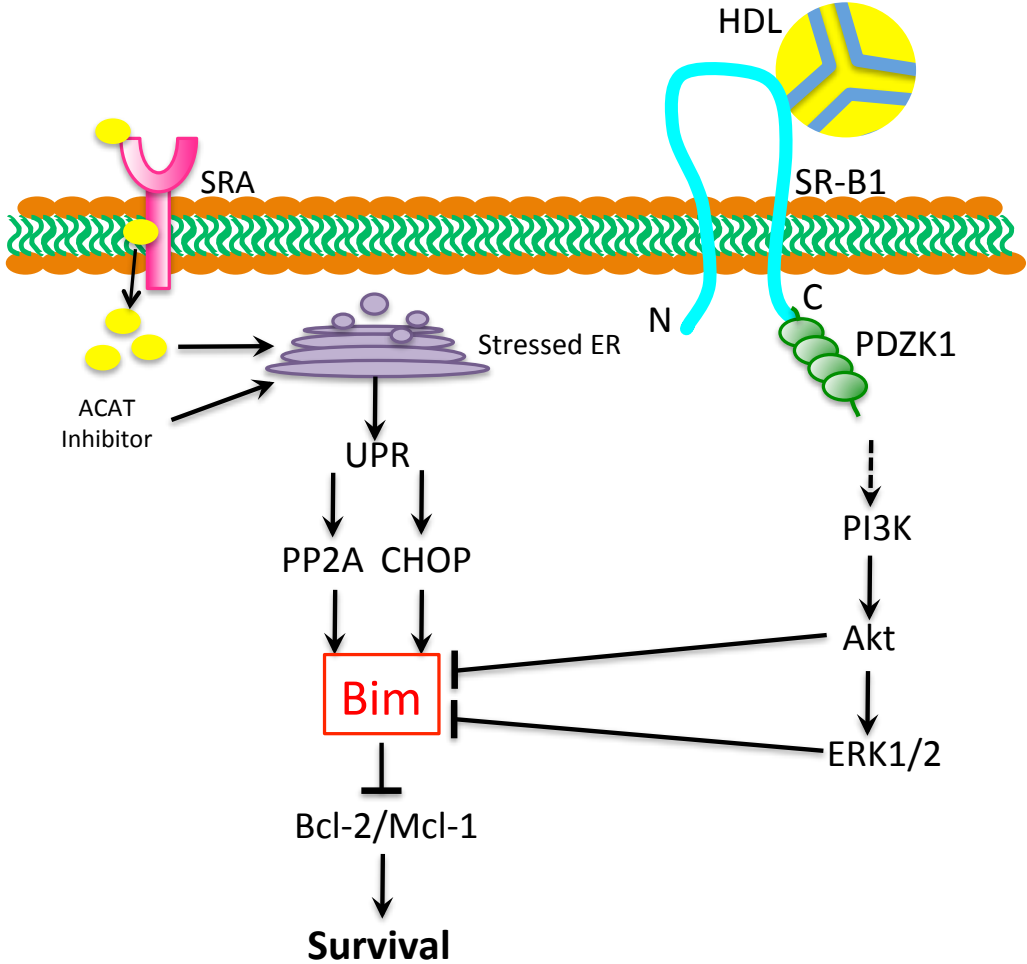
5.1 Summary of HDL anti-apoptotic signaling pathway in macrophages

Macrophage apoptosis has been effectively induced by various triggers (e.g. FC, oxysterols, Fas ligand and TNF α), which are present or abundantly accumulate in atherosclerotic plaques (Canault et al., 2006; Feng et al., 2003a; Myoishi et al., 2007; Zadelaar et al., 2005). However, the exact mechanism mediating macrophage apoptosis is still under investigation. One well-established mechanism is FC-induced ER stress, which triggers macrophage apoptosis via the activation of UPR and CHOP (Tabas, 2004). A CHOP binding site has been found in the first intron of the Bim genes, enabling CHOP as a transcription factor of Bim transcription (Puthalakath et al., 2007). Protein Phosphatase 2A (PP2A), which is also activated by ER stress, dephosphorylated Bim and prevented Bim from ubiquitination and proteosomal degradation (Puthalakath et al., 2007) (Figure 5.1).

FC-induced apoptosis was shown by my colleagues to be suppressed by co-incubating cells with HDL (Zhang and Al-Jarallah, manuscript in revision). The protection by HDL is dependent on the HDL receptor SR-B1 (Zhang and Al-Jarallah, manuscript in revision) and the adapter PDZK1 (Chapter 2), which is followed by the activation of PI3K/Akt pathway. Since HDL did not affect Bim mRNA levels in ER stressed macrophages (Chapter 3), HDL more likely regulates Bim at post-transcriptional level. It has been shown that the PI3K/Akt pathway stimulated the activation of MAPK pathway, and the activation of ERK1/2 mediated the phosphorylation of Bim at Ser65, leading to the dissociation of Bim from pro-survival

Bcl-2 proteins and the proteasomal degradation of Bim proteins (Ewings et al., 2007a; Ley et al., 2003). It has also been shown that Akt activation directly suppressed Bim activity by phosphorylating Bim at Ser87 (Qi et al., 2006). However, there are still some important questions that can be addressed to delineate the HDL-dependent signaling pathway in macrophages:

Figure 5.1: The working model of SR-B1-mediated HDL anti-apoptotic signaling pathway in macrophages. Extracellular cholesterol (*e.g.* acetylated LDL) is taken up via the scavenger receptor A (SRA). Acetyl-coenzyme A acetyltransferase (ACAT) inhibitor is added to induce free cholesterol accumulation in ER, leading to ER stress and UPR. UPR activates CHOP and PP2A, which increase Bim protein by up-regulating transcription and inhibiting degradation. In contrast, HDL activates PI3K/Akt pathway via SR-B1 and PDZK1. Akt, on one hand, was shown to inhibit Bim activation; on the other hand, Akt activates ERK1/2, which phosphorylates Bim and tags Bim for ubiquitination and proteasomal degradation.



(1) Which component in HDL is the ligand interacting with SR-B1 and initiating the signaling pathway in macrophages?

It has been demonstrated by Dr. Krieger that SR-B1 is a multi-ligand receptor, binding with not only HDL, but also other lipoproteins, including VLDL, IDL and LDL (Krieger, 2001). My data suggests that only HDL, but not LDL, is able to protect cells from apoptosis (Figure 2.1), suggesting that not all SR-B1 ligands exert this effect. Moreover, SR-B1 also interacts with the isolated apolipoproteins contained in HDL, such as apoA-I, apoA-II and apoC-III (Xu et al., 1997). However, it is unknown which component(s) in HDL activates the pro-survival signaling pathway in macrophages by binding to SR-B1. Chapter 3 showed that the knockout of apoA-I significantly increased the plaque size and necrotic core size in LDLR^{-/-} mice (Figure 3.5). This may indicate a role of apoA-I as SR-B1's ligand *in vivo*. However, since apoA-I participates in HDL *de novo* synthesis, the deficiency of apoA-I led to over 60 % decrease of plasma HDL (Figure 3.4). Thus, it is unclear if the increased atherosclerosis was the result of reduced HDL levels or the fact that what HDL was present lacked apoA-I. Purified apolipoproteins and reconstituted HDL have been widely used to test the effects of these HDL components in vascular cells *in vitro* (Cockerill et al., 2001; Di Bartolo et al., 2011a; Dimayuga et al., 1999; Feng et al., 2012). However, purified apoA-I can be lipidated and transformed into HDL particle during tissue culturing, as a consequence of cholesterol efflux from cells (Asztalos et al., 1997). Thus, in order to test the effect of apoA-I *in vitro*, we can isolate plasma HDL from apoA-I^{-/-} mice to test if HDL lacking apoA-I can still protect macrophages from apoptosis.

(2) How is PI3K/Akt1 activated by SR-B1/PDZK1?

Akt, or specifically Akt1, activation in macrophages by HDL is dependent on the expression of both SR-B1 and PDZK1 (Zhang and Al-Jarallah, manuscript in revision; Chapter 2, Yu and Fernandes, manuscript in preparation). Also, Zhang *et al.* showed that the ability of HDL to rescue FC-treated macrophages was reversed by co-incubating with PI3K inhibitor LY294002 (Zhang and Al-Jarallah, manuscript in revision). However, it is unknown how PI3K/Akt pathway is activated by SR-B1 and PDZK1. It was demonstrated in endothelial cells that non-receptor kinase Src, which was the upstream factor of PI3K/Akt, coimmunoprecipitated with SR-B1 independently of PDZK1 (Mineo *et al.*, 2003; Zhu *et al.*, 2008). However, the phosphorylation of Src by SR-B1 was abolished by either PDZK1 knockdown or overexpression of truncated PDZK1 lacking the two C-terminal PDZ domains (Zhu *et al.*, 2008), suggesting that the entire PDZK1 is required for the activation of Src by SR-B1. However, whether Src is also involved in the HDL signaling pathway in macrophages remains to be tested. Furthermore, more studies are needed to clarify the mechanism of Src activation. *e.g.* Which SR-B1 domain does Src interact with? How do the two C-terminal PDZ domains of PDZK1 participate in Src activation? Does PDZK1 anchor or regulate certain molecule(s) required for Src phosphorylation by SR-B1?

(3) Is the SR-B1/PDZK1 pathway involved in macrophage efferocytosis?

In Chapter 2, we observed an increased percentage of cleaved caspase-3(+) cells in the peritoneal cavity of tunicamycin-injected PDZK1^{-/-} mice or the LDLR^{-/-} mice transplanted with PDZK1^{-/-} BM. It can be explained by the increased sensitivity of PDZK1^{-/-} macrophages to apoptosis. However, we do not exclude the possibility that inactivation of PDZK1 abolished macrophage efferocytosis, leading to increased accumulation of apoptotic macrophages in the peritoneal cavity. It was shown recently that SR-B1 recognized and interacted with the phosphatidylserine on the surface of apoptotic macrophages, resulting in the activation of Src/PI3K/Akt pathway, which activated Rac1 and mediated apoptotic cell engulfment (Tao et al., 2015). PDZK1 has been shown to be indispensable for the activation of Src induced by HDL via SR-B1 in endothelial cells (Zhu et al., 2008). However, it is unclear if PDZK1 is also involved in SR-B1-regulated Src activation in macrophages. To test if PDZK1 mediates the engulfment of apoptotic cells by macrophages, a standard *in vivo* macrophage efferocytosis assay can be performed (Seimon et al., 2009). Briefly, WT and PDZK1^{-/-} mice will be injected i.p. with thioglycollate to recruit macrophages into the peritoneal cavity. Three days later, apoptotic Jurkat T cells (labeled with a fluorescent dye and induced to undergo apoptosis by UV irradiation) will be injected into the peritoneal cavity. After 30 min, peritoneal cells will be collected, and stained for a macrophage marker and analyzed by flow cytometry for the fluorophores used to label the apoptotic T cells and the macrophage marker (Wojcik et al., 2008). Macrophages that have performed efferocytosis will be identified as the cells positive for both macrophage marker and T cell fluorophore.

5.2 Akt1 as a therapeutic target for atherosclerosis

All three Akt isoforms are expressed in various tissues: Akt1 and Akt3 are abundant in the brain and heart, while Akt2 is expressed in the insulin-responsive tissues such as brown fat and skeletal muscle (Bellacosa et al., 2004; Shiojima and Walsh, 2002). These Akt isoforms function differently as shown in Akt isoform knockout mice. For example: Akt1^{-/-} mice exhibit defects in both fetal and postnatal growth, while Akt2^{-/-} mice show impaired metabolism of insulin and glucose (Cho et al., 2001). Unlike Akt1, the deficiency of which causes decrease in the sizes of all the organs, Akt3 knockout specifically reduces brain size (Easton et al., 2005). Moreover, these Akt isoforms play quite different, even opposite roles, in the same cell type. For example, Akt1 promotes tumor endothelial cell growth and migration, while Akt3 acts in an opposite manner (Phung et al., 2015). It has been known that Akt mediated the eNOS activation in endothelial cells (Fulton et al., 1999; Mineo et al., 2003), which was likely to be attributed by Akt1, and compensated by Akt2 when Akt1 was knocked out (Lee et al., 2014). In macrophages, Akt1 is the main factor stimulating cell migration (Al-Jarallah et al., 2014) and survival (Figure 2.5). Akt1^{-/-} apoE^{-/-} mice showed increased aortic atherosclerosis and coronary atherosclerosis, compared to apoE^{-/-} mice (Fernandez-Hernando et al., 2007). In contrast, knockout of Akt2 in macrophages shows decreased plaque size in both early and advanced stage of atherosclerosis (Babaev et al., 2014). Also, Akt2^{-/-} macrophages are more prone to undergo M2 polarization than WT macrophages (Babaev et al., 2014). For future investigation, the effects of

individual isoform and the isoform-specific effects of therapeutic compounds should be demonstrated in the context of atherosclerosis.

My data in Chapter 2 demonstrate that Akt1 plays a central role in mediating HDL dependent protection against macrophage apoptosis. This is consistent with the central role of PI3K/Akt in HDL signaling in endothelial cells, as well as the finding that Akt1^{-/-}/apoE^{-/-} mice exhibit increased diet induced atherosclerosis, macrophage apoptosis and coronary artery disease compared to apoE^{-/-} mice (Fernandez-Hernando et al., 2007). These suggest that PI3K/Akt1 may be therapeutic target for atherosclerosis.

Andrographolide, an active component isolated from the Chinese herb *Andrographis paniculata*, has been reported to inhibit LPS-induced inducible nitric oxide synthase (iNOS) in macrophages (Chiou et al., 1998) and phorbol-12-myristate-13-acetate (PMA)-induced ROS production in neutrophils (Shen et al., 2000). Yen and colleagues demonstrated the ability of andrographolide to protect endothelial cells from growth factor deprivation-induced mitochondrial pathway of apoptosis (Chen et al., 2004). More importantly, they noticed that andrographolide induced the activation of Akt in endothelial cells and the suppression of Akt activity by PI3K inhibitors abolished the inhibitory effect of andrographolide on cell apoptosis (Chen et al., 2004). Even though their study did not clarify which isoform(s) of Akt was activated by andrographolide, research done by other's lab showed that an andrographolide analogue, andrographolide-lipoic acid conjugate (AL-1), protected ROS-induced cell death by activating Akt1 and ERK1/2 pathways (Yan et al., 2013). This may suggest

andrographolide as a potentially specific Akt1 activator in the treatment of atherosclerosis.

5.3 Study of atherosclerosis in macrophage-specific Bim knockout mice

Bim in macrophages can be increased by not only ER stress, but also phagocytosis of bacteria, which is regulated by Toll-like receptor (TLR) and the adaptor protein MyD88 (Kirschnek et al., 2005). Similar to our observation that Bim^{-/-} macrophages were resistant to ER stress-induced apoptosis, Bim^{-/-} macrophages were also shown to be more prone to survive *E. coli* phagocytosis-induced apoptosis than WT macrophages (Kirschnek et al., 2005). *In vivo*, Bim is highly expressed in hematopoietic cells (Bouillet et al., 1999). Bim global knockout mice are characterized by dramatically increased circulating leukocytes, including lymphocytes, monocytes and granulocytes (Bouillet et al., 1999). Even though Bim was only knocked out in BM-derived cells, the LDLR^{-/-} mice with Bim deficient BM still exhibit alterations in lymphocyte counts and even plasma cholesterol (Figure 3.7, 3.9). Therefore, it would be relevant to investigate on the atherosclerosis in macrophage-specific Bim knockout mice to eliminate the effects of Bim deficiency on blood lymphocytes. LysM-Cre mice, which express Cre-recombinase under the control of the murine M lysozyme, had been bred with Bim conditional knockout mice, in which the first 4 exons of Bim are flanked by LoxP sequences (Steimer et al., 2009; Takeuchi et al., 2005), to generate macrophage-specific Bim^{-/-} mice (Steimer et al., 2009). It was shown that the LysM-Cre-LoxP system completely deleted Bim expression in BM-derived macrophages (Steimer et al., 2009). Of note, selectively knocking out of Bim in macrophages did not cause leukemia in

those mice (Steimer et al., 2009), which is different from the phenotypes of Bim global knockout mice (Bouillet et al., 1999). These mice could be used to evaluate the effect of macrophage-expressed Bim on atherosclerotic plaque development.

5.4 Characterization of coronary atherosclerotic plaques in SR-B1^{-/-}/apoE^{-/-} mice

Our research showed that SR-B1^{-/-}/apoE^{-/-} mice spontaneously developed severe coronary atherosclerosis, thrombosis and myocardial infarction (Chapter 4), which resemble what were observed in atherogenic diet-fed SR-B1^{-/-}/LDLR^{-/-} mice (Fuller et al., 2014a). This suggests that SR-B1 deficient atherogenic mice may be useful mouse models of coronary artery atherosclerotic plaque development, instability and rupture. Therefore, the plaque morphology in the coronary arteries of SR-B1^{-/-}/apoE^{-/-} mice should be further characterized. It has been suggested that mouse models of plaque rupture should display the three steps of human plaque rupture (Matoba et al., 2013):

(1) Plaque destabilization:

Vulnerable plaques are characterized by large necrotic lipid core and thin fibrous cap. In light of our research showing that macrophage lacking SR-B1 are prone to undergo apoptosis, and that the atherogenic mice transplanted with SR-B1^{-/-} BM developed big necrotic cores in atherosclerotic lesions (Tao et al., 2015)(Zhang and Al-Jarallah, manuscript in revision), it is conceivable that SR-B1^{-/-}/apoE^{-/-} mice may develop large necrotic cores in the coronary atherosclerotic plaques. We also tested if rosuvastatin could protect SR-B1^{-/-}/apoE^{-/-} BM-derived macrophages from ER stress-

induced apoptosis by treating these macrophages with or without 20 μ M rosuvastatin in the presence of tunicamycin. The preliminary data showed that rosuvastatin reduced the percentage of TUNEL⁺ cells by around 50 % (Pei Yu, unpublished data). To test the effect of rosuvastatin on cell apoptosis *in vivo*, heart sections from control and rosuvastatin-treated dKO mice can be stained by TUNEL method, so that the apoptotic cells in the coronary atherosclerotic plaques can be quantified. Also, Haematoxylin & Eosin (H&E) and Trichrome staining of coronary atherosclerotic lesions can be carried out to analyze the composition of the plaques, including necrotic core size and fibrous cap thickness. However, there exist technical difficulties to observe the morphology and cellular structures of the plaques in the coronary arteries, due to the small diameter of coronary arteries compared to aortic sinus, and the small size of the dKO mice resulting from the spontaneous nature of the coronary artery disease and early death (mice were only 14 g and 5 weeks of age). In order to analyze coronary atherosclerosis in mouse, we need to: 1) move to a different, diet-inducible atherosclerotic mouse model (e.g. SR-B1^{-/-}LDLR^{-/-} mice) where coronary atherosclerosis can be induced in fully grown adult mice which will have larger hearts and coronary arteries with larger diameter; 2) focus on the proximal segments of coronary arteries of serial sections spanning a significant length of the CA in order to evaluate apoptosis over a defined volume of plaque rather than a single section; 3) utilize paraffin sectioning (rather than frozen sectioning) to improve histology and morphology and better discriminate necrotic cores and fibrous caps.

(2) Plaque rupture:

Plaque rupture is featured by a spontaneous disruption of the fibrous cap over large necrotic core, may accompanied by inflammatory cell infiltration and intra-plaque hemorrhage (Matoba et al., 2013). However, the advanced plaques in conventional atherosclerotic mouse models rarely progress to plaque rupture (Matoba et al., 2013). The mechanism of plaque rupture is not clear, but may be associated with changes in shear stress (Matoba et al., 2013). For future study, the serial sections of coronary arteries from the dKO mice can be stained with Trichrome or Elastica van Gieson to visualize the incidence of fibrous cap disruption.

(3) Thrombosis formation:

Brachiocephalic artery has been identified as the most susceptible site for atherosclerosis in apoE^{-/-} mice fed high fat diet, in which the advanced plaques even showed some features of erosion and rupture (Johnson et al., 2005; Johnson and Jackson, 2001). However, thrombosis formation overlying pre-existing plaques was never seen in these mouse models (Bentzon and Falk, 2010; Johnson et al., 2005; Rosenfeld et al., 2000; Schwartz et al., 2007). It has been demonstrated that the abnormal circulating lipoproteins [high unesterified cholesterol (UC): cholesterol ester (CE) ratio] in SR-B1^{-/-} mice was associated with increased cholesterol content in platelets, leading to rapid clearance of platelets and thrombocytopenia (Dole et al., 2008; Korporaal et al., 2011). SR-B1 also regulates platelet function. Hepatic SR-B1 deficiency-induced hypercholesterolemia increased platelet activity (Korporaal et al., 2011; Ma et al., 2010).

On the contrary, inactivation of SR-B1 expressed on platelets had an inhibitory effect on platelet activation (Ma et al., 2010). Even though SR-B1^{-/-} mice are thrombocytopenic, and SR-B1^{-/-} platelets are resistant to activation, SR-B1^{-/-}/apoE^{-/-} mice exhibit increased platelet activation, which has been linked to increased platelet UC content (due to the abnormally high UC:TC ratio in circulating lipoproteins of these mice) (Braun et al., 2003). Korporaal *et al.* showed that platelets in the whole blood collected from dKO mice were activated without the stimulation of agonists, may suggesting that the platelets in dKO mice were circulating in an activated state (Korporaal et al., 2011). In chapter 4, we showed that CD41, marker of activated platelets were abundantly observed in the proximal segments of atherosclerotic coronary arteries of SR-B1^{-/-}/apoE^{-/-} mice, but not in the distal segments or in the aortic sinus with preexisting atherosclerotic plaques (data not shown). This is consistent with the distribution of the human plaques susceptible to rupture, and likely suggests that the platelet accumulation in the coronary arteries is the result of plaque rupture, but not due to the platelets themselves just being over-activated.

5.5 The effects of SR-B1 deficiency on the components and functions of HDL

SR-B1 in hepatocytes, mediates the cholesterol reverse transport by selectively taking up cholesterol from circulating HDL into hepatocytes (Huby et al., 2006). Therefore, knockout of SR-B1 disrupts the unloading of cholesterol from HDL particles, and causes enlargement of HDL particles due to cholesterol accumulation (Huby et al., 2006; Rigotti et al., 1997). An alternative pathway of cholesterol transport from HDL to

the liver is via apoE-mediated catabolism of HDL particles in hepatocytes (Miller, 1990). In SR-B1^{-/-}/apoE^{-/-} mice, however, the HDL particles were further enlarged (Figure 4.1B), due to the shutdown of both cholesterol transport pathways. The composition of HDL in SR-B1 deficient mice was also different from that of WT mice. SR-B1^{-/-} mice had significantly higher UC:CE ratio than SR-B1^{+/+} control (Braun et al., 2003; Van Eck et al., 2003). It has been shown that the HDL from SR-B1^{-/-} mice had increased apoE (Rigotti et al., 1997). Compared to ApoE^{-/-} mice, we found a significant increase of pro-inflammatory SAA in SR-B1^{-/-}/apoE^{-/-} mice (Pei Yu, unpublished data), which has been reported to bind to HDL particles in circulation, and may overtake apoA-I as the predominant apolipoprotein during acute phase (Artl et al., 2000). This suggests that the HDL in SR-B1^{-/-}/apoE^{-/-} mice may exhibit inflammatory rather than the normal anti-inflammatory properties. In preliminary experiments, I tested the effect of HDL from SR-B1^{-/-} mice on protecting macrophages from apoptosis. We isolated HDL from pooled plasma of either control WT or SR-B1^{-/-} mice by KBr density gradient ultracentrifugation. As described in Chapter 2 and 3, apoptosis of mouse peritoneal macrophages was induced by tunicamycin. Cells were co-incubated with 50 µg of HDL from WT and SR-B1^{-/-} mice for 24 hrs. As seen for human HDL (Figure 2.1), HDL from WT mice was also able to protect macrophages from tunicamycin-induced apoptosis in a dose-dependent manner. However, this protection was not observed in the macrophages treated with HDL isolated from SR-B1^{-/-} mice (Pei Yu, unpublished data). We speculated that the dysfunctional HDL in SR-B1 deficient mice might also contribute to their susceptibility to atherosclerosis. In light of the complexity of HDL

particles, the components of HDL and their functions in mediating cardioprotection are worthy of further investigation. This is particularly important in light of a number of clinical trials using HDL cholesterol-raising agents, such as torcetrapib, dalcetrapib and niacin, which did not show a significant reduction of the mortality of cardiovascular events (Kingwell et al., 2014). This suggests that it is not just the amount but rather the composition and function of the altered HDL that more likely influence cardiovascular outcomes. Notably, increasing evidence suggest a relationship between the heterogeneity and functions of HDL particles (Akinkuolie et al., 2014; Kingwell et al., 2014; Navab et al., 2001; Yan et al., 2014). Lipidomic and proteomic studies can be performed for future investigation to screen the differences between HDLs from WT (healthy control) and SR-B1^{-/-} (atherosclerosis model) mice, which may reveal some elements essential for HDL to exert anti-atherosclerotic protection, and thereby shed some light on the strategies to control the quality of HDL increased by candidate medication.

5.6 Summary and Significance

Low plasma HDL level has been widely accepted as an indicator of CHD. It has been shown by our lab and others that HDL protected macrophages from apoptosis induced by various inducers in a SR-B1-dependent manner. In order to extend our understanding about HDL's signaling pathway in macrophages, the downstream factors were investigated. The data presented in Chapter 2 showed an indispensable role of PDZK1 and Akt1 in mediating HDL signaling in macrophages *in vitro*, and the effect of

BM-derived cell expressed PDZK1 in inhibiting cell apoptosis and necrotic core formation in atherosclerotic plaques. Chapter 3 further explored the signaling pathway by showing that HDL reduced Bim protein in macrophages, and that Bim deficiency in macrophages conferred protection against ER stress-induced apoptosis even in the absence of HDL, suggesting that Bim is the target of HDL's anti-apoptotic signaling pathway in macrophages. It is the first time that the mechanism by which HDL protected macrophages from apoptosis was demonstrated. Since macrophage apoptosis is one of the major contributors of necrotic core formation and plaque instability, our research may lead to the identification of novel therapeutic targets for vascular disease.

SR-B1 plays a vital role in mediating HDL's signaling to protect against atherosclerosis. The knockout of SR-B1 increased the susceptibility of apoE^{-/-} mice to atherosclerosis in aortic sinus. Interestingly, the dKO mice developed atherosclerosis in coronary arteries spontaneously, leading to coronary stenosis and occlusions. Of note, our lab first observed the platelet accumulation in atherosclerotic coronary arteries in spontaneous (SR-B1^{-/-}/apoE^{-/-}) (Chapter 4) and diet-induced (SR-B1^{-/-}/LDLR^{-/-}) (Fuller et al., 2014a) CHD mouse models, respectively, suggesting the potential of these mice as novel models of atherothrombosis. This is the first time that rosuvastatin has been tested in a mouse model of spontaneous coronary artery atherosclerosis involving platelet accumulation in atherosclerotic coronary artery plaques and cardiac fibrosis. This study demonstrated that treatment with rosuvastatin significantly attenuated the development of atherosclerosis, deposition of platelets in atherosclerotic coronary arteries, and

attenuated cardiac fibrosis and cardiac enlargement in SR-BI^{-/-}/apoE^{-/-} mice. These beneficial effects of rosuvastatin occurred despite increased plasma cholesterol levels and appear to involve reduced accumulation of oxidized LDL in plasma and in the walls of affected arteries, and reduced macrophage foam cell formation. These findings provide insight into mechanisms by which rosuvastatin protects against atherosclerosis and subsequent myocardial infarction by pathways independent of cholesterol lowering.

REFERENCES

- Acton, S., Rigotti, A., Landschulz, K.T., Xu, S., Hobbs, H.H., and Krieger, M. (1996). Identification of scavenger receptor SR-BI as a high density lipoprotein receptor. *Science* 271, 518-520.
- Adachi, M., Zhao, X., and Imai, K. (2005). Nomenclature of dynein light chain-linked BH3-only protein Bim isoforms. *Cell death and differentiation* 12, 192-193.
- Ai, D., Chen, C., Han, S., Ganda, A., Murphy, A.J., Haeusler, R., Thorp, E., Accili, D., Horton, J.D., and Tall, A.R. (2012). Regulation of hepatic LDL receptors by mTORC1 and PCSK9 in mice. *The Journal of clinical investigation* 122, 1262-1270.
- Akinkuolie, A.O., Paynter, N.P., Padmanabhan, L., and Mora, S. (2014). High-density lipoprotein particle subclass heterogeneity and incident coronary heart disease. *Circulation Cardiovascular quality and outcomes* 7, 55-63.
- Al-Jarallah, A., Chen, X., Gonzalez, L., and Trigatti, B.L. (2014). High density lipoprotein stimulated migration of macrophages depends on the scavenger receptor class B, type I, PDZK1 and Akt1 and is blocked by sphingosine 1 phosphate receptor antagonists. *PloS one* 9, e106487.
- Al-Jarallah, A., Igdoura, F., Zhang, Y., Tenedero, C.B., White, E.J., MacDonald, M.E., Igdoura, S.A., and Trigatti, B.L. (2013). The effect of pomegranate extract on coronary artery atherosclerosis in SR-BI/APOE double knockout mice. *Atherosclerosis* 228, 80-89.

Al-Jarallah, A., and Trigatti, B.L. (2010). A role for the scavenger receptor, class B type I in high density lipoprotein dependent activation of cellular signaling pathways. *Biochimica et biophysica acta* *1801*, 1239-1248.

Amano, S.U., Cohen, J.L., Vangala, P., Tencerova, M., Nicoloso, S.M., Yawe, J.C., Shen, Y., Czech, M.P., and Aouadi, M. (2014). Local proliferation of macrophages contributes to obesity-associated adipose tissue inflammation. *Cell metabolism* *19*, 162-171.

Anantharamaiah, G.M., Jones, J.L., Brouillette, C.G., Schmidt, C.F., Chung, B.H., Hughes, T.A., Bhowm, A.S., and Segrest, J.P. (1985). Studies of synthetic peptide analogs of the amphipathic helix. Structure of complexes with dimyristoyl phosphatidylcholine. *The Journal of biological chemistry* *260*, 10248-10255.

Arai, T., Wang, N., Bezouevski, M., Welch, C., and Tall, A.R. (1999). Decreased atherosclerosis in heterozygous low density lipoprotein receptor-deficient mice expressing the scavenger receptor BI transgene. *J Biol Chem* *274*, 2366-2371.

Argraves, K.M., and Argraves, W.S. (2007). HDL serves as a S1P signaling platform mediating a multitude of cardiovascular effects. *Journal of lipid research* *48*, 2325-2333.

Argraves, K.M., Sethi, A.A., Gazzolo, P.J., Wilkerson, B.A., Remaley, A.T., Tybjaerg-Hansen, A., Nordestgaard, B.G., Yeatts, S.D., Nicholas, K.S., Barth, J.L., *et al.* (2011). S1P, dihydro-S1P and C24:1-ceramide levels in the HDL-containing fraction of serum inversely correlate with occurrence of ischemic heart disease. *Lipids in health and disease* *10*, 70.

- Artl, A., Marsche, G., Lestavel, S., Sattler, W., and Malle, E. (2000). Role of serum amyloid A during metabolism of acute-phase HDL by macrophages. *Arteriosclerosis, thrombosis, and vascular biology* *20*, 763-772.
- Assanasen, C., Mineo, C., Seetharam, D., Yuhanna, I.S., Marcel, Y.L., Connelly, M.A., Williams, D.L., de la Llera-Moya, M., Shaul, P.W., and Silver, D.L. (2005). Cholesterol binding, efflux, and a PDZ-interacting domain of scavenger receptor-BI mediate HDL-initiated signaling. *The Journal of clinical investigation* *115*, 969-977.
- Assmann, G., and Nofer, J.R. (2003). Atheroprotective effects of high-density lipoproteins. *Annual review of medicine* *54*, 321-341.
- Asztalos, B., Zhang, W., Roheim, P.S., and Wong, L. (1997). Role of free apolipoprotein A-I in cholesterol efflux. Formation of pre-alpha-migrating high-density lipoprotein particles. *Arteriosclerosis, thrombosis, and vascular biology* *17*, 1630-1636.
- Asztalos, B.F., Roheim, P.S., Milani, R.L., Lefevre, M., McNamara, J.R., Horvath, K.V., and Schaefer, E.J. (2000). Distribution of ApoA-I-containing HDL subpopulations in patients with coronary heart disease. *Arteriosclerosis, thrombosis, and vascular biology* *20*, 2670-2676.
- Averous, J., Bruhat, A., Jousse, C., Carraro, V., Thiel, G., and Fafournoux, P. (2004). Induction of CHOP expression by amino acid limitation requires both ATF4 expression and ATF2 phosphorylation. *The Journal of biological chemistry* *279*, 5288-5297.

Awan, Z., Seidah, N.G., MacFadyen, J.G., Benjannet, S., Chasman, D.I., Ridker, P.M., and Genest, J. (2012). Rosuvastatin, proprotein convertase subtilisin/kexin type 9 concentrations, and LDL cholesterol response: the JUPITER trial. *Clinical chemistry* 58, 183-189.

Babaev, V.R., Hebron, K.E., Wiese, C.B., Toth, C.L., Ding, L., Zhang, Y., May, J.M., Fazio, S., Vickers, K.C., and Linton, M.F. (2014). Macrophage deficiency of Akt2 reduces atherosclerosis in Ldlr null mice. *Journal of lipid research* 55, 2296-2308.

Badimon, J.J., Badimon, L., and Fuster, V. (1990). Regression of atherosclerotic lesions by high density lipoprotein plasma fraction in the cholesterol-fed rabbit. *The Journal of clinical investigation* 85, 1234-1241.

Badimon, J.J., Badimon, L., Galvez, A., Discche, R., and Fuster, V. (1989). High density lipoprotein plasma fractions inhibit aortic fatty streaks in cholesterol-fed rabbits. *Laboratory investigation; a journal of technical methods and pathology* 60, 455-461.

Baitsch, D., Bock, H.H., Engel, T., Telgmann, R., Muller-Tidow, C., Varga, G., Bot, M., Herz, J., Robenek, H., von Eckardstein, A., *et al.* (2011). Apolipoprotein E induces antiinflammatory phenotype in macrophages. *Arterioscler Thromb Vasc Biol* 31, 1160-1168.

Baldan, A., Pei, L., Lee, R., Tarr, P., Tangirala, R.K., Weinstein, M.M., Frank, J., Li, A.C., Tontonoz, P., and Edwards, P.A. (2006). Impaired development of atherosclerosis in hyperlipidemic Ldlr^{-/-} and ApoE^{-/-} mice transplanted with Abcg1^{-/-} bone marrow. *Arteriosclerosis, thrombosis, and vascular biology* 26, 2301-2307.

Bantel, H., Sinha, B., Domschke, W., Peters, G., Schulze-Osthoff, K., and Janicke, R.U. (2001). alpha-Toxin is a mediator of *Staphylococcus aureus*-induced cell death and activates caspases via the intrinsic death pathway independently of death receptor signaling. *The Journal of cell biology* 155, 637-648.

Barter, P., Gotto, A.M., LaRosa, J.C., Maroni, J., Szarek, M., Grundy, S.M., Kastelein, J.J., Bittner, V., Fruchart, J.C., and Treating to New Targets, I. (2007). HDL cholesterol, very low levels of LDL cholesterol, and cardiovascular events. *The New England journal of medicine* 357, 1301-1310.

Basseri, S., and Austin, R.C. (2012). Endoplasmic reticulum stress and lipid metabolism: mechanisms and therapeutic potential. *Biochemistry research international* 2012, 841362.

Baumgartner-Parzer, S.M., Wagner, L., Pettermann, M., Grillari, J., Gessl, A., and Waldhausl, W. (1995). High-glucose--triggered apoptosis in cultured endothelial cells. *Diabetes* 44, 1323-1327.

Bellacosa, A., Testa, J.R., Moore, R., and Larue, L. (2004). A portrait of AKT kinases: human cancer and animal models depict a family with strong individualities. *Cancer biology & therapy* 3, 268-275.

Bentzon, J.F., and Falk, E. (2010). Atherosclerotic lesions in mouse and man: is it the same disease? *Current opinion in lipidology* 21, 434-440.

Bielicki, J.K., and Oda, M.N. (2002). Apolipoprotein A-I(Milano) and apolipoprotein A-I(Paris) exhibit an antioxidant activity distinct from that of wild-type apolipoprotein A-I. *Biochemistry* 41, 2089-2096.

Blaho, V.A., and Hla, T. (2014). An update on the biology of sphingosine 1-phosphate receptors. *Journal of lipid research* 55, 1596-1608.

Blair, A., Shaul, P.W., Yuhanna, I.S., Conrad, P.A., and Smart, E.J. (1999). Oxidized low density lipoprotein displaces endothelial nitric-oxide synthase (eNOS) from plasmalemmal caveolae and impairs eNOS activation. *The Journal of biological chemistry* 274, 32512-32519.

Blanche, P.J., Gong, E.L., Forte, T.M., and Nichols, A.V. (1981). Characterization of human high-density lipoproteins by gradient gel electrophoresis. *Biochimica et biophysica acta* 665, 408-419.

Boisvert, W.A., Black, A.S., and Curtiss, L.K. (1999). ApoA1 reduces free cholesterol accumulation in atherosclerotic lesions of ApoE-deficient mice transplanted with ApoE-expressing macrophages. *Arteriosclerosis, thrombosis, and vascular biology* 19, 525-530.

Bouillet, P., Metcalf, D., Huang, D.C., Tarlinton, D.M., Kay, T.W., Kontgen, F., Adams, J.M., and Strasser, A. (1999). Proapoptotic Bcl-2 relative Bim required for certain apoptotic responses, leukocyte homeostasis, and to preclude autoimmunity. *Science* 286, 1735-1738.

Braun, A., Rigotti, A., and Trigatti, B.L. (2008a). Myocardial infarction following atherosclerosis in murine models. *Current drug targets* 9, 217-223.

Braun, A., Trigatti, B.L., Post, M.J., Sato, K., Simons, M., Edelberg, J.M., Rosenberg, R.D., Schrenzel, M., and Krieger, M. (2002). Loss of SR-BI expression leads to the early onset of occlusive atherosclerotic coronary artery disease, spontaneous

myocardial infarctions, severe cardiac dysfunction, and premature death in apolipoprotein E-deficient mice. *Circulation research* 90, 270-276.

Braun, A., Yesilaltay, A., Acton, S., Broschat, K.O., Krul, E.S., Napawan, N., Stagliano, N., and Krieger, M. (2008b). Inhibition of intestinal absorption of cholesterol by ezetimibe or bile acids by SC-435 alters lipoprotein metabolism and extends the lifespan of SR-BI/apoE double knockout mice. *Atherosclerosis* 198, 77-84.

Braun, A., Zhang, S., Miettinen, H.E., Ebrahim, S., Holm, T.M., Vasile, E., Post, M.J., Yoerger, D.M., Picard, M.H., Krieger, J.L., *et al.* (2003). Probucol prevents early coronary heart disease and death in the high-density lipoprotein receptor SR-BI/apolipoprotein E double knockout mouse. *Proceedings of the National Academy of Sciences of the United States of America* 100, 7283-7288.

Brunelle, J.K., and Letai, A. (2009). Control of mitochondrial apoptosis by the Bcl-2 family. *Journal of cell science* 122, 437-441.

Caligiuri, G., Levy, B., Pernow, J., Thoren, P., and Hansson, G.K. (1999). Myocardial infarction mediated by endothelin receptor signaling in hypercholesterolemic mice. *Proc Natl Acad Sci U S A* 96, 6920-6924.

Canault, M., Peiretti, F., Kopp, F., Bonardo, B., Bonzi, M.F., Coudeyre, J.C., Alessi, M.C., Juhan-Vague, I., and Nalbone, G. (2006). The TNF alpha converting enzyme (TACE/ADAM17) is expressed in the atherosclerotic lesions of apolipoprotein E-deficient mice: possible contribution to elevated plasma levels of soluble TNF alpha receptors. *Atherosclerosis* 187, 82-91.

Cande, C., Cecconi, F., Dessen, P., and Kroemer, G. (2002). Apoptosis-inducing factor (AIF): key to the conserved caspase-independent pathways of cell death? *Journal of cell science* *115*, 4727-4734.

Castelli, W.P., Garrison, R.J., Wilson, P.W., Abbott, R.D., Kalousdian, S., and Kannel, W.B. (1986). Incidence of coronary heart disease and lipoprotein cholesterol levels. The Framingham Study. *Jama* *256*, 2835-2838.

Chen, J.H., Hsiao, G., Lee, A.R., Wu, C.C., and Yen, M.H. (2004). Andrographolide suppresses endothelial cell apoptosis via activation of phosphatidyl inositol-3-kinase/Akt pathway. *Biochemical pharmacology* *67*, 1337-1345.

Cheng, A.M., Handa, P., Tateya, S., Schwartz, J., Tang, C., Mitra, P., Oram, J.F., Chait, A., and Kim, F. (2012). Apolipoprotein A-I attenuates palmitate-mediated NF-kappaB activation by reducing Toll-like receptor-4 recruitment into lipid rafts. *PloS one* *7*, e33917.

Cheng-Lai, A. (2003). Rosuvastatin: a new HMG-CoA reductase inhibitor for the treatment of hypercholesterolemia. *Heart Dis* *5*, 72-78.

Chinetti-Gbaguidi, G., Colin, S., and Staels, B. (2015). Macrophage subsets in atherosclerosis. *Nature reviews Cardiology* *12*, 10-17.

Chiou, W.F., Lin, J.J., and Chen, C.F. (1998). Andrographolide suppresses the expression of inducible nitric oxide synthase in macrophage and restores the vasoconstriction in rat aorta treated with lipopolysaccharide. *British journal of pharmacology* *125*, 327-334.

Cho, H., Thorvaldsen, J.L., Chu, Q., Feng, F., and Birnbaum, M.J. (2001).

Akt1/PKBalpha is required for normal growth but dispensable for maintenance of glucose homeostasis in mice. *The Journal of biological chemistry* 276, 38349-38352.

Christoffersen, C., Obinata, H., Kumaraswamy, S.B., Galvani, S., Ahnstrom, J., Sevvana, M., Egerer-Sieber, C., Muller, Y.A., Hla, T., Nielsen, L.B., *et al.* (2011).

Endothelium-protective sphingosine-1-phosphate provided by HDL-associated apolipoprotein M. *Proceedings of the National Academy of Sciences of the United States of America* 108, 9613-9618.

Clybouw, C., Merino, D., Nebl, T., Masson, F., Robati, M., O'Reilly, L., Hubner, A., Davis, R.J., Strasser, A., and Bouillet, P. (2012). Alternative splicing of Bim and Erk-mediated Bim(EL) phosphorylation are dispensable for hematopoietic homeostasis in vivo. *Cell death and differentiation* 19, 1060-1068.

Cockerill, G.W., Huehns, T.Y., Weerasinghe, A., Stocker, C., Lerch, P.G., Miller, N.E., and Haskard, D.O. (2001). Elevation of plasma high-density lipoprotein concentration reduces interleukin-1-induced expression of E-selectin in an in vivo model of acute inflammation. *Circulation* 103, 108-112.

Cockerill, G.W., Rye, K.A., Gamble, J.R., Vadas, M.A., and Barter, P.J. (1995). High-density lipoproteins inhibit cytokine-induced expression of endothelial cell adhesion molecules. *Arteriosclerosis, thrombosis, and vascular biology* 15, 1987-1994.

- Cockerill, G.W., Saklatvala, J., Ridley, S.H., Yarwood, H., Miller, N.E., Oral, B., Nithyanathan, S., Taylor, G., and Haskard, D.O. (1999). High-density lipoproteins differentially modulate cytokine-induced expression of E-selectin and cyclooxygenase-2. *Arteriosclerosis, thrombosis, and vascular biology* 19, 910-917.
- Colin, S., Fanchon, M., Belloy, L., Bochem, A.E., Copin, C., Derudas, B., Stroes, E.S., Hovingh, G.K., Kuivenhoven, J.A., Dallinga-Thie, G.M., *et al.* (2014). HDL does not influence the polarization of human monocytes toward an alternative phenotype. *International journal of cardiology* 172, 179-184.
- Collins, T., Read, M.A., Neish, A.S., Whitley, M.Z., Thanos, D., and Maniatis, T. (1995). Transcriptional regulation of endothelial cell adhesion molecules: NF-kappa B and cytokine-inducible enhancers. *FASEB journal : official publication of the Federation of American Societies for Experimental Biology* 9, 899-909.
- Collot-Teixeira, S., Martin, J., McDermott-Roe, C., Poston, R., and McGregor, J.L. (2007). CD36 and macrophages in atherosclerosis. *Cardiovascular research* 75, 468-477.
- Cory, S., and Adams, J.M. (2002). The Bcl2 family: regulators of the cellular life-or-death switch. *Nature reviews Cancer* 2, 647-656.
- Covey, S.D., Krieger, M., Wang, W., Penman, M., and Trigatti, B.L. (2003). Scavenger receptor class B type I-mediated protection against atherosclerosis in LDL receptor-negative mice involves its expression in bone marrow-derived cells. *Arteriosclerosis, thrombosis, and vascular biology* 23, 1589-1594.

- Cullen, S.P., and Martin, S.J. (2009). Caspase activation pathways: some recent progress. *Cell death and differentiation* 16, 935-938.
- Damirin, A., Tomura, H., Komachi, M., Liu, J.P., Mogi, C., Tobo, M., Wang, J.Q., Kimura, T., Kuwabara, A., Yamazaki, Y., *et al.* (2007). Role of lipoprotein-associated lysophospholipids in migratory activity of coronary artery smooth muscle cells. *American journal of physiology Heart and circulatory physiology* 292, H2513-2522.
- Datta, S.R., Brunet, A., and Greenberg, M.E. (1999). Cellular survival: a play in three Acts. *Genes & development* 13, 2905-2927.
- Daugherty, A., Dunn, J.L., Rateri, D.L., and Heinecke, J.W. (1994). Myeloperoxidase, a catalyst for lipoprotein oxidation, is expressed in human atherosclerotic lesions. *The Journal of clinical investigation* 94, 437-444.
- Davignon, J. (2004). Beneficial cardiovascular pleiotropic effects of statins. *Circulation* 109, III39-43.
- Davignon, J., and Ganz, P. (2004). Role of endothelial dysfunction in atherosclerosis. *Circulation* 109, III27-32.
- De Lalla, O.F., and Gofman, J.W. (1954). Ultracentrifugal analysis of serum lipoproteins. *Methods of biochemical analysis* 1, 459-478.
- de Martin, R., Vanhove, B., Cheng, Q., Hofer, E., Csizmadia, V., Winkler, H., and Bach, F.H. (1993). Cytokine-inducible expression in endothelial cells of an I kappa B alpha-like gene is regulated by NF kappa B. *The EMBO journal* 12, 2773-2779.
- de Silva, H.V., Mas-Oliva, J., Taylor, J.M., and Mahley, R.W. (1994). Identification of apolipoprotein B-100 low density lipoproteins, apolipoprotein B-48 remnants, and

apolipoprotein E-rich high density lipoproteins in the mouse. *J Lipid Res* 35, 1297-1310.

Decaudin, D., Marzo, I., Brenner, C., and Kroemer, G. (1998). Mitochondria in chemotherapy-induced apoptosis: a prospective novel target of cancer therapy (review). *International journal of oncology* 12, 141-152.

DeMeester, S.L., Qiu, Y., Buchman, T.G., Hotchkiss, R.S., Dunnigan, K., Karl, I.E., and Cobb, J.P. (1998). Nitric oxide inhibits stress-induced endothelial cell apoptosis. *Critical care medicine* 26, 1500-1509.

Devries-Seimon, T., Li, Y., Yao, P.M., Stone, E., Wang, Y., Davis, R.J., Flavell, R., and Tabas, I. (2005). Cholesterol-induced macrophage apoptosis requires ER stress pathways and engagement of the type A scavenger receptor. *The Journal of cell biology* 171, 61-73.

Di Bartolo, B.A., Nicholls, S.J., Bao, S., Rye, K.A., Heather, A.K., Barter, P.J., and Bursill, C. (2011a). The apolipoprotein A-I mimetic peptide ETC-642 exhibits anti-inflammatory properties that are comparable to high density lipoproteins. *Atherosclerosis* 217, 395-400.

Di Bartolo, B.A., Vanags, L.Z., Tan, J.T., Bao, S., Rye, K.A., Barter, P.J., and Bursill, C.A. (2011b). The apolipoprotein A-I mimetic peptide, ETC-642, reduces chronic vascular inflammation in the rabbit. *Lipids in health and disease* 10, 224.

Dijkers, P.F., Medema, R.H., Lammers, J.W., Koenderman, L., and Coffey, P.J. (2000). Expression of the pro-apoptotic Bcl-2 family member Bim is regulated by the forkhead transcription factor FKHR-L1. *Current biology : CB* 10, 1201-1204.

Dimayuga, P., Zhu, J., Oguchi, S., Chyu, K.Y., Xu, X.O., Yano, J., Shah, P.K., Nilsson, J., and Cercek, B. (1999). Reconstituted HDL containing human apolipoprotein A-1 reduces VCAM-1 expression and neointima formation following periadventitial cuff-induced carotid injury in apoE null mice. *Biochemical and biophysical research communications* *264*, 465-468.

Dimmeler, S., Haendeler, J., and Zeiher, A.M. (2002). Regulation of endothelial cell apoptosis in atherothrombosis. *Current opinion in lipidology* *13*, 531-536.

Dimmeler, S., Rippmann, V., Weiland, U., Haendeler, J., and Zeiher, A.M. (1997). Angiotensin II induces apoptosis of human endothelial cells. Protective effect of nitric oxide. *Circulation research* *81*, 970-976.

Ding, A., Wright, S.D., and Nathan, C. (1987). Activation of mouse peritoneal macrophages by monoclonal antibodies to Mac-1 (complement receptor type 3). *The Journal of experimental medicine* *165*, 733-749.

Dole, V.S., Matuskova, J., Vasile, E., Yesilaltay, A., Bergmeier, W., Bernimoulin, M., Wagner, D.D., and Krieger, M. (2008). Thrombocytopenia and platelet abnormalities in high-density lipoprotein receptor-deficient mice. *Arteriosclerosis, thrombosis, and vascular biology* *28*, 1111-1116.

Dong, Y., Zhang, M., Liang, B., Xie, Z., Zhao, Z., Asfa, S., Choi, H.C., and Zou, M.H. (2010). Reduction of AMP-activated protein kinase $\alpha 2$ increases endoplasmic reticulum stress and atherosclerosis in vivo. *Circulation* *121*, 792-803.

Douglas, G., Bendall, J.K., Crabtree, M.J., Tatham, A.L., Carter, E.E., Hale, A.B., and Channon, K.M. (2012). Endothelial-specific Nox2 overexpression increases vascular

superoxide and macrophage recruitment in ApoE(-)/(-) mice. *Cardiovascular research* 94, 20-29.

Drechsler, M., Megens, R.T., van Zandvoort, M., Weber, C., and Soehnlein, O. (2010). Hyperlipidemia-triggered neutrophilia promotes early atherosclerosis. *Circulation* 122, 1837-1845.

Dzau, V.J., Braun-Dullaeus, R.C., and Sedding, D.G. (2002). Vascular proliferation and atherosclerosis: new perspectives and therapeutic strategies. *Nature medicine* 8, 1249-1256.

Easton, R.M., Cho, H., Roovers, K., Shineman, D.W., Mizrahi, M., Forman, M.S., Lee, V.M., Szabolcs, M., de Jong, R., Oltersdorf, T., *et al.* (2005). Role for Akt3/protein kinase Bgamma in attainment of normal brain size. *Molecular and cellular biology* 25, 1869-1878.

Eliseev, R.A., Zuscik, M.J., Schwarz, E.M., O'Keefe, R.J., Drissi, H., and Rosier, R.N. (2005). Increased radiation-induced apoptosis of Saos2 cells via inhibition of NFkappaB: a role for c-Jun N-terminal kinase. *Journal of cellular biochemistry* 96, 1262-1273.

Emerging Risk Factors, C., Di Angelantonio, E., Sarwar, N., Perry, P., Kaptoge, S., Ray, K.K., Thompson, A., Wood, A.M., Lewington, S., Sattar, N., *et al.* (2009). Major lipids, apolipoproteins, and risk of vascular disease. *Jama* 302, 1993-2000.

Enari, M., Sakahira, H., Yokoyama, H., Okawa, K., Iwamatsu, A., and Nagata, S. (1998). A caspase-activated DNase that degrades DNA during apoptosis, and its inhibitor ICAD. *Nature* 391, 43-50.

Enomoto, S., Sata, M., Fukuda, D., Nakamura, K., and Nagai, R. (2009). Rosuvastatin prevents endothelial cell death and reduces atherosclerotic lesion formation in ApoE-deficient mice. *Biomedicine & pharmacotherapy = Biomedecine & pharmacotherapie* 63, 19-26.

Erbay, E., Babaev, V.R., Mayers, J.R., Makowski, L., Charles, K.N., Snitow, M.E., Fazio, S., Wiest, M.M., Watkins, S.M., Linton, M.F., *et al.* (2009). Reducing endoplasmic reticulum stress through a macrophage lipid chaperone alleviates atherosclerosis. *Nature medicine* 15, 1383-1391.

Ewings, K.E., Hadfield-Moorhouse, K., Wiggins, C.M., Wickenden, J.A., Balmanno, K., Gilley, R., Degenhardt, K., White, E., and Cook, S.J. (2007a). ERK1/2-dependent phosphorylation of BimEL promotes its rapid dissociation from Mcl-1 and Bcl-xL. *The EMBO journal* 26, 2856-2867.

Ewings, K.E., Wiggins, C.M., and Cook, S.J. (2007b). Bim and the pro-survival Bcl-2 proteins: opposites attract, ERK repels. *Cell cycle* 6, 2236-2240.

Falk, E., Shah, P.K., and Fuster, V. (1995). Coronary plaque disruption. *Circulation* 92, 657-671.

Fazio, S., Babaev, V.R., Murray, A.B., Hasty, A.H., Carter, K.J., Gleaves, L.A., Atkinson, J.B., and Linton, M.F. (1997). Increased atherosclerosis in mice reconstituted with apolipoprotein E null macrophages. *Proc Natl Acad Sci U S A* 94, 4647-4652.

Feig, J.E., Rong, J.X., Shamir, R., Sanson, M., Vengrenyuk, Y., Liu, J., Rayner, K., Moore, K., Garabedian, M., and Fisher, E.A. (2011). HDL promotes rapid atherosclerosis regression in mice and alters inflammatory properties of plaque monocyte-derived

cells. *Proceedings of the National Academy of Sciences of the United States of America* *108*, 7166-7171.

Feng, B., Yao, P.M., Li, Y., Devlin, C.M., Zhang, D., Harding, H.P., Sweeney, M., Rong, J.X., Kuriakose, G., Fisher, E.A., *et al.* (2003a). The endoplasmic reticulum is the site of cholesterol-induced cytotoxicity in macrophages. *Nature cell biology* *5*, 781-792.

Feng, B., Zhang, D., Kuriakose, G., Devlin, C.M., Kockx, M., and Tabas, I. (2003b). Niemann-Pick C heterozygosity confers resistance to lesional necrosis and macrophage apoptosis in murine atherosclerosis. *Proceedings of the National Academy of Sciences of the United States of America* *100*, 10423-10428.

Feng, Y., Schoutedden, S., Geenens, R., Van Duppen, V., Herijgers, P., Holvoet, P., Van Veldhoven, P.P., and Verfaillie, C.M. (2012). Hematopoietic stem/progenitor cell proliferation and differentiation is differentially regulated by high-density and low-density lipoproteins in mice. *PloS one* *7*, e47286.

Fernandez-Hernando, C., Ackah, E., Yu, J., Suarez, Y., Murata, T., Iwakiri, Y., Prendergast, J., Miao, R.Q., Birnbaum, M.J., and Sessa, W.C. (2007). Loss of Akt1 leads to severe atherosclerosis and occlusive coronary artery disease. *Cell metabolism* *6*, 446-457.

Fitch, W.M. (1977). Phylogenies constrained by the crossover process as illustrated by human hemoglobins and a thirteen-cycle, eleven-amino-acid repeat in human apolipoprotein A-I. *Genetics* *86*, 623-644.

Frank, P.G., and Marcel, Y.L. (2000). Apolipoprotein A-I: structure-function relationships. *Journal of lipid research* *41*, 853-872.

Fruchart, J.C., Ailhaud, G., and Bard, J.M. (1993). Heterogeneity of high density lipoprotein particles. *Circulation* 87, III22-27.

Fuller, M., Dadoo, O., Serkis, V., Abutouk, D., MacDonald, M., Dhingani, N., Macri, J., Igdoura, S.A., and Trigatti, B.L. (2014a). The effects of diet on occlusive coronary artery atherosclerosis and myocardial infarction in scavenger receptor class B, type 1/low-density lipoprotein receptor double knockout mice. *Arteriosclerosis, thrombosis, and vascular biology* 34, 2394-2403.

Fuller, M., Dadoo, O., Serkis, V., Abutouk, D., MacDonald, M., Dhingani, N., Macri, J., Igdoura, S.A., and Trigatti, B.L. (2014b). The Effects of Diet on Occlusive Coronary Artery Atherosclerosis and Myocardial Infarction in Scavenger Receptor Class B, Type 1/Low-Density Lipoprotein Receptor Double Knockout Mice. *Arteriosclerosis, thrombosis, and vascular biology*.

Fulton, D., Gratton, J.P., McCabe, T.J., Fontana, J., Fujio, Y., Walsh, K., Franke, T.F., Papapetropoulos, A., and Sessa, W.C. (1999). Regulation of endothelium-derived nitric oxide production by the protein kinase Akt. *Nature* 399, 597-601.

Galkina, E., and Ley, K. (2007). Vascular adhesion molecules in atherosclerosis. *Arteriosclerosis, thrombosis, and vascular biology* 27, 2292-2301.

Galkina, E., and Ley, K. (2009). Immune and inflammatory mechanisms of atherosclerosis (*). *Annual review of immunology* 27, 165-197.

Galluzzi, L., Brenner, C., Morselli, E., Touat, Z., and Kroemer, G. (2008). Viral control of mitochondrial apoptosis. *PLoS pathogens* 4, e1000018.

Galvani, S., Sanson, M., Blaho, V.A., Swendeman, S.L., Conger, H., Dahlback, B., Kono, M., Proia, R.L., Smith, J.D., and Hla, T. (2015). HDL-bound sphingosine 1-phosphate acts as a biased agonist for the endothelial cell receptor S1P1 to limit vascular inflammation. *Science signaling* *8*, ra79.

Gao, M., Zhao, D., Schouteden, S., Sorci-Thomas, M.G., Van Veldhoven, P.P., Eggermont, K., Liu, G., Verfaillie, C.M., and Feng, Y. (2014). Regulation of high-density lipoprotein on hematopoietic stem/progenitor cells in atherosclerosis requires scavenger receptor type BI expression. *Arteriosclerosis, thrombosis, and vascular biology* *34*, 1900-1909.

Garcia-Cardena, G., Martasek, P., Masters, B.S., Skidd, P.M., Couet, J., Li, S., Lisanti, M.P., and Sessa, W.C. (1997). Dissecting the interaction between nitric oxide synthase (NOS) and caveolin. Functional significance of the nos caveolin binding domain in vivo. *The Journal of biological chemistry* *272*, 25437-25440.

Gaut, J.R., and Hendershot, L.M. (1993). The modification and assembly of proteins in the endoplasmic reticulum. *Current opinion in cell biology* *5*, 589-595.

Gautier, E.L., Huby, T., Witztum, J.L., Ouzilleau, B., Miller, E.R., Saint-Charles, F., Aucouturier, P., Chapman, M.J., and Lesnik, P. (2009). Macrophage apoptosis exerts divergent effects on atherogenesis as a function of lesion stage. *Circulation* *119*, 1795-1804.

Ghiselli, G., Schaefer, E.J., Gascon, P., and Breser, H.B., Jr. (1981). Type III hyperlipoproteinemia associated with apolipoprotein E deficiency. *Science* *214*, 1239-1241.

Gilbert, H.S., and Ginsberg, H. (1983). Hypocholesterolemia as a manifestation of disease activity in chronic myelocytic leukemia. *Cancer* 51, 1428-1433.

Goldstein, J.L., and Brown, M.S. (1979). The LDL receptor locus and the genetics of familial hypercholesterolemia. *Annu Rev Genet* 13, 259-289.

Goldstein, J.L., and Brown, M.S. (1987). Regulation of low-density lipoprotein receptors: implications for pathogenesis and therapy of hypercholesterolemia and atherosclerosis. *Circulation* 76, 504-507.

Gordon, D.J., and Rifkind, B.M. (1989). High-density lipoprotein--the clinical implications of recent studies. *The New England journal of medicine* 321, 1311-1316.

Gordon, S. (2007). Macrophage heterogeneity and tissue lipids. *The Journal of clinical investigation* 117, 89-93.

Gordon, T., Castelli, W.P., Hjortland, M.C., Kannel, W.B., and Dawber, T.R. (1977). High density lipoprotein as a protective factor against coronary heart disease. The Framingham Study. *The American journal of medicine* 62, 707-714.

Green, D.R., and Kroemer, G. (2004). The pathophysiology of mitochondrial cell death. *Science* 305, 626-629.

Gronros, J., Wikstrom, J., Brandt-Eliasson, U., Forsberg, G.B., Behrendt, M., Hansson, G.I., and Gan, L.M. (2008). Effects of rosuvastatin on cardiovascular morphology and function in an ApoE-knockout mouse model of atherosclerosis. *American journal of physiology Heart and circulatory physiology* 295, H2046-2053.

Guicciardi, M.E., and Gores, G.J. (2009). Life and death by death receptors. *FASEB journal : official publication of the Federation of American Societies for Experimental Biology* 23, 1625-1637.

Han, J., Zhou, X., Yokoyama, T., Hajjar, D.P., Gotto, A.M., Jr., and Nicholson, A.C. (2004). Pitavastatin downregulates expression of the macrophage type B scavenger receptor, CD36. *Circulation* 109, 790-796.

Han, S., Liang, C.P., DeVries-Seimon, T., Ranalletta, M., Welch, C.L., Collins-Fletcher, K., Accili, D., Tabas, I., and Tall, A.R. (2006). Macrophage insulin receptor deficiency increases ER stress-induced apoptosis and necrotic core formation in advanced atherosclerotic lesions. *Cell metabolism* 3, 257-266.

Harfouche, R., Gratton, J.P., Yancopoulos, G.D., Nosedá, M., Karsan, A., and Hussain, S.N. (2003). Angiotensin-1 activates both anti- and proapoptotic mitogen-activated protein kinases. *FASEB journal : official publication of the Federation of American Societies for Experimental Biology* 17, 1523-1525.

Heinloth, A., Brune, B., Fischer, B., and Galle, J. (2002). Nitric oxide prevents oxidised LDL-induced p53 accumulation, cytochrome c translocation, and apoptosis in macrophages via guanylate cyclase stimulation. *Atherosclerosis* 162, 93-101.

Hers, I., Vincent, E.E., and Tavaré, J.M. (2011). Akt signalling in health and disease. *Cellular signalling* 23, 1515-1527.

Hewing, B., Parathath, S., Barrett, T., Chung, W.K., Astudillo, Y.M., Hamada, T., Ramkhalawon, B., Tallant, T.C., Yusufshaq, M.S., Didonato, J.A., *et al.* (2014). Effects of native and myeloperoxidase-modified apolipoprotein a-I on reverse cholesterol

transport and atherosclerosis in mice. *Arteriosclerosis, thrombosis, and vascular biology* *34*, 779-789.

Hinds, M.G., Smits, C., Fredericks-Short, R., Risk, J.M., Bailey, M., Huang, D.C., and Day, C.L. (2007). Bim, Bad and Bmf: intrinsically unstructured BH3-only proteins that undergo a localized conformational change upon binding to prosurvival Bcl-2 targets. *Cell death and differentiation* *14*, 128-136.

Hla, T. (2003). Signaling and biological actions of sphingosine 1-phosphate. *Pharmacological research* *47*, 401-407.

Holm, T.M., Braun, A., Trigatti, B.L., Brugnara, C., Sakamoto, M., Krieger, M., and Andrews, N.C. (2002). Failure of red blood cell maturation in mice with defects in the high-density lipoprotein receptor SR-BI. *Blood* *99*, 1817-1824.

Holvoet, P., Vanhaecke, J., Janssens, S., Van de Werf, F., and Collen, D. (1998). Oxidized LDL and malondialdehyde-modified LDL in patients with acute coronary syndromes and stable coronary artery disease. *Circulation* *98*, 1487-1494.

Horton, J.D., Cohen, J.C., and Hobbs, H.H. (2007). Molecular biology of PCSK9: its role in LDL metabolism. *Trends in biochemical sciences* *32*, 71-77.

Hovingh, G.K., Bochem, A.E., and Kastelein, J.J. (2010). Apolipoprotein A-I mimetic peptides. *Current opinion in lipidology* *21*, 481-486.

Huby, T., Doucet, C., Datchet, C., Ouzilleau, B., Ueda, Y., Afzal, V., Rubin, E., Chapman, M.J., and Lesnik, P. (2006). Knockdown expression and hepatic deficiency reveal an atheroprotective role for SR-BI in liver and peripheral tissues. *The Journal of clinical investigation* *116*, 2767-2776.

- Hughes, S.D., Verstuyft, J., and Rubin, E.M. (1997). HDL deficiency in genetically engineered mice requires elevated LDL to accelerate atherogenesis. *Arteriosclerosis, thrombosis, and vascular biology* 17, 1725-1729.
- Ikemoto, M., Arai, H., Feng, D., Tanaka, K., Aoki, J., Dohmae, N., Takio, K., Adachi, H., Tsujimoto, M., and Inoue, K. (2000). Identification of a PDZ-domain-containing protein that interacts with the scavenger receptor class B type I. *Proceedings of the National Academy of Sciences of the United States of America* 97, 6538-6543.
- Imaizumi, K. (2011). Diet and atherosclerosis in apolipoprotein E-deficient mice. *Biosci Biotechnol Biochem* 75, 1023-1035.
- Ishibashi, S., Brown, M.S., Goldstein, J.L., Gerard, R.D., Hammer, R.E., and Herz, J. (1993). Hypercholesterolemia in low density lipoprotein receptor knockout mice and its reversal by adenovirus-mediated gene delivery. *J Clin Invest* 92, 883-893.
- Jansen, H., Verhoeven, A.J., and Sijbrands, E.J. (2002). Hepatic lipase: a pro- or anti-atherogenic protein? *J Lipid Res* 43, 1352-1362.
- Jedidi, I., Couturier, M., Therond, P., Gardes-Albert, M., Legrand, A., Barouki, R., Bonnefont-Rousselot, D., and Aggerbeck, M. (2006). Cholesteryl ester hydroperoxides increase macrophage CD36 gene expression via PPARalpha. *Biochemical and biophysical research communications* 351, 733-738.
- Jeffers, J.R., Parganas, E., Lee, Y., Yang, C., Wang, J., Brennan, J., MacLean, K.H., Han, J., Chittenden, T., Ihle, J.N., *et al.* (2003). Puma is an essential mediator of p53-dependent and -independent apoptotic pathways. *Cancer cell* 4, 321-328.

Jiang, X., and Wang, X. (2004). Cytochrome C-mediated apoptosis. *Annual review of biochemistry* *73*, 87-106.

Johnson, J., Carson, K., Williams, H., Karanam, S., Newby, A., Angelini, G., George, S., and Jackson, C. (2005). Plaque rupture after short periods of fat feeding in the apolipoprotein E-knockout mouse: model characterization and effects of pravastatin treatment. *Circulation* *111*, 1422-1430.

Johnson, J.L., and Jackson, C.L. (2001). Atherosclerotic plaque rupture in the apolipoprotein E knockout mouse. *Atherosclerosis* *154*, 399-406.

Johnson, J.L., and Newby, A.C. (2009). Macrophage heterogeneity in atherosclerotic plaques. *Current opinion in lipidology* *20*, 370-378.

Ju, H., Zou, R., Venema, V.J., and Venema, R.C. (1997). Direct interaction of endothelial nitric-oxide synthase and caveolin-1 inhibits synthase activity. *The Journal of biological chemistry* *272*, 18522-18525.

Karackattu, S.L., Picard, M.H., and Krieger, M. (2005). Lymphocytes are not required for the rapid onset of coronary heart disease in scavenger receptor class B type I/apolipoprotein E double knockout mice. *Arterioscler Thromb Vasc Biol* *25*, 803-808.

Karackattu, S.L., Trigatti, B., and Krieger, M. (2006). Hepatic lipase deficiency delays atherosclerosis, myocardial infarction, and cardiac dysfunction and extends lifespan in SR-BI/apolipoprotein E double knockout mice. *Arterioscler Thromb Vasc Biol* *26*, 548-554.

- Karuna, R., Park, R., Othman, A., Holleboom, A.G., Motazacker, M.M., Sutter, I., Kuivenhoven, J.A., Rohrer, L., Matile, H., Hornemann, T., *et al.* (2011). Plasma levels of sphingosine-1-phosphate and apolipoprotein M in patients with monogenic disorders of HDL metabolism. *Atherosclerosis* 219, 855-863.
- Kattan, O.M., Kasravi, F.B., Elford, E.L., Schell, M.T., and Harris, H.W. (2008). Apolipoprotein E-mediated immune regulation in sepsis. *J Immunol* 181, 1399-1408.
- Kelly, M.E., Clay, M.A., Mistry, M.J., Hsieh-Li, H.M., and Harmony, J.A. (1994). Apolipoprotein E inhibition of proliferation of mitogen-activated T lymphocytes: production of interleukin 2 with reduced biological activity. *Cell Immunol* 159, 124-139.
- Kimura, T., Sato, K., Malchinkhuu, E., Tomura, H., Tamama, K., Kuwabara, A., Murakami, M., and Okajima, F. (2003). High-density lipoprotein stimulates endothelial cell migration and survival through sphingosine 1-phosphate and its receptors. *Arteriosclerosis, thrombosis, and vascular biology* 23, 1283-1288.
- Kimura, T., Tomura, H., Mogi, C., Kuwabara, A., Damirin, A., Ishizuka, T., Sekiguchi, A., Ishiwara, M., Im, D.S., Sato, K., *et al.* (2006a). Role of scavenger receptor class B type I and sphingosine 1-phosphate receptors in high density lipoprotein-induced inhibition of adhesion molecule expression in endothelial cells. *The Journal of biological chemistry* 281, 37457-37467.
- Kimura, T., Tomura, H., Mogi, C., Kuwabara, A., Ishiwara, M., Shibasawa, K., Sato, K., Ohwada, S., Im, D.S., Kurose, H., *et al.* (2006b). Sphingosine 1-phosphate receptors

mediate stimulatory and inhibitory signalings for expression of adhesion molecules in endothelial cells. *Cellular signalling* 18, 841-850.

Kingwell, B.A., Chapman, M.J., Kontush, A., and Miller, N.E. (2014). HDL-targeted therapies: progress, failures and future. *Nature reviews Drug discovery* 13, 445-464.

Kirschnek, S., Ying, S., Fischer, S.F., Hacker, H., Villunger, A., Hochrein, H., and Hacker, G. (2005). Phagocytosis-induced apoptosis in macrophages is mediated by up-regulation and activation of the Bcl-2 homology domain 3-only protein Bim. *Journal of immunology* 174, 671-679.

Kiryu-Seo, S., Hirayama, T., Kato, R., and Kiyama, H. (2005). Noxa is a critical mediator of p53-dependent motor neuron death after nerve injury in adult mouse. *The Journal of neuroscience : the official journal of the Society for Neuroscience* 25, 1442-1447.

Kocher, O., Birrane, G., Tsukamoto, K., Fenske, S., Yesilaltay, A., Pal, R., Daniels, K., Ladas, J.A., and Krieger, M. (2010). In vitro and in vivo analysis of the binding of the C terminus of the HDL receptor scavenger receptor class B, type I (SR-BI), to the PDZ1 domain of its adaptor protein PDZK1. *The Journal of biological chemistry* 285, 34999-35010.

Kocher, O., Birrane, G., Yesilaltay, A., Shechter, S., Pal, R., Daniels, K., and Krieger, M. (2011). Identification of the PDZ3 domain of the adaptor protein PDZK1 as a second, physiologically functional binding site for the C terminus of the high

density lipoprotein receptor scavenger receptor class B type I. *The Journal of biological chemistry* 286, 25171-25186.

Kocher, O., Pal, R., Roberts, M., Cirovic, C., and Gilchrist, A. (2003a). Targeted disruption of the PDZK1 gene by homologous recombination. *Molecular and cellular biology* 23, 1175-1180.

Kocher, O., Yesilaltay, A., Cirovic, C., Pal, R., Rigotti, A., and Krieger, M. (2003b). Targeted disruption of the PDZK1 gene in mice causes tissue-specific depletion of the high density lipoprotein receptor scavenger receptor class B type I and altered lipoprotein metabolism. *The Journal of biological chemistry* 278, 52820-52825.

Kocher, O., Yesilaltay, A., Shen, C.H., Zhang, S., Daniels, K., Pal, R., Chen, J., and Krieger, M. (2008). Influence of PDZK1 on lipoprotein metabolism and atherosclerosis. *Biochimica et biophysica acta* 1782, 310-316.

Kolodgie, F.D., Narula, J., Burke, A.P., Haider, N., Farb, A., Hui-Liang, Y., Smialek, J., and Virmani, R. (2000). Localization of apoptotic macrophages at the site of plaque rupture in sudden coronary death. *The American journal of pathology* 157, 1259-1268.

Kontush, A., Lhomme, M., and Chapman, M.J. (2013). Unraveling the complexities of the HDL lipidome. *Journal of lipid research* 54, 2950-2963.

Korporaal, S.J., Meurs, I., Hauer, A.D., Hildebrand, R.B., Hoekstra, M., Cate, H.T., Pratico, D., Akkerman, J.W., Van Berkel, T.J., Kuiper, J., *et al.* (2011). Deletion of the high-density lipoprotein receptor scavenger receptor BI in mice modulates thrombosis susceptibility and indirectly affects platelet function by elevation of

plasma free cholesterol. *Arteriosclerosis, thrombosis, and vascular biology* 31, 34-42.

Kozarsky, K.F., Donahee, M.H., Glick, J.M., Krieger, M., and Rader, D.J. (2000). Gene transfer and hepatic overexpression of the HDL receptor SR-BI reduces atherosclerosis in the cholesterol-fed LDL receptor-deficient mouse. *Arterioscler Thromb Vasc Biol* 20, 721-727.

Krieger, M. (2001). Scavenger receptor class B type I is a multiligand HDL receptor that influences diverse physiologic systems. *The Journal of clinical investigation* 108, 793-797.

Kwon, Y.G., Min, J.K., Kim, K.M., Lee, D.J., Billiar, T.R., and Kim, Y.M. (2001). Sphingosine 1-phosphate protects human umbilical vein endothelial cells from serum-deprived apoptosis by nitric oxide production. *The Journal of biological chemistry* 276, 10627-10633.

Kzhyshkowska, J., Neyen, C., and Gordon, S. (2012). Role of macrophage scavenger receptors in atherosclerosis. *Immunobiology* 217, 492-502.

Lee, A.S. (2005). The ER chaperone and signaling regulator GRP78/BiP as a monitor of endoplasmic reticulum stress. *Methods* 35, 373-381.

Lee, C.D., Folsom, A.R., Nieto, F.J., Chambless, L.E., Shahar, E., and Wolfe, D.A. (2001). White blood cell count and incidence of coronary heart disease and ischemic stroke and mortality from cardiovascular disease in African-American and White men and women: atherosclerosis risk in communities study. *American journal of epidemiology* 154, 758-764.

Lee, M.Y., Luciano, A.K., Ackah, E., Rodriguez-Vita, J., Bancroft, T.A., Eichmann, A., Simons, M., Kyriakides, T.R., Morales-Ruiz, M., and Sessa, W.C. (2014). Endothelial Akt1 mediates angiogenesis by phosphorylating multiple angiogenic substrates. *Proceedings of the National Academy of Sciences of the United States of America* *111*, 12865-12870.

Lee, W.R., Sacharidou, A., Behling-Kelly, E., Oltmann, S.C., Zhu, W., Ahmed, M., Gerard, R.D., Hui, D.Y., Abe, J., Shaul, P.W., *et al.* (2015). PDZK1 prevents neointima formation via suppression of breakpoint cluster region kinase in vascular smooth muscle. *PloS one* *10*, e0124494.

Leitinger, N., and Schulman, I.G. (2013). Phenotypic polarization of macrophages in atherosclerosis. *Arteriosclerosis, thrombosis, and vascular biology* *33*, 1120-1126.

Ley, R., Balmanno, K., Hadfield, K., Weston, C., and Cook, S.J. (2003). Activation of the ERK1/2 signaling pathway promotes phosphorylation and proteasome-dependent degradation of the BH3-only protein, Bim. *The Journal of biological chemistry* *278*, 18811-18816.

Ley, R., Hadfield, K., Howes, E., and Cook, S.J. (2005). Identification of a DEF-type docking domain for extracellular signal-regulated kinases 1/2 that directs phosphorylation and turnover of the BH3-only protein BimEL. *The Journal of biological chemistry* *280*, 17657-17663.

Li, A.C., Binder, C.J., Gutierrez, A., Brown, K.K., Plotkin, C.R., Pattison, J.W., Valledor, A.F., Davis, R.A., Willson, T.M., Witztum, J.L., *et al.* (2004). Differential inhibition of

macrophage foam-cell formation and atherosclerosis in mice by PPARalpha, beta/delta, and gamma. *The Journal of clinical investigation* *114*, 1564-1576.

Li, G., Tokuno, S., Tahep Id, P., Vaage, J., Lowbeer, C., and Valen, G. (2001).

Preconditioning protects the severely atherosclerotic mouse heart. *Ann Thorac Surg* *71*, 1296-1303; discussion 1303-1294.

Li, W., Asagami, T., Matsushita, H., Lee, K.H., and Tsao, P.S. (2005). Rosuvastatin attenuates monocyte-endothelial cell interactions and vascular free radical production in hypercholesterolemic mice. *The Journal of pharmacology and experimental therapeutics* *313*, 557-562.

Liao, F., Andalibi, A., deBeer, F.C., Fogelman, A.M., and Lusis, A.J. (1993). Genetic control of inflammatory gene induction and NF-kappa B-like transcription factor activation in response to an atherogenic diet in mice. *J Clin Invest* *91*, 2572-2579.

Liao, J.K., and Laufs, U. (2005). Pleiotropic effects of statins. *Annual review of pharmacology and toxicology* *45*, 89-118.

Lichtman, A.H., Clinton, S.K., Iiyama, K., Connelly, P.W., Libby, P., and Cybulsky, M.I. (1999). Hyperlipidemia and atherosclerotic lesion development in LDL receptor-deficient mice fed defined semipurified diets with and without cholate. *Arterioscler Thromb Vasc Biol* *19*, 1938-1944.

Lim, W.S., Timmins, J.M., Seimon, T.A., Sadler, A., Kolodgie, F.D., Virmani, R., and Tabas, I. (2008). Signal transducer and activator of transcription-1 is critical for apoptosis in macrophages subjected to endoplasmic reticulum stress in vitro and in advanced atherosclerotic lesions in vivo. *Circulation* *117*, 940-951.

Lin, K.R., Li, C.L., Yen, J.J., and Yang-Yen, H.F. (2013). Constitutive phosphorylation of GATA-1 at serine(2)(6) attenuates the colony-forming activity of erythrocyte-committed progenitors. *PloS one* 8, e64269.

Liu, M., Seo, J., Allegood, J., Bi, X., Zhu, X., Boudyguina, E., Gebre, A.K., Avni, D., Shah, D., Sorci-Thomas, M.G., *et al.* (2014). Hepatic apolipoprotein M (apoM) overexpression stimulates formation of larger apoM/sphingosine 1-phosphate-enriched plasma high density lipoprotein. *The Journal of biological chemistry* 289, 2801-2814.

Llodra, J., Angeli, V., Liu, J., Trogan, E., Fisher, E.A., and Randolph, G.J. (2004). Emigration of monocyte-derived cells from atherosclerotic lesions characterizes regressive, but not progressive, plaques. *Proceedings of the National Academy of Sciences of the United States of America* 101, 11779-11784.

Ludman, A., Venugopal, V., Yellon, D.M., and Hausenloy, D.J. (2009). Statins and cardioprotection--more than just lipid lowering? *Pharmacology & therapeutics* 122, 30-43.

Lv, Y., Song, S., Zhang, K., Gao, H., and Ma, R. (2013). CHIP regulates AKT/FoxO/Bim signaling in MCF7 and MCF10A cells. *PloS one* 8, e83312.

Ma, Y., Ashraf, M.Z., and Podrez, E.A. (2010). Scavenger receptor BI modulates platelet reactivity and thrombosis in dyslipidemia. *Blood* 116, 1932-1941.

Mantovani, A., Locati, M., Vecchi, A., Sozzani, S., and Allavena, P. (2001). Decoy receptors: a strategy to regulate inflammatory cytokines and chemokines. *Trends in immunology* 22, 328-336.

Maron, D.J., Fazio, S., and Linton, M.F. (2000). Current perspectives on statins. *Circulation* *101*, 207-213.

Matoba, T., Sato, K., and Egashira, K. (2013). Mouse models of plaque rupture. *Current opinion in lipidology* *24*, 419-425.

Mazor, R., Shurtz-Swirski, R., Farah, R., Kristal, B., Shapiro, G., Dorlechter, F., Cohen-Mazor, M., Meilin, E., Tamara, S., and Sela, S. (2008). Primed polymorphonuclear leukocytes constitute a possible link between inflammation and oxidative stress in hyperlipidemic patients. *Atherosclerosis* *197*, 937-943.

McCullough, K.D., Martindale, J.L., Klotz, L.O., Aw, T.Y., and Holbrook, N.J. (2001). Gadd153 sensitizes cells to endoplasmic reticulum stress by down-regulating Bcl2 and perturbing the cellular redox state. *Molecular and cellular biology* *21*, 1249-1259.

McNeill, E., Channon, K.M., and Greaves, D.R. (2010). Inflammatory cell recruitment in cardiovascular disease: murine models and potential clinical applications. *Clinical science* *118*, 641-655.

McNeish, J., Aiello, R.J., Guyot, D., Turi, T., Gabel, C., Aldinger, C., Hoppe, K.L., Roach, M.L., Royer, L.J., de Wet, J., *et al.* (2000). High density lipoprotein deficiency and foam cell accumulation in mice with targeted disruption of ATP-binding cassette transporter-1. *Proceedings of the National Academy of Sciences of the United States of America* *97*, 4245-4250.

Mehrabian, M., Demer, L.L., and Lusis, A.J. (1991). Differential accumulation of intimal monocyte-macrophages relative to lipoproteins and lipofuscin corresponds

to hemodynamic forces on cardiac valves in mice. *Arteriosclerosis and thrombosis : a journal of vascular biology / American Heart Association* *11*, 947-957.

Meisinger, C., Baumert, J., Khuseyinova, N., Loewel, H., and Koenig, W. (2005).

Plasma oxidized low-density lipoprotein, a strong predictor for acute coronary heart disease events in apparently healthy, middle-aged men from the general population. *Circulation* *112*, 651-657.

Michel, J.B., Feron, O., Sacks, D., and Michel, T. (1997). Reciprocal regulation of endothelial nitric-oxide synthase by Ca²⁺-calmodulin and caveolin. *The Journal of biological chemistry* *272*, 15583-15586.

Miller, N.E. (1990). HDL metabolism and its role in lipid transport. *European heart journal* *11 Suppl H*, 1-3.

Mineo, C., and Shaul, P.W. (2007). Role of high-density lipoprotein and scavenger receptor B type I in the promotion of endothelial repair. *Trends in cardiovascular medicine* *17*, 156-161.

Mineo, C., and Shaul, P.W. (2012a). Novel biological functions of high-density lipoprotein cholesterol. *Circulation research* *111*, 1079-1090.

Mineo, C., and Shaul, P.W. (2012b). Regulation of eNOS in caveolae. *Advances in experimental medicine and biology* *729*, 51-62.

Mineo, C., Yuhanna, I.S., Quon, M.J., and Shaul, P.W. (2003). High density lipoprotein-induced endothelial nitric-oxide synthase activation is mediated by Akt and MAP kinases. *The Journal of biological chemistry* *278*, 9142-9149.

Monetti, M., Canavesi, M., Camera, M., Parente, R., Paoletti, R., Tremoli, E., Corsini, A., and Bellosta, S. (2007). Rosuvastatin displays anti-atherothrombotic and anti-inflammatory properties in apoE-deficient mice. *Pharmacological research : the official journal of the Italian Pharmacological Society* 55, 441-449.

Moolenaar, W.H., and Hla, T. (2012). SnapShot: Bioactive lysophospholipids. *Cell* 148, 378-378 e372.

Moore, K.J., Sheedy, F.J., and Fisher, E.A. (2013). Macrophages in atherosclerosis: a dynamic balance. *Nature reviews Immunology* 13, 709-721.

Moore, K.J., and Tabas, I. (2011). Macrophages in the pathogenesis of atherosclerosis. *Cell* 145, 341-355.

Moore, R.E., Kawashiri, M.A., Kitajima, K., Secreto, A., Millar, J.S., Pratico, D., and Rader, D.J. (2003). Apolipoprotein A-I deficiency results in markedly increased atherosclerosis in mice lacking the LDL receptor. *Arteriosclerosis, thrombosis, and vascular biology* 23, 1914-1920.

Mouhamad, S., Besnault, L., Auffredou, M.T., Leprince, C., Bourgeade, M.F., Leca, G., and Vazquez, A. (2004). B cell receptor-mediated apoptosis of human lymphocytes is associated with a new regulatory pathway of Bim isoform expression. *Journal of immunology* 172, 2084-2091.

Mozaffarian, D., Benjamin, E.J., Go, A.S., Arnett, D.K., Blaha, M.J., Cushman, M., de Ferranti, S., Despres, J.P., Fullerton, H.J., Howard, V.J., *et al.* (2015). Heart disease and stroke statistics--2015 update: a report from the American Heart Association. *Circulation* 131, e29-322.

- Muller, K., Dulku, S., Hardwick, S.J., Skepper, J.N., and Mitchinson, M.J. (2001). Changes in vimentin in human macrophages during apoptosis induced by oxidised low density lipoprotein. *Atherosclerosis* 156, 133-144.
- Murata, N., Sato, K., Kon, J., Tomura, H., Yanagita, M., Kuwabara, A., Ui, M., and Okajima, F. (2000). Interaction of sphingosine 1-phosphate with plasma components, including lipoproteins, regulates the lipid receptor-mediated actions. *The Biochemical journal* 352 Pt 3, 809-815.
- Murohara, T., Witzendichler, B., Spyridopoulos, I., Asahara, T., Ding, B., Sullivan, A., Losordo, D.W., and Isner, J.M. (1999). Role of endothelial nitric oxide synthase in endothelial cell migration. *Arteriosclerosis, thrombosis, and vascular biology* 19, 1156-1161.
- Murphy, A.J., Woollard, K.J., Hoang, A., Mukhamedova, N., Stirzaker, R.A., McCormick, S.P., Remaley, A.T., Sviridov, D., and Chin-Dusting, J. (2008). High-density lipoprotein reduces the human monocyte inflammatory response. *Arteriosclerosis, thrombosis, and vascular biology* 28, 2071-2077.
- Murphy, A.J., Woollard, K.J., Suhartoyo, A., Stirzaker, R.A., Shaw, J., Sviridov, D., and Chin-Dusting, J.P. (2011). Neutrophil activation is attenuated by high-density lipoprotein and apolipoprotein A-I in in vitro and in vivo models of inflammation. *Arteriosclerosis, thrombosis, and vascular biology* 31, 1333-1341.
- Murray, P.J., and Wynn, T.A. (2011). Protective and pathogenic functions of macrophage subsets. *Nature reviews Immunology* 11, 723-737.

Myoishi, M., Hao, H., Minamino, T., Watanabe, K., Nishihira, K., Hatakeyama, K., Asada, Y., Okada, K., Ishibashi-Ueda, H., Gabbiani, G., *et al.* (2007). Increased endoplasmic reticulum stress in atherosclerotic plaques associated with acute coronary syndrome. *Circulation* *116*, 1226-1233.

Nagao, T., Qin, C., Grosheva, I., Maxfield, F.R., and Pierini, L.M. (2007). Elevated cholesterol levels in the plasma membranes of macrophages inhibit migration by disrupting RhoA regulation. *Arteriosclerosis, thrombosis, and vascular biology* *27*, 1596-1602.

Nakashima, Y., Plump, A.S., Raines, E.W., Breslow, J.L., and Ross, R. (1994). ApoE-deficient mice develop lesions of all phases of atherosclerosis throughout the arterial tree. *Arteriosclerosis and thrombosis : a journal of vascular biology / American Heart Association* *14*, 133-140.

Nakaya, H., Summers, B.D., Nicholson, A.C., Gotto, A.M., Jr., Hajjar, D.P., and Han, J. (2009). Atherosclerosis in LDLR-knockout mice is inhibited, but not reversed, by the PPARgamma ligand pioglitazone. *The American journal of pathology* *174*, 2007-2014.

Napoli, C., Paolisso, G., Casamassimi, A., Al-Omran, M., Barbieri, M., Sommese, L., Infante, T., and Ignarro, L.J. (2013). Effects of nitric oxide on cell proliferation: novel insights. *Journal of the American College of Cardiology* *62*, 89-95.

Napoli, C., Williams-Ignarro, S., De Nigris, F., Lerman, L.O., Rossi, L., Guarino, C., Mansueto, G., Di Tuoro, F., Pignalosa, O., De Rosa, G., *et al.* (2004). Long-term combined beneficial effects of physical training and metabolic treatment on

atherosclerosis in hypercholesterolemic mice. *Proceedings of the National Academy of Sciences of the United States of America* *101*, 8797-8802.

Navab, M., Hama, S.Y., Hough, G.P., Subbanagounder, G., Reddy, S.T., and Fogelman, A.M. (2001). A cell-free assay for detecting HDL that is dysfunctional in preventing the formation of or inactivating oxidized phospholipids. *Journal of lipid research* *42*, 1308-1317.

Navab, M., Reddy, S.T., Van Lenten, B.J., and Fogelman, A.M. (2011). HDL and cardiovascular disease: atherogenic and atheroprotective mechanisms. *Nature reviews Cardiology* *8*, 222-232.

Niculescu, L.S., Sanda, G.M., and Sima, A.V. (2013). HDL inhibits endoplasmic reticulum stress by stimulating apoE and CETP secretion from lipid-loaded macrophages. *Biochemical and biophysical research communications* *434*, 173-178.

Nissen, S.E., Tsunoda, T., Tuzcu, E.M., Schoenhagen, P., Cooper, C.J., Yasin, M., Eaton, G.M., Lauer, M.A., Sheldon, W.S., Grines, C.L., *et al.* (2003). Effect of recombinant ApoA-I Milano on coronary atherosclerosis in patients with acute coronary syndromes: a randomized controlled trial. *Jama* *290*, 2292-2300.

Nofer, J.R., Bot, M., Brodde, M., Taylor, P.J., Salm, P., Brinkmann, V., van Berkel, T., Assmann, G., and Biessen, E.A. (2007). FTY720, a synthetic sphingosine 1 phosphate analogue, inhibits development of atherosclerosis in low-density lipoprotein receptor-deficient mice. *Circulation* *115*, 501-508.

Nofer, J.R., Geigenmuller, S., Gopfert, C., Assmann, G., Buddecke, E., and Schmidt, A. (2003). High density lipoprotein-associated lysosphingolipids reduce E-selectin

expression in human endothelial cells. *Biochemical and biophysical research communications* 310, 98-103.

Nofer, J.R., Levkau, B., Wolinska, I., Junker, R., Fobker, M., von Eckardstein, A., Seedorf, U., and Assmann, G. (2001). Suppression of endothelial cell apoptosis by high density lipoproteins (HDL) and HDL-associated lysosphingolipids. *The Journal of biological chemistry* 276, 34480-34485.

Nofer, J.R., van der Giet, M., Tolle, M., Wolinska, I., von Wnuck Lipinski, K., Baba, H.A., Tietge, U.J., Godecke, A., Ishii, I., Kleuser, B., *et al.* (2004). HDL induces NO-dependent vasorelaxation via the lysophospholipid receptor S1P3. *The Journal of clinical investigation* 113, 569-581.

Okajima, F., Sato, K., and Kimura, T. (2009). Anti-atherogenic actions of high-density lipoprotein through sphingosine 1-phosphate receptors and scavenger receptor class B type I. *Endocrine journal* 56, 317-334.

Olivera, A., and Spiegel, S. (1993). Sphingosine-1-phosphate as second messenger in cell proliferation induced by PDGF and FCS mitogens. *Nature* 365, 557-560.

Oram, J.F. (2000). Tangier disease and ABCA1. *Biochimica et biophysica acta* 1529, 321-330.

Oram, J.F., and Vaughan, A.M. (2006). ATP-Binding cassette cholesterol transporters and cardiovascular disease. *Circulation research* 99, 1031-1043.

Overbergh, L., Valckx, D., Waer, M., and Mathieu, C. (1999). Quantification of murine cytokine mRNAs using real time quantitative reverse transcriptase PCR. *Cytokine* 11, 305-312.

Oyadomari, S., and Mori, M. (2004). Roles of CHOP/GADD153 in endoplasmic reticulum stress. *Cell death and differentiation* 11, 381-389.

Paigen, B., Holmes, P.A., Mitchell, D., and Albee, D. (1987). Comparison of atherosclerotic lesions and HDL-lipid levels in male, female, and testosterone-treated female mice from strains C57BL/6, BALB/c, and C3H. *Atherosclerosis* 64, 215-221.

Paigen, B., Morrow, A., Brandon, C., Mitchell, D., and Holmes, P. (1985). Variation in susceptibility to atherosclerosis among inbred strains of mice. *Atherosclerosis* 57, 65-73.

Paik, J.H., Chae, S., Lee, M.J., Thangada, S., and Hla, T. (2001). Sphingosine 1-phosphate-induced endothelial cell migration requires the expression of EDG-1 and EDG-3 receptors and Rho-dependent activation of alpha vbeta3- and beta1-containing integrins. *The Journal of biological chemistry* 276, 11830-11837.

Pandolfino, J., Hakimian, D., Rademaker, A.W., and Tallman, M.S. (1997). Hypocholesterolemia in hairy cell leukemia: a marker for proliferative activity. *American journal of hematology* 55, 129-133.

Park, S.J., Lee, K.P., Kang, S., Lee, J., Sato, K., Chung, H.Y., Okajima, F., and Im, D.S. (2014). Sphingosine 1-phosphate induced anti-atherogenic and atheroprotective M2 macrophage polarization through IL-4. *Cellular signalling* 26, 2249-2258.

Paszy, C., Maeda, N., Verstuyft, J., and Rubin, E.M. (1994). Apolipoprotein AI transgene corrects apolipoprotein E deficiency-induced atherosclerosis in mice. *The Journal of clinical investigation* 94, 899-903.

Pei, Y., Chen, X., Aboutouk, D., Fuller, M.T., Dadoo, O., Yu, P., White, E.J., Igdoura, S.A., and Trigatti, B.L. (2013). SR-BI in bone marrow derived cells protects mice from diet induced coronary artery atherosclerosis and myocardial infarction. *PloS one* 8, e72492.

Peng, Z.Y., Zhao, S.P., He, B.M., Peng, D.Q., and Hu, M. (2011). Protective effect of HDL on endothelial NO production: the role of DDAH/ADMA pathway. *Molecular and cellular biochemistry* 351, 243-249.

Perk, J., De Backer, G., Gohlke, H., Graham, I., Reiner, Z., Verschuren, W.M., Albus, C., Benlian, P., Boysen, G., Cifkova, R., *et al.* (2012). European Guidelines on cardiovascular disease prevention in clinical practice (version 2012): The Fifth Joint Task Force of the European Society of Cardiology and Other Societies on Cardiovascular Disease Prevention in Clinical Practice (constituted by representatives of nine societies and by invited experts). *Atherosclerosis* 223, 1-68.

Phillips, M.C. (2014). Molecular mechanisms of cellular cholesterol efflux. *The Journal of biological chemistry* 289, 24020-24029.

Phung, T.L., Du, W., Xue, Q., Ayyaswamy, S., Gerald, D., Antonello, Z., Nhek, S., Perruzzi, C.A., Acevedo, I., Ramanna-Valmiki, R., *et al.* (2015). Akt1 and akt3 exert opposing roles in the regulation of vascular tumor growth. *Cancer research* 75, 40-50.

Piedrahita, J.A., Zhang, S.H., Hagaman, J.R., Oliver, P.M., and Maeda, N. (1992). Generation of mice carrying a mutant apolipoprotein E gene inactivated by gene targeting in embryonic stem cells. *Proc Natl Acad Sci U S A* 89, 4471-4475.

Plump, A.S., Azrolan, N., Odaka, H., Wu, L., Jiang, X., Tall, A., Eisenberg, S., and Breslow, J.L. (1997). ApoA-I knockout mice: characterization of HDL metabolism in homozygotes and identification of a post-RNA mechanism of apoA-I up-regulation in heterozygotes. *Journal of lipid research* 38, 1033-1047.

Plump, A.S., Scott, C.J., and Breslow, J.L. (1994). Human apolipoprotein A-I gene expression increases high density lipoprotein and suppresses atherosclerosis in the apolipoprotein E-deficient mouse. *Proceedings of the National Academy of Sciences of the United States of America* 91, 9607-9611.

Plump, A.S., Smith, J.D., Hayek, T., Aalto-Setälä, K., Walsh, A., Verstuyft, J.G., Rubin, E.M., and Breslow, J.L. (1992). Severe hypercholesterolemia and atherosclerosis in apolipoprotein E-deficient mice created by homologous recombination in ES cells. *Cell* 71, 343-353.

Powell-Braxton, L., Veniant, M., Latvala, R.D., Hirano, K.I., Won, W.B., Ross, J., Dybdal, N., Zlot, C.H., Young, S.G., and Davidson, N.O. (1998). A mouse model of human familial hypercholesterolemia: markedly elevated low density lipoprotein cholesterol levels and severe atherosclerosis on a low-fat chow diet. *Nat Med* 4, 934-938.

Prosser, H.C., Ng, M.K., and Bursill, C.A. (2012). The role of cholesterol efflux in mechanisms of endothelial protection by HDL. *Current opinion in lipidology* 23, 182-189.

Puthalakath, H., O'Reilly, L.A., Gunn, P., Lee, L., Kelly, P.N., Huntington, N.D., Hughes, P.D., Michalak, E.M., McKimm-Breschkin, J., Motoyama, N., *et al.* (2007). ER stress triggers apoptosis by activating BH3-only protein Bim. *Cell* *129*, 1337-1349.

Qi, X.J., Wildey, G.M., and Howe, P.H. (2006). Evidence that Ser87 of BimEL is phosphorylated by Akt and regulates BimEL apoptotic function. *The Journal of biological chemistry* *281*, 813-823.

Qiao, J.H., Tripathi, J., Mishra, N.K., Cai, Y., Tripathi, S., Wang, X.P., Imes, S., Fishbein, M.C., Clinton, S.K., Libby, P., *et al.* (1997). Role of macrophage colony-stimulating factor in atherosclerosis: studies of osteopetrotic mice. *The American journal of pathology* *150*, 1687-1699.

Qin, C., Nagao, T., Grosheva, I., Maxfield, F.R., and Pierini, L.M. (2006). Elevated plasma membrane cholesterol content alters macrophage signaling and function. *Arteriosclerosis, thrombosis, and vascular biology* *26*, 372-378.

Rajavashisth, T., Qiao, J.H., Tripathi, S., Tripathi, J., Mishra, N., Hua, M., Wang, X.P., Loussararian, A., Clinton, S., Libby, P., *et al.* (1998). Heterozygous osteopetrotic (op) mutation reduces atherosclerosis in LDL receptor- deficient mice. *The Journal of clinical investigation* *101*, 2702-2710.

Ranger, A.M., Zha, J., Harada, H., Datta, S.R., Danial, N.N., Gilmore, A.P., Kutok, J.L., Le Beau, M.M., Greenberg, M.E., and Korsmeyer, S.J. (2003). Bad-deficient mice develop diffuse large B cell lymphoma. *Proceedings of the National Academy of Sciences of the United States of America* *100*, 9324-9329.

Read, M.A., Neish, A.S., Luscinskas, F.W., Palombella, V.J., Maniatis, T., and Collins, T. (1995). The proteasome pathway is required for cytokine-induced endothelial-leukocyte adhesion molecule expression. *Immunity* 2, 493-506.

Read, M.A., Whitley, M.Z., Williams, A.J., and Collins, T. (1994). NF-kappa B and I kappa B alpha: an inducible regulatory system in endothelial activation. *The Journal of experimental medicine* 179, 503-512.

Reddick, R.L., Zhang, S.H., and Maeda, N. (1994). Atherosclerosis in mice lacking apo E. Evaluation of lesional development and progression. *Arteriosclerosis and thrombosis : a journal of vascular biology / American Heart Association* 14, 141-147.

Reddy, S.T., Navab, M., Anantharamaiah, G.M., and Fogelman, A.M. (2014). Apolipoprotein A-I mimetics. *Current opinion in lipidology* 25, 304-308.

Renehan, A.G., Booth, C., and Potten, C.S. (2001). What is apoptosis, and why is it important? *Bmj* 322, 1536-1538.

Reverter, J.C., Sierra, J., Marti-Tutusaus, J.M., Montserrat, E., Granena, A., and Rozman, C. (1988). Hypocholesterolemia in acute myelogenous leukemia. *European journal of haematology* 41, 317-320.

Riddell, D.R., Graham, A., and Owen, J.S. (1997). Apolipoprotein E inhibits platelet aggregation through the L-arginine:nitric oxide pathway. Implications for vascular disease. *J Biol Chem* 272, 89-95.

Rigotti, A., Miettinen, H.E., and Krieger, M. (2003). The role of the high-density lipoprotein receptor SR-BI in the lipid metabolism of endocrine and other tissues. *Endocr Rev* 24, 357-387.

Rigotti, A., Trigatti, B.L., Penman, M., Rayburn, H., Herz, J., and Krieger, M. (1997). A targeted mutation in the murine gene encoding the high density lipoprotein (HDL) receptor scavenger receptor class B type I reveals its key role in HDL metabolism. *Proceedings of the National Academy of Sciences of the United States of America* 94, 12610-12615.

Robbins, C.S., Chudnovskiy, A., Rauch, P.J., Figueiredo, J.L., Iwamoto, Y., Gorbatov, R., Etzrodt, M., Weber, G.F., Ueno, T., van Rooijen, N., *et al.* (2012). Extramedullary hematopoiesis generates Ly-6C(high) monocytes that infiltrate atherosclerotic lesions. *Circulation* 125, 364-374.

Robbins, C.S., Hilgendorf, I., Weber, G.F., Theurl, I., Iwamoto, Y., Figueiredo, J.L., Gorbatov, R., Sukhova, G.K., Gerhardt, L.M., Smyth, D., *et al.* (2013). Local proliferation dominates lesional macrophage accumulation in atherosclerosis. *Nature medicine* 19, 1166-1172.

Roger, V.L., Go, A.S., Lloyd-Jones, D.M., Benjamin, E.J., Berry, J.D., Borden, W.B., Bravata, D.M., Dai, S., Ford, E.S., Fox, C.S., *et al.* (2012). Heart disease and stroke statistics--2012 update: a report from the American Heart Association. *Circulation* 125, e2-e220.

Rong, J.X., Li, J., Reis, E.D., Choudhury, R.P., Dansky, H.M., Elmalem, V.I., Fallon, J.T., Breslow, J.L., and Fisher, E.A. (2001). Elevating high-density lipoprotein cholesterol

in apolipoprotein E-deficient mice remodels advanced atherosclerotic lesions by decreasing macrophage and increasing smooth muscle cell content. *Circulation* *104*, 2447-2452.

Roselaar, S.E., and Daugherty, A. (1998). Apolipoprotein E-deficient mice have impaired innate immune responses to *Listeria monocytogenes* in vivo. *J Lipid Res* *39*, 1740-1743.

Rosenfeld, M.E., Polinsky, P., Virmani, R., Kauser, K., Rubanyi, G., and Schwartz, S.M. (2000). Advanced atherosclerotic lesions in the innominate artery of the ApoE knockout mouse. *Arteriosclerosis, thrombosis, and vascular biology* *20*, 2587-2592.

Rosenson, R.S., Brewer, H.B., Jr., Davidson, W.S., Fayad, Z.A., Fuster, V., Goldstein, J., Hellerstein, M., Jiang, X.C., Phillips, M.C., Rader, D.J., *et al.* (2012). Cholesterol efflux and atheroprotection: advancing the concept of reverse cholesterol transport. *Circulation* *125*, 1905-1919.

Rubin, E.M., Krauss, R.M., Spangler, E.A., Verstuyft, J.G., and Clift, S.M. (1991). Inhibition of early atherogenesis in transgenic mice by human apolipoprotein AI. *Nature* *353*, 265-267.

Saelens, X., Festjens, N., Vande Walle, L., van Gurp, M., van Loo, G., and Vandenabeele, P. (2004). Toxic proteins released from mitochondria in cell death. *Oncogene* *23*, 2861-2874.

Sakahira, H., Enari, M., and Nagata, S. (1998). Cleavage of CAD inhibitor in CAD activation and DNA degradation during apoptosis. *Nature* *391*, 96-99.

- Sakakura, K., Nakano, M., Otsuka, F., Ladich, E., Kolodgie, F.D., and Virmani, R. (2013). Pathophysiology of atherosclerosis plaque progression. *Heart Lung Circ* 22, 399-411.
- Sanan, D.A., Newland, D.L., Tao, R., Marcovina, S., Wang, J., Mooser, V., Hammer, R.E., and Hobbs, H.H. (1998). Low density lipoprotein receptor-negative mice expressing human apolipoprotein B-100 develop complex atherosclerotic lesions on a chow diet: no accentuation by apolipoprotein(a). *Proc Natl Acad Sci U S A* 95, 4544-4549.
- Sanson, M., Distel, E., and Fisher, E.A. (2013). HDL induces the expression of the M2 macrophage markers arginase 1 and Fizz-1 in a STAT6-dependent process. *PloS one* 8, e74676.
- Saraste, A., and Pulkki, K. (2000). Morphologic and biochemical hallmarks of apoptosis. *Cardiovascular research* 45, 528-537.
- Sattler, K.J., Elbasan, S., Keul, P., Elter-Schulz, M., Bode, C., Graler, M.H., Brocker-Preuss, M., Budde, T., Erbel, R., Heusch, G., *et al.* (2010). Sphingosine 1-phosphate levels in plasma and HDL are altered in coronary artery disease. *Basic research in cardiology* 105, 821-832.
- Sawant, P.B., Bera, A., Dasgupta, S., Sawant, B.T., Chadha, N.K., and Pal, A.K. (2014). p53 dependent apoptotic cell death induces embryonic malformation in *Carassius auratus* under chronic hypoxia. *PloS one* 9, e102650.
- Schaefer, E.J., and Asztalos, B.F. (2007). Increasing high-density lipoprotein cholesterol, inhibition of cholesteryl ester transfer protein, and heart disease risk reduction. *The American journal of cardiology* 100, n25-31.

Schafer, A., Fraccarollo, D., Eigenthaler, M., Tas, P., Firmschild, A., Frantz, S., Ertl, G., and Bauersachs, J. (2005a). Rosuvastatin reduces platelet activation in heart failure: role of NO bioavailability. *Arteriosclerosis, thrombosis, and vascular biology* *25*, 1071-1077.

Schafer, K., Kaiser, K., and Konstantinides, S. (2005b). Rosuvastatin exerts favourable effects on thrombosis and neointimal growth in a mouse model of endothelial injury. *Thrombosis and haemostasis* *93*, 145-152.

Schmidt, A., Geigenmuller, S., Volker, W., and Buddecke, E. (2006). The antiatherogenic and antiinflammatory effect of HDL-associated lysosphingolipids operates via Akt -->NF-kappaB signalling pathways in human vascular endothelial cells. *Basic research in cardiology* *101*, 109-116.

Scholzen, T., and Gerdes, J. (2000). The Ki-67 protein: from the known and the unknown. *Journal of cellular physiology* *182*, 311-322.

Schroder, M., and Kaufman, R.J. (2005). The mammalian unfolded protein response. *Annual review of biochemistry* *74*, 739-789.

Schroeter, M.R., Humboldt, T., Schafer, K., and Konstantinides, S. (2009). Rosuvastatin reduces atherosclerotic lesions and promotes progenitor cell mobilisation and recruitment in apolipoprotein E knockout mice. *Atherosclerosis* *205*, 63-73.

Schwartz, S.M., Galis, Z.S., Rosenfeld, M.E., and Falk, E. (2007). Plaque rupture in humans and mice. *Arteriosclerosis, thrombosis, and vascular biology* *27*, 705-713.

Scull, C.M., and Tabas, I. (2011). Mechanisms of ER stress-induced apoptosis in atherosclerosis. *Arteriosclerosis, thrombosis, and vascular biology* 31, 2792-2797.

Seetharam, D., Mineo, C., Gormley, A.K., Gibson, L.L., Vongpatanasin, W., Chambliss, K.L., Hahner, L.D., Cummings, M.L., Kitchens, R.L., Marcel, Y.L., *et al.* (2006). High-density lipoprotein promotes endothelial cell migration and reendothelialization via scavenger receptor-B type I. *Circulation research* 98, 63-72.

Seimon, T., and Tabas, I. (2009). Mechanisms and consequences of macrophage apoptosis in atherosclerosis. *Journal of lipid research* 50 *Suppl*, S382-387.

Seimon, T.A., Wang, Y., Han, S., Senokuchi, T., Schrijvers, D.M., Kuriakose, G., Tall, A.R., and Tabas, I.A. (2009). Macrophage deficiency of p38alpha MAPK promotes apoptosis and plaque necrosis in advanced atherosclerotic lesions in mice. *The Journal of clinical investigation* 119, 886-898.

Senokuchi, T., Liang, C.P., Seimon, T.A., Han, S., Matsumoto, M., Banks, A.S., Paik, J.H., DePinho, R.A., Accili, D., Tabas, I., *et al.* (2008). Forkhead transcription factors (FoxOs) promote apoptosis of insulin-resistant macrophages during cholesterol-induced endoplasmic reticulum stress. *Diabetes* 57, 2967-2976.

Shah, A.S., Tan, L., Long, J.L., and Davidson, W.S. (2013). Proteomic diversity of high density lipoproteins: our emerging understanding of its importance in lipid transport and beyond. *Journal of lipid research* 54, 2575-2585.

Shah, P.K., Yano, J., Reyes, O., Chyu, K.Y., Kaul, S., Bisgaier, C.L., Drake, S., and Cercek, B. (2001). High-dose recombinant apolipoprotein A-I(milano) mobilizes tissue cholesterol and rapidly reduces plaque lipid and macrophage content in

apolipoprotein e-deficient mice. Potential implications for acute plaque stabilization. *Circulation* *103*, 3047-3050.

Sharrett, A.R., Ballantyne, C.M., Coady, S.A., Heiss, G., Sorlie, P.D., Catellier, D., Patsch, W., and Atherosclerosis Risk in Communities Study, G. (2001). Coronary heart disease prediction from lipoprotein cholesterol levels, triglycerides, lipoprotein(a), apolipoproteins A-I and B, and HDL density subfractions: The Atherosclerosis Risk in Communities (ARIC) Study. *Circulation* *104*, 1108-1113.

Shashkin, P., Dragulev, B., and Ley, K. (2005). Macrophage differentiation to foam cells. *Current pharmaceutical design* *11*, 3061-3072.

Shellman, Y.G., Howe, W.R., Miller, L.A., Goldstein, N.B., Pacheco, T.R., Mahajan, R.L., LaRue, S.M., and Norris, D.A. (2008). Hyperthermia induces endoplasmic reticulum-mediated apoptosis in melanoma and non-melanoma skin cancer cells. *The Journal of investigative dermatology* *128*, 949-956.

Shen, Y.C., Chen, C.F., and Chiou, W.F. (2000). Suppression of rat neutrophil reactive oxygen species production and adhesion by the diterpenoid lactone andrographolide. *Planta medica* *66*, 314-317.

Shinkai, Y., Rathbun, G., Lam, K.P., Oltz, E.M., Stewart, V., Mendelsohn, M., Charron, J., Datta, M., Young, F., Stall, A.M., *et al.* (1992). RAG-2-deficient mice lack mature lymphocytes owing to inability to initiate V(D)J rearrangement. *Cell* *68*, 855-867.

Shiojima, I., and Walsh, K. (2002). Role of Akt signaling in vascular homeostasis and angiogenesis. *Circulation research* *90*, 1243-1250.

Silva, R.A., Huang, R., Morris, J., Fang, J., Gracheva, E.O., Ren, G., Kontush, A., Jerome, W.G., Rye, K.A., and Davidson, W.S. (2008). Structure of apolipoprotein A-I in spherical high density lipoproteins of different sizes. *Proceedings of the National Academy of Sciences of the United States of America* 105, 12176-12181.

Silver, D.L. (2002). A carboxyl-terminal PDZ-interacting domain of scavenger receptor B, type I is essential for cell surface expression in liver. *The Journal of biological chemistry* 277, 34042-34047.

Smith, J.D., Trogan, E., Ginsberg, M., Grigaux, C., Tian, J., and Miyata, M. (1995). Decreased atherosclerosis in mice deficient in both macrophage colony-stimulating factor (op) and apolipoprotein E. *Proceedings of the National Academy of Sciences of the United States of America* 92, 8264-8268.

Smythies, L.E., White, C.R., Maheshwari, A., Palgunachari, M.N., Anantharamaiah, G.M., Chaddha, M., Kurundkar, A.R., and Datta, G. (2010). Apolipoprotein A-I mimetic 4F alters the function of human monocyte-derived macrophages. *American journal of physiology Cell physiology* 298, C1538-1548.

Song, G., Ouyang, G., and Bao, S. (2005). The activation of Akt/PKB signaling pathway and cell survival. *Journal of cellular and molecular medicine* 9, 59-71.

Springer, T.A. (1994). Traffic signals for lymphocyte recirculation and leukocyte emigration: the multistep paradigm. *Cell* 76, 301-314.

Stahl, M., Dijkers, P.F., Kops, G.J., Lens, S.M., Coffey, P.J., Burgering, B.M., and Medema, R.H. (2002). The forkhead transcription factor FoxO regulates

transcription of p27Kip1 and Bim in response to IL-2. *Journal of immunology* 168, 5024-5031.

Stannard, A.K., Riddell, D.R., Sacre, S.M., Tagalakis, A.D., Langer, C., von Eckardstein, A., Cullen, P., Athanasopoulos, T., Dickson, G., and Owen, J.S. (2001). Cell-derived apolipoprotein E (ApoE) particles inhibit vascular cell adhesion molecule-1 (VCAM-1) expression in human endothelial cells. *J Biol Chem* 276, 46011-46016.

Steimer, D.A., Boyd, K., Takeuchi, O., Fisher, J.K., Zambetti, G.P., and Opferman, J.T. (2009). Selective roles for antiapoptotic MCL-1 during granulocyte development and macrophage effector function. *Blood* 113, 2805-2815.

Stein, M., Keshav, S., Harris, N., and Gordon, S. (1992). Interleukin 4 potently enhances murine macrophage mannose receptor activity: a marker of alternative immunologic macrophage activation. *The Journal of experimental medicine* 176, 287-292.

Stoekenbroek, R.M., Stroes, E.S., and Hovingh, G.K. (2015). ApoA-I mimetics. *Handbook of experimental pharmacology* 224, 631-648.

Stoger, J.L., Gijbels, M.J., van der Velden, S., Manca, M., van der Loos, C.M., Biessen, E.A., Daemen, M.J., Lutgens, E., and de Winther, M.P. (2012). Distribution of macrophage polarization markers in human atherosclerosis. *Atherosclerosis* 225, 461-468.

Suc, I., Escargueil-Blanc, I., Troly, M., Salvayre, R., and Negre-Salvayre, A. (1997). HDL and ApoA prevent cell death of endothelial cells induced by oxidized LDL. *Arteriosclerosis, thrombosis, and vascular biology* 17, 2158-2166.

Sugano, M., Tsuchida, K., and Makino, N. (2000). High-density lipoproteins protect endothelial cells from tumor necrosis factor-alpha-induced apoptosis. *Biochemical and biophysical research communications* 272, 872-876.

Sullivan, P.M., Mezdour, H., Quarfordt, S.H., and Maeda, N. (1998). Type III hyperlipoproteinemia and spontaneous atherosclerosis in mice resulting from gene replacement of mouse Apoe with human Apoe*2. *J Clin Invest* 102, 130-135.

Suzuki, M., Pritchard, D.K., Becker, L., Hoofnagle, A.N., Tanimura, N., Bammler, T.K., Beyer, R.P., Bumgarner, R., Vaisar, T., de Beer, M.C., *et al.* (2010). High-density lipoprotein suppresses the type I interferon response, a family of potent antiviral immunoregulators, in macrophages challenged with lipopolysaccharide. *Circulation* 122, 1919-1927.

Sweetnam, P.M., Thomas, H.F., Yarnell, J.W., Baker, I.A., and Elwood, P.C. (1997). Total and differential leukocyte counts as predictors of ischemic heart disease: the Caerphilly and Speedwell studies. *American journal of epidemiology* 145, 416-421.

Swertfeger, D.K., and Hui, D.Y. (2001). Apolipoprotein E receptor binding versus heparan sulfate proteoglycan binding in its regulation of smooth muscle cell migration and proliferation. *J Biol Chem* 276, 25043-25048.

Swirski, F.K., Libby, P., Aikawa, E., Alcaide, P., Luscinskas, F.W., Weissleder, R., and Pittet, M.J. (2007). Ly-6Chi monocytes dominate hypercholesterolemia-associated monocytosis and give rise to macrophages in atheromata. *The Journal of clinical investigation* 117, 195-205.

Tabas, I. (2004). Apoptosis and plaque destabilization in atherosclerosis: the role of macrophage apoptosis induced by cholesterol. *Cell death and differentiation* *11 Suppl 1*, S12-16.

Tabas, I. (2005). Consequences and therapeutic implications of macrophage apoptosis in atherosclerosis: the importance of lesion stage and phagocytic efficiency. *Arteriosclerosis, thrombosis, and vascular biology* *25*, 2255-2264.

Tabas, I. (2009). Macrophage apoptosis in atherosclerosis: consequences on plaque progression and the role of endoplasmic reticulum stress. *Antioxidants & redox signaling* *11*, 2333-2339.

Tabet, F., Vickers, K.C., Cuesta Torres, L.F., Wiese, C.B., Shoucri, B.M., Lambert, G., Catherinet, C., Prado-Lourenco, L., Levin, M.G., Thacker, S., *et al.* (2014). HDL-transferred microRNA-223 regulates ICAM-1 expression in endothelial cells. *Nature communications* *5*, 3292.

Tacke, F., Alvarez, D., Kaplan, T.J., Jakubzick, C., Spanbroek, R., Llodra, J., Garin, A., Liu, J., Mack, M., van Rooijen, N., *et al.* (2007). Monocyte subsets differentially employ CCR2, CCR5, and CX3CR1 to accumulate within atherosclerotic plaques. *The Journal of clinical investigation* *117*, 185-194.

Takeuchi, O., Fisher, J., Suh, H., Harada, H., Malynn, B.A., and Korsmeyer, S.J. (2005). Essential role of BAX,BAK in B cell homeostasis and prevention of autoimmune disease. *Proceedings of the National Academy of Sciences of the United States of America* *102*, 11272-11277.

Tamama, K., Tomura, H., Sato, K., Malchinkhuu, E., Damirin, A., Kimura, T., Kuwabara, A., Murakami, M., and Okajima, F. (2005). High-density lipoprotein inhibits migration of vascular smooth muscle cells through its sphingosine 1-phosphate component. *Atherosclerosis* 178, 19-23.

Tangirala, R.K., Rubin, E.M., and Palinski, W. (1995). Quantitation of atherosclerosis in murine models: correlation between lesions in the aortic origin and in the entire aorta, and differences in the extent of lesions between sexes in LDL receptor-deficient and apolipoprotein E-deficient mice. *J Lipid Res* 36, 2320-2328.

Tao, H., Yancey, P.G., Babaev, V.R., Blakemore, J.L., Zhang, Y., Ding, L., Fazio, S., and Linton, M.F. (2015). Macrophage SR-BI mediates efferocytosis via Src/PI3K/Rac1 signaling and reduces atherosclerotic lesion necrosis. *Journal of lipid research* 56, 1449-1460.

Terasaka, N., Wang, N., Yvan-Charvet, L., and Tall, A.R. (2007). High-density lipoprotein protects macrophages from oxidized low-density lipoprotein-induced apoptosis by promoting efflux of 7-ketocholesterol via ABCG1. *Proceedings of the National Academy of Sciences of the United States of America* 104, 15093-15098.

Tesh, V.L. (2010). Induction of apoptosis by Shiga toxins. *Future microbiology* 5, 431-453.

Thorp, E., Li, G., Seimon, T.A., Kuriakose, G., Ron, D., and Tabas, I. (2009). Reduced apoptosis and plaque necrosis in advanced atherosclerotic lesions of Apoe^{-/-} and Ldlr^{-/-} mice lacking CHOP. *Cell metabolism* 9, 474-481.

Timmins, J.M., Ozcan, L., Seimon, T.A., Li, G., Malagelada, C., Backs, J., Backs, T., Bassel-Duby, R., Olson, E.N., Anderson, M.E., *et al.* (2009). Calcium/calmodulin-dependent protein kinase II links ER stress with Fas and mitochondrial apoptosis pathways. *The Journal of clinical investigation* 119, 2925-2941.

Tolani, S., Pagler, T.A., Murphy, A.J., Bochem, A.E., Abramowicz, S., Welch, C., Nagareddy, P.R., Holleran, S., Hovingh, G.K., Kuivenhoven, J.A., *et al.* (2013). Hypercholesterolemia and reduced HDL-C promote hematopoietic stem cell proliferation and monocytosis: studies in mice and FH children. *Atherosclerosis* 229, 79-85.

Tolle, M., Pawlak, A., Schuchardt, M., Kawamura, A., Tietge, U.J., Lorkowski, S., Keul, P., Assmann, G., Chun, J., Levkau, B., *et al.* (2008). HDL-associated lysosphingolipids inhibit NAD(P)H oxidase-dependent monocyte chemoattractant protein-1 production. *Arteriosclerosis, thrombosis, and vascular biology* 28, 1542-1548.

Trigatti, B., Rayburn, H., Vinals, M., Braun, A., Miettinen, H., Penman, M., Hertz, M., Schrenzel, M., Amigo, L., Rigotti, A., *et al.* (1999). Influence of the high density lipoprotein receptor SR-BI on reproductive and cardiovascular pathophysiology. *Proceedings of the National Academy of Sciences of the United States of America* 96, 9322-9327.

Trigatti, B.L., Mangroo, D., and Gerber, G.E. (1991). Photoaffinity labeling and fatty acid permeation in 3T3-L1 adipocytes. *The Journal of biological chemistry* 266, 22621-22625.

Trogan, E., Choudhury, R.P., Dansky, H.M., Rong, J.X., Breslow, J.L., and Fisher, E.A. (2002). Laser capture microdissection analysis of gene expression in macrophages from atherosclerotic lesions of apolipoprotein E-deficient mice. *Proceedings of the National Academy of Sciences of the United States of America* 99, 2234-2239.

Tsukamoto, K., Mani, D.R., Shi, J., Zhang, S., Haagensen, D.E., Otsuka, F., Guan, J., Smith, J.D., Weng, W., Liao, R., *et al.* (2013). Identification of apolipoprotein D as a cardioprotective gene using a mouse model of lethal atherosclerotic coronary artery disease. *Proc Natl Acad Sci U S A* 110, 17023-17028.

Tsukano, H., Gotoh, T., Endo, M., Miyata, K., Tazume, H., Kadomatsu, T., Yano, M., Iwawaki, T., Kohno, K., Araki, K., *et al.* (2010). The endoplasmic reticulum stress-C/EBP homologous protein pathway-mediated apoptosis in macrophages contributes to the instability of atherosclerotic plaques. *Arteriosclerosis, thrombosis, and vascular biology* 30, 1925-1932.

Tuttolomondo, A., Di Raimondo, D., Pecoraro, R., Arnao, V., Pinto, A., and Licata, G. (2012). Atherosclerosis as an inflammatory disease. *Current pharmaceutical design* 18, 4266-4288.

Ueda, Y., Gong, E., Royer, L., Cooper, P.N., Francone, O.L., and Rubin, E.M. (2000). Relationship between expression levels and atherogenesis in scavenger receptor class B, type I transgenics. *J Biol Chem* 275, 20368-20373.

Uehara, Y., Ando, S., Yahiro, E., Oniki, K., Ayaori, M., Abe, S., Kawachi, E., Zhang, B., Shioi, S., Tanigawa, H., *et al.* (2013). FAMP, a novel apoA-I mimetic peptide,

suppresses aortic plaque formation through promotion of biological HDL function in ApoE-deficient mice. *Journal of the American Heart Association* 2, e000048.

Uittenbogaard, A., Shaul, P.W., Yuhanna, I.S., Blair, A., and Smart, E.J. (2000). High density lipoprotein prevents oxidized low density lipoprotein-induced inhibition of endothelial nitric-oxide synthase localization and activation in caveolae. *The Journal of biological chemistry* 275, 11278-11283.

Urban, D., Poss, J., Bohm, M., and Laufs, U. (2013). Targeting the proprotein convertase subtilisin/kexin type 9 for the treatment of dyslipidemia and atherosclerosis. *Journal of the American College of Cardiology* 62, 1401-1408.

Urbano, A., McCaffrey, R., and Foss, F. (1998). Isolation and characterization of NUC70, a cytoplasmic, hematopoietic apoptotic endonuclease. *The Journal of biological chemistry* 273, 34820-34827.

van der Meij, E., Koning, G.G., Vriens, P.W., Peeters, M.F., Meijer, C.A., Kortekaas, K.E., Dalman, R.L., van Bockel, J.H., Hanemaaijer, R., Kooistra, T., *et al.* (2013). A clinical evaluation of statin pleiotropy: statins selectively and dose-dependently reduce vascular inflammation. *PloS one* 8, e53882.

van der Wal, A.C., and Becker, A.E. (1999). Atherosclerotic plaque rupture--pathologic basis of plaque stability and instability. *Cardiovascular research* 41, 334-344.

Van Eck, M., Herijgers, N., Yates, J., Pearce, N.J., Hoogerbrugge, P.M., Groot, P.H., and Van Berkel, T.J. (1997). Bone marrow transplantation in apolipoprotein E-deficient

mice. Effect of ApoE gene dosage on serum lipid concentrations, (beta)VLDL catabolism, and atherosclerosis. *Arterioscler Thromb Vasc Biol* 17, 3117-3126.

Van Eck, M., Hoekstra, M., Hildebrand, R.B., Yaong, Y., Stengel, D., Kruijt, J.K., Sattler, W., Tietge, U.J., Ninio, E., Van Berkel, T.J., *et al.* (2007). Increased oxidative stress in scavenger receptor BI knockout mice with dysfunctional HDL. *Arterioscler Thromb Vasc Biol* 27, 2413-2419.

Van Eck, M., Twisk, J., Hoekstra, M., Van Rij, B.T., Van der Lans, C.A., Bos, I.S., Kruijt, J.K., Kuipers, F., and Van Berkel, T.J. (2003). Differential effects of scavenger receptor BI deficiency on lipid metabolism in cells of the arterial wall and in the liver. *The Journal of biological chemistry* 278, 23699-23705.

Van Vre, E.A., Ait-Oufella, H., Tedgui, A., and Mallat, Z. (2012). Apoptotic cell death and efferocytosis in atherosclerosis. *Arteriosclerosis, thrombosis, and vascular biology* 32, 887-893.

Verreth, W., De Keyzer, D., Davey, P.C., Geeraert, B., Mertens, A., Herregods, M.C., Smith, G., Desjardins, F., Balligand, J.L., and Holvoet, P. (2007). Rosuvastatin restores superoxide dismutase expression and inhibits accumulation of oxidized LDL in the aortic arch of obese dyslipidemic mice. *British journal of pharmacology* 151, 347-355.

Vinals, M., Martinez-Gonzalez, J., Badimon, J.J., and Badimon, L. (1997). HDL-induced prostacyclin release in smooth muscle cells is dependent on cyclooxygenase-2 (Cox-2). *Arteriosclerosis, thrombosis, and vascular biology* 17, 3481-3488.

Voight, B.F., Peloso, G.M., Orho-Melander, M., Frikke-Schmidt, R., Barbalic, M., Jensen, M.K., Hindy, G., Holm, H., Ding, E.L., Johnson, T., *et al.* (2012). Plasma HDL cholesterol and risk of myocardial infarction: a mendelian randomisation study. *Lancet* *380*, 572-580.

von Harsdorf, R., Li, P.F., and Dietz, R. (1999). Signaling pathways in reactive oxygen species-induced cardiomyocyte apoptosis. *Circulation* *99*, 2934-2941.

Voyiaziakis, E., Goldberg, I.J., Plump, A.S., Rubin, E.M., Breslow, J.L., and Huang, L.S. (1998). ApoA-I deficiency causes both hypertriglyceridemia and increased atherosclerosis in human apoB transgenic mice. *Journal of lipid research* *39*, 313-321.

Watson, L.M., Chan, A.K., Berry, L.R., Li, J., Sood, S.K., Dickhout, J.G., Xu, L., Werstuck, G.H., Bajzar, L., Klamut, H.J., *et al.* (2003). Overexpression of the 78-kDa glucose-regulated protein/immunoglobulin-binding protein (GRP78/BiP) inhibits tissue factor procoagulant activity. *The Journal of biological chemistry* *278*, 17438-17447.

Weinmann, M., Jendrossek, V., Handrick, R., Guner, D., Goecke, B., and Belka, C. (2004). Molecular ordering of hypoxia-induced apoptosis: critical involvement of the mitochondrial death pathway in a FADD/caspase-8 independent manner. *Oncogene* *23*, 3757-3769.

Wiersma, H., Nijstad, N., de Boer, J.F., Out, R., Hogewerf, W., Van Berkel, T.J., Kuipers, F., and Tietge, U.J. (2009). Lack of Abcg1 results in decreased plasma HDL cholesterol levels and increased biliary cholesterol secretion in mice fed a high cholesterol diet. *Atherosclerosis* *206*, 141-147.

Wilkerson, B.A., Grass, G.D., Wing, S.B., Argraves, W.S., and Argraves, K.M. (2012).

Sphingosine 1-phosphate (S1P) carrier-dependent regulation of endothelial barrier: high density lipoprotein (HDL)-S1P prolongs endothelial barrier enhancement as compared with albumin-S1P via effects on levels, trafficking, and signaling of S1P1. *The Journal of biological chemistry* 287, 44645-44653.

Williamson, R., Lee, D., Hagaman, J., and Maeda, N. (1992). Marked reduction of high density lipoprotein cholesterol in mice genetically modified to lack apolipoprotein A-I. *Proceedings of the National Academy of Sciences of the United States of America* 89, 7134-7138.

Wojcik, A.J., Skafien, M.D., Srinivasan, S., and Hedrick, C.C. (2008). A critical role for ABCG1 in macrophage inflammation and lung homeostasis. *Journal of immunology* 180, 4273-4282.

Wouters, K., Shiri-Sverdlov, R., van Gorp, P.J., van Bilsen, M., and Hofker, M.H. (2005). Understanding hyperlipidemia and atherosclerosis: lessons from genetically modified apoe and ldlr mice. *Clin Chem Lab Med* 43, 470-479.

Wu, B.J., Shrestha, S., Ong, K.L., Johns, D., Hou, L., Barter, P.J., and Rye, K.A. (2015). Cholesteryl ester transfer protein inhibition enhances endothelial repair and improves endothelial function in the rabbit. *Arteriosclerosis, thrombosis, and vascular biology* 35, 628-636.

Xu, S., Laccotripe, M., Huang, X., Rigotti, A., Zannis, V.I., and Krieger, M. (1997). Apolipoproteins of HDL can directly mediate binding to the scavenger receptor SR-

BI, an HDL receptor that mediates selective lipid uptake. *Journal of lipid research* 38, 1289-1298.

Yamamoto, K., Takahara, K., Oyadomari, S., Okada, T., Sato, T., Harada, A., and Mori, K. (2010). Induction of liver steatosis and lipid droplet formation in ATF6alpha-knockout mice burdened with pharmacological endoplasmic reticulum stress. *Mol Biol Cell* 21, 2975-2986.

Yamashita, S., and Matsuzawa, Y. (2009). Where are we with probucol: a new life for an old drug? *Atherosclerosis* 207, 16-23.

Yan, G.R., Zhou, H.H., Wang, Y., Zhong, Y., Tan, Z.L., Wang, Y., and He, Q.Y. (2013). Protective effects of andrographolide analogue AL-1 on ROS-induced RIN-mbeta cell death by inducing ROS generation. *PloS one* 8, e63656.

Yan, L.R., Wang, D.X., Liu, H., Zhang, X.X., Zhao, H., Hua, L., Xu, P., and Li, Y.S. (2014). A pro-atherogenic HDL profile in coronary heart disease patients: an iTRAQ labelling-based proteomic approach. *PloS one* 9, e98368.

Yancey, P.G., Jerome, W.G., Yu, H., Griffin, E.E., Cox, B.E., Babaev, V.R., Fazio, S., and Linton, M.F. (2007). Severely altered cholesterol homeostasis in macrophages lacking apoE and SR-BI. *Journal of lipid research* 48, 1140-1149.

Yao, P.M., and Tabas, I. (2001). Free cholesterol loading of macrophages is associated with widespread mitochondrial dysfunction and activation of the mitochondrial apoptosis pathway. *The Journal of biological chemistry* 276, 42468-42476.

Yesilaltay, A., Daniels, K., Pal, R., Krieger, M., and Kocher, O. (2009). Loss of PDZK1 causes coronary artery occlusion and myocardial infarction in Paigen diet-fed apolipoprotein E deficient mice. *PloS one* 4, e8103.

Yesilaltay, A., Kocher, O., Pal, R., Leiva, A., Quinones, V., Rigotti, A., and Krieger, M. (2006). PDZK1 is required for maintaining hepatic scavenger receptor, class B, type I (SR-BI) steady state levels but not its surface localization or function. *The Journal of biological chemistry* 281, 28975-28980.

Yin, X.M., Wang, K., Gross, A., Zhao, Y., Zinkel, S., Klocke, B., Roth, K.A., and Korsmeyer, S.J. (1999). Bid-deficient mice are resistant to Fas-induced hepatocellular apoptosis. *Nature* 400, 886-891.

Yla-Herttuala, S., Rosenfeld, M.E., Parthasarathy, S., Sigal, E., Sarkioja, T., Witztum, J.L., and Steinberg, D. (1991). Gene expression in macrophage-rich human atherosclerotic lesions. 15-lipoxygenase and acetyl low density lipoprotein receptor messenger RNA colocalize with oxidation specific lipid-protein adducts. *The Journal of clinical investigation* 87, 1146-1152.

Yu, H., Littlewood, T., and Bennett, M. (2015). Akt isoforms in vascular disease. *Vascular pharmacology* 71, 57-64.

Yu, H., Zhang, W., Yancey, P.G., Koury, M.J., Zhang, Y., Fazio, S., and Linton, M.F. (2006). Macrophage apolipoprotein E reduces atherosclerosis and prevents premature death in apolipoprotein E and scavenger receptor-class BI double-knockout mice. *Arteriosclerosis, thrombosis, and vascular biology* 26, 150-156.

Yuhanna, I.S., Zhu, Y., Cox, B.E., Hahner, L.D., Osborne-Lawrence, S., Lu, P., Marcel, Y.L., Anderson, R.G., Mendelsohn, M.E., Hobbs, H.H., *et al.* (2001). High-density lipoprotein binding to scavenger receptor-BI activates endothelial nitric oxide synthase. *Nature medicine* 7, 853-857.

Yvan-Charvet, L., Pagler, T., Gautier, E.L., Avagyan, S., Siry, R.L., Han, S., Welch, C.L., Wang, N., Randolph, G.J., Snoeck, H.W., *et al.* (2010a). ATP-binding cassette transporters and HDL suppress hematopoietic stem cell proliferation. *Science* 328, 1689-1693.

Yvan-Charvet, L., Pagler, T.A., Seimon, T.A., Thorp, E., Welch, C.L., Witztum, J.L., Tabas, I., and Tall, A.R. (2010b). ABCA1 and ABCG1 protect against oxidative stress-induced macrophage apoptosis during efferocytosis. *Circulation research* 106, 1861-1869.

Yvan-Charvet, L., Ranalletta, M., Wang, N., Han, S., Terasaka, N., Li, R., Welch, C., and Tall, A.R. (2007). Combined deficiency of ABCA1 and ABCG1 promotes foam cell accumulation and accelerates atherosclerosis in mice. *The Journal of clinical investigation* 117, 3900-3908.

Zabalawi, M., Bhat, S., Loughlin, T., Thomas, M.J., Alexander, E., Cline, M., Bullock, B., Willingham, M., and Sorci-Thomas, M.G. (2003). Induction of fatal inflammation in LDL receptor and ApoA-I double-knockout mice fed dietary fat and cholesterol. *The American journal of pathology* 163, 1201-1213.

Zadelaar, A.S., von der Thusen, J.H., Boesten, L.S., Hoeben, R.C., Kockx, M.M., Versnel, M.A., van Berkel, T.J., Havekes, L.M., Biessen, E.A., and van Vlijmen, B.J. (2005).

Increased vulnerability of pre-existing atherosclerosis in ApoE-deficient mice following adenovirus-mediated Fas ligand gene transfer. *Atherosclerosis* 183, 244-250.

Zadelaar, S., Kleemann, R., Verschuren, L., de Vries-Van der Weij, J., van der Hoorn, J., Princen, H.M., and Kooistra, T. (2007). Mouse models for atherosclerosis and pharmaceutical modifiers. *Arteriosclerosis, thrombosis, and vascular biology* 27, 1706-1721.

Zannis, V.I., Chroni, A., and Krieger, M. (2006). Role of apoA-I, ABCA1, LCAT, and SR-BI in the biogenesis of HDL. *Journal of molecular medicine* 84, 276-294.

Zerneck, A., Bot, I., Djalali-Talab, Y., Shagdarsuren, E., Bidzhekov, K., Meiler, S., Krohn, R., Schober, A., Sperandio, M., Soehnlein, O., *et al.* (2008). Protective role of CXC receptor 4/CXC ligand 12 unveils the importance of neutrophils in atherosclerosis. *Circulation research* 102, 209-217.

Zhang, H.L., Wu, J., and Zhu, J. (2010a). The immune-modulatory role of apolipoprotein E with emphasis on multiple sclerosis and experimental autoimmune encephalomyelitis. *Clin Dev Immunol* 2010, 186813.

Zhang, S., Picard, M.H., Vasile, E., Zhu, Y., Raffai, R.L., Weisgraber, K.H., and Krieger, M. (2005). Diet-induced occlusive coronary atherosclerosis, myocardial infarction, cardiac dysfunction, and premature death in scavenger receptor class B type I-deficient, hypomorphic apolipoprotein ER61 mice. *Circulation* 111, 3457-3464.

Zhang, S.H., Reddick, R.L., Burkey, B., and Maeda, N. (1994). Diet-induced atherosclerosis in mice heterozygous and homozygous for apolipoprotein E gene disruption. *J Clin Invest* 94, 937-945.

Zhang, S.H., Reddick, R.L., Piedrahita, J.A., and Maeda, N. (1992). Spontaneous hypercholesterolemia and arterial lesions in mice lacking apolipoprotein E. *Science* 258, 468-471.

Zhang, W., Yancey, P.G., Su, Y.R., Babaev, V.R., Zhang, Y., Fazio, S., and Linton, M.F. (2003). Inactivation of macrophage scavenger receptor class B type I promotes atherosclerotic lesion development in apolipoprotein E-deficient mice. *Circulation* 108, 2258-2263.

Zhang, X., Zhu, X., and Chen, B. (2010b). Inhibition of collar-induced carotid atherosclerosis by recombinant apoA-I cysteine mutants in apoE-deficient mice. *Journal of lipid research* 51, 3434-3442.

Zhang, Y., Ahmed, A.M., McFarlane, N., Capone, C., Boreham, D.R., Truant, R., Igdoura, S.A., and Trigatti, B.L. (2007). Regulation of SR-BI-mediated selective lipid uptake in Chinese hamster ovary-derived cells by protein kinase signaling pathways. *Journal of lipid research* 48, 405-416.

Zhong, J.C., Yu, X.Y., Lin, Q.X., Li, X.H., Huang, X.Z., Xiao, D.Z., and Lin, S.G. (2008). Enhanced angiotensin converting enzyme 2 regulates the insulin/Akt signalling pathway by blockade of macrophage migration inhibitory factor expression. *British journal of pharmacology* 153, 66-74.

Zhou, J., Lhotak, S., Hilditch, B.A., and Austin, R.C. (2005). Activation of the unfolded protein response occurs at all stages of atherosclerotic lesion development in apolipoprotein E-deficient mice. *Circulation* *111*, 1814-1821.

Zhu, W., Saddar, S., Seetharam, D., Chambliss, K.L., Longoria, C., Silver, D.L., Yuhanna, I.S., Shaul, P.W., and Mineo, C. (2008). The scavenger receptor class B type I adaptor protein PDZK1 maintains endothelial monolayer integrity. *Circulation research* *102*, 480-487.

Zinszner, H., Kuroda, M., Wang, X., Batchvarova, N., Lightfoot, R.T., Remotti, H., Stevens, J.L., and Ron, D. (1998). CHOP is implicated in programmed cell death in response to impaired function of the endoplasmic reticulum. *Genes & development* *12*, 982-995.

Zizzo, G., Hilliard, B.A., Monestier, M., and Cohen, P.L. (2012). Efficient clearance of early apoptotic cells by human macrophages requires M2c polarization and MerTK induction. *Journal of immunology* *189*, 3508-3520.

Zong, W.X., and Thompson, C.B. (2006). Necrotic death as a cell fate. *Genes & development* *20*, 1-15.